50444

T 180

28/02/13   50447

26/12/11

EMULSION POLYMERIZATION OF STYRENE AND SYNTHESIS OF POLYSTYRENE NANOCOMPOSITES IN SUPERCRITICAL CARBON DIOXIDE MEDIUM

A thesis submitted

in partial fulfillment of the requirements for the degree of

Doctor of Philosophy

By

Isha Ruhulla Kamrupi

Registration No. 014 of 2010

School of Science and Technology

Department of Chemical Sciences

Tezpur University

Assam, India

April, 2011

Dedicated to

BABA and

MAAI

Emulsion polymerization of styrene and synthesis of polystyrene nanocomposites in supercritical carbon dioxide medium

ABSTRACT

THE THESIS

The present thesis deals with the study of polymerization of styrene using fluorine and siloxane based stabilizers and their physical properties. A considerable effort has been devoted to the standardization of the different process parameters for polymerization of styrene in sc-CO_2 medium. The synthesis of stable dispersion of metal nanoparticles like Ag, Cu etc. in water in sc-CO_2 medium using polydimethyl siloxane (PDMS) stabilizer and their nanocomposites with polystyrene is also illustrated in the thesis. The physical properties of metal nanoparticles encapsulated polystyrene particles like antibacterial activity is described in the thesis. Finally, concluding remarks and proposed future research efforts have been included in the thesis.

The thesis includes six chapters which are briefly described below.

Chapter 1 includes with the general introduction of supercritical carbon dioxide (sc-CO_2), its invention, properties, advantages over conventional organic solvents, its solubility in different reactants, design of surfactant for sc-CO_2 etc. Different types of polymerization reactions in sc-CO_2 medium are briefly described with the latest literature survey up to 2011. The different synthetic methods for the synthesis of nanoparticles like rapid expansion of supercritical solutions (RESS), supercritical anti-solvent precipitation (SAS), synthesis of nanoparticles by reduction in sc-CO_2, synthesis of metal nanoparticles by hydrolysis of metal salts in sc-CO_2, etc. are described. The technique for synthesis of nanocomposites in sc-CO_2 medium is also elaborately described in this chapter.

Chapter 2 deals with the polymerization of styrene using siloxane and fluorine based stabilizers in sc-CO_2 medium. The successful emulsion polymerization of styrene monomers in sc-CO_2 using different fluorinated and siloxane based stabilizers and

standardization of the reaction parameters are reported in this chapter. In all the syntheses, azo-bis-isobutyronitrile (AIBN) is used as the initiator. The stabilizers used in these syntheses are (trifluoromethyl)undecafluorocyclohexane (C_7F_{14}), polydimethylsiloxane (PDMS), etc. The polymers were characterized by gel permeation chromatograpyu (GPC), scanning electron micrograph (SEM) and Thermogravimetric analysis (TGA). The influence of different process parameters (stabilizer concentration, initiator concentration and pressure of CO_2) on conversion, molecular weight, particle size and polydispersity index are elaborately studied in this chapter.

Chapter 3 describes the synthesis and characterization of metal (Ag, Cu) nanoparticles and their nanocomposites with polystyrene using water in supercritical carbon dioxide (sc-CO_2) medium. polydimethylsiloxane (PDMS) was used as stabilizer and sodium borohydrate ($NaBH_4$) was used as the reducing agent in the synthesis of metal nanoparticles. The synthesized metal nanoparticles (Ag, Cu) were encapsulated into polystyrene particles in sc-CO_2 medium. The antibacterial activity of these nanocomposites particles are also described elaborately in this chapter.

Chapter 4 contains the synthesis of polystyrene/bentonite clay nanocomposites by emulsion polymerization in aqueous and in supercritical carbon dioxide (sc-CO_2) medium. The modified clay is dispersed within the monomer via ultrasonication and the mixture is allowed to undergo in-situ emulsion polymerization resulting in the formation of polymer/clay nanocomposites. A comparative study of the properties of the nanocomposites synthesized in the two media is carried out. The effects of clay concentration on polymer conversion, molecular weight, morphology and mechanical properties have been investigated. The mechanical properties of the nanocomposite synthesized in sc-CO_2 medium are higher than in aqueous medium. Similarly, thermal properties and the particle forming efficiency of the nanocomposite are far better in supercritical carbon dioxide medium than in aqueous medium.

Chapter 5 reports the synthesis of microporous polymer particles by suspension polymerization using sc-CO_2 as a pressure-adjustable porogen. In this chapter it is emphasized that sc-CO_2 can also be used as a porogenic solvent for the synthesis of microporous polymer particles. The solvent property of sc-CO_2 can be tuned over a

this chapter it is emphasized that sc-CO_2 can also be used as a porogenic solvent for the synthesis of microporous polymer particles. The solvent property of sc-CO_2 can be tuned over a wide range for the synthesis of macroporous polymer particles by changing the pressure inside the reactor. The pore size, pore size distribution, surface area and the average diameter of the particles can be effectively controlled by controlling the pressure. The diameter of the particles increases with the increase in pressure. Similarly the surface area of the particles also increases with the increase in pressure. The use of sc-CO_2 for synthesizing porous polymer particles is superior to the other conventional systems that are used for synthesizing porous particles regarding the purification of the products and environmental pollution. By depressurizing the gas simply, the porogens from the porous particles can be removed completely; no extra washing or drying steps are required.

Chapter 6 outlines the concluding remarks, highlights of the findings followed by future scopes of the present investigations. It is concluded that sc-CO_2 can be used as a versatile and green synthesis medium of different polymers, metal nanoparticles, nanocomposites and microporous polymer particles. Using sc-CO_2, one can directly synthesize powdered polymer particles without any solvent residue in the product. Metal nanoparticles like Ag, Cu etc. can be synthesized using water in sc-CO_2 medium, the size of the nanoparticles can be controlled be tailoring the pressure of CO_2. Polymer/clay nanocomposites can be easily synthesized in sc-CO_2 medium. The processing of the clay layers is very excellent in sc-CO_2 medium, which facilitates different properties of the nanocomposites like mechanical strength, thermal stability etc. Again sc-CO_2 can be used as a pressure adjustable porogens for synthesizing microporous polymer particles. The pore diameter of the particles can be controlled by controlling the pressure of CO_2.
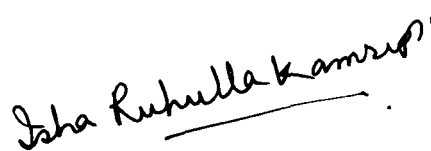
DECLARATION BY THE CANDIDATE

The thesis entitled "*Emulsion polymerization of styrene and synthesis of polystyrene nanocomposites in supercritical carbon dioxide medium*" is being submitted to the Tezpur University in partial fulfillment for the award of the degree of Doctor of Philosophy in *Chemical Sciences* is a record of bonafide research work accomplished by me under the supervision of Prof. S. K. Dolui.

All helps received from various sources have been duly acknowledged.

No part of this thesis has been submitted elsewhere for award of any other degree.

Date: 21 – 04 – 2011

Place: Tezpur

Isha Ruhulla Kamrupi

Department of Chemical Sciences

Tezpur University

iv

TEZPUR UNIVERSITY

(A Central University by an Act of Parliament)

DISTRICT: SONITPUR:: ASSAM:: INDIA
Napaam, Tezpur-784028

Ph: 03712-267004(O) 9957198489 (M)   Fax: 03712-267006 *Email : dolui@tezu.ernet.in*

CERTIFICATE OF THE PRINCIPAL SUPERVISOR

This is to certify that the thesis entitled "*Emulsion polymerization of styrene and synthesis of polystyrene nanocomposites in supercritical carbon dioxide medium*" submitted to the School of *Science and Technology*, Tezpur University in partial fulfillment for the award of the **degree of Doctor of Philosophy** in *Chemical Sciences* is a record of research work **carried** out by ***Mr. Isha Ruhulla Kamrupi*** under my supervision and guidance.

All help received by **him from** various sources **have** been duly acknowledged.

No part of this thesis has been submitted elsewhere for award of any other degree.

Date: 21 April 2011

Place: Tezpur

S. K. Dolui

Professor

Department of Chemical Sciences

School of Science and Technology

TEZPUR UNIVERSITY

(A Central University by an Act of Parliament)

DISTRICT: SONITPUR:: ASSAM:: INDIA

Napaam, Tezpur-784028

Fax: 03712-267006 Ph: 03712-267004 *Email : adm@agnigarh.tezu.ernet.in*

CERTIFICATE OF THE EXTERNAL EXAMINER AND ODEC

This is to certify that the thesis entitled *"Emulsion polymerization of styrene and synthesis of polystyrene nanocomposites in supercritical carbon dioxide medium"* submitted by *Mr. Isha Ruhulla Kamrupi* to Tezpur University in the **Department of Chemical Sciences** under the school of **Science and Technology** in partial fulfillment of the requirement for the award of the degree of Doctor of Philosophy in **Chemical Sciences** has been examined by us on _____ and found to be satisfactory.

Signature of:

Principal Supervisor   External Examiner

Date: _____

Preface

Synthesis of polymers and polymer nanocomposites in a greener route is highly demanded in the current scenario due to different environmental aspects. The advancement made in this regard compelled the researchers and scientists to turn into supercritical carbon dioxide (sc-CO_2) medium as it has advantages over conventional organic solvents.

Sc-CO_2 offers several advantages over conventional organic solvents like inexpensiveness, recyclability, nonflammability and green nature for polymer synthesis and processing. Supercritical carbon dioxide possesses many properties that have allowed it to emerge as most extensively studied supercritical fluid for polymerization reactions. Sc-CO_2 is one of the viable and promising alternatives to traditional solvents used for polymerization reactions to date. It is extensively used in the extraction of natural products, synthesis of organic compounds and inorganic complexes. It can also be used as a polymerization medium for the different monomers, synthesis of metal nanoparticles and its nanocomposites with polymers, synthesis of macroporous polymer particles etc.

The major problem encountered in the synthesis of polymers in sc-CO_2 medium is solubility. Since CO_2 is a non-polar solvent, it can only dissolve small non-polar molecules and hydrocarbons up to 20 carbons. Organic molecules such as aldehydes, ketones, esters are soluble in it. Large molecules like waxes, oil, polymers. cannot be dissolved in sc-CO_2 medium. But these molecules can be emulsified in sc-CO_2 using suitable fluorinated and siloxane based stabilizers. A considerable effort has been devoted to the synthesis of powdered polystyrene microparticles, metal nanoparticles and their nanocomposites with special reference to antibacterial activity, polystyrene/clay nanocomposites and macroporous polymer particles. The contents of the thesis have been compiled into six chapters. Chapter 1 deals with the general introduction of supercritical fluids. Chapter 2 describes the synthesis and characterization of polystyrene particles and their thermal properties. In chapter 3, synthesis and characterization of metal nanoparticles like Ag, Cu and its nanocomposites with polystyrene are discussed. The antibacterial activity of these nanocomposites has been tested against a number of bacterial strains. Chapter 4 includes the synthesis and characterization of polystyrene/clay nanocomposites in supercritical carbon dioxide medium. Chapter 5 deals with the synthesis and characterization of macroporous polystyrene particles in supercritical carbon dioxide medium. Chapter 6 is the last chapter includes the concluding remarks, highlights of the findings and future scopes of the present investigation.

I hope that this study contributes a little knowledge to the rapidly advancing field of polymerization in sc-CO$_2$ medium and also opens up the possibilities of further research on the subject.

This research was carried out in the Department of Chemical Sciences, Tezpur University with financial assistance from the Naval Research Board (NRB), India (Grant no NRB-56/MAT/05-06) under sponsored research scheme.

Isha Ruhulla Kamrupi

Acknowledgement

Isha Ruhulla Kamrupi

Contents

List of Tables

List of Figures

Abbreviations used in the thesis

sc-CO_2	Supercritical carbon dioxide
SCF	Supercritical fluids
AOT	Sodium bis-ethylhexyl sulfosuccinate
SANS	Small angle neutron scattering
EO	Ethylene Oxide
PO	Propylene Oxide
FTIR	Fourier transformed infrared spectroscopy
PFPE	Perfluoropolyethylene
PDMS	Polydimethylsiloxane
RPM	Rotation per minute
VOC	Volatile organic compounds
CFC	Chlorofluorocarbon
μm	Micro meter
PEHA	Poly(1,1-dihydroper-fluorooctyl acrylate)
CFD	Critical flocculation density
MMA	Methylmethacrylate
PMMA	Polymethylmethacrylate
HDPE	High-density polyethylene
PTFE	Polytetrafluoroethylene
PS	Polystyrene
RESS	Rapid expansion of supercritical solutions
DSP	2,5-distyrylpyrazine
RESOLV	Rapid expansion of supercritical solution into solvent
PVP	Poly(N-vinyl-2-pyrrolidone
PHDFDE	Poly(heptadecafluorodecylacrylate)
SAS	Supercritical anti-solvent
VLE	Vapor-liquid equilibria
SCW	Supercritical water

TTIP	Titanium tetra-isopropoxide
BSA	Bovine serum albumin
TEM	Transmission electron micrograph
SEM	Scanning electron micrograph
AFM	Atomic force microscope
TRIM	Trimethylolpropane trimethacrylate
sc-CH$_3$OH	Supercritical methanol
sc-EtOH	Supercritical ethanol
GPC	Gel permeation chromatography
XRD	X-Ray diffraction
STM	Scanning tunneling microscope
UV-vis	Ultra-violet visible
TGA	Thermogravimetric analysis
DSC	Differential scanning calorimetry
UTM	Universal testing machine
BET	Brunauer Emmett Teller theory
ASB	Anchor soluble balance
AIBN	Azobisisobutyronitrile
THF	Tetrahydrofuran
PSI	Pounds per square inch
HPLC	High performance liquid chromatography
M$_n$	Number average molecular weight
PDI	Polydispersity index
Ag	Silver
Cu	Copper
AOT-TMH	Sodium bis(3,5,5-trimethyl-1-hexyl)sulfosuccinate)
SDS	Sodium dodecyl sulfonate
MPa	Mega pascal
BS3	Pseudomonas fluorescens
BP2	Bacillus circulens

DHSα	Eschericia coli
FCC	Face-centered cubic
DNA	Deoxy ribonucelic acid
SDBS	Sodium dodecylbenzene sulfonate
ASTM	American society for testing and materials
T_g	Glass transition temperature

CHAPTER 1

GENERAL

INTRODUCTION

1.1 Introduction

1.1.1 Supercritical Fluids

"There is no point in doing something in a supercritical fluid just because it's neat. Using the fluids must have some real advantage"

These words were expressed 22 years ago at the first international symposium on supercritical fluids in 1988 and still hold true today. Working with supercritical fluids involves high pressures and sometimes high temperatures. It is always easier to carry out an experiment under conventional conditions than supercritically. But reactions in supercritical conditions have some real advantages over conventional organic reaction media.[1-3]

A French scientist, Baron Charles Cagniard de la Tour, in 1821 first discovered the supercritical state.[4] However, intensive research in the area actually belongs to the last few decades. The supercritical phase of a compound is a phase in which the compound is above its critical pressure (P_c), and critical temperature, (T_c).[5-11] In this phase, the properties of both a gas and a liquid exist. The most important property of a supercritical fluid is its tunability in the temperature range since small changes in temperature will cause drastic changes in the pressure, followed by changes in other physical variables related to pressure and temperature.[12] The main variables that are affected by such changes and that play important roles in supercritical applications are the density (ρ) and the dielectric constant (ε). The density is a variable known to be directly proportional to the solvency power, and this is the basis for supercritical fluid extraction processes. The tunability of the dielectric constant also gives power to tune the solvency power, since it relates to the solvent polarity and other important solvent effects. Supercritical fluids bear many important properties that increase their utility. Their high diffusivity, low viscosity and high density make them suitable for

1

continuous-flow processes. The critical conditions of several common solvents[13] and gases are summarized in Table 1.1.

Table.1.1: Critical conditions of several substances

Solvent	$T_c(K)$	$P_c(MPa)$	Solvent	$T_c(K)$	$P_c(MPa)$
Acetone	508.1	4.70	Hexafluoroethane	293.0	3.06
Ammonia	405.6	11.3	Methane	190.4	4.60
Carbon dioxide	304.1	7.38	Methanol	512.6	8.09
Cyclohexane	553.5	4.07	n-hexane	507.5	3.01
Diethyl ether	466.7	3.64	Propane	369.8	4.25
Difluoromethane	351.6	5.83	Propylene	364.9	4.60
Difluoroethane	386.7	4.50	Sulfur hexafluoride	318.7	3.76
Dimethyl ether	400.0	5.24	Tetrafluoromethane	227.6	3.74
Ethane	305.3	4.87	Toluene	591.8	41.1
Ethylene	282.4	5.04	Trifluoromethane	299.3	4.86
Ethyne	308.3	6.14	Water	647.3	22.1

1.1.2 Supercritical Carbon dioxide (sc-CO$_2$)

Among all the substances, carbon dioxide has attracted the scientific community as a reaction medium due to its unique properties. Carbon dioxide is a non-flammable, inexpensive, recyclable and tunable solvent.[14-19] Moreover, it has less solvent residues in products, lower environmental impacts, solvent power of a liquid, and penetrating power of a gas. In 1875, Andrews first discovered the critical conditions for carbon dioxide and since then it has been used in various applications. It offers a unique combination of properties. Compared to liquids, sc-CO$_2$ possesses highly variable densities, much higher diffusivities, and much lower viscosities. Their solvent properties can be varied continuously from gas like to nearly liquid like by increasing pressure. Many applications have either proposed or developed to take advantage of the

advantage of the adjustability of supercritical fluids. The phase diagram of carbon dioxide is shown in Fig. 1.1[20]
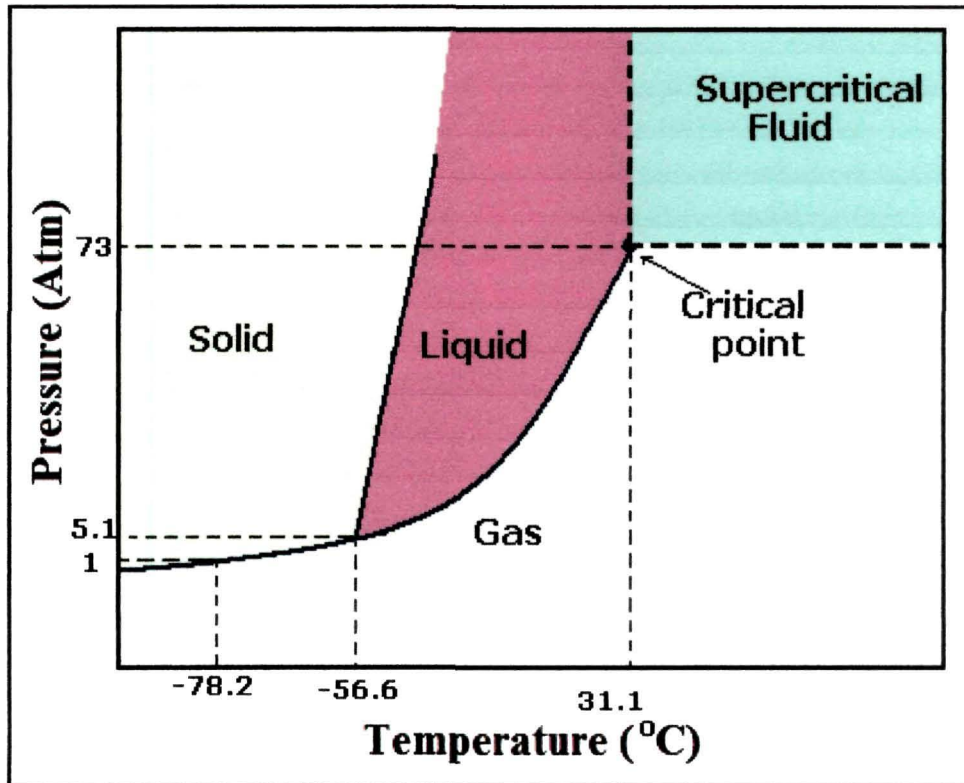
Fig.1.1: A phase diagram showing supercritical state of CO₂

Density of CO_2 as a function of pressure at different temperatures and at the vapor-liquid equilibrium line is shown in Fig.1.2. The solid line is the density versus pressure line and the dashed line is the liquid-vapour equilibrium line.[21]

3
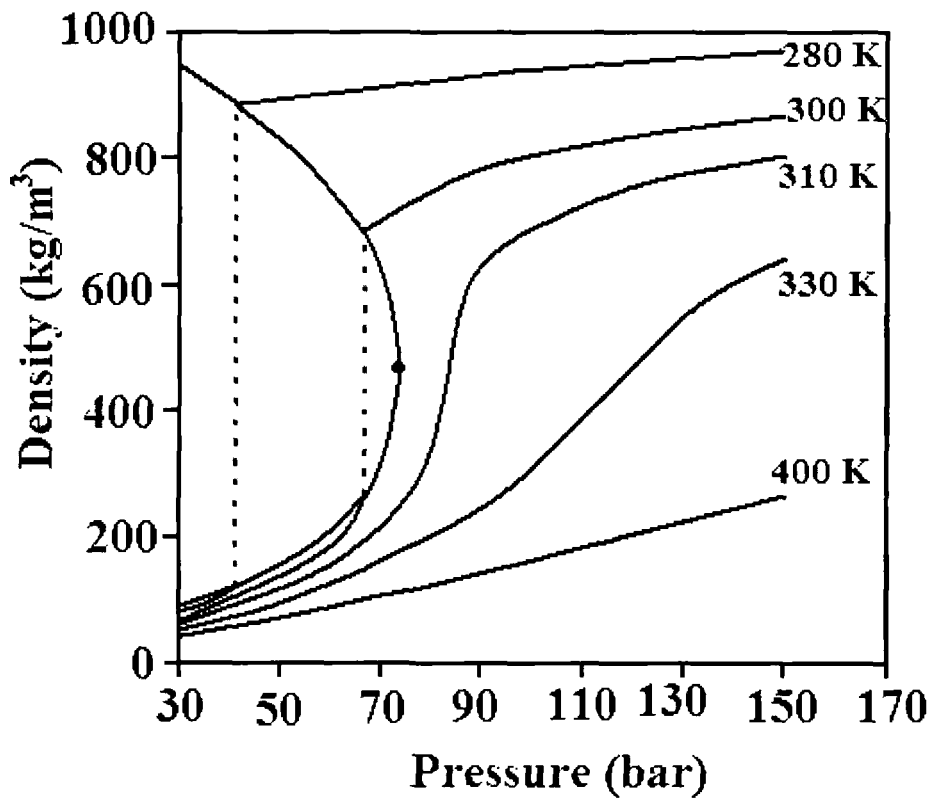
Fig.1.2: Density of CO_2 as a function of pressure at different temperatures (Solid lines) and at the vapor-liquid equilibrium line (dashed line)

The merits of supercritical carbon dioxide as an industrial solvent[22] are summarized in Table1.2.

Table.1.2: Benefits of supercritical carbon dioxide as an industrial solvent

Environmental Benefits	Health and Safety Benefits	Chemical Benefits	Process Benefits
Does not contribute to smog	Non carcinogenic	High miscibility with gases	No solvent residues
Does not damage ozone layer	Less toxic	Altered cage strength	Facile separation of products
No acute ecotoxicity	Non flammable	Variable dielectric constant	High diffusion rates
No liquid waste		High compressibility	Low viscosity
		Local density augmentation	Adjustable solvent power
		High diffusion rate	Adjustable density
			Inexpensive

1.1.3 Solubility in supercritical carbon dioxide (sc-CO_2)

In addition to gases, other reagents including low molecular weight organic compounds (e.g. cyclohexene, different monomers and caffeine) possess good miscibility or solubility in supercritical fluids (SCFs). It is important to assess the solubility and phase behavior of reactants as the reaction might be occurring as a 'solvent free' process under an atmosphere of carbon dioxide and not actually accessing the full benefits of using sc-CO_2.[23-28] The traditional method for obtaining solubility data for substances in SCFs is cloud point. Temperature and pressure are varied for a solvent–solute system and a graph is acquired that indicates when the substance falls out of solution and forms 'clouds'.

The schematic representation of the solute-solvent clustering in carbon dioxide medium is shown in Fig.1.3.[29]

(a) Low Pressure
2 phases, solvent
(gas), solute (liquid
or solid)

(b) Moderate pressure
1phase, solvent (SCF)
Clustering around solute

(c) High pressure
1 phase, solvent (liquid
or SCF) clustering around
solute
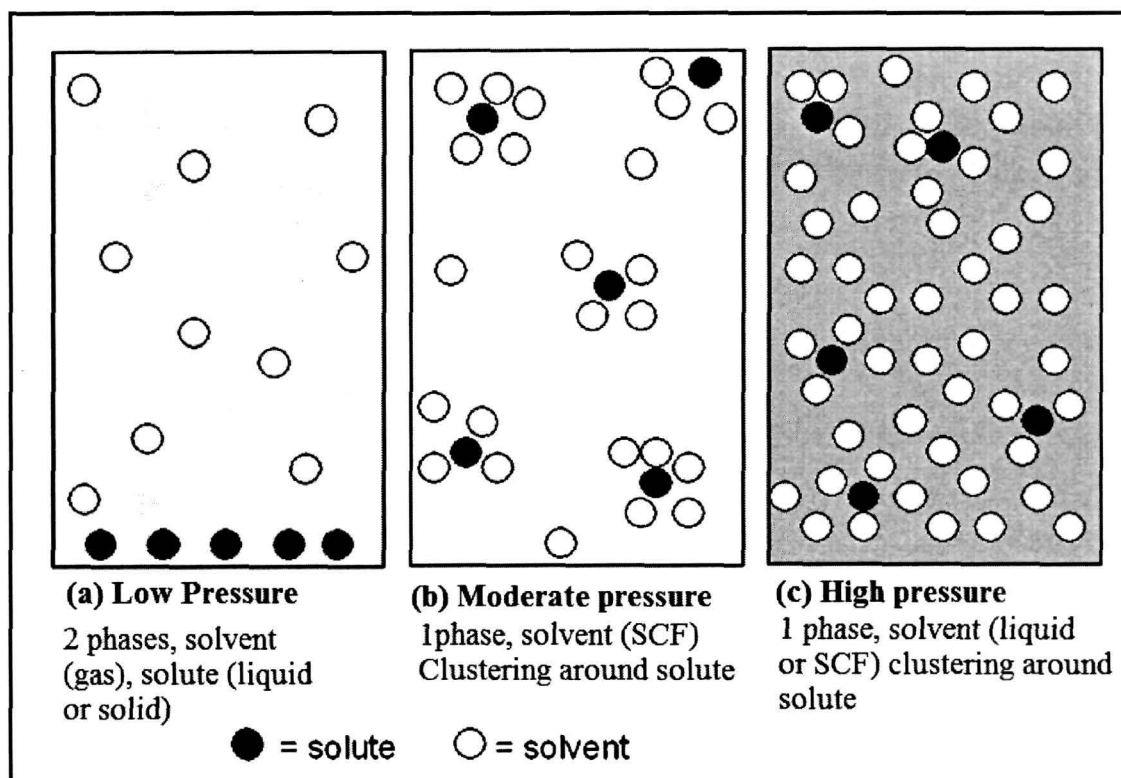
● = solute   ○ = solvent

Fig.1.3: Schematic presentation of solute-solvent clustering in CO₂ medium

Carbon dioxide, being a non-polar solvent, and it can dissolve small non-polar molecules and hydrocarbons up to 20 carbon. Organic molecules such as aldehydes, ketones, esters are also soluble in sc-CO_2. Large molecules like waxes, oil, polymer etc. cannot be dissolved in sc-CO_2 medium. That is why it is necessary to design surfactants to increase its solubility in desired purposes.

1.2   Design of surfactant for sc-CO₂ medium

Surfactants are being designed to overcome the limitations associated with the use of CO_2 as a solvent.[30] Generally, the aim is to allow solubilization or dispersion of molecules that are incompatible with sc-CO_2, e.g. water or macromolecules.[31] In the preparation of stable dispersions, surfactants are used. In all these cases, the surfactant

6

sterically stabilizes the dispersion of solid particles or water droplets in the sc-CO_2 phase. Surfactants used in CO_2 are amphiphilic molecules containing both a CO_2-phobic and a CO_2-philic portions. The CO_2-phobic portion displays poor solubility in CO_2 and therefore prefers to reside away from the continuous phase; the CO_2-philic tail has good solubility in CO_2 and extends out into the bulk solvent.[31] To achieve this, the CO_2-phobic part of the surfactant must have a high affinity for the compound being dispersed. This portion is thus hydrophilic in the case of water-in-CO_2 emulsions, or has some affinity for the polymer particles being formed in polymer synthesis. In a typical CO_2/water/surfactant mixture, water partitions into the core of the surfactant micelles leading to the formation of a microemulsion or macro-emulsion depending on the stabilizing ability of the surfactant used. Macroemulsions are composed of kinetically stable large droplets within the size of 0.1 to a few micrometers. They are normally formed in the presence of vigorous agitation and collapse in the absence of this. However, microemulsions are thermodynamically stable and optically clear as they are composed of nanodroplets (within the range 2-5 nm). As the polarizability per unit volume is relatively low for sc-CO_2 compared to organic solvents, it is difficult to overcome the strong attractive van der Waals interactions between water droplets and to obtain a stable W/C microemulsion. Therefore relatively few materials have been found as effective surfactants. The surfactants used in conventional water-in oil emulsions, for example sodium bisethylhexyl sulfosuccinate (AOT) does not work alone in CO_2 but can be used in association with other co-surfactants. Incorporation of fluorinated or silicone units in the CO_2-philic portion of a surfactant encourages good solubility in dense CO_2. Recent molecular stimulation of the surfactant $(C_7F_{15})_2CHSO_4^-Na^+$ shown that the CO_2-philic groups actually provide a protective layer around the droplets leading to weaker van der Walls interactions at the droplet interface, thus preventing the destabilization of the emulsion.

The formation of micelle in sc-CO_2 medium is shown schematically in Fig 1.4.
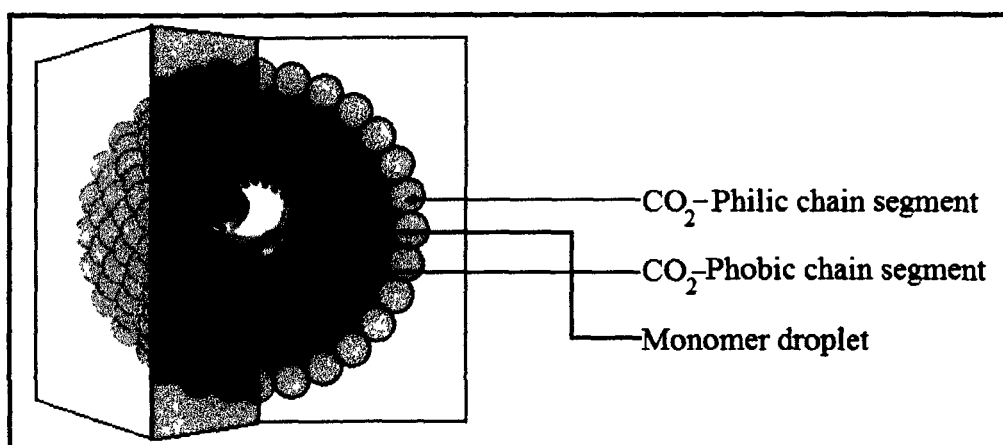
Fig.1.4: Micelle formation in supercritical carbon dioxide medium

The high cost of fluorinated stabilizers and their potential toxicity are the major barriers facing the implementation of sc-CO_2 microemulsions in industrial applications. Researchers are now focusing on the development of effective hydrocarbon based surfactants. Although AOT is ineffective as a surfactant when used alone, the addition of methylated groups at the end of the hydrocarbon tail considerably increases its solubility in sc-CO_2 allowing the formation of W/C emulsions as demonstrated by small angle neutron scattering (SANS). The ability of these methylated analogues of AOT to form stable microemulsion has been demonstrated, but stable microemulsions were not formed. This limitation comes from the inability of CO_2 to fully solvate the surfactant tails, which is required to determine inter-droplet interactions. The commercially available, nonionic surfactant Triton X100 that has a trimethyl group at one end did not show good solubility in CO_2 and demonstrated no surfactant ability. However, these molecules formed aggregates in dense CO_2 by aggregation of their ethylene oxide (EO) chains and were successfully used in reactions to extract metal ions. A new class of non-ionic amphiphiles with very short and bulky CO_2-philic trisiloxane head groups [$(CH_3)_3SiO)_2Si(CH_3)(CH_2)_3$-EOn] have been shown to be surface active at CO_2/air interfaces. They are found to stabilize concentrated and dilute emulsions of water in sc-CO_2. Similar results were obtained for a trifunctional hydrocarbon surfactant incorporating EO and propylene oxide (PO) groups. The low molecular weight (below

8

600 g mol^{-1}) of these compounds and the presence of branched methyl groups cause them to have relatively high solubility in CO_2. They are able to form W/C micro emulsions but with only a low water uptake (with water-to surfactant mole ratios, Wo~8). Further research has demonstrated that incorporation of a short highly branched hydrocarbon block leads to stable W/C micro-emulsions with nanodroplet radii in the range 1.6–3 nm. Sugar pentaacetates have also been found to have a high degree of solubility in CO_2, in part due to favourable specific polar interactions, and these are stable for the design of 'low-cost' surfactant tails.[31]

The main differences between the two surfactants are the dergree of fluorination on the side chains end group character. By end group character, we mean the availability of a hydrogen atom on this group. The effect of this hydrogen atom was also discussed by Eastoe et al.[36-38]

High molecular weight surfactants (>600 g mol^{-1}) are also referred to as polymeric surfactants and may consist of a CO_2- philic tail, which is usually fluorinated and an ionic CO_2-phobic head group. Ionic derivatives of perfluoropolyethers have been studied in detail.[32] Johnston and co-workers reported the formation of stable reverse micelles in sc-CO_2. FTIR spectroscopic measurements revealed that the chain length of PFPE surfactants used for sc-CO_2 surfactant strongly affects its ability to form W/C microemulsions. Amongst the surfactants, perfluoropolyethylyne (PFPE)[32-34] tail with an average molecular weight of 2500 g mol^{-1} led to W/C microemulsions with the highest water content. The surfactant head group was found to have a significant effect. Nonionic carboxylic acids did not form micelles in dense CO_2 but cationic species led to the formation of W/C emulsions with $W_0 \approx 28$ and droplet radii in the range 1.6–3.6 nm. Da Rocha and Johnston measured the interfacial tension at the water/CO_2 interface and determined that the surface area per molecule of surfactant was considerably larger than the surface area per molecule of surfactant at a water/oil interface. This is a result of the much smaller interfacial tension at the water/CO_2 interface as well as the increased penetration of small CO_2 molecules into the extended tails of the surfactant

molecules.[35] A thick, structured monolayer is formed around the water droplets, comparable to the assembly of analogous hydrocarbon surfactants at water/oil interfaces.

Some commonly used surfactants are polydimethylsiloxane (PDMS), poly(tetrafluoroethylene) (PTFE) and poly(ether-carbonate) copolymer (Fig. 1.5 and Fig.1.6.[29])
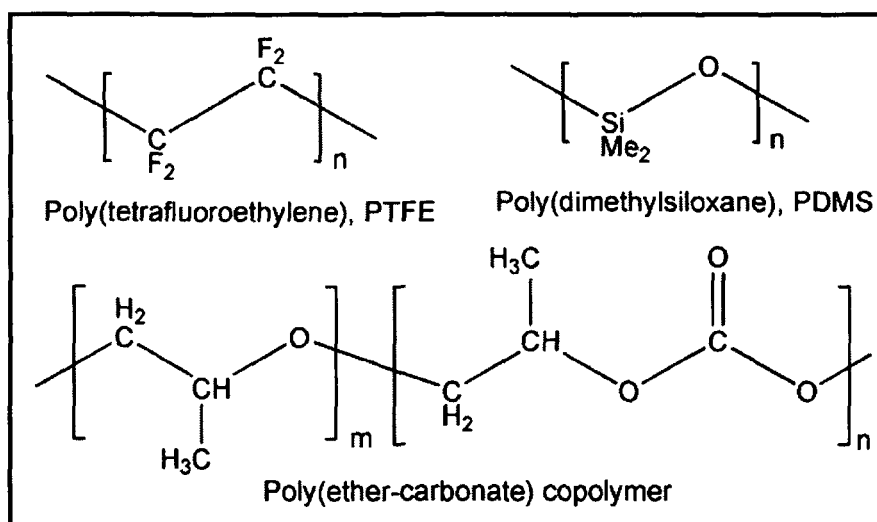
Fig.1.5: Polymeric stabilizers used in supercritical carbon dioxide
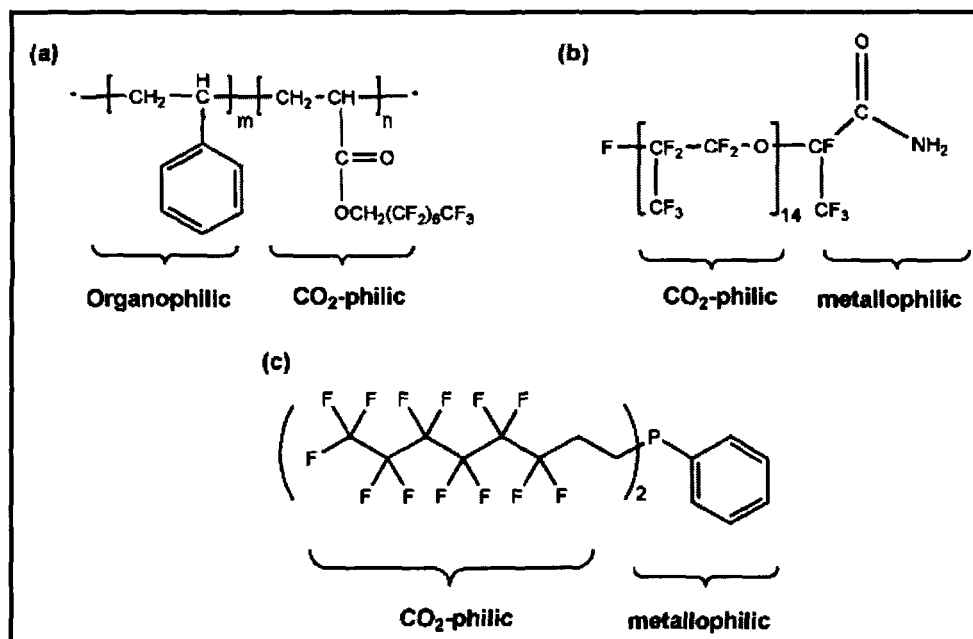
Fig.1.6: Some fluoropolymer derived materials used in sc-CO_2 technologies

(a) copolymer used as stabilizer in emulsion polymerizations of styrene; (b) end functionalized polymer used in metal extraction studies; (c) a ligand used for homogeneous catalysis in sc-CO_2.

1.3 Interactions of carbon dioxide with polymers and monomers

For application of sc-CO_2 as a medium in polymer processing, it is important to consider its interactions with polymers and monomers. In general, the thermodynamic properties of pure substances and mixtures of molecules are determined by intermolecular forces acting between the molecules or polymer segments. By examining these potentials between molecules in a mixture, insight into the solution behavior of the mixture can be obtained.[39] The most commonly occurring interactions are dispersion, dipole-dipole, dipole-quadrupole, and quadrupole-quadrupole (Fig.1.7). For small molecules, the contribution of each interaction to the intermolecular potential energy Γij (r,T) is given by the polarizability α, the dipole moment μ, the quadruple moment Q, and in some cases specific interactions such as complex formation or hydrogen bonding.[40]
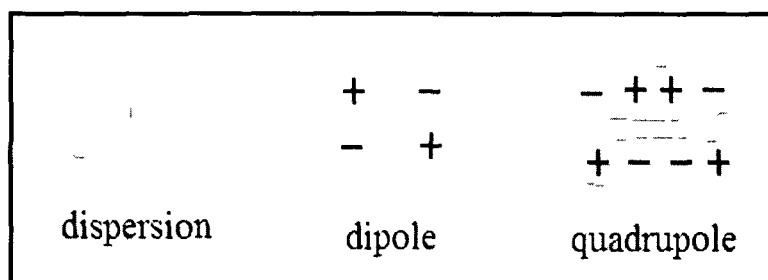
Fig.1.7: Most commonly occurring interactions

The interactions work over different distances, with the longest range for dispersion and dipole interactions. It is noteworthy that the dispersion interaction depends on the polarizability only and not on the temperature. Consequently, an increased polarizability of the supercritical solvent is expected to decrease the pressure that is needed in dissolving a nonpolar solute or polymer. At elevated temperatures, the configurational alignment of directional interactions as dipoles or quadrupoles is disrupted by the thermal energy, leading to a nonpolar behaviour. Hence, it may be possible to dissolve a nonpolar solute or a polymer in a polar supercritical fluid. However, to obtain sufficient density for dissolving the solutes at these elevated temperatures, substantially higher pressures need to be applied.[40] Additionally, specific interactions such as complex formation and hydrogen bonding can increase the solvent strength of the supercritical fluid. These interactions are also highly temperature sensitive. The solvent strength of carbon dioxide for solutes is dominated by low polarizability and a strong quadrupole moment. Consequently, supercritical carbon dioxide is difficult to compare to conventional solvents because of this ambivalent character. With its low polarizability and nonpolarity, supercritical carbon dioxide is similar to perfluoromethane, perfluoroethane, and methane. In general, supercritical carbon dioxide is a reasonable solvent for small molecules, both polar and non polar. With the exception of water, for many compounds, including most common monomers are complete miscible at elevated pressures. However, the critical point of the mixture, i.e. the lowest pressure at a given temperature where CO_2 is still completely miscible, rises sharply with increasing molecule size. Larger components and polymers exhibit

very limited solubility in carbon dioxide. Polymers which exhibit high solubility in carbon dioxide are typically characterized by a flexible backbone and high free volume (hence a low glass transition temperature T_g), weak interactions between the polymer segments, and a weakly basic interaction site such as a carbonyl group. Carbon dioxide-soluble polymers incorporating these characteristics include polyalkene oxides, perfluorinated polypropylene oxide, polymethyl acrylate, polyvinyl acetate, polyalkyl siloxanes, and polyether carbonate. Although the solubility of polymers in CO_2 is typically very low, the solubility of carbon dioxide in many polymers is substantial.[41-44] The sorption of carbon dioxide by the polymers and the resulting swelling influence their mechanical and physical properties of the polymer. The most important effect is plasticization, i.e. the reduction of the T_g of glassy polymers. The plasticization effect, characterized by increased segmental and chain mobility as well as an increase in inter-chain distance, is largely determined by polymer-solvent interactions and solvent size. The molecular weight of the polymer is of little influence on the swelling once the entanglement molecular weight has been exceeded.[44]

The interaction of CO_2 and polymers can be divided into three application areas: processing of polymers, swollen or dissolved polymers and applications where carbon dioxide does not interact with the polymer. An extensive review on polymer processing using supercritical fluids has been written by Kazarian[45], including possible applications based on the specific interaction of CO_2 and the polymer system involved.

Obviously, the sorption and swelling of polymers by CO_2 are crucial in designing polymer processing based on high-pressure technology. The important properties such as diffusivity, viscosity, glass transition, melting point, compressibility, and expansion get changed with pressure. The plasticization effect of CO_2 facilitates mass transfer properties of solutes into and out of the polymer phase, which leads to many applications: increased monomer diffusion for polymer synthesis, enhanced diffusion of small components in polymers for impregnation and extraction purposes, polymer fractionation, and polymer extrusion. Another important requirement for the

13

development of polymer processing based on sc-CO_2 is about the phase behavior of the mixture involved, which enables the process variables to be tuned properly to achieve maximum process efficiency. The phase behavior of mixture of polymers, sc-CO_2 and other ingredients are dependent on the solvent quality, the molecular weight, chain branching, and chemical architecture of the polymer as well as the effect of end groups and the addition of a co-solvent or an antisolvent.[46-50]

1.4 Apparatus for polymerization in sc-CO_2 medium

The schematic diagram of the supercritical carbon dioxide reactor is shown in Fig.1.8. The SCF reactor is connected with the high pressure CO_2 cylinder, high pressure metering pump and an efficient cooler. The pressure inside the reactor can be raised up to 6,000 psi. The pressure inside the reactor is measured with a pressure transducer. The temperature is measured digitally and maintained by an efficient thermocouple. The maximum temperature achievable in the reactor is 350°C. The reaction mixture is agitated inside the reactor with the help of a high efficient magnetically coupled mechanical stirrer the maximum achievable rotation per minute (rpm) of 3,000 rpm. The cooling of the reaction mixture can be done internally with the help of some cooling tubes inside the reactor.[61]
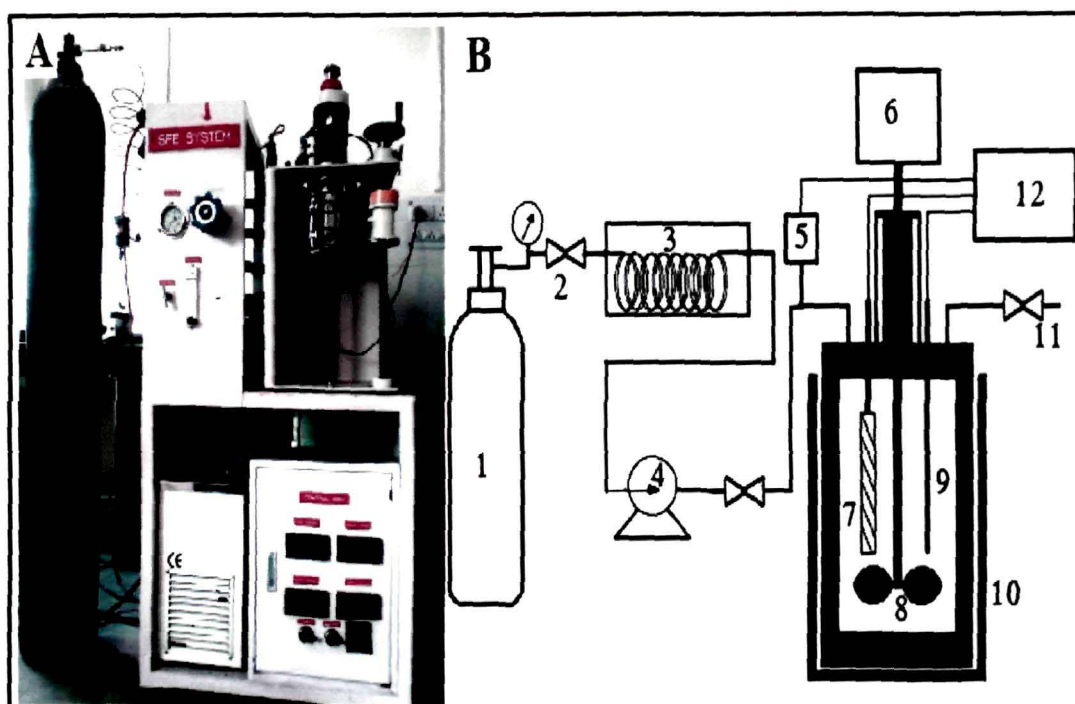
Fig.1.8: Schematic diagram of the apparatus

A. Apparatus available in our laboratory (Reaction engineering Inc., Korea), B. Flow diagram of the apparatus 1. Carbon dioxide cylinder 2. Back pressure valve 3. Refrigeration Unit 4. High pressure liquid Pump 5. Back pressure Gauge 6. Motor for mechanical stirrer 7. Cooling unit 8. Mechanical stirrer 9. Heating probe 10. SFE Vessel 11. Vent 12. Digital display unit.

1.5 Polymerizations in supercritical carbon dioxide

Polymers have become an inextricable part of our daily life. Not only the synthesis but also the processing of polymers has been given a major attention. Processed polymers are used for particular applications in particular forms such as foam, film, sheet, powder etc. For example, powder industries always seek the particles of micron or nano size with a narrow particle size distribution. Most of the commercial methods use environmentally hazardous volatile organic solvents (VOC) and chlorofluorocarbons (CFC) for processing and synthesis of polymers. Due to the enormous increment of VOC/CFC emissions and also the generation of aqueous waste streams, chemical engineers and chemists have already been looking for new and

15

cleaner alternatives. One of these methods is the use of supercritical fluids as a processing solvent.[51-54]

An intense research activity concentrated in the last decade has demonstrated that dense carbon dioxide is an attractive solvent for polymer synthesis as it is environmentally benign, inexpensive, with tunable physico-chemical properties and substantially inert towards chain transfer reactions. It can be easily separable from the product as on the release of pressure it returns to a gas thus leaving negligible solvent residues.[55] Supercritical carbon dioxide possesses many properties that have allowed it to emerge as most extensively studied supercritical fluid for polymerization reactions. Supercritical carbon dioxide is a viable and promising alternative to traditional solvent used for polymerization reactions. Supercritical carbon dioxide has the best of two words: they can have gas-like diffusivities (which have important implications for reaction kinetics) while having liquid-like densities that allow for solvation of many compounds. They exhibit changes in solvent density with small changes in temperature or pressure without altering solvent composition.[56] Because of these advantages, chemists have explored reaction mechanisms and solvent cage effects in supercritical fluids.[57-58] Changing solvent quality also has substantial effects on the molecular weight distribution and it can affect the separation of the polymer from starting materials and catalysts. In addition, the low viscosity of supercritical fluids and their ability to plasticize glassy polymers have implications on polymer processing and kinetics. The low viscosity supercritical fluid decreases solvent cage effects in free-radical initiator decompositions.[59]

When carbon dioxide is used as the supercritical solvent, additional advantages can be realized. The chemical industry has become increasingly aware of environmental concerns over the use of volatile organic solvents and chlorofluorocarbons in the manufacture and processing of commercial polymer products. The use of water alleviates these problems somewhat, but still results in large amounts of hazardous aqueous waste that require further treatment. As a result of these environmental

concerns, supercritical CO_2 represents a more environmental friendly alternative to traditional solvents. CO_2 is naturally occurring and abundant: it exists in natural reservoirs of high purity located throughout the world. In addition, it is generated in large quantities as a byproduct in ammonia, hydrogen, and ethanol plants and in thermal power generation stations that burn fossil fuels.[60]

1.5.1 Chain growth polymerization in CO_2

The major types of chain-growth polymerization routes include free-radical, cationic, anionic, and metal-catalyzed reactions. Most chain-growth polymerizations in CO_2 have focused on free-radical polymerizations. There are a number of reports in the areas of cationic and metal-catalyzed reactions.[55] We are unaware of any reports of anionic polymerizations in CO_2: reactive anions would attack the Lewis acid CO_2, and thus anionic polymerizations in CO_2 are unlikely unless extremely weak nucleophiles are involved, such as siloxanolates.

1.5.2 Free-radical polymerizations

Free-radical polymerizations can be classified as either homogeneous or heterogeneous reactions. In a homogeneous polymerization, all components, including monomer, initiator, and polymer are soluble throughout the duration of the reaction; a heterogeneous polymerization contains at least one insoluble component at some point during the reaction. Because the terminology to describe heterogeneous polymerization processes has been used inconsistently in the literature, a brief treatment of this subject is necessary to avoid confusion.[62] The four most widely studied heterogeneous processes (precipitation, suspension, dispersion, and emulsion) can be clearly distinguished on the basis of the initial state of the polymerization mixture, the kinetics of polymerization, the mechanism of particle formation, and the shape and size of the final polymer particles.[63] Other heterogeneous processes include miniemulsion polymerization and microemulsion polymerization.[64-66] In a precipitation

17

polymerization, an initially homogeneous mixture of monomer, initiator, and solvent becomes heterogeneous during the reaction as insoluble polymer chains aggregate to form a separate polymer phase. In a suspension polymerization, on the other hand, neither the monomer nor the initiator is soluble in the continuous phase. The resulting polymer is also insoluble in the continuous phase, which simply acts as a dispersant and heat-dissipation agent during the polymerization. As a result of the high solubility of many common monomers and organic initiators in compressed CO_2, suspension polymerizations in CO_2 are not common and will not be presented herein. Dispersion and emulsion polymerizations constitute the colloid forming polymerization methods that have been recently explored using CO_2. A brief discussion of the traditional definitions of these colloid forming processes follows. A dispersion polymerization begins as a homogeneous mixture because of the solubility of both the monomer and the initiator in the continuous phase. Once the growing oligomeric radicals reach a critical molecular weight, the chains are no longer soluble in the reaction medium and phase separation occurs. At this point the surface active stabilizing molecule adsorbs to or becomes chemically attached to the polymer colloid and prevents coagulation or agglomeration of the particles. In this respect, a dispersion polymerization is often considered to be a "modified precipitation polymerization".[67] Polymerization persists both in the continuous phase and in the growing polymer particles. Since the initiator and monomer are not segregated or compartmentalized, dispersion polymerizations do not follow Smith-Ewart kinetics. However, enhanced rates of polymerization are often observed due to the auto acceleration (Gel or Trommsdorf) effect within a growing polymer particle. The product from a dispersion polymerization exists as spherical polymer particles, typically ranging in size from 100 nm to 10 μm. Due to the good solubility of many small organic molecules in CO_2, dispersion polymerization constitutes the best heterogeneous method that has been developed thus far for producing high molecular weight, CO_2- insoluble, industrially important hydrocarbon polymers.[62,68]

In contrast to dispersion polymerization, the reaction mixture in an emulsion polymerization is initially heterogeneous due to the low solubility of the monomer in the continuous phase. Emulsion polymerization is a very active area of research, and several recent books and reviews have been published in this realm of research.[69-71] For a reaction to take advantage of the desirable Smith-Ewart/Harkins kinetics, the monomer and initiator must be segregated with the initiator preferentially dissolved in the continuous phase and not in the monomer phase.[72] Traditionally, emulsion polymerizations employ oil-soluble monomers such as acrylics or styrenics dispersed in an aqueous medium containing a water-soluble initiator such as sodiumpersulfate. While "inverse emulsion polymerization" employs water-soluble monomers, such as acrylamide, dispersed in an organic medium containing an oil-soluble initiator such as an organic azo or peroxide species. In either case, the insoluble polymer is stabilized as colloidal particles. The repulsive forces, which result from the surface charges imparted by an ionic initiating species, an added small molecule ionic surfactant, an added amphiphilic macromolecular stabilizer, or a combination of these to provide a charged surface, prevent the coagulation of the growing particles and lead to a stabilized colloid. As a result of the kinetics of an emulsion polymerization, high molecular weight polymer can be produced at high rates, with the rate of polymerization dependent upon the number of polymer particles. The polymer which results from an emulsion polymerization exists as spherical particles typically smaller than 1 μm in diameter. Due to the high solubility of most vinyl monomers in CO_2, emulsion polymerization in CO_2 probably will not be a very useful process for the majority of commercially important monomers, although there are exceptions. For example, inverse emulsion polymerization of acrylamide in a water/CO_2 system has been reported.[73]

1.5.3 Dispersion and emulsion polymerizations in sc-CO_2

The key to a successful dispersion or emulsion polymerization is the surfactant. Its role is to adsorb or chemically attach to the surface of the growing polymeric particles and prevent the particles from aggregating by electrostatic and steric stabilization. Consani and Smith had studied the solubility of over 130 surfactants in CO_2 at 50°C and 100-500 bar.[74] They concluded that microemulsions of commercial surfactants are formed much more readily in other low polarity supercritical fluids such as alkanes in CO_2. Since traditional surfactants for emulsion and dispersion polymerizations were designed for use in an aqueous or organic continuous phase and are completely insoluble in CO_2. An exciting area of research is the design and synthesis of novel surfactants specifically for CO_2. Polymeric surfactants for steric stabilization are effective in solvents with low dielectric constants. It is rather steric stabilization, than electrostatic stabilization which provides the stabilization mechanism of choice for CO_2-based systems. The polymeric stabilizer is a macromolecule that preferentially exists at the polymer-solvent interface and prevents aggregation of particles by coating the surface of each particle and imparting long-range repulsions between them. These long-range repulsions must be great enough to compensate for the long-range van der Waals attractions of the particles.[62] This complex phenomenon depends not only on the amount and molecular weight of adsorbed stabilizer, but also on its conformation, which is affected by the nature of the solvent. When steric stabilization acts effectively in a heterogeneous system, the stabilizing molecules attach to the surface of the polymer particles by either chemical grafting or physical adsorption. Amphiphilic materials such as block and graft copolymers posses two components. One component remains in the continuous phase and another component, the anchor, which prefers to reside in the polymer phase offering the highest probability for physical adsorption. The other route to stabilization includes the chemical grafting of the stabilizer to the particle surface, either through chain transfer to stabilizer or by using a functional stabilizer that can serve as an initiator, monomer, or terminating agent. In this case, the chemically grafted stabilizer cannot physically desorb from the

particle surface, and as a result, grafted stabilizers impart better colloidal stability than physically adsorbed stabilizers. In CO_2-based systems, the types of surfactants that have been used for steric stabilization include CO_2-philic (CO_2-soluble) homopolymers, copolymers (statistical, block, or graft) containing a CO_2-philic component and a CO_2-phobic (CO_2-insoluble) anchoring component, and CO_2-philic reactive macromonomers.

Recently, the traditional Napper theory for steric stabilization in colloidal systems has been evaluated for applicability in highly compressible supercritical media. Peck and Johnston have developed a lattice fluid self-consistent field theory to describe a surfactant chain at an interface in a compressible fluid, allowing traditional colloidal stabilization theory[75] to be extended to supercritical fluid continuous phases.[76,77] In their theory, "holes" have been introduced into the lattice to account for the decreased concentration of molecules in the less dense supercritical phase. In this way, they are able to account for the compressibility of the continuous phase. The mechanism of steric stabilization was further studied by the Johnston group experimentally by turbidity and tensionmetry measurements of emulsion stability, critical flocculation density, and reversibility of flocculation.[78] The emulsions of poly(2-ethylhexyl acrylate) (PEHA) in CO_2 in the presence of a surfactant, either poly(1,1-dihydroper-fluorooctyl acrylate) (PFOA) homopolymer, PS-b- PFOA, or PFOA-b-poly(vinyl acetate)-b-PFOA were studied in details. A distinct change in the emulsion stability was observed at the critical flocculation density (CFD), which corresponded with the θ-point (where the second virial coefficient equals zero) for PFOA in bulk CO_2. The CFD is the density at which particles flocculate due to collapse of the soluble portion of the surfactant. While PFOA resulted in bridging flocculation of PEHA particles below the CFD, PS-b-PFOA was more strongly adsorbed and flocculation below the CFD was slower. The dynamic light scattering confirmed the correlation between the CFD and the θ-point density of PFOA in CO_2 by monitoring the PEHA droplet size as a function of time and CO_2 density in the presence of surfactant. Further theoretical developments have been made by Meredith and Johnston for homopolymer stabilizers,[79] copolymers and end graft

stabilizers in a supercritical fluid.[80] The adsorption of surfactant at a planar surface and the free energies of interaction between two such surfaces were modeled. The effects of solvent density on the adsorbed amount of stabilizer and layer thickness, both of which would influence colloid stability, were examined. General design criteria were provided for copolymers and end-graft stabilizers. It is clear from these studies on steric stabilization in CO_2 that for effective stabilization, the surfactant must anchor to the particle surface and must not be in a collapsed state at the reaction density.

The majority of the work in dispersion polymerizations in supercritical CO_2 has focused on methyl methacrylate (MMA). In 1994, DeSimone reported the dispersion polymerization of MMA in supercritical CO_2.[81] Further study on MMA dispersion polymerizations with PFOA stabilization investigated the influence of helium concentration in CO_2 on the resulting PMMA particle sizes and distribution.[82,83] This study was important since many tanks of CO_2 are sold with a helium head pressure. It was found that the presence of 2.4 mol % helium in CO_2 increased the PMMA average particle diameters from 1.9 to 2.7 μm, while decreasing particle size distribution from 1.29 to 1.03. Furthermore, the small percentage of helium in the reaction mixture decreases the solvent strength of the medium, as determined by solvatochromic investigations. Scientists have noted the increase in retention times in SCF chromatography[84-86] and the reduced extraction rate in SCF extractions[87] when helium is present in the CO_2. An acoustic technique, used by Kordikowski and co-workers to measure the composition of helium in CO_2-tanks and showed the content to be unpredictable, presumably due to common lack of equilibration in the cylinder.[88] Therefore, these diverse experiments illustrate that even seemingly "benign" components such as an inert gas can affect the solvent quality of CO_2, and the CO_2 purity needs to be taken into consideration for process development and scale-up issues if the process, such as dispersion polymerization, is to be commercialized.

1.5.4   Synthesis of polymer blends

The plasticization of polymers by supercritical CO_2 has been exploited for the synthesis of polymer blends. In general, CO_2 is used to swell a CO_2-insoluble polymer substrate and to infuse a CO_2-soluble monomer and initiator into the substrate. Subsequent polymerization of the monomer generates the polymer blend. Watson and McCarthy used supercritical CO_2 to swell solid polymer substrates, including poly(chlorotrifluoroethylene), poly(4-methyl-1-pentene), high-density polyethylene (HDPE), nylon-66, poly(oxymethylene), and bisphenol-A carbonate, and to infuse styrene monomer and a free radical initiator into the swollen polymer.[89-91] The polymerization reaction was run either before decompression of the CO_2 or after decompression and recompression with N_2. Mass uptake is of up to 118% based on the original polymer were reported. As expected, diffusion rates in CO_2-swollen polymers were dramatically increased over nonswollen polymers. Using ethyl benzene as a model for styrene, the equilibrium for monomer uptake was 25 times faster with CO_2 under the conditions studied than without CO_2. X-ray analysis showed that the polystyrene existed in phase-segregated regions throughout the matrix polymer, and thermal analysis showed that radical grafting reactions were not significant. In a related study, styrene (with and without cross-linker) was infused into three fluoropolymer substrates polymerized, and subsequently sulfonated in order to provide surface modification to the polymeric substrates.[92] Polystyrene was shown to be present throughout the blends and semi-interpenetrating networks of each of the three polymer substrates, PTFE, poly(TFE-co-hexafluoropropylene), and poly-(chlorotrifluoroethylene). The modified surfaces were characterized by X-ray photoelectron spectroscopy and by water contact angle measurements. The wettability of all modified fluoropolymer substrates was increased by the surface modification. In a separate study, the morphology and mechanical performance of PS/HDPE composites were evaluated.[93] As in the previous experiments, the polymer substrate, HDPE, was swollen with CO_2 in the presence of styrene and initiator. The subsequent polymerization produced the blend, with PS located in the amorphous interlamellar regions of the polyethylene spherulite and in the

spherulite centers. The PS/HDPE blends exhibited a modulus enhancement in modulus, improvement in strength with increasing PS content, loss in fracture toughness, and increase in brittleness.

1.6 Nanoparticles in supercritical carbon dioxide

There is a great interest in the preparation and application of nanometer size materials since they can exhibit new properties of industrial interest. Which are the matter properties that can show dramatic changes at nanoscale range? Mainly the properties related to the ratio between surface and volume: at nanoscale, surface properties become relevant with respect to volume properties. For example, surface molecules can impart hardness to metals and higher energy to propellants and explosives. Electronic devices and pharmaceuticals with improved performance can also be produced by tuning surface properties.[94]

Different interpretations of the dimensions that set the boundary between normal materials and nano materials have been proposed. In this work, we assume that a nano product should have at least one dimension smaller than 200 nm; though, more restrictive definitions have been proposed that set the upper limit at 100 nm. Nanoparticles, nanofilms and nanowires are nanometric along three, two and one dimension, respectively. In the case of nanostructured materials, at least one of the components has nanometric dimensions.[94]

The various processes that have been proposed to obtain nanomaterials follow two main approaches: top down and bottom up. Top-down is characterized by the production of nanoproducts departing from normal size materials; i.e., reducing the dimensions of the original material; for example, using special size reduction techniques (Fig.1). Bottom-up approach is related to the "synthesis" of man-sized materials, starting from the molecular scale (Fig.1.9); for example, the formation of particles by precipitation from a fluid phase.

24
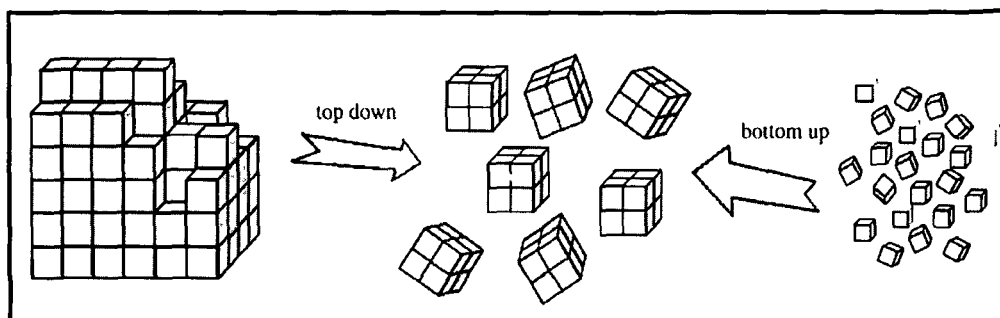
Fig.1.9: Top down and bottom up approaches

Supercritical fluids (SCFs) have also been proposed as media to produce nanomaterials. The properties that make supercritical fluids particularly attractive, as a rule, are gas-like diffusivities, the continuously tunable solvent power/selectivity and the possibility of complete elimination at the end of the process. Particularly, the mixing of gas-like and liquid-like properties can be useful in many applications related to nanotechnologies.

The most widely used supercritical fluid is carbon dioxide (CO_2), which is cheap and non polluting, and whose critical parameters are simple to be obtained in an industrial apparatus. However, ammonia, alcohols, light hydrocarbons and water have been proposed, among the others for nano materials production at supercritical conditions.

Among all the nano products, two main areas have been explored using supercritical fluids: nanoparticles and nano structured materials. Nanoparticles cover a wide range of applications. It will be possible to produce explosives with a higher potential; i.e., approaching the ideal detonation; coloring matter with brighter colors; toners with a higher resolution; polymers and biopolymers with improved functional and structural properties. Pharmaceutical products can also be designed which can enhanced pharmaceutical activity or use of different delivery routes and/or overcome human body internal barriers. Metals, metal oxides and ceramic compounds at nano dimensions can exhibit unusual strength and/or can be used as fillers in nano structured

materials. Composite nano spheres and nano capsules can be used, for example, in pharmaceutical applications for controlled and sustained release of drugs. The production of nanowires, nanofilms and nanotubes has also been considered in supercritical fluid assisted processes. Nanostructured polymers can be generated in the form of nanocellular foams and membranes. For example, nanocomposite polymers can be obtained modifying the host polymer properties using nanofillers (nanoparticles, nanoclays).[95] Several supercritical based techniques have been proposed in the literature for the production of micro and nano materials, since several processes can operate in the micronic or in the nano-metric domain depending on the operating conditions and on the process arrangement.[95-100]

1.6.1 Rapid expansion of supercritical solution (RESS)

The rapid expansion of supercritical solutions (RESS) consists of the saturation of the supercritical fluid with dispersed particles of polymer and other metal nanoparticles followed by the depressurization of the solution through a heated nozzle into a low pressure chamber produces a rapid nucleation of the substrate in the form of very small particles that are collected from the gaseous stream. The morphology of the resulting solid material depends on the chemical structure of the material and on the RESS parameters (temperature, pressure drop, impact distance of the jet against a surface, nozzle geometry, etc.).[97] The fast release of the solute in the gaseous medium should assure the production of very small particles. This process is particularly attractive due to the absence of organic solvents.

The process for RESS[101,102] was patented with respect to the possibility of producing nanoparticles and films (Smith *et al.*[103-105]). However, the scientific literature published several years later that confirmed this possibility. For example, Turk *et al.*[106] used the RESS process to produce β-sitosterol (an anticholesteremic) nanoparticles with a mean diameter of about 200 nm. They tested the process in sc-CO_2 at different pre-expansion temperatures and pressures and observed that the variation of pre-expansion

conditions does not lead to appreciable variations in nanoparticles diameters in the case of β-sitosterol. They also used this process for the production of griseofulvin (an antibiotic) nanoparticles using supercritical CHF_3.

Sane *et al.* used RESS to produce fluorinated tetraphenylporphyrin (a photosensitizer for photodynamic therapy) spherical, agglomerated nanoparticles with average particle sizes from 60 to 80 nm, at different pre-expansion temperatures.[107] Pestov *et al.* used RESS to produce nanoparticles of 2,5-distyrylpyrazine (DSP), (a polymer that can change properties upon exposure to light or chemicals, with application as optical data storage and chemical sensor).[108] The schematic diagram for RESS process is given in Fig.1.10.
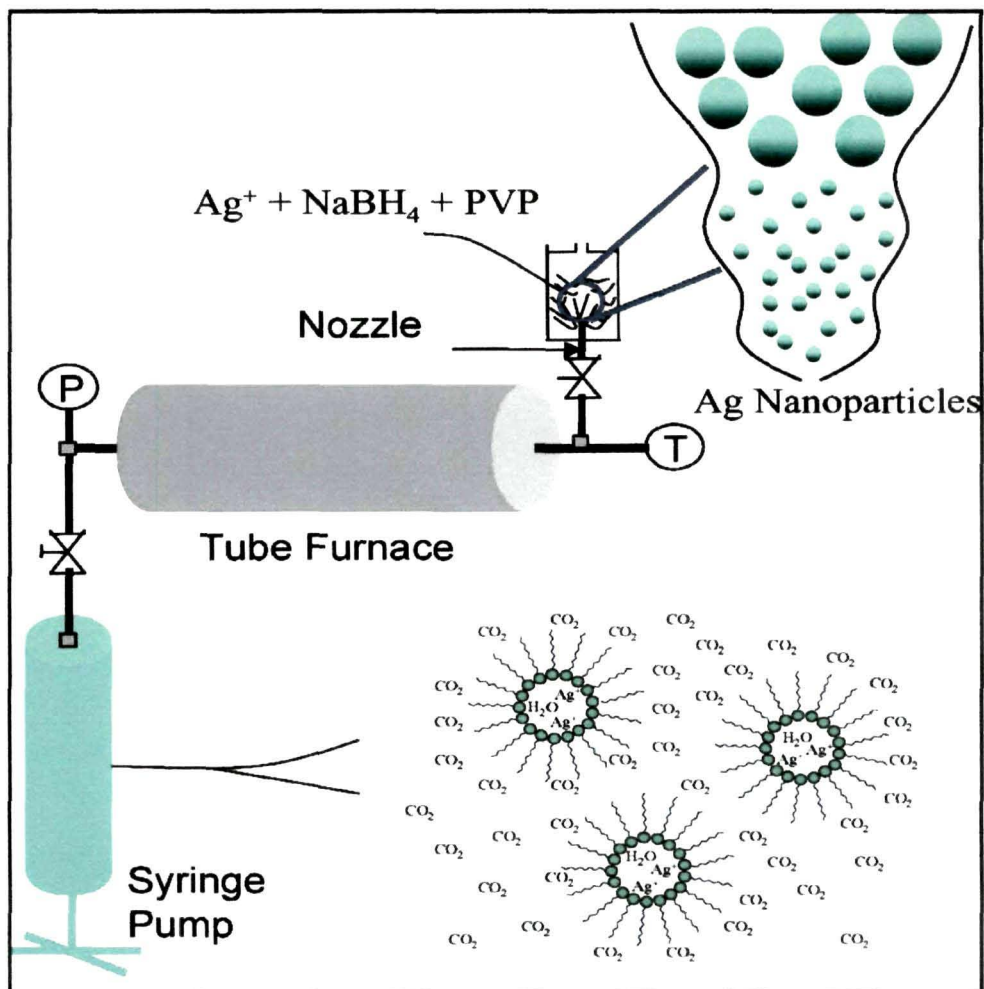
Fig.1.10: Schematic diagram for RESS process

An interesting variation of the RESS process is the rapid expansion of a supercritical solution into a liquid solvent (RESOLV) that involves spraying of supercritical solution into a liquid. It is possible to quench particles growth in the precipitator, thus improving the RESS process performance. Moreover, by interaction among the nucleating solid particles and the compounds contained in the liquid phase, a chemical reaction step can also be added. For example, Sun and Rollins proposed a RESOLV process in which the liquid receiving the spray of the supercritical solution also contains a reactant for the solute that nucleates from the expanding jet.[109] They performed the rapid expansion of $Cd(NO_3)_2$ in sc-NH_3 into a room-temperature solution of Na_2S in water or ethanol, producing cadmium sulfide (CdS) nanoparticles with an

28

average diameter of 3.3 nm. The Na_2S solution also contained poly(N-vinyl-2-pyrrolidone) (PVP) to stabilize the produced nanoparticles. Using the same process arrangement, they produced an homogeneous solution of $Pb(NO_3)_2$ in sc-NH_3, expanding in an ethanol solution of Na_2S, produced nanoparticles of PbS. PbS nanoparticles was stabilized by PVP in liquid solution. Nanoparticles with mean diameters of about 4 nm were produced.[110] The same research group used the RESOLV process to produce ibuprofen (anti-inflammatory) nanoparticles with an average diameter of 40 nm.[111] Naproxen (anti-inflammatory, analgesic, antipyretic) nanoparticles with an average size of 64 nm with a standard deviation of 10 nm were also prepared using this process. In both cases, they used high molecular weight PVP as stabilizer in the aqueous solution to reduce the agglomeration process and to control the average diameter of nanoparticles. RESOLV process was also applied for processing of polymers.[112,113] Poly(heptadecafluorodecylacrylate) (PHDFDE) that is highly soluble in sc-CO_2, but insoluble in water. Therefore, the supercritical solution (CO_2 + PHDFDE) was expanded directly into an aqueous NaCl solution. However, even the presence of NaCl could not shun agglomeration of nanoparticles. The problem was resolved by adding a surfactant (sodium dodecyl sulfate) to a basic acqueous solution.

Kropf et al.[114] patented a RESS-like process in which the supercritical solution is expanded into a gas or liquid to produce nanoparticles of size between 10 and 300 nm. Subsequently, Foerster et al.[115] and Kropf et al.[116] used this process to patent the generation of nanometric particles of chitosan and sterols.

A further modification of the RESOLV process consists of the use of a water in supercritical CO_2 (w/c) microemulsion used as a modified supercritical solvent to dissolve $AgNO_3$.[117] A w/c microemulsion containing $AgNO_3$ was rapidly expanded into a room temperature solution of sodium borohydride. Ag nanoparticles with the average particle size of 7.8 nm were finally obtained. In a subsequent work the reductive solution at the receiving end of the rapid expansion was adjusted to be highly basic.[118]

Nanocrystalline Ag particles with a bimodal distribution were obtained, with the smaller ones centered around 3.1 nm (S.D. 0.8 nm) and large ones around 10 nm (S.D. 2 nm).

The potential features of RESS are very interesting from the theoretical point of view; but, the results have not been particularly good in several cases. In many cases, it is problematic to control the particle size of the precipitates. During the expansion, the particles coalesce in the supersonic free jet generated in the precipitation vessel and, therefore, needlelike particles have been obtained. Sometimes, the formation of oriented needles can be explained by the presence of electrostatic charges on the surface of the particles, induced by the fast relative motion between the particles and the gas contained in the expansion chamber.[119]

RESOLV configuration has been demonstrated to be more effective in producing nanoparticles, since the liquid that receives the expanding jet can suppress the particle growth. The addition of a stabilizing agent in the liquid also protects particles from agglomeration. The major limitation of RESS and RESOLV processes is that they are applicable only to products that show a reasonable solubility in the selected supercritical fluid. Unfortunately, many solid compounds with high molecular weight and polar bonds, that could be candidate to nanoparticles generation, show a very low or negligible solubility in sc-CO_2. RESOLV has also the problem of the recovery of particles from the liquid as this process is no more solventless.

1.6.2 Supercritical anti-solvent precipitation (SAS)

Supercritical anti-solvent precipitation (SAS) has been proposed using various acronyms; but the process is substantially the same in all the cases. A liquid solution contains the solute to be micronized; at the process conditions, the supercritical fluid should be completely miscible with the liquid solvent; whereas, the solute should be insoluble in the SCF. Therefore, contacting the liquid solution with the SCF induces the formation of a solution, producing super saturation and precipitation of the solute. The

30

formation of the liquid mixture is very fast due to the enhanced mass transfer rates that characterize supercritical fluids and, as a result, nanoparticles could be produced. This process has been used by several authors using different process arrangements. However, the most significant differences are related to the way the process operates: in batch or semi-continuous mode. In batch operation (GAS: Gas anti-solvent) the precipitation vessel is loaded with a given quantity of the liquid solution and, then the supercritical antisolvent is added until the final pressure is obtained. In the semi-continuous operation (SAS), the liquid solution and the supercritical anti-solvent are continuously delivered to the precipitation vessel in co-current or counter-current mode.[96] An important role is also played by the liquid solution injection device.[120] The injector is designed to produce liquid jet break-up and the formation of small droplets to produce a large mass transfer surface between the liquid and the gaseous phases. Several injector configurations have been proposed in the literature and patented.[121-123] High pressure vapor-liquid equilibria (VLEs) and mass transfer between the liquid and the SCF also play a relevant role in SAS. Particularly, VLEs of the ternary system solute-solvent-SC antisolvent and the position of the operating point in SAS processing with respect to these VLEs, can be decisive for the success of the process. The formation of a single supercritical phase is the key step for the successful production of nanoparticles.[124] The washing step with pure supercritical anti-solvent at the end of the precipitation process is also fundamental to avoid the condensation of the liquid phase that otherwise rains on the precipitate modifying its characteristics.

1.6.3 Synthesis of nanoparticles by reduction in sc-CO_2

Shah et al.[125] demonstrated that it is possible to stabilize Ag nanocrystals in sc-CO_2 using appropriate surfactants (alkanethiols). The process, called by the authors arrested growth, consisting of the reduction with H_2 in a batch reactor of sc-CO_2 soluble organo-metallic precursors in the presence of a stabilizing perfluoro-octanediol ligand. The stabilizing agent binds to the surface of metal nanoparticles and arrests particle growth. The key characteristics of this process are: (a) precursors soluble in sc-CO_2 (b)

polar products not soluble in sc-CO_2. Using the same process[126], they synthesized nanocrystals of Ag, In and Pt with diameters ranging between about 2nm to 12 nm. Moreover, analyzing the arrested precipitation of Ag nanocrystals in sc-CO_2, they studied the influence of the process parameters on particles diameter and polydispersity[127], concluding that CO_2 density is the major parameter affecting particle size and distribution in this process. The crystals of about 2 nm in diameter was obtained at higher CO_2 density due to the strong barrier formed by the surfactant; whereas, at lower CO_2 densities, larger Ag crystals of about 4 nm were obtained with higher polydispersity, since particles grew to a larger size before the coverage of surfactant was sufficient to prevent their further coagulation. Precursor concentration, thiol/precursor ratio and reaction time do not appreciably affect the crystals size, though they can affect their polydispersity. Korgel et al.[128] synthesized Ag nanoparticles using arrested precipitation in sc-CO_2 by reduction of silver acetilacetonate in presence of organic ligands that acted as stabilizers of the nanoparticles. Using the same technique silicon nanocrystals ranging between 2 and 20 nm were also synthesized in sc-hexane.

Kameo et al.[129] produced Ag and Pd nanoparticles by reduction of silver acetylacetonate and palladium acetate in supercritical CO_2. The precursors and a surfactant (FOMBLIN) were loaded into small fixed volume vessel; CO_2 was added to the reactor, forming a solution. Then, dimethylamine borane in ethanol solution was injected into the solution and the reactor was stirred. Nanoparticles with mean diameters ranging between 3-12 nm and between 3-6 nm were obtained for Ag and Pd, respectively.

McLeod et al.[130] produced metallic nanoparticles of Pd and Ag, spraying a sc-CO_2 solution containing CO_2-soluble metal precursors into a second CO_2 solution containing a reducing agent and a stabilizer used to limit the growth of nanoparticles. Ag particles with a mean diameter of 3 nm and a distribution ranging between 1.5 and 9 nm were obtained.

1.6.4 Synthesis of metal nanoparticles by hydrolysis of metal salts in sc-CO_2

Ziegler et al.[131] synthesized cuprous oxide (Cu_2O) nanoparticles from copper nitrate by hydrolysis in SCW. They performed the reaction with and without ligands. Cu_2O polydisperse particles with diameters ranging from 10 to 35 nm were obtained by hydrolysis when they did not use alkanethiol ligands. In presence of ligand 1-hexanethiol was added in the reactor, Cu nanocrystals of about 7 nm in diameter were obtained. The alkanethiol ligand stabilized the synthesis of nanocrystals by the reduction of copper nitrate to Cu nanoparticles. Ligands which bind on the nanoparticles surface can block the growth of nanoparticles, with a stabilization process analogous to the arrested growth discussed in the previous section.[126] The authors also studied different precursors to obtain the particles with different morphologies.

Titanium hydroxide nanoparticles were produced by hydrolysis of titanium tetra-isopropoxide (TTIP) in sc-CO_2 using a continuous large scale plant (5 dm^3 reactor volume) operated at mild pressure conditions (80–140 bar) and in the temperature range between 40 and 60°C.[132] Two solutions of TTIP and water in sc-CO_2 were prepared by flowing sc-CO_2 in two contactors, containing TTIP and water, respectively. Then, the two supercritical solutions were injected into the reactor and $Ti(OH)_4$ was produced upon subsequent hydrolysis. $Ti(OH)_4$ spherical nanoparticles with mean diameters ranging between 70 and 110 nm were produced, with surface areas larger than 300 m^2/g. Calcination of the product to TiO_2 was also performed.

Stallings and Lamb also performed the hydrolysis of TTIP, but they injected pure TTIP into water in SC-CO_2 dispersions using a batch reactor.[133] A surfactant was also added in some experiments to stabilize the water-sc-CO_2 dispersion. Spherical particles with a broad particle size distribution ranging between 20-800 nm were obtained, independently from the use of the surfactant. According to the authors, these particles were formed by agglomerates of primary particles of about 20 nm in diameter.

1.7 Synthesis of nanocomposite materials in sc-CO_2 medium

The production of composite nanomaterials can be of interest in several applications: particularly for the controlled release of pharmaceuticals, medical devices, semiconductors and superconductors, microelectronic applications and barrier materials (gas barriers, oxygen barriers, food packaging).[134]

From a general point of view, composite nanoparticles can be classified as nanospheres, nanocapsules, nanofibers, nanotubes etc. Nanospheres are formed by the random dispersion of two or more compounds (for example, a polymer and a drug); nanocapsules, instead, are formed by a shell of one component and a core of the active compound. Nanocomposite materials in form of nanofibers, nanotubes plus fillers and nanoparticles on nanowires have also been proposed for specific applications. Conventional techniques used to produce composite nanoparticles are generally an extension of the processes used for the generation of single compound nanoparticles. The same consideration is valid for supercritical fluids based processes that are, as a rule, an extension of the techniques discussed in the previous chapters. Therefore, RESOLV, SAS, w/c microemulsions, sc-water, sc-based reactions, etc., have also been adapted to produce composite materials. RESOLV has been used by Sun et al.[135] to produce polymer protected nickel, cobalt and iron nanoparticles precipitated from SC-ethanol. These authors used the RESOLV plus chemical reaction process adding in the receiving solution PVP at concentrations large enough to cover the nanoparticles formed in the first part of the process. Using the same technique Meziani et al.[136] produced nanocrystalline Ag particles by precipitation from SC-ammonia. As covering materials they selected PVP and bovine serum albumin (BSA) that were dissolved in the receiving liquid solution that also contained the reducing agent (an aqueous solution for BSA and an ethanolic solution for PVP). Particles with average diameters in the range of 4.8-43 nm were obtained depending on the coating agent and on the composition of the receiving solution. The RESOLV plus reaction process was also used for the preparation of BSA protein-conjugated silver sulfide nanoparticles.[137] The

aim of the authors was to prepare core-shell nanocapsules in which albumin acts as the coating agent. To obtain this result they dissolved $AgNO_3$ in sc-ammonia and the supercritical solution was RESS-sprayed into an aqueous solution containing BSA. TEM analysis confirmed that particles with an average diameter of 6.3 nm (and a standard deviation of 1.6 nm) were produced. AFM images showed that well-dispersed Ag_2S nanoparticles surrounded by soft material were obtained with an overall diameter of 20-30 nm.

The production of nanocapsules formed by silica and Eudragit (a polymer) was the scope of the work proposed by Wang et al.[138] using the SAS process. A polymer solution was prepared by dissolving Eudragit in acetone. Silica nanoparticles were suspended in this solution at the desired polymer-silica ratio. The suspension was supercritical antisolvent (SAS) treated with sc-CO_2 causing heterogeneous polymer nucleation with spherical silica nanoparticles acting as nuclei for the growth of the polymer. The original diameter of silica nanoparticles was in the range of 16 to 30 nm and the obtained nanocapsules were in the range of 50 to 100 nm. However, a different morphology was obtained, due to the non uniform distribution of the polymer on the surface of the particles and to the aggregation of the composite nanoparticles in multiparticulate systems contained in a polymer matrix. When simultaneous precipitation is attempted, the loading efficiency by SAS varies in a wide range whereas the process parameters have only a minor effect on loading capacity. This is due to the fact that in this case the nanoparticles are formed by co-precipitation of the compounds from their solutions. Therefore, they are substantially solvent induced physical blending processes and largely depend on the similarity of compounds involved.[139] These conditions are particularly difficult to be obtained: therefore, SAS co-precipitation is rarely successful.

Sue et al.[140] precipitated Ni nanoparticles on Fe_3O_4 nuclei in a continuous reactor. The composite particles were formed in two steps: formation of Fe_3O_4 nuclei by HTS and, then, Ni precipitation on the surface of nuclei by H_2 reduction of a precursor

in an aqueous solution. In the synthesis of Fe_3O_4 composite particles the crystallite size increased with temperature, when Ni nanoparticles were formed on the surface of Fe_3O_4. According to the authors, this result indicates that Ni coating was fast and probably inhibited further Fe_3O_4 particle growth. They obtained particles as small as 59 nm with a standard deviation of 19 nm.

The use of sc-H_2O to produce composite nanoparticles has also been proposed using two SCW reactors operated in series.[141] In the first one ZnO nanoparticles were produced, then ZnO nanoparticles were immediately sent to the second reactor where TiO_2 was produced obtaining the composite nanoparticles. The composite particles are not in the core-shell form and the two metals are not mixed: the composite particle is formed by the random coalescence of nanoparticles of the two oxides.

Composite nanoparticles have also been produced by a variation of the w/o reverse micelles process. In a first work Han and coworkers[142] proposed the mixing of two micellar solutions containing precursor compounds forming ZnS/CdS composite nanoparticles in the reverse micelles due to the exchange of contents. Supercritical CO_2 was used as solvent-catcher to eliminate the liquid solvent and the surfactant. The same research group reported preparation of Ag nanoparticles in a w/o reverse micelle and added PS in the liquid solution.[143] Then, sc-CO_2 was added as solvent-catcher to eliminate the liquid solvent (cyclohexane) and the surfactant and to induce the precipitation of the polymer on the Ag nanoparticles trapped or wrapped in the polymer. The reduction of the size of the composite nanoparticles with increasing pressure and temperature was explained by the reduction of the physical coalescence of the nanoparticles. The same process was also used to produce CdS/PMMA and PVP-Prussian blue (PB) composite nanoparticles.[144, 145]

1.8 Porous materials synthesis using sc-CO_2 medium

Microporous particles are of particular interest because they possess characteristics such as high surface-to-volume ratio, low density, and low coefficients of thermal expansion.[145-150] These characteristics facilitate the manipulation of the surface properties of the interior or the exterior of the microspheres. Microporous polymeric particles with high and uniform pore interiors and high surface area play an important role in microencapsulation and have been used in both drug delivery and biomedical imaging.[151,152] Microporous polymers are important in a wide range of applications such as ion-exchange resins, chromatographic separation media, solid-supported reagents, and supports for combinatorial synthesis. They are commonly prepared by dispersion polymerization, emulsion polymerization, phase separation, suspension polymerization etc. by adding some suitable porogens. These porogens are mainly some organic solvents which are completely miscible with the monomers and are "good" solvent for the growing polymer networks. But the complete removal of the solvent and porogenic material from the polymer particles is not possible. That is why these microporous polymer particles are not advisable for particular applications like drug delivery, temporary artificial matrix for cell seeding, chromatographic separation media, ion exchange resin etc., which demand high purity of the product.[153] But by using sc-CO_2 as pressure adjustable porogen, we can overcome these problems and can obtain highly pure porous polymeric particles. Again in this case, one can have very fine control over the pore size and the diameter of the microparticles which is not possible in conventional porogenic solvents.

There are several specific reasons to consider supercritical carbon dioxide as alternative solvents for the synthesis and processing of porous materials: [154]

1. The production of porous materials is often solvent intensive, so that more sustainable alternatives could offer significant environmental benefits.

2. Drying steps can be energy intensive. With the exception of water, most SCF solvents studied so far are gases under ambient conditions.

3. Collapsing of pores may occur in certain materials (e.g. aerogels) when removing conventional liquid solvents. This can be avoided by the use of SCF solvents, which do not give rise to a liquid–vapour interface.

4. Porous structures are important in biomedical applications (e.g. tissue engineering), where there are strict limits on the amounts of residual organic solvent that may remain in the materials. This provides a strong driving force to seek non-toxic solvent alternatives.

5. Surface modification of porous materials frequently requires the use of solvents that will wet the pore structure efficiently. Supercritical fluids (and certain liquefied gases, such as CO_2) are extremely versatile wetting agents because of their low surface tensions (e.g. liquid CO_2 will wet teflon).

6. Surface modification or templating of nanoporous materials presents special problems because organic solvents are often too viscous to fill such small pores. Even gaseous species (when below the critical.temperature) can condense within small pores, thus forming a relatively viscous liquid "plug" that blocks the pore, preventing further penetration. SCF solvents have much lower viscosities than organic liquids and cannot condense into the liquid state. Moreover, mass transfer rates in SCF solvents tend to be high because of low solvent viscosity.

7. As a result of their compressed state, SCF solvents are highly suited to the generation of polymer foams. Moreover, polymer foaming requires that the material is either melted or highly plasticized, and many SCF solvents are excellent plasticizing agents (while being non-solvents) for a wide range of polymers.

In many applications, more than one of these considerations is important. Therefore, the synthesis and processing of porous materials is a particularly fertile area for research in SCF.

Cooper *et al.* in 2001 first reported the synthesis of microporous polymeric beads by using sc-CO_2 as the porogens.[155] They showed that these reaction conditions could be modified to generate well-defined microporous polymer monoliths, thereby using sc-CO_2 as a porogenic solvent. They used [trimethylolpropane trimethacrylate (TRIM)] monomer for synthesizing the microporous polymer beads. In earlier all works sc-CO_2 was used as the polymerizing medium and the resulting polymer particles are all nonporous in nature. The solvent properties of supercritical carbon dioxide can be tuned in such a way that it can be used for the synthesis of microporous polymer beads and the porosity in the beads can be controlled by varying the CO_2 pressure.[156]

1.9 Objectives of this research

Supercritical carbon dioxide is an attractive substitute for organic non polar solvents for a variety of chemical reactions. Supercritical carbon dioxide (sc-CO_2) has attracted extensive interest as a polymerization and processing medium, primarily driven by the need to replace conventional solvents with more environmentally benign and economically viable systems. It has many advantages over conventional organic solvents because of its non toxic, non flammable, inexpensive, high diffusivity and compressibility nature. Moreover the product can easily be separated out from solvent gas by depressurizing the gases. Many reagents/ chemicals are not soluble in CO_2. However it can easily be emulsified in sc-CO_2 by selecting proper fluorinated or siloxane based surfactants/stabilizers. There are many supercritical fluids like supercritical SO_2 (sc-SO_2), supercritical CO_2 (sc-CO_2), supercritical water (sc-H_2O), supercritical methanol (sc-CH_3OH), supercritical ethanol (sc-EtOH) etc. Out of all these, sc-CO_2 is more commonly used because it has an easy accessible critical point with $T_c=31°C$ and $P_c=73.8bar$.

Supercritical carbon dioxide (sc-CO_2) can be used as a green synthesis medium for the synthesis of different polymers. Using sc-CO_2 medium, one can achieve directly free flowing powdered polymer particles in a single step reaction. Heterogeneous polymerizations involve at least two phases during polymerizations. The polymers are insoluble in the continuous phase and may be dispersed by addition of stabilizers as CO_2 is a poor solvent for most oligomers.

Polymers that are produced by dispersion polymerization are used extensively in the surface coatings industry. For many applications, the polymers are prepared directly as stable latexes in a solvent that is suitable for application of the coatings. Alternatively, the dry, isolated latex particles can also be redispersed in a suitable solvent prior to application. Dry, redispersible coatings are appealing since it is much less expensive to transport dry powders than it is to transport solvent-borne latexes.

Polymer/metal nanocomposites synthesis is an ongoing challenge in materials research. A number of techniques are being used currently, but till now no general, effective and green preparative method is available. Synthesis of nanoparticles has been investigated widely because of their effective application in catalysis and antimicrobial activity. The antimicrobial potential of nanoparticles (Ag, Cu etc.) is a subject of great interest to chemists, biologists in the recent years. Numerous methods for the preparation of metallic nanoparticles have been reported. Supercritical carbon dioxide can also be used as a medium for synthesizing metal nanoparticles and their nanocomposites in a greener way.

1.9.1 Objective of the present investigation

Keeping in view the above aspects, the following objectives have been set

1. Synthesis of polymer microparticles by emulsion polymerization using siloxane and fluorine based stabilizers in supercritical carbon dioxide (sc-CO_2) medium and optimization of the reaction parameters.

2. Synthesis and characterization of different metal nanoparticles (Ag & Cu) and their nanocomposites using water in supercritical carbon dioxide (sc-CO_2) medium with special reference to their antibacterial activity.

3. Synthesis of polystyrene/clay nanocomposites by emulsion polymerization have been carried out in aqueous and in supercritical carbon dioxide and compare their physical and mechanical properties.

4. Synthesis of macroporous polystyrene particles by suspension polymerization in supercritical carbon dioxide (sc-CO_2) medium.

5. Characterization of nanocomposites by UV- visible spectroscopy, XRD, SEM, TEM, GPC, TGA, BET, DSC analysis, mechanical properties by UTM etc.

REFERENCES

1. Hamley, P.A.; Field, C.N.; Han, B.; Poliakoff, M. In Proc. 5th Meeting on Supercritical Fluids; Nice, France **T2**, 895 (1998).

2. Sloan, R.; Hollowood, M.E.; Humphreys, G.O.; Ashraf, W.; York, P. Supercritical fluid processing: preparation of stable protein particles. In: Perrut M, Subra P, eds. Proceedings of the 5th meeting of supercritical fluids, Nice, France, **1**, 1301–306 (1998).

3. Perrut, M. Supercritical fluid application: industrial developments and economical issues, Proceedings of 5th Italian conference on supercritical fluids and their applications. Garda (Verona), Italy, 13-16 June, 1-8 (1999).

4. C. Cagniard de la Tour, Exposure of some results obtained by the action combination of the heat and compression on some liquids, such as water, alcohol, ether petroleum ether, *Ann. Chem. Phys.* **21**, 127-132 (1822)

5. Canelas, D.A.; DeSimone, J.M. Polymerizations in liquid and supercritical carbon dioxide, *Adv. Polym. Sci.* **133**, 103-140 (1997).

6. Kendall, J.L.; Canelas, D.A.; Young, J.L.; DeSimone, J.M. Polymerizations in supercritical carbon dioxide, *Chem. Rev.* **99**, 543 (1999).

7. Sajfrtov, M.; Lickov, I.; Wimmerov, M.; Sovov, H.; Wimmer, Z. β-Sitosterol: Supercritical Carbon Dioxide Extraction from Sea Buckthorn (Hippophae rhamnoides L.) Seeds, *Int. J. Mol. Sci.* **11(4)**, 1842-1850 (2010).

8. Leitner, W. *In Modern Solvents in Organic Chemistry* (Springer-Verlag, Berlin 107–132, 1999).

9. Cooper, A. I.; Synthesis and processing of polymers using supercritical carbon dioxide, *J. Mater. Chem.* **10**, 207–234 (2000).

10. DeSimone, J.M.; Tumas, W.; Young, J.L.; Anastas, P.A. *Green Chemistry Using Liquid and Supercritical Carbon Dioxide* (Oxford University Press, Oxford, 2000).

11. Aymonier, C.; Serani, A.L.; Reveron, H.; Garrabos, Y.; Cansell, F. Review of supercritical fluids in inorganic materials sciences, *J. Supercrit. Fluid.* **38**, 242-251 (2006).

12. Leitner, W.; Jessop, P.G. *Chemical synthesis using supercritical fluids* (Wiley-VCH, Weinheim 1999).

13. Cooper, A.I. Polymer synthesis and processing using supercritical carbon dioxide, *J. Mater. Chem.* **10 (2)**, 207–234 (2000).

14. Kendall, J.L. et al., Polymerizations in supercritical carbon dioxide, *Chem. Rev.* **99(2)**, 543–563 (1999).

15. Tomasko, D.L. et al., A review of CO_2 applications in the processing of polymers, *Ind. Eng. Chem. Res.* **42(25)**, 6431–6456 (2003).

16. Woods, H.M. et al., Materials processing in supercritical carbon dioxide: surfactants, polymers and biomaterials, *J. Mater. Chem.* **14(11)**, 1663–1678 (2004).

17. Yeo, S.D.; Kiran, E. Formation of polymer particles with supercritical fluids: a review, *J. Supercrit. Fluid.* **34(3)**, 287–308 (2005).

18. Beckman, E.J. A challenge for green chemistry: designing molecules that readily dissolve in carbon dioxide, *Chem. Commun.* **17**, 1885–1888 (2004).

19. Zagrobelny, J.; Betts, T.A.; Bright, F.V. Steady-state and time-resolved fluorescence investigations of pyrene excimer formation in supercritical CO_2, *J. Am. Chem. Soc.* **114**, 5249-5257 (1992).

20. Angus, S.; Armstrong, B.; de Reuck, K.M. *International thermodynamic tables of the fluid state. Carbon dioxide* (Pergamon Press, Oxford, 1976).

21. Span, R.; Wagner, W. A new equation of state for carbon dioxide covering the fluid region from the triple point temperature to 1000 K at Pressures up to 800 MPa, *J. Phys. Chem.* **25/6**, 1509-1596 (1996).

22. Menceloglu, Y. *Processing in supercritical carbon dioxide. Report presentation*, (Tuzla: Sabanci University, 2002).

23. Pantoula, M.; Panayiotou, C. Sorption and swelling in glassy polymer/carbon dioxide systems Part I. Sorption, *J. Supercrit. Fluid.* **37(2)**, 254–262 (2006).

24. Rajendran, A. *et al.*, Simultaneous measurement of swelling and sorption in a supercritical CO_2-poly(methyl methacrylate) system, *Ind. Eng. Chem. Res.* **44**, 82549–2560 (2005).

25. Shieh, Y.T.; Liu, K.H. Solubility of CO_2 in glassy PMMA and PS over a wide pressure range: the effect of carbonyl groups, *J. Pol. Res.-Taiwan.* **9(2)**, 107–113 (2002).

26. Duarte, A.R.C. *et al.*, A comparison between gravimetric and in situ spectroscopic methods to measure the sorption of CO_2 in a biocompatible polymer, *J. Supercrit. Fluid.* **36(2)**, 160–165 (2005).

27. Kazarian, S.G. *et al.*, Specific intermolecular interaction of carbon dioxide with polymers, *J. Am. Chem. Soc.* **118(7)**, 1729–1736 (1996).

28. Nalawade, S.P. *et al.*, The FT-IR studies of the interactions of CO_2 and polymers having different chain groups, *J. Supercrit. Fluid.* **36 (3)**, 236–244 (2006).

29. Kerton, F.M. *Alternative solvents for green chemistry*, (RSC Green Chemistry book series Royal Society of Chemistry, Chapter 4, 2009).

30. Zhang, D.; Cui, L.; Wei, X.; Zhang, S. Preparation of polymer microspheres in supercritical carbon dioxide and their evaluation as cold-flow improvers in diesel, *J. Appl. Polym. Sci.* **117**, 2749–2753 (2010).

31. Harrison K.; Goveas J.; Johnston, K. P. Water-in-carbondioxide Microemulsions With Fluorocarbon-Hydrocarbon Hybrid Surfactant, *Langmuir* **10**, 3536–3541 (1994).

32. Clarke, M.J.; Harrison, K.L.; Johnson, K.P.; Howdle, S.M. Water in Supercritical Carbon Dioxide Microemulsions: Spectroscopic Investigation of a New Environment For Aqueous Inorganic Chemistry, *J. Am. Chem. Soc.* **119**, 6399–6406 (1997).

33. Fremgen, D.E.; Gerald, R.E.; Smotkin, E.S.; Klingler, R.J. Rathke, J.W. Microemulsions of water in supercritical carbon dioxide: An in-situ NMR investigation of micelle formation and structure, *J. Supercrit. Fluid.* **19**, 287–298 (2001).

34. Lee, C.T.; Bhargava, P.; Johnston, K.P. Percolation in Concentrated Water-in-Carbon Dioxide Microemulsions, *J. Phys. Chem.* **104**, 4448-4456 (2000).

35. Eastoe, Julian, Alison, P.; Downer, A. Effects of fluorocarbon surfactant chain structure on stability of water-in carbon dioxide microemulsions: Links between aqueous surface tension and microemulsion stability, *Langmur.* **18**, 3014-3017 (2002).

36. Eastoe, J.; Audrey, D.; Steytler D.C. Fluorinated surfactants in supercritical CO_2, *Curr. Opin. Colloid In.* **8**, 267-273 (2003).

37. Bruice,; Yurkanis, P. *Conformations of Alkenes, In Organic Chemistry,* (Ed. Paula Yurkanis Bruice, Englewood Cliffs: Prentice-Hall 2nd ed: 89-93 1998).

38. Sheppard,; Sheppard,C.; McClay, R.E. United States Patent 19- 4101522.

39. Kemmere, M. *Supercritical carbon dioxide for sustainable polymer processes, Supercritical carbon dioxide: In polymer Reaction Engineering* (Wiley-VCH Verlag GmbH & Co, Chapter 1, 2005).

40. Prausnitz, J.M.; Lichtenthaler, R.N.; de Azevedo, E.G. *Molecular thermodynamics of fluid phase equilibria,* (prentice-hall, Englewood Cliffs, 2nd edn. 1986).

41. Rindfleisch, F.; DiNoia, T.P.; McHugh, M.A. Solubility of polymers and copolymers in supercritical CO_2, *J. Phys. Chem.* **100**, 15581-15587 (1996).

42. Sarbu, T.; Styranec, T;. Beckman, E.J. Correlations for direct calculation of vapor pressures from cubic equations of state, *Ind. Eng. Chem. Res.* **39**, 1673-1678 (2000).

43. Sarbu, T.; Styranec, T.; Beckman, E.J. Non-fluorous polymers with very high solubility in supercritical CO_2 down to low pressures, *Nature.* **405**, 165-168 (2000).

44. Kazarian, S.G.; Vincent, M.F.; Bright, F.V.; Liotta, C.L.; Eckert, C.A. Specific intermolecular interaction of carbon dioxide with polymers, *J. Am. Chem. Soc.* **118**, 1729-1736 (1996).

45. Kazarian, S.G. Polymer processing with supercritical fuids, *Polym. Sci., Ser. C.* **42(1)**, 78-101 (2000).

46. Yuvaraj, H. *et al*. Dispersion polymerization of styrene in supercritical CO_2 in the presence of non-fluorous random copolymeric stabilizers, *J. of Supercrit. Fluid.* **42**, 351–358 (2007).

47. Shaffer, K.A.; DeSimone, J.M. Chain polymerizations in inert near- and supercritical fluids trends. *Polym. Sci.* **3(5)**, 146-153 (1995).

48. Kendall, J.L.; Canelas, D.A.; Young, J.L.; DeSimone, J.M. Polymerizations in supercritical carbon dioxide, *Chem. Rev.* **99(2)**, 553-543 (1999).

49. Cooper, A.I. Polymer synthesis and processing using supercritical carbon dioxide *Mater. Chem.* **10**, 207-234 (2000).

50. Kemmere, M.F. *Recent developments in polymer processes, Handbook for polymer reaction engineering*, (Wiley-VCH, Weinheim, 2005).

51. Cooper, A.I. Synthesis and processing of polymers using supercritical carbon dioxide, *J. Mater. Chem.* **10**, 207-234 (2000).

52. Tomasko, D.L. *et al*. A review of CO_2 applications in the processing of polymers, *Ind. Eng. Chem. Res.* **42**, 6431-6456 (2003).

53. Kendall, J.L.; Canelas, D.A.; Young, J.L.; DeSimone, J.M. Polymerizations in supercritical carbon dioxide, *Chem. Rev.* **99**, 543-564 (1999).

54. Mchugh, M.A.; Krukonis, V.J. *Supercritical fluid extraction*, (Boston: Butterworth- Heinemann, 1994).

55. Zagrobelny, J.; Bright, F.V. Probing solute-entrainer interactions in matrix-modified supercritical CO_2, *J. Am. Chem. Soc.* **115**, 701-707 (1993).

56. McHugh, M.A.; Krukonis, V.J. *Supercritical fluid extraction: Principles and practice*,(2nd ed. Butterworth-Heineman, Stoneham, 1993).

57. Jessop, P.G.; Ikariya, T.; Noyori, R. Selectivity for hydrogenation or hydroformylation of olefins by hydridopentacarbonyl-manganese(I) in supercritical carbon dioxide, *Organometallics* **14**, 1510-1513 (1995).

58. Kaupp, G. Reactions in supercritical carbon dioxide, *Angew. Chem. Int. Ed. Engl.* **33**, 1452-1455 (1994).

59. DeSimone, J.M.; Guan, Z.; Elsbernd, C.S. Synthesis of fluoropolymers in supercritical carbon dioxide, *Science* **257**, 945-947 (1992).

60. Barer, S.J.; Stern, K.M. *Catalytic activation of carbon dioxide*, (American Chemical Society, Washington DC, 1988).

61. Munson, C.A.; Page, P.M.; Bright, F.V. Effects of fluid density on a poly(dimethylsiloxane)-based junction in pure and methanol-modified carbon dioxide, *Macromolecules* **38**, 1341-1348 (2005).

62. Barrett, K.E.J. *Dispersion Polymerization in Organic Media*, (John Wiley and Sons, New York, 1975).

63. Arshady, R. Suspension, emulsion, and dispersion polymerization: A methodological survey, *Colloid Polym. Sci.* **270**, 717-732 (1992).

64. Miller, C.M.; Blythe, P.J.; Sudol, E.D.; Silebi, C.A.; El-Aasser, M.S. Effect of the presence of polymer in miniemulsion droplets on the kinetics of polymerization, *J. Polym. Sci.: Part A: Polym. Chem.* **32**, 2365-2376 (1994).

65. El-Aasser, M.S.; Miller, C.M. *Polymeric dispersions: principles and applications*, (Kluwer academic press. Boston, **335**, 109-126, 1997).

66. Candau, F. *Polymeric dispersions: principles and applications*, (Academic Press. Boston, **335**, 127, 1997).

67. Bright, F.V. *et al.* The photophysics of 6-(1-Pyrenyl)hexyl-11(1-pyrenyl)undecanoate dissolved in neat liquids and supercritical carbon dioxide: impact on olefin metathesis, *J. Phys. Chem. B* **106**, 1820-1832 (2002).

68. Sudol, E.D. *Polymeric dispersions: principles and applications*, (Kluwer academic Press, Boston, **335**, 141-153, 1997).

69. Gilbert, R.G. *Emulsion polymerization: A mechanistic approach*, (Academic Press, London, 1995).

70. Dardin, A.; Cain, J.B.; DeSimone, J.M.; Johnson, J.C.S.; Samulski, E.T. High-pressure NMR of polymers dissolved in supercritical carbon dioxide, *Macromolecules* **30**, 3593-3599 (1997).

71. Kane, M.A.; Pandey, S.; Baker, G.A.; Perez, S.A.; Bukowski, E.J.; Hoth, D.C.; Bright, F.V. Effects of density on the intramolecular hydrogen bonding, tail-tail cyclization, and mean-free tail-to-tail distances of pyrene end-labeled poly(dimethylsiloxane) oligomers dissolved in supercritical CO_2, *Macromolecules* **34,** 6831-6838 (2001).

72. Desislava, E.G. *et al.* Particle formation in ab-initio RAFT mediated emulsion polymerization systems, *Macromolecules* **40,** 6181-6189 (2007).

73. Adamsky, F. A.; Beckman, E.J. Inverse emulsion polymerization of acrylamide in supercritical carbon dioxide, *Macromolecules* **27,** 312-314 (1994).

74. Consani, K.A.; Smith, R.D. Observations on the solubility of surfactants and related molecules in carbon dioxide at 50°C, *J. Supercrit. Fluids.* **3,** 51-65 (1990).

75. Napper, D. H. *Polymeric stabilization of colloidal dispersions*, (Academic press, New York, 1983).

76. Peck, D.G.; Johnston, K.P. Prediction of interfacial properties of microemulsions: the lattice fluid self-consistent field theory, *J. Phys. Chem.* **97,** 5661- 5667 (1993).

77. Peck, D. G.; Johnston, K. P. Lattice fluid self-consistent field theory of surfaces with anchored chains, *Macromolecules* **26,** 1537- 1545 (1993).

78. O'Neill, M.L.*et al.* Emulsion stabilization and flocculation in CO_2: 1. Turbidimetry and tensiometry, *Macromolecules* **30,** 5050-5059 (1997).

79. Meredith, J.C.; Johnston, K.P. Theory of polymer adsorption and colloid stabilization in supercritical fluids. 1. Homopolymer stabilizers, *Macromolecules* **31,** 5507- 5517 (1998).

80. Meredith, J.C.; Johnston, K.P. Theory of polymer adsorption and colloid stabilization in supercritical fluids. 2. Copolymer and end-grafted stabilizers, *Macromolecules* **31,** 5518-5528 (1998).

81. DeSimone, J.M. *et al.* Dispersion polymerizations in supercritical carbon dioxide. *Science* **265,** 356-359 (1994).

82. Hsiao, Y.L.; DeSimone, J.M. Dispersion polymerizations of methyl methacrylate in supercritical carbon dioxide: The influence of helium concentration on particle size and particle size distribution, *J. Polym. Sci.* 2009-2013 (1997).

83. Hsiao, Y.L.; Maury, E.E.; DeSimone, J.M. Dispersion polymerization of methyl methacrylate stabilized with poly(1,1-dihydroperfluorooctyl acrylate) in supercritical carbon dioxide, *Macromolecules* **28**, 8159-8166 (1995).

84. Gorner, T.; Dellacherif, J.; Perut, M. Comparison of helium head pressure carbon dioxide and pure carbon dioxide as mobile phases in supercritical fluid chromatography, *J. Chromatogr.* **514**, 309-316 (1990).

85. Rosselli, A.C.; Boyer, D.S.; Houck, R.K. Reproducibility of packed-column supercritical-fluid chromatography with helium head-pressure carbon dioxide, *J. Chromatogr.* **465**, 11-15 (1989).

86. Leichter, E.; Strode, J.T.B.; Taylor, L.T.; Schweighardt, F.K. Effect of helium headspace carbon dioxide cylinders on packed column supercritical fluid chromatography, *Anal. Chem.* **68**, 894-898 (1996).

87. Raynie, D.E; Delaney, T. Effect of entrained helium on the kinetics of supercritical fluid extraction with carbon dioxide, *J. Chromatogr. Sci.* **32**, 298-300 (1994).

88. Kordikowski, A.; Robertson, D.G.; Poliakoff, M. Acoustic determination of the helium content of CO_2 from helium head pressure cylinders and FT-IR studies of the density of the resulting supercritical CO_2: Implications for reproducibility in supercritical experiments, *Anal. Chem.* **68**, 4436-4440 (1996).

89. Watkins, J.J.; McCarthy, T. J. Polymerization in supercritical fluid-swollen polymers: A new route to polymer blends, *Macromolecules* **27**, 4845-4847 (1994).

90. Watkins, J.J.; McCarthy, T. J. Polymerization of styrene in supercritical CO_2-swollen poly(chlorotrifluoroethylene), *Macromolecules* **28**, 4067- 4074 (1995).

91. Wang, J.; Ran, Y.; Zou, E.; Dong, Q. Supercritical CO_2 assisted ternary-monomer grafting copolymerization of polypropylene, *J. Polym. Res* **16**, 739–744 (2009).

92. Rajagopalan, P.; McCarthy, T. J. Two-step surface modification of chemically resistant polymers: blend formation and subsequent chemistry, *Macromolecules* **31**, 4791-4797 (1998).

93. Kung, E.; Lesser, A.J.; McCarthy, T.J. The morphology and mechanical performance of polystyrene/polyethylene composites prepared using supercritical carbon dioxide, *Macromolecules* **31**, 4160-4169 (1998).

94. Reverchon, E.; Adami, R. Nanomaterials and supercritical fluids, *J. Supercrit. Fluid.* **37**, 1-22 (2006).

95. Tomasko, D.L.; Han, X.; Liu, D.; Gao, W. Supercritical fluid applications in polymer nanocomposites, *Curr. Opin. Solid State Mater. Sci.* **7**, 407-420 (2003).

96. Reverchon, E. Supercritical antisolvent precipitation of micro- and nano-particles, *J. Supercrit. Fluid.* **15**, 1-21 (1999).

97. Jung, J.; Perrut, M. Particle design using supercritical fluids: Literature and patent survey, *J. Supercrit. Fluid.* **20**, 179-219 (2001).

98. Knez, Z.; Weidner, E. Particles formation and particle design using supercritical fluids, *Curr. Opin. Solid State Mater. Sci.* **7**, 353-361 (2003).

99. Shariati, A.; Peters, C.J. Recent developments in particle design using supercritical fluids, *Curr. Opin. Solid State Mater. Sci.* **7**, 371-383 (2003).

100. Hakuta, Y.; Hayashi, H.; Arai, K. Fine particle formation using supercritical fluids, *Curr. Opin. Solid State Mater. Sci.* **7**, 341-351 (2003).

101. Petersen, R.C.; Matson, D.W.; Smith, R.D. Rapid precipitation of low vapor pressure solids from supercritical fluid solutions: the formation of thin films and powders, *J. Am. Chem. Soc.* **108**, 2100-2102 (1986).

102. Matson, D.W.; Fulton, J.L.; Petersen, R.C.; Smith, R.D. Rapid expansion of supercritical fluid solutions: solute formation of powders, thin films, and fibers, *Ind. Eng. Chem. Res.* **26**, 2298-2306 (1987).

103. Smith, R.D. Supercritical fluid molecular spray film deposition and powder formation, US A 4582731 (19860415).

104. Smith, R.D. Method of making supercritical fluid molecular spray films, powder and fibers, US 4734227 (19880329).

105. Smith, R.D. Supercritical fluid molecular spray thin films and fine powders, US A 4734451 (19880329).

106. Turk, M.; Hils, P.; Helfgen, B.; Schaber, K.; Martin, H.J.; Wahl, M.A. Micronization of pharmaceutical substances by the rapid expansion of supercritical solutions (RESS): a promising method to improve bioavailability of poorly soluble pharmaceutical agents, *J. Supercrit. Fluid.* **22**, 75-84 (2002).

107. Pestov, D.; Levit, N.; Kessick, R.; Tepper, G. Photosensitive 2,5-distyrylpyrazine particles produced from rapid expansion of supercritical solutions, *Polymer* **44**, 3177 (2003).

108. Pestov, D.; Levit, N.; Guney, A.O.; Tepper, G. Development of encapsulated microspheres from a multiple-component, rapidly expanding supercritical solution for sensing applications, in: G. Brunner, I. Kikic, M. Perrut (Eds.), (Proceedings of the sixth International Symposium on Supercritical Fluids, tome 3, Versailles, France, 1911 (2003).

109. Sun, Y.P.; Rollins, H.W. Preparation of polymer-protected semiconductor nanoparticles through the rapid expansion of supercritical fluid solution, *Chem. Phys. Lett.* **288**, 585-588 (1998).

110. Sun, Y.P.; Guduru, R.; Lin, F.; Whiteside, T. Preparation of nanoscale semiconductors through the rapid expansion of supercritical solution (RESS) into liquid solution, *Ind. Eng. Chem. Res.* **39**, 4663-4669 (2000).

111. Pathak, P.; Meziani, M.J.; Desai, T.; Sun, Y.P. Nanosizing drug particles in supercritical fluid processing, *J. Am. Chem. Soc.* **126**, 10842-10843 (2004).

112. Meziani, M.J. *et al.* Supercritical-fluid processing technique for nanoscale polymer particles, *Angew. Chem. Int. Ed.* **43**, 704-707 (2004).

113. Sun, Y.P.; Meziani, M.J.; Pathak, P.; Qu, L. Polymeric nanoparticles from rapid expansion of supercritical fluid solution, *Chem. Eur. J.* **11**, 1366-1373 (2005).

114. Kropf, C. *et al.* Method for producing nanoparticles by expansion of supercritical solutions, WO A1 2000015329 (20000323).

115. Foerster, T.; Fabry, B.; Hollenbrock, M.; Kropf, C. Use of nanoscale sterols and sterol esters for producing cosmetic and/or pharmaceutical preparations, WO A1 2000021490 (20000420).

116. Kropf, C. *et al.* Use of nanoscale chitosans and/or chitosan derivatives, WO A1 2000047177 (20000817).

117. Sun, Y.P.; Atorngitjawat, P.; Meziani, M.J. Preparation of silver nanoparticles via rapid expansion of water in carbon dioxide microemulsion into reductant solution, *Langmuir* **17**, 5707-5710 (2001).

118. Meziani, M.J.; Pathak, P.; Beacham, F.; Allard, L.F.; Sun, Y.P. Nanoparticle formation in rapid expansion of water-in-supercritical carbon dioxide microemulsion into liquid solution, *J. Supercrit. Fluids.* **34**, 91-94 (2005).

119. Reverchon, E.; Della Porta, G.; Taddeo, R.; Pallado, P.; Stassi, A. Solubility and micronization of griseofulvin in supercritical CHF_3, *Ind. Eng. Chem. Res.* **34**, 4087-4091 (1995).

120. Dehghani, F.; Foster, N.R. Dense gas anti-solvent processes for pharmaceutical formulation, *Curr. Opin. Solid State Mater. Sci.* **7**, 363-369 (2003).

121. York, P.; Hanna, M. Salmeterol xinafoate with controlled particle size, WO A1 9501324 (19950112).

122. Gupta, R.B.; Chattopadhyay, P. Method of forming nanoparticles and microparticles of controllable size using supercritical fluids and ultrasound, US A1 2002000681 (20020103).

123. Subramaniam, B.; Said, S.; Rajewski, R.A.; Stella, V. Methods and apparatus for particle precipitation and coating using near-critical and supercritical antisolvents, WO A1 9731691 (19970904).
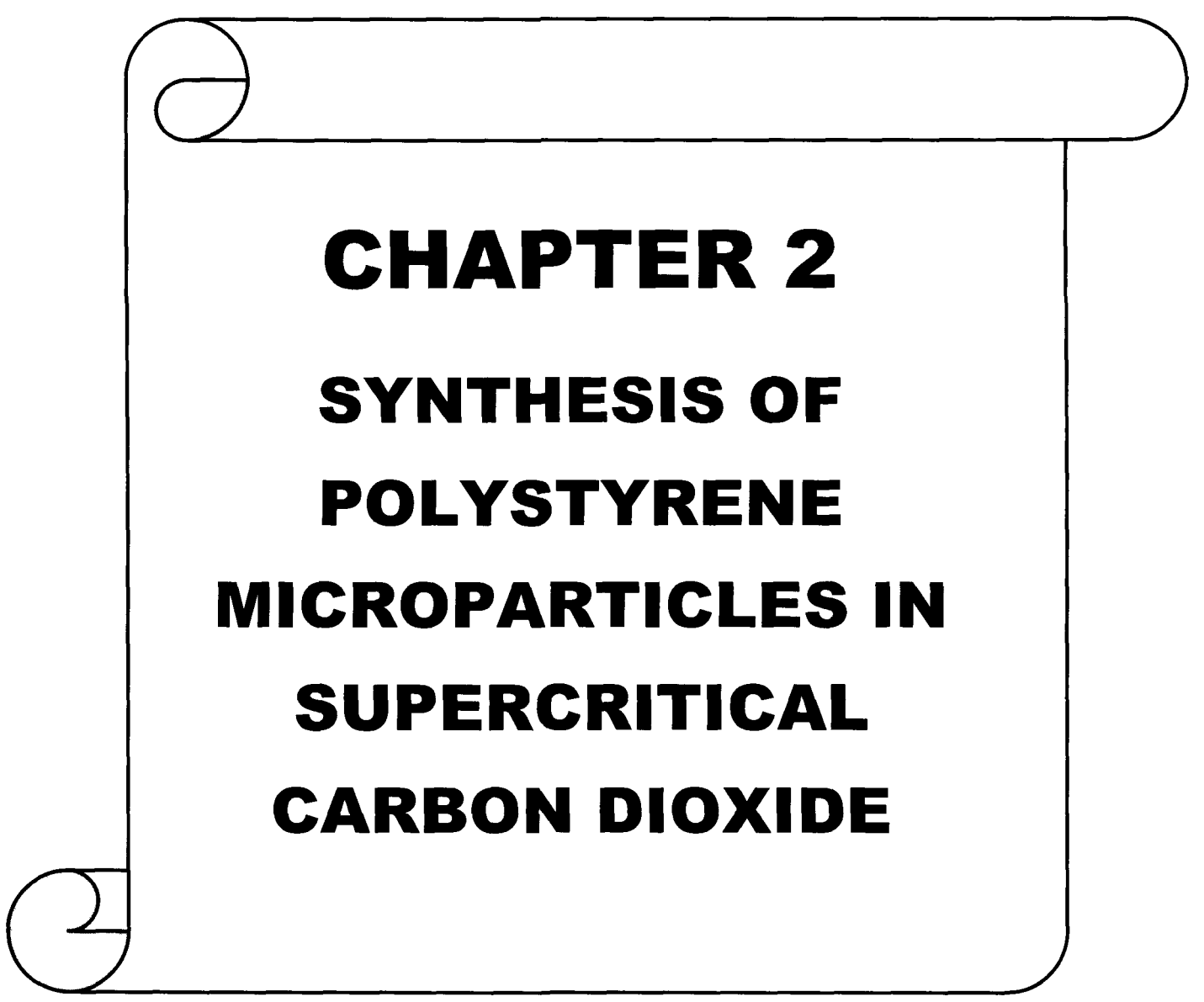
124. Reverchon, E.; Caputo, G.; DeMarco, I. Role of phase behavior and atomization in the supercritical antisolvent precipitation, *Ind. Eng. Chem. Res.* **42**, 6406-6414 (2003).

125. Shah, P.S.; Holmes, J.D.; Doty, R.C.; Johnston, K.P.; Korgel, B.A. Steric stabilization of nanocrystals in supercritical CO_2 using fluorinated ligands, *J. Am. Chem. Soc.* **122**, 4245-4246 (2000).

126. Shah, P.S.; Husain, S.; Johnston, K.P.; Korgel, B.A. Nanocrystal arrested precipitation in supercritical carbon dioxide, *J. Phys. Chem. B.* **105**, 9433-9440 (2001).

127. Shah, P.S.; Husain, S.; Johnston, K.P.; Korgel, B.A. Role of steric stabilization on the arrested growth of silver nanocrystals in supercritical carbon dioxide, *J. Phys. Chem. B* **106**, 12178-12185 (2002).

128. Korgel, B.A.; Shah, P.S.; Pell, L.E.; Johnston, K.P. Nanocrystal stabilization and synthesis in supercritical solvents, in: A. Bertucco (Ed.), Proceedings fourth international symposium on high pressure technology and Chemical Engineering, Venice, Italy, 2, 633 (2002).

129. Kameo, A.; Yoshimura, T.; Esumi, K. Preparation of noble metal nanoparticles in supercritical carbon dioxide, *Colloids Surf. A.* **215**, 181-189 (2003).

130. McLeod, M.C.; Gale, W.F.; Roberts, C.B. Metallic nanoparticle production utilizing a supercritical carbon dioxide flow process, *Langmuir* **20**, 7078-7082 (2004).

131. Ziegler, K.J.; Doty, R.C.; Johnston, K.P.; Korgel, B.A. Synthesis of organic monolayer-stabilized copper nanocrystals in supercritical water, *J. Am. Chem. Soc.* **123**, 7797-7803 (2001).

132. Reverchon, E.; Caputo, G.; Correra, S.; Cesti, P. Synthesis of titanium hydroxide nanoparticles in supercritical carbon dioxide on the pilot scale, *J. Supercrit. Fluid.* **26**, 253-261 (2003).

133. Stallings, W.E.; Lamb, H.H. Synthesis of nanostructured titania powders via hydrolysis of titanium isopropoxide in supercritical carbon dioxide, *Langmuir* **19**, 2989-2994 (2003).

134. Kamrupi, I.R.; Phukon, P.; Konwer, B.K.; Dolui, S.K. Synthesis of silver-polystyrene nanocomposites particles using water in supercritical carbon dioxide medium and its antimicrobial activity, *J. Supercrit. Fluid.* **55**, 1089-1094 (2011).

135. Sun, Y.P.; Rollins, H.W.; Guduru, R. Preparations of nickel, cobalt, and iron nanoparticles through the rapid expansion of supercritical fluid solutions (RESS) and chemical reduction, *Chem. Mater.* **11(1)**, 7-9 (1999).

136. Meziani, M.J.; Rollins, H.W.; Allard, L.F.; Sun, Y.P. Protein-protected nanoparticles from rapid expansion of supercritical solution into aqueous solution, *J. Phys. Chem. B* **106**, 11178-11182 (2002).

137. Meziani, M.J.; Sun, Y.P. Protein-conjugated nanoparticles from rapid expansion of supercritical fluid solution into aqueous solution, *J. Am. Chem. Soc.* **125**, 8015-8018 (2003).

138. Wang, Y.; Dave, R.N.; Pfeffer, R. Polymer coating/encapsulation of nanoparticles using a supercritical anti-solvent process, *J. Supercrit. Fluid* **28**, 85-99 (2004).

139. Yeo, S.D.; Kiran, E. Formation of polymer particles with supercritical fluids: a review, *J. Supercrit. Fluid* **34**, 287-308 (2005).

140. Sue, K.; Kakinuma, N.; Adschiri, T.; Arai, K. Continuous production of nickel fine particles by hydrogen reduction in near-critical water, *Ind. Eng. Chem. Res.* **43**, 2073-2078 (2004).

141. Viswanathan, R.; Lilly, G.D.; Gale, W.F.; Gupta, R.B. Formation of zinc oxide-titanium dioxide composite nanoparticles in supercritical water, *Ind. Eng. Chem. Res.* **42**, 5535-5540 (2003).

142. Zhang, J. *et al.* Preparation of ZnS/CdS composite nanoparticles by coprecipitation from reverse micelles using CO_2 as antisolvent, *J. Colloid. Interf. Sci.* **273**, 160-164 (2004).

143. Zhang, J. *et al*. A novel method to synthesize polystyrene nanospheres immobilized with silver nanoparticles by using compressed CO_2, *Chem. Eur. J.* **10**, 3531-3536 (2004).

144. Li, Z. *et al*. Preparation of cadmium sulfide/poly(methyl methacrylate) composites by precipitation with compressed CO_2, *J. Appl. Polym. Sci.* **94**, 1643-1648 (2004).

145. Li, Z. *et al*. Preparation of polyvinylpyrrolidone-protected Prussian blue nanocomposites in microemulsion, *Colloids Surf. A.* **243**, 63-66 (2004).

146. Sherrington, D.C. Preparation, structure and morphology of polymer supports, *Chem. Commun.* 2275-2286 (1998).

147. Tanev, P.T.; Chibwe, M.; Pinnavaia, T. J. Titanium-containing mesoporous molecular sieves for catalytic oxidation of aromtic compounds, *Nature.* **368**, 321-323 (1994).

148. Dong, A. *et al*. Mechanically stable zeolite monoliths with three-dimensional ordered macropores through the transformation of mesoporous silica spheres, *Adv. Mater.* **14**, 1506-1510 (2002).

149. Brandhuber, D. *et al*. Glycol-modified silanes in the synthesis of mesoscopically organized silica monoliths with hierarchical porosity, *Chem. Mater.* **17**, 4262-4271 (2005).

150. Kuang, D.; Brezesinski, T.; Smarsly, B. Hierarchical porous silica materials with a trimodal pore system using surfactant templates, *J. Am.Chem. Soc.* **126**, 10534-10535 (2004).

151. Hodge, P. Sherrington, D.C. *Syntheses and separations using functional polymers*, (Wiley: New York, 1989).

152. Sherrington, D.C. Preparation, structure and morphology of polymer supports, *Chem. Commun.* 2275-2286 (1998).

153. Park, Y.J. *et al*. Porous poly(lactide) membranes for guided tissue regeneration and controlled drug delivery: membrane fabrication and characterization, *J Control Release.* **43**, 151-160 (1997).

154. Cooper, A.I. Porous materials and supercritical fluids, *Adv. Mater.* **15**, 1049-1059 (2003).

155. Wood, C.D.; Cooper, A.I. Synthesis of macroporous polymer beads by suspension polymerization using supercritical carbon dioxide as a pressure-adjustable porogens, *Macromolecules.* **34(1)**, 5-8 (2001).

156. Cooper, A.I.; Wood, C.D.; Holmes, A.B. Synthesis of well-defined macroporous Polymer monoliths by sol-gel polymerization in supercritical CO_2, *Ind. Eng. Chem. Res.* **39**, 4741-4744 (2000).

CHAPTER 2

SYNTHESIS OF POLYSTYRENE MICROPARTICLES IN SUPERCRITICAL CARBON DIOXIDE

Polymerization of styrene using siloxane and fluorine based stabilizers in supercritical carbon dioxide (sc-CO$_2$) medium.

2.1 Introduction

Carbon dioxide is an environmentally benign, inexpensive, tunable, nonflammable and alternative solvent to the aqueous and organic solvents which are traditionally used in the synthesis of different polymers.[1-20] It can be obtained from natural reservoirs or recovered as a byproduct of industrial chemical processes such as cement industry, fermentation industry etc. Although CO$_2$ is a gas at ambient conditions, its liquid and supercritical states can be easily obtained by compression and application of heat.[21] Liquid CO$_2$ is a compressible fluid, while supercritical CO$_2$ has relatively high densities like liquid and low viscositiy like gases.[22] Silicones and fluoropolymers are the only classes of polymers found to be highly soluble in CO$_2$ at easily accessible temperature and high pressure.[23] Hydrocarbon based polymers are relatively less soluble in CO$_2$. Polystyrene (PS) is insoluble in CO$_2$ even at 225°C and 210 bar.[24] However, CO$_2$ acts as a plasticizing agent for PS[25-30] and this phenomenon facilitates the diffusion of monomer inside the swollen polymer phase during polymerization. De Simone et al.[31] reported the first dispersion polymerization of methyl methacrylate supercritical carbon dioxide (sc-CO$_2$) by using highly soluble amorphous fluorinated polymers as the stabilizer. Heterogeneous polymerizations involve at least two phases during polymerizations.

The polymers are insoluble in the continuous phase and may be dispersed by addition of stabilizers as CO_2 is a poor solvent for most oligomers. Terricarson et al.[32] studied the successful dispersion polymerization of 1-vinyl-2-pyrolidene in supercritical carbon dioxide (sc-CO$_2$) with the various amounts of polyfluorooctylacrylate (poly-FOA). They reported that increasing concentrations of poly-(FOA) yielded a decrease in particle diameter, while increasing the monomer concentration produced larger particle size. No significant change was observed in the particle morphology for polymerizations conducted at different pressures. Wang et al.[33] studied the successful dispersion polymerization of methyl methacrylate in supercritical carbon dioxide (sc-CO$_2$) with a novel ester end-capped perfluoropolyether stabilizer. With the increase in crytox butyl ester stabilizer (0-1%), the yield of the product (29-95%) and the molecular weight increases (17,000-175,000). Canelas et al.[34] studied the dispersion polymerization of styrene in supercritical carbon dioxide (sc-CO$_2$) stabilized with poly (styrene-b-dimethylsiloxane) block copolymers as sterric stabilizers. It was explained that the anchor soluble balance (ASB) of the stabilizer has a dramatic effect on both the progress of reaction and morphology of the polystyrene products. They performed the dispersion polymerizations under a series of different pressures (143-439 bar) resulted in variations in the conversion, molecular weight, and particle diameter. It is suggested that the reaction is extremely sensitive to the density of the continuous phase. Weijum Ye et al.[35] studied the emulsion polymerization of N-ethylacrylamide in supercritical carbon dioxide (sc-CO$_2$). The emulsion polymerization of a water soluble vinylic monomer in supercritical carbon dioxide (sc-CO$_2$) was carried out. The influence of the reaction parameters on the particle diameter and distribution of particle sizes were investigated. They observed that higher temperature and higher surfactant and initiator concentrations resulted in particles with smaller sizes.

In this chapter, we report the emulsion polymerization of styrene monomers in supercritical carbon dioxide (sc-CO$_2$) using different fluorine and siloxane based stabilizers. In all the syntheses, azobisisobutyronitrile (AIBN) is used as the initiator. The stabilizers used in these syntheses are (Trifluoromethyl)-undecafluorocyclohexane

(C_7F_{14}) as a fluorine based stabilizer and Polydimethylsiloxane (PDMS) as the siloxane based stabilizer. The emulsion polymerizations were carried out at different percentages of stabilizers (0.2%-10%), different initiator concentrations (0.1%-0.5%) and at different pressures (2100-2500 psi). The synthesized polymer particles were characterized by GPC, SEM and TGA. The influence of different process parameters (stabilizer concentration, initiator concentration and pressure of CO_2) on conversion, molecular weight, particle size and polydispersity index were elaborately studied.

2.2 Experimental

2.2.1 Materials

Styrene (Merck) was purified and deinhibited by washing it with 10% NaOH solution and followed by washing with double distilled water. (Trifluoromethyl)-undecafluorocyclohexane (C_7F_{14}) (Aldrich) and Polydimethylsiloxane (PDMS) (Aldrich) were used as received. Azobisisobutyronitrile (AIBN) (G.S. Chemical Testing Lab. & Allied Industries, Bombay) was used after recrystallization twice from methanol. Methanol (Merck), n-heptane (Merck) was used as received. Tetrahydrofuran (THF, Ranbaxy) was distilled from a sodium/ benzophenone solution. Carbon dioxide (Rass Chryogenics) (99.99% pure) was used as received.

2.2.2 Experimental set-up

All experiments were conducted in a 60 ml, high-pressure reactor (SFE-System, Reaction Eng. Inc. Korea). The schematic diagram of the apparatus is shown in (Fig.2.1). The SCF equipment is attached with the high pressure CO_2 cylinder, high pressure metering pump and the efficient cooler. The pressure inside the reactor can be raised up to 6,000 Psi. The pressure inside the reactor was measured with a pressure transducer and the internal temperature of the reactor was measured with thermocouple.
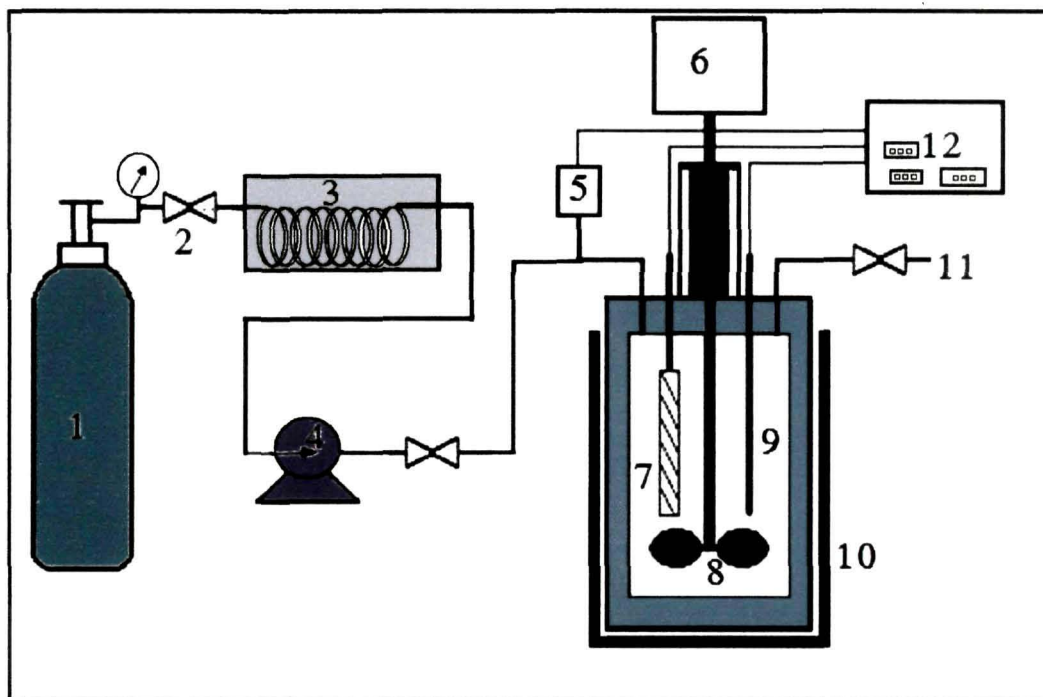
Fig.2.1. Schematic diagram of the SCF Reactor

1. Carbon dioxide cylinder 2. Back pressure valve 3. Refrigeration Unit 4. High pressure liquid Pump
5. Back pressure Gauge 6. Motor for mechanical stirrer 7. Cooling unit 8. Mechanical stirrer
9. Heating probe 10. SFE Vessel 11. Vent 12. Digital display unit.

2.3 Procedure

2.3.1 Emulsion polymerization of styrene in Supercritical carbon dioxide (sc-CO$_2$) stabilized with (Trifluoromethyl)undecafluorocyclohexane (C$_7$F$_{14}$)

The reactor was charged with styrene monomer (10mL), stabilizer C$_7$F$_{14}$ (0.5g) and initiator AIBN (0.1g). After a well mixing, a slow stream of CO$_2$ was purged to remove any oxygen present inside the reactor. The meter pump was started to feed more CO$_2$ pressure inside the reactor. The temperature of the reactor was set at 75°C to ensure the dissociation of the initiator, simultaneously the pump was also run to maintain the

60

pressure inside the reactor. The rotation speed of the stirrer was maintained at 900 rotations per minute (rpm) value. The polymerization reaction was allowed to run for about 9 hr. At the end of the reaction, the reactor was allowed to cool to room temperature and CO$_2$ was slowly vented off from the reactor. The polymer was removed and allowed to dry at 80°C in the vacuum oven. The yield of the dry polymer was determined gravimetrically, and all reactions were repeated at least twice with reproducible results. The polymer was washed thoroughly with n-heptane to remove the excess amount of stabilizers.

The following sets of experiments were carried out

2.3.1.1.1 The emulsion polymerization of styrene with different percentages of stabilizers (0.2-10.0%).

2.3.1.1.2 Emulsion polymerization of styrene with different initiator concentration (0.1-0.5%).

2.3.1.1.3 Emulsion polymerization of styrene with different pressure (2,100-2,500 psi).

2.3.2 Emulsion polymerization of styrene in supercritical carbon dioxide Sc-CO$_2$ using polydimethylsiloxane (PDMS) as the stabilizer

The polymerization was performed in high pressure stainless steel reactor equipped with a magnetically coupled overhead stirrer. At first, reactor was charged with PDMS (0.5 g) stabilizer. Then AIBN (0.1 g) and styrene (10 mL) was added into the reactor and mixed thoroughly. The reactor was pressurized by filling with CO$_2$ to a pressure of 1,000 psi, and heated to the desired reaction temperature (75°C). With the increase in temperature, the pressure gradually increases. Once the reaction temperature was reached, the desired pressure (2,000-2,600 psi) was maintained with the help of

metering pump. The reaction was allowed to proceed for 6-8 hours at temperature 75°C and pressure (2,000-2,600 psi). At the end, the reactor was allowed to cool down to room temperature. The pressure was then slowly released and at atmospheric pressure the polymeric product was recovered from the reactor as a fine white powder.

The following sets of experiments were carried out-

2.3.2.1 Emulsion polymerization of styrene at different stabilizer (PDMS) concentrations (0.3-2.5%).

2.3.2.2 Emulsion polymerization of styrene at different pressures (2,000-2,600 psi).

2.4 CHARACTERIZATION

The monomer conversion was determined gravimetrically.

2.4.1 GPC analysis

Molecular weights of the polymers were determined by gel permeation chromatography (GPC, Waters, USA, Model 515) solvent delivery system at a flow rate of 1.0 ml/min through a set of three ultrastyregel columns. Analysis was performed at controlled temperature at 45°C using HPLC grade tetrahydrofuran (THF) as eluent, and the instrument was standardized with polystyrene standards.

2.4.2 SEM analysis

Morphology of the powdered polymer particles were obtained from Jeol-Jsm-6390LV scanning electron microscope (SEM). For SEM analysis, samples were mounted on an aluminum stub using an adhesive carbon tape and were coated with platinum to a thickness of 200 A°.

2.4.3 TGA analysis

Thermal analysis was carried out with the thermo gravimetric analyzer (TGA, Model TGA-50, Shimadzu). In TGA analysis, the heating rate was maintained at 10°C/min. under the nitrogen flow rate of 30 mL/min.

2.5 Results and Discussions

The primary requirement for the dispersion or emulsion polymerization in supercritical carbon dioxide (sc-CO$_2$) is the solubility of the stabilizer in the medium. The fluorinated stabilizers and the siloxane based stabilizers are excellent stabilizers in sc-CO$_2$ medium.[33,34] In this case we have used the polydimethylsiloxane (PDMS) and (trifluoromethyl)-undecafluorocyclohexane (C$_7$F$_{14}$) as the stabilizers for the dispersion/emulsion polymerization. In the initial stage of the reaction, the monomer mixed with initiator form micro-droplets in sc-CO$_2$ medium. The stabilizer covers these droplets to form microemulsions and thereby imparts stability to the microemulsions. In the second stage, the initiator gets decomposed at 75°C, and initiates the polymerization reaction. After complete polymerization, the free flowing, white powdered polymer particles are obtained by slowly depressurizing the reactor.

2.5.1 Emulsion polymerization of styrene in Supercritical carbon dioxide (sc-CO$_2$) stabilized with (Trifluoromethyl)undecafluorocyclohexane (C$_7$F$_{14}$)

2.5.1.1 Effect of stabilizer concentration

The reaction was carried out at pressure 2,100 psi and temperature 75°C using different concentration of stabilizer- (0.2%, 0.5%, 2.5%, 5% and 10%). Under reaction conditions styrene was insoluble in CO$_2$ and the reaction occurred heterogeneously. The heterogeneous phase was stabilized with the help of CO$_2$-philic stabilizer,

(trifluoromethyl)undecafluorocyclohexane (C$_7$F$_{14}$). The yield of the reaction, molecular weight and morphology of the polymer are reported in the (Table.2.1).

Table 2.1. Physical properties of polymers synthesized at different stabilizer conc.

Sl. no	[S],wt %	Final state	Yield, %	Mol. wt.[b] M$_n$	PDI[a]	Average Size (µm)	Morphology
1	10	sticky polymer	85	37,000	2.33	0.25	Spherical
2	5	sticky polymer	87	34,000	2.00	0.7	Spherical
3	2.5	sticky polymer	86	36,000	1.89	0.9	Spherical
4	0.5	white powder	85	32,000	1.70	1.3	Spherical
5	0.2	white powder	84	39,000	1.43	1.8	Spherical

(a = Polydispersity index, b = number average molecular weight, Pressure of CO$_2$ = 2,100 Psi, Temperature= 75°C and initiator concentration = 0.2% for all the reactions)

The stabilizer concentration did not have significant effect on the yield of the polymerization reaction (for all the cases in the range of 84-87%). The final form of polymer after depressurizing of CO$_2$ is sticky polymer when the stabilizer concentration is > 0.5%. The stickiness is observed due to plasticization effect of CO$_2$ as it contains large amount of fluorinated stabilizers. If the sticky product is dried in oven at 80 °C for 2 hours, the product become granular in nature. The molecular weights of polymers (Table 2.1) are in the range of 32,000 to 39,000 g/mol. Molecular weight is not affected by the different concentrations of stabilizer. However it is observed that the molecular weight is quite low in comparison to the usual polymer prepared via free radical polymerization. Thus this method is suitable for synthesizing polymers of moderate molecular weight. It is found that polydispersity is in the range of 1.43 to 2.33. The polydispersity index decreases with the decrease in stabilizer concentration. The lowest polydispersity is observed with the lowest amount of stabilizer.

The SEM micrographs of the polymer particles are shown below-
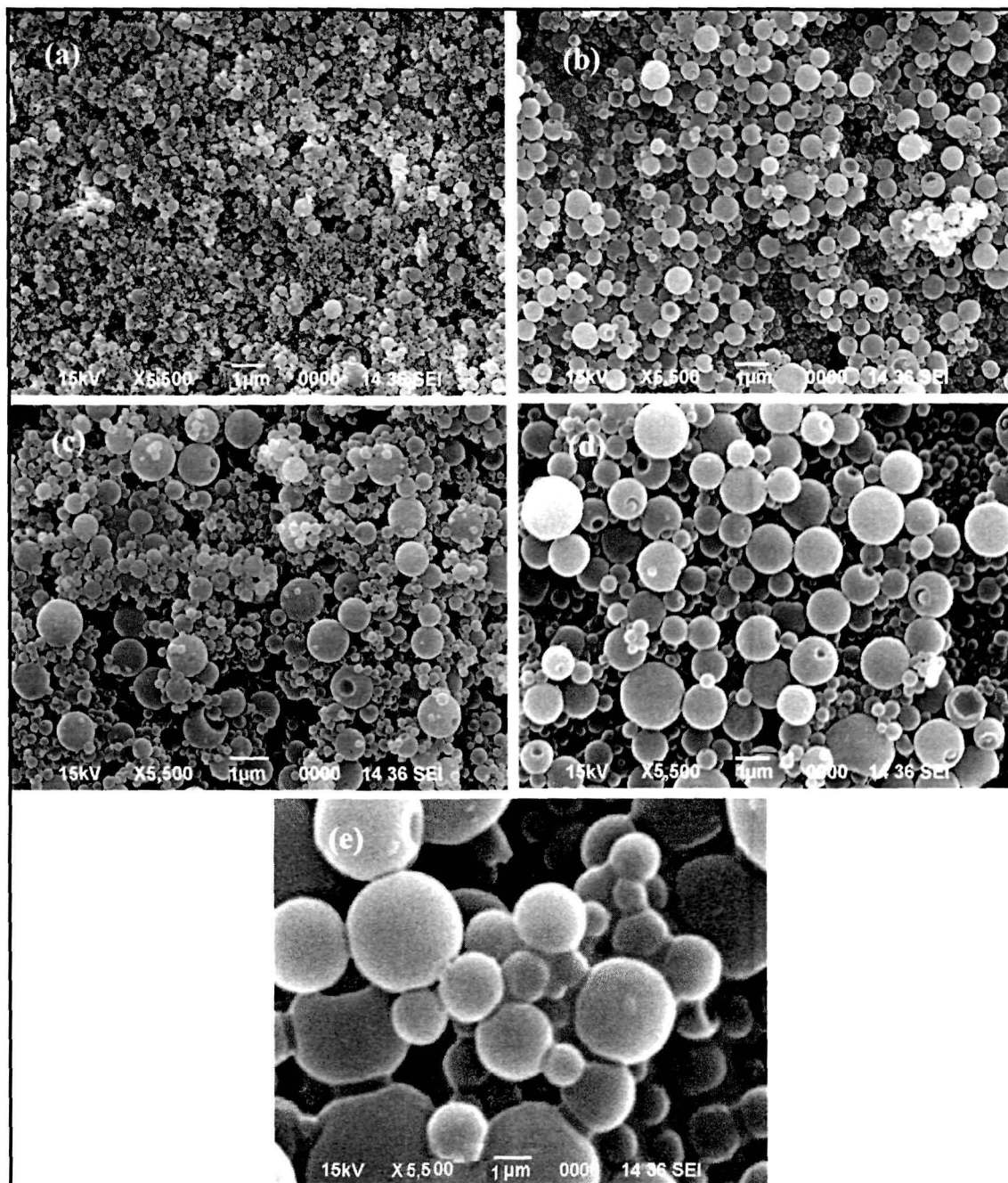
Fig.2.2. SEM micrographs of polystyrene particles at different stabilizer conc.

(a) 10% stabilizer (C$_7$F$_{14}$), (b) % stabilizer (C$_7$F$_{14}$), (c) 2.5 % stabilizer (C$_7$F$_{14}$), (d) 0.5 % stabilizer (C$_7$F$_{14}$), (e) 0.2 % stabilizer (C$_7$F$_{14}$)

SEM shows (Fig.2.2) the formation of uniform spherical particles in all the reactions. The size of the polymer particles decreases with the increase in stabilizer concentrations. The lowest size of particles was formed with the highest stabilizer concentration (10%) (Table.2.1). The relation of concentration of stabilizer and particle size follows the usual trend for emulsion polymerization. At higher concentrations of surfactant, the initial state of the mixture of the reactants was an emulsion and the final state was in a sticky polymer state. But as the concentrations of the surfactant decreased, the final state of the product was a fine white powdered polymer. In an emulsion polymerization, the number of polymer particles formed is associated with the surfactant concentration. As the number of surfactant molecules increases, the number of surfactant stabilized micelles also increases resulting in smaller particles.[36] At low surfactant concentrations, we obtained surprisingly some large particles with a size much larger than the other particles (Fig.2.2) in addition to the submicron sized particles. It is believed that these large particles were produced from the polymerized monomer droplets (bulk polymerization as in suspension) as the AIBN initiator is soluble in both the CO$_2$ and liquid monomer phase. The initiation took place not only in the polymerization medium, but also inside the monomer droplets. Gardon et al.[37] studied emulsion polymerization and experimental data in the context of the revised Smith-Ewart theory. Excellent quantitative agreements were obtained between theoretical and experimental particle size values for different polymers. The size of polymerized monomer droplets depended strongly on the surfactant concentration. Weijun Ye et al.[35] studied the emulsion polymerization of N-ethylacrylamide in supercritical carbon dioxide (sc-CO$_2$) and reported the similar result in the dependence of the size of the polymer particles on the surfactant concentrations during polymerizations.

2.5.1.2 Effect of initiator concentration (AIBN)

The emulsion polymerization of styrene was carried out at the pressure of 2,100 psi and 75° C temperature with fixed amount of stabilizer (0.2%). The emulsion

polymerization of styrene was carried out at three different initiator (AIBN) concentrations: 0.5, 0.2, and 0.1 wt% that were based on the monomer weight. The results are summarized in (Table 2.2)

Table.2.2: Physical properties of polymers synthesized at different initiator conc.

Sl. no	[I] wt.%	Final state	Yield (%)	Mol. weight (M_n) (g/mol)	Average Size (μm)	Morphology
1	0.1	white powder	82	55,000	4	spherical
2	0.2	white powder	87	49,000	3.2	spherical
3	0.5	white powder	85	43,000	1.8	spherical

(Pressure = 2,100 psi, temperature = 75 °C and 0.2% of stabilizer in all the reactions)

In all the reactions, dry, white, free-flowing powdered polymer products are observed. The yields of the products are found to be independent of the initiator concentration and in all reactions it is above 82%.
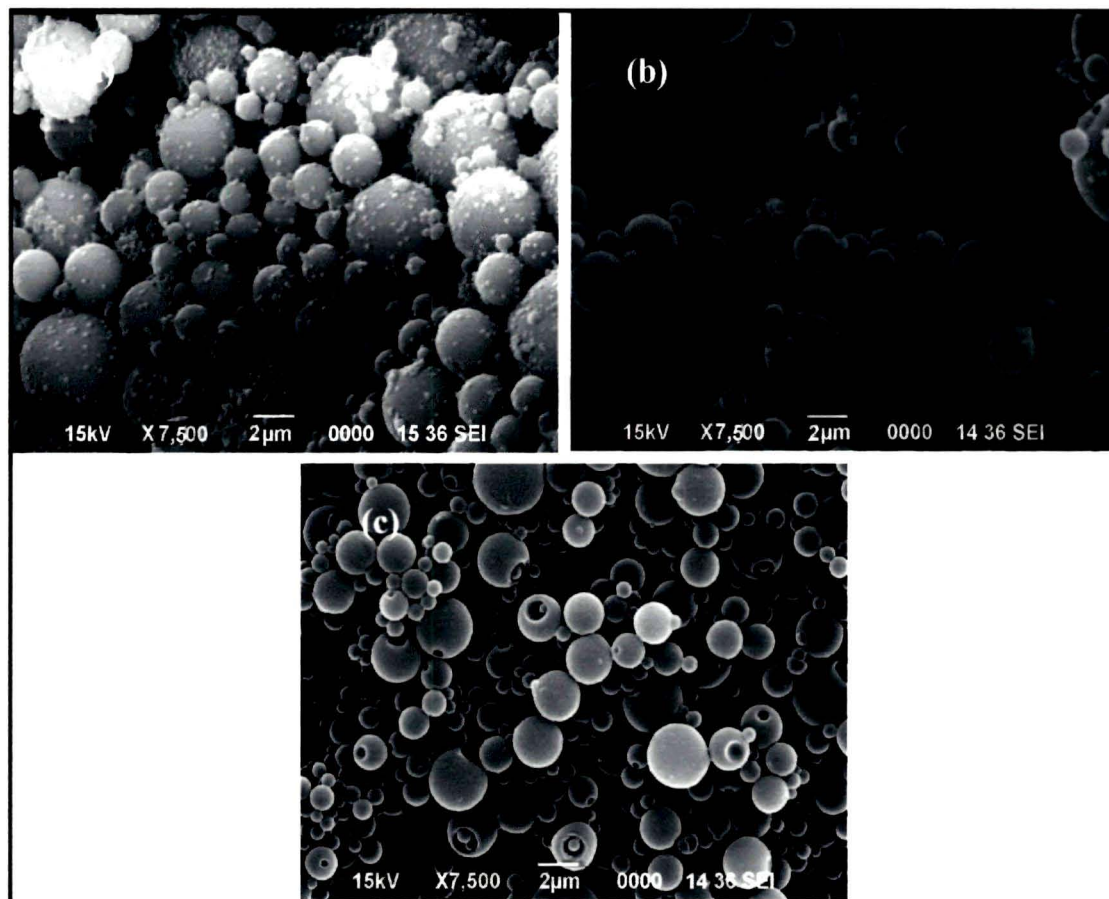
Fig. 2.3: SEM micrographs products at different initiator concentrations.

(a) 0.1% initiator (AIBN) (b) 0.2% initiator (AIBN) (c) 0.5% initiator (AIBN)

The molecular weight of the polymer particles were obtained in the range of 43,000-55,000 g/mol. The molecular weight of the polymer particles decreases with increasing initiator concentration. As the initiator concentration is low, fewer free radicals are available and thus allow chain to grow more. The number of free radicals generated increases as the initiator concentration increases. The monomers are attracted to these sites and because there are many active sites, short chains will form. The molecular weight of polystyrene decreases as the concentration of the initiator increases.

The morphology of the polymer particles were studied by SEM analysis (Fig. 2.3) which shows that particle size decreases with the increase in initiator

concentrations. The smallest particle size (1.8μm) formed at highest concentration of initiator (0.5%). Many authors had also reported the similar results[32,30,33] which are in accordance with the nucleation mechanism of an emulsion polymerization. In case of emulsion polymerization the nucleation of the particles take place in either the monomer swollen micelles or the precipitated solution polymerized oligomer radicals.

Formation of the polymer particles through micellar and homogeneous nucleation involve the absorption of surfactant from the micelles, medium, and monomer droplets, and the number of polymer particles, N, is dependent on the total surfactant surface area present in the system and the initiation rate. The same result (eq. 1) has been derived for both micellar and homogeneous nucleation.[38,39]

$$N = k \, (R_i / \mu)^{0.4} \, S^{0.6} = KI^{0.4} \, S^{0.6} \quad \text{---------------------- (1)}$$

Where k and K are constants, í is the rate of volume increase of a polymer particle, R$_i$ and I the initiation rate and the initiator concentration, and S the surfactant concentration. Obviously, with more initiator and surfactant, the emulsion polymerization leads to more polymer particles, which are associated with a smaller particle size.

2.5.1.3 Effect of pressure

One of the great advantages of using supercritical fluids as a reaction medium is the ability to adjust its solvent quality in the reactor through its easily tunable density and dielectric constant by changing either pressure or temperature according to reaction condition. Moreover, for free radical reactions, CO$_2$ offers no chain transfer to solvent and high free-radical initiation efficiency with acceptable initiator decomposition kinetics. The emulsion polymerization of styrene in sc-CO$_2$ was conducted at three different pressures (2100, 2300, 2500 Psi) (Table 2.3).

Table.2.3. Physical properties of the polymers synthesized at different pressures

Sl. no.	Pressure, psi	Yield, %	Mol. wt. (M_n)	Particle Size (μm)	Morphology	PDI
1	2,100	82	34,000	1	Spherical	1.78
2	2,300	84	35,000	1.5	Spherical	1.82
3	2,500	81	36,000	2.2	Spherical	1.86

The yield of the reactions was observed in the range of 81-84%. The operating pressure has significant effect on the molecular weight, polydispersity index and on particle size. Molecular weight (M_n) of the polymer particles were in the range of 34,000-36,000 g/mol. PDI of the polymer particles increases with increase in pressure and found to be in the range of 1.78 to 1.86. This is because, as the pressure of carbon dioxide inside the reactor is increased, its solvency power towards the monomers and growing polymer chains increased.[40] This higher CO$_2$ solvency can affect the fraction of the monomer molecularly dissolve in the polymerizing medium, which has a great role in determining the size of the final polymer particles. Moreover, at higher pressure, there is a chance of coalescence of the small polymer particles due to which, larger particles are obtained.
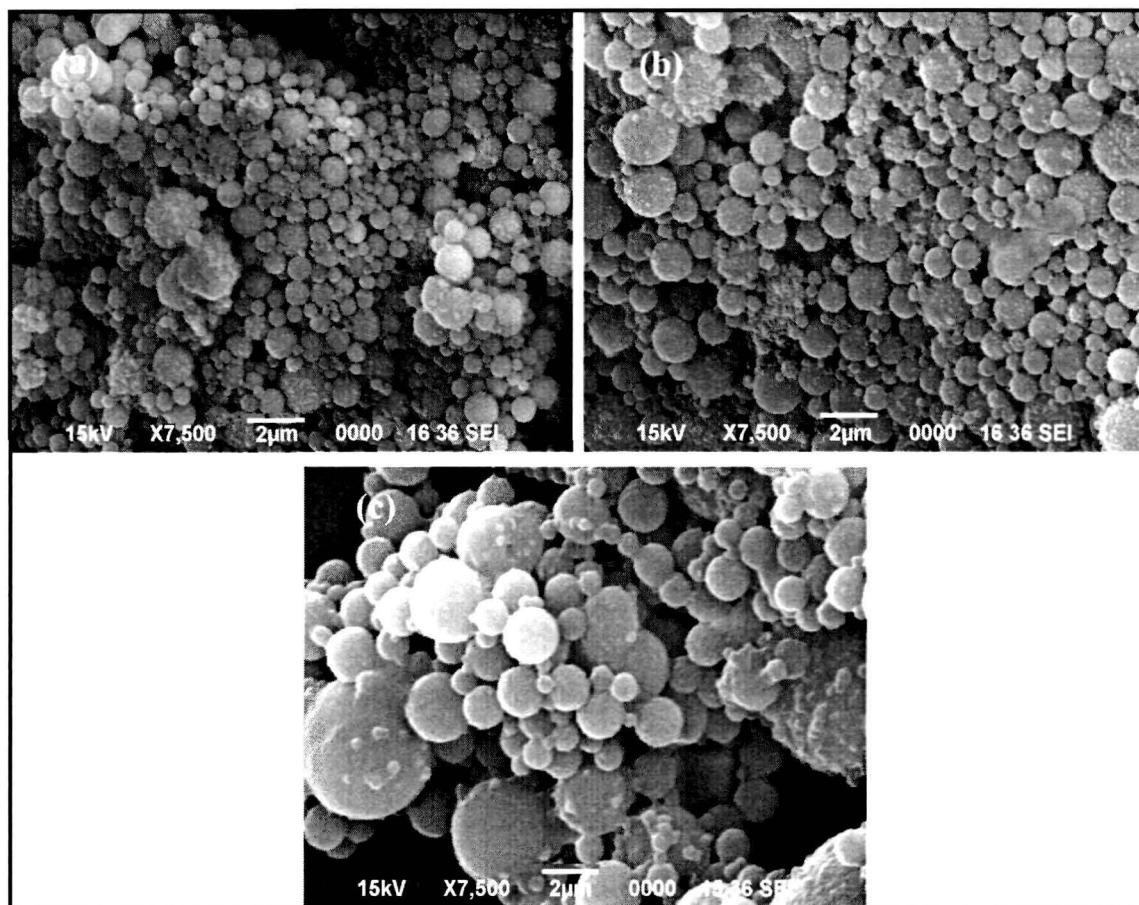
Fig.2.4: SEM micrographs of products at different pressures

(a) At 2,100 psi, (b) At 2,300 psi, (c) At 2,500 psi

The increased pressure may also affect the initiation rate of polymerization. Weijun Ye *et al.*[35] investigated the AIBN thermal decomposition in sc-CO$_2$ as a function of pressure and observed that there were two opposite effects on the decomposition rate of AIBN in supercritical carbon dioxide (sc-CO$_2$). These are the solvation effect and the intrinsic activation volume effect. In the low-pressure region, the AIBN decomposition rate was enhanced with pressure due to the solvation effect. However, as the pressure is increased, the intrinsic activation volume effect dominated, which leads to the lower rate of decomposition. We have observed the pronounced effect of pressure on particle size of polymer. With the increase in pressure, particle size gradually increases (Fig.2.4.). At 2,100 psi pressure the particle size is 1μm and at

71

2,500 Psi pressure, the particle size is 2.2μm. The high pressure facilitates the nucleation of growing particles and hence results in formation of larger particles.
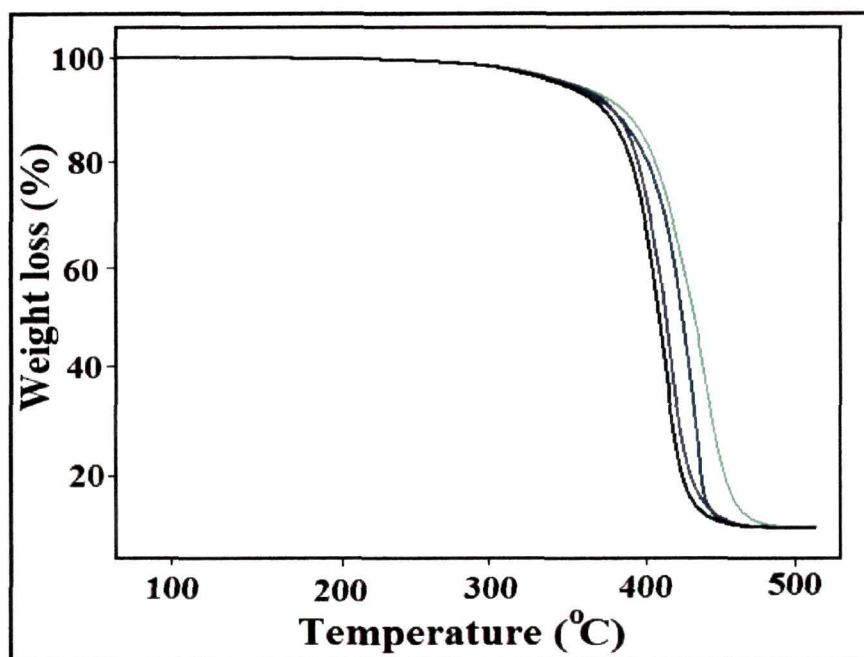
Fig.2.5. TGA thermogram of the polymer samples

The thermal stability of all the polymer samples was studied by TGA analysis. TGA thermograph shows no difference in the thermal stability. As seen in (Fig. 2.5) it was observed that all the polymeric products were stable upto the temperature of 370 °C.

2.5.2   Emulsion polymerization of styrene in supercritical carbon dioxide sc-CO₂ using Polydimethylsiloxane (PDMS) as the stabilizer

Fluorinated and siloxane based stabilizers are found to be excellent stabilizers in sc-CO₂ medium. In this case, we have used the siloxane based polydimethylsiloxane (PDMS) as the stabilizer for the emulsion polymerization in sc-CO₂ medium. In the initial stage of the reaction, the monomers and the initiators form micro-droplets in sc-CO₂ medium. PDMS covers these micro-droplets to form microemulsions and thereby imparts stability to the microemulsions. As soon as the initiator gets decomposed at

75°C, and initiates the polymerization reaction and is continued the reaction for 8 hours. After complete polymerization, the free flowing, white powdered polymer particles are obtained by slowly depressurizing the reactor.

The formation of free flowing powdered polymer particles in the sc-CO$_2$ medium is shown schematically in Fig.2.6.
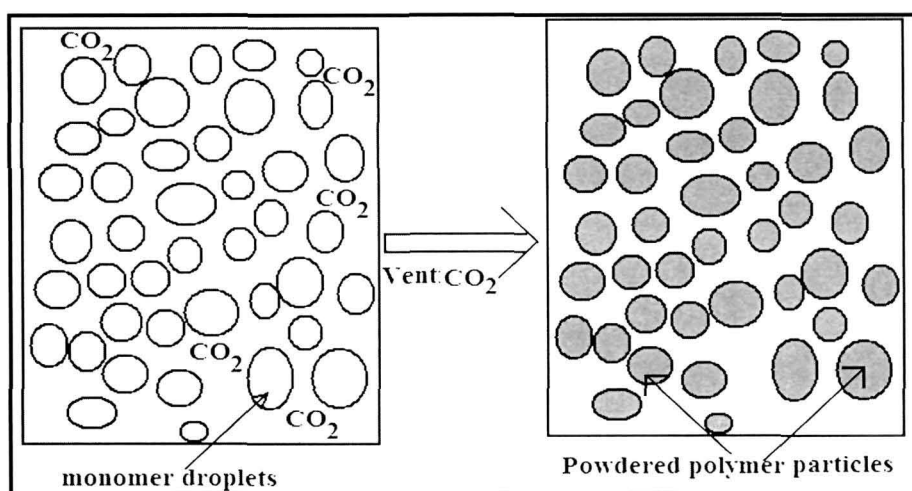
Fig.2.6: Formation of powder polymeric particles

2.5.2.1 Effect of stabilizer concentration

The polymerization reactions in supercritical carbon dioxide (sc-CO$_2$) medium was conducted by varying the stabilizer concentration (0.3%, 0.6%, 1.5% and 2.5%) keeping other parameters constant viz. pressure 2,200 psi, stirring speed 900 rpm and temperature 75°C and is summarized in Table 2.4. The polymerization reactions were conducted at constant pressure (2,200 psi) in presence of various concentrations of PDMS stabilizer produced free flowing powdered polymer products.

Table 2.4: Physical properties of polymers synthesized at different stabilizer conc.

Sl no	Stabilizer Conc. %	Yield %	Mol. Wt.	PDI	Final state	Morphology	Particle size (μm)
1	0.3	82	34,000	1.32	Agglomerated powder	spherical	1.3
2	0.6	79	36,000	1.46	Free flowing powder	Spherical	1.1
3	1.5	81	33,000	1.64	Free flowing powder	Spherical	0.8
4	2.5	80	35,000	1.86	Free flowing powder	spherical	0.6

(All the polymerizations were performed at constant pressure 2,200 psi, stirring speed 900 rpm and 75°C)

The stabilizer concentration did not have significant effect on yield of the polymers (79-82%). The molecular weight of the polymer was obtained in the range of 33,000 to 36,000 g/mol and it is not found to be affected by the different concentrations of stabilizers. However, the molecular weight of the polymer synthesized in sc-CO$_2$ is quite low in comparison with that of the polymers prepared by the usual free radical polymerization carried out in organic solvents. That is why this method may be useful for synthesizing polymers having moderate molecular weights.
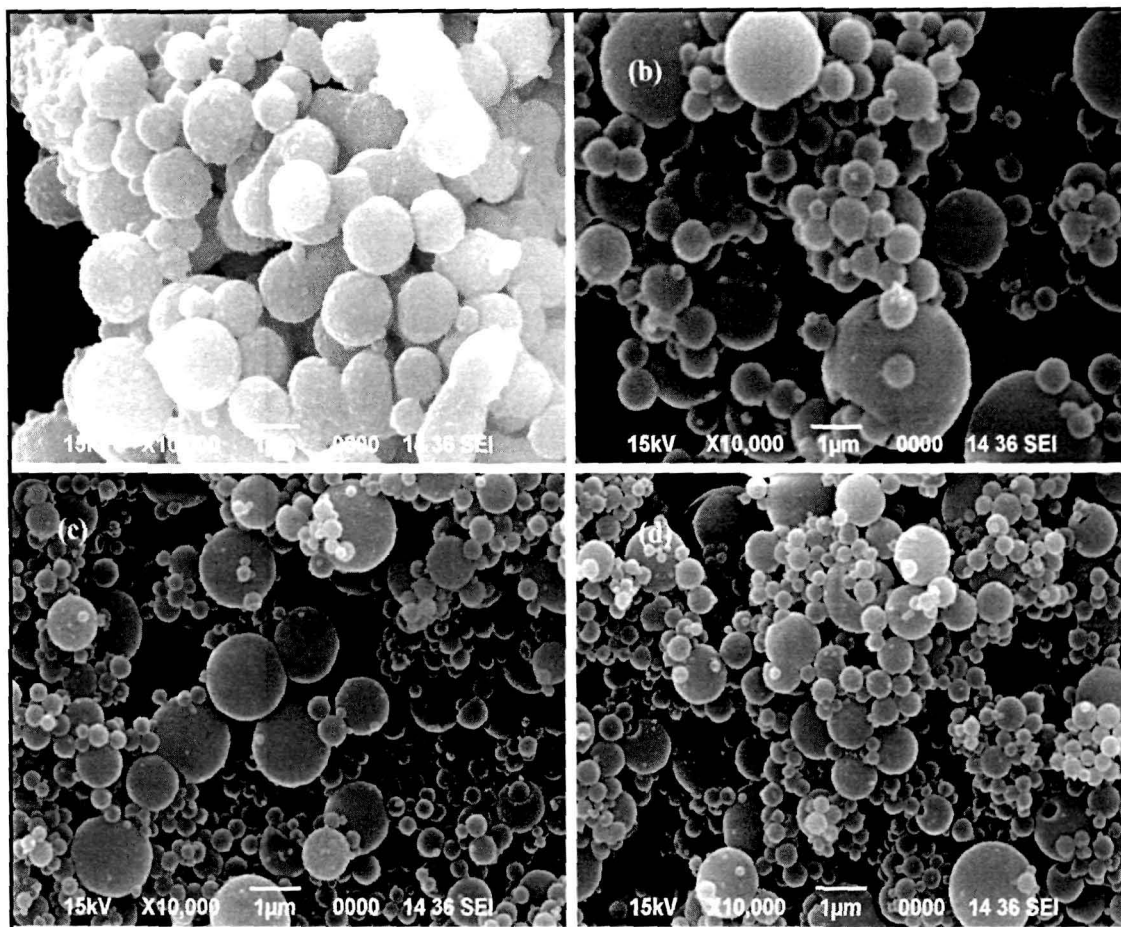
Fig.2.7. SEM images of the polymers synthesized at different stabilizer conc.
(a) At 0.3%, (b) 0.6%, (c) 1.5% and (d) 2.5%

The morphology of the polymer particles was studied by SEM analysis, and the product was found to exhibit discrete spherical polymer particles with particular diameter in micrometer range. The SEM images of the polymers are depicted in Fig.2.7. It was observed that particle size decreased as the stabilizer concentration was increased. These results are in agreement with the finding of Gardon et al.[37] who observed that the particle size of the final latex decreases with increasing stabilizer concentration. The particle size dependence on stabilizer concentration can be explained in terms of surface area of the polymer particles. The increasing surfactant/stabilizer concentration permits more surface area stabilization. It is also observed that at higher stabilizer concentrations, the particle size distribution is broader. In emulsion

polymerization, the number of polymer particles formed is associated with the surfactant concentration. As the number of surfactant molecules increased, the number of surfactant stabilized micelles also increases, resulting the formation of smaller sized particles at higher stabilizer concentrations.

2.5.2.2 Effect of pressure

The emulsion polymerizations were carried out in supercritical carbon dioxide (sc-CO2) medium in the presence of PDMS stabilizers at different pressures. The effects of operating pressure on different physical properties of the synthesized polymer particles were studied. It is observed that the operating pressure has significant effect on the polymer particle size, molecular weight and on polydispersity index (PDI). All these data are summarized in the following table (Table 2.5).

Table. 2.5 Physical properties for the synthesis of powdered polystyrene particles

Sl no	Pressure (psi)	Yield (%)	Final state	(M_n) Mol. Wt. g/mol	Particle size morphology	PDI
1	2,000	90	Agglomerate particles	35,542	(3.3 µm), spherical	1.45
2	2,100	84	Agglomerate particles	36,765	(3.25µm) Spherical	1.78
3	2,300	85	Fine white powder	37,645	(4.1µm) Spherical	1.82
4	2,500	81	Fine white powder	40,667	(5.2µm) Spherical,	1.86
5	2,600	83	Fine white powder	45,078	(6.3µm) Spherical	1.87

(Temperature=75°C, Monomer conc., Stabilizer conc. and the Time of reaction was kept constant)

The density of CO_2 increases with increasing pressure. With increase in density of CO_2, the solvency power increases and thereby increases the solubility of the monomer and the stabilizer in the medium. The morphology of the polymers synthesized at different pressures is as shown in Fig.2.8. In all the reactions free flowing white powdered

particles was obtained. Discrete polymer particles were obtained in all cases. From these set of reactions it is clear that the increase in pressure inside the reactor did not have so much influence on the yield. The yield of the polymer is found to be above 81%. The higher solvency of CO$_2$ can affect the fraction of the monomer molecularly dissolve in the polymerizing medium, which has a great role in determining the size of the final polymer particles. Moreover, at higher pressure, the monomer droplets coalesces each other resulting the formation of larger particles and hence with the increase in pressure, the particle size increases. Another interesting observation that was made during these experiments involved the change in pressure during the course of the reaction. As styrene has a negative reaction volume, a decrease in pressure as the monomer is converted to polymer is expected for homogeneous solution polymerization. However, for low initial pressures we observed an increase in pressure during the course of the reaction. This is due to the thermodynamics of mixing, which favors the expulsion of the CO$_2$ and monomer from the polymer phase. The amount of CO$_2$ dissolved in the polystyrene phase increases with increase in pressure. Thus the CO$_2$ residing in the interstitial space or continuous phase for reactions conducted at lower pressure will be higher than the reactions conducted at higher pressures. As the reactions are conducted in very high pressures and CO$_2$ used in this system is roughly the same, the change in pressure might be due to different degrees of partitioning of CO$_2$ in the continuous phase and particle phase as well as the volume contraction in the polymerization reaction. Further studies are necessary in rationalizing the pressure changes in the reaction at high pressures.

The molecular weight of the polymer is in the range of (35,000-45,000 g/mol). The molecular weight is quite low in comparison to the normal free radical polymerization.
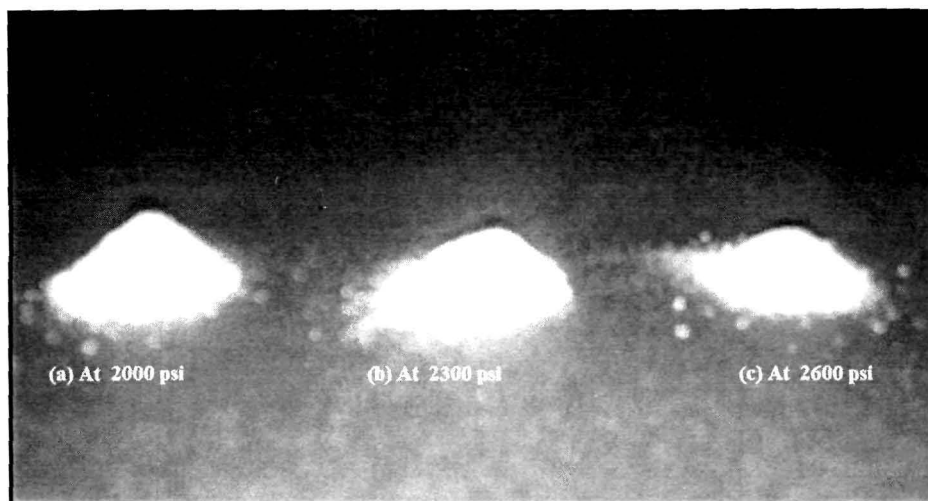
Fig.2.8. Powdered polymeric particles obtained from sc-CO$_2$ reactor

Fig.2.8. shows the powdered polymeric particles obtained directly from the sc-CO$_2$ reactor after depressurizing the CO$_2$. Generally low molecular weight polymer is obtained if the solvent acts as a chain transferring agent. But CO$_2$ is not taking part in chain transfer reactions as it is evident (Table.2.5) from the narrow polydispersity indx (1.45-1.87).[36] Weijun Ye *et al.*[35] investigated the thermal decomposition of AIBN in sc-CO$_2$ as a function of pressure. The decomposition rate of AIBN was enhanced with pressure due to the solvation effect.

Therefore it is expected the enhancement of rate of polymerization reaction in sc-CO$_2$. This enhanced rate of reaction causes the decrease in molecular weight in comparison to the normal free radical polymerization.

The SEM micrograhs of the polystyrene particles (Fig. 2.9) shows the formation of uniform sized spherical particles.
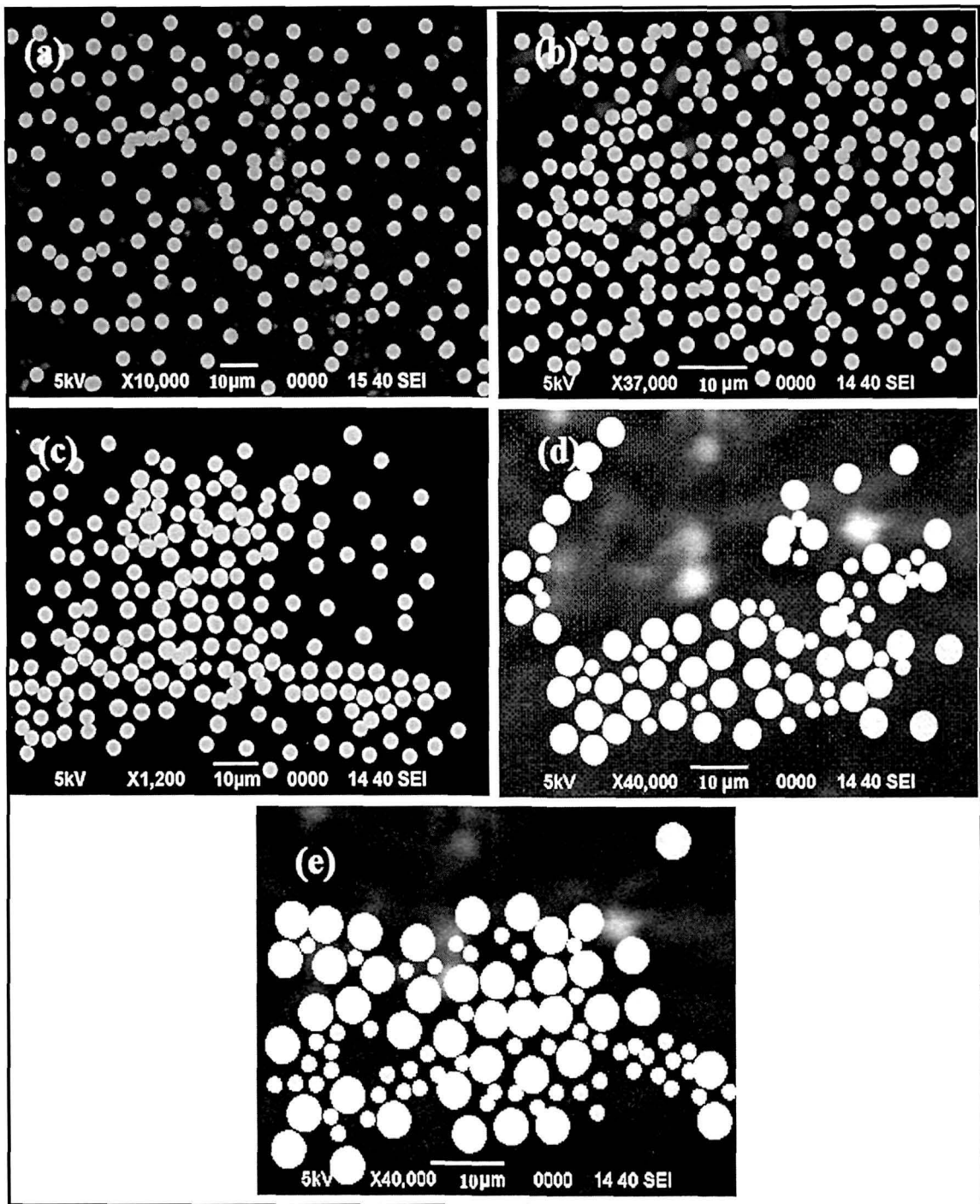
Fig.2.9. SEM micrograph of the powder polymeric particles

(a) At 2,000 psi, (b) at 2,100 psi, (c) 2,300 psi, (d) 2,500 psi and (e) at 2,600 psi

It is observed that the molecular weight gradually increases with increasing pressure (Fig.2.10). Thus controlling pressure inside the reactor in free radical emulsion polymerization, the molecular weight of the polymer particles can be controlled. The polydispersity indices of the polymer particles synthesized in sc-CO$_2$ are found to be in the range of 1.45-1.86. The polydispersity index is quite narrow which indicates less branching in the polymerization. The polydispersity index of the polymer increases with the increase in pressure.
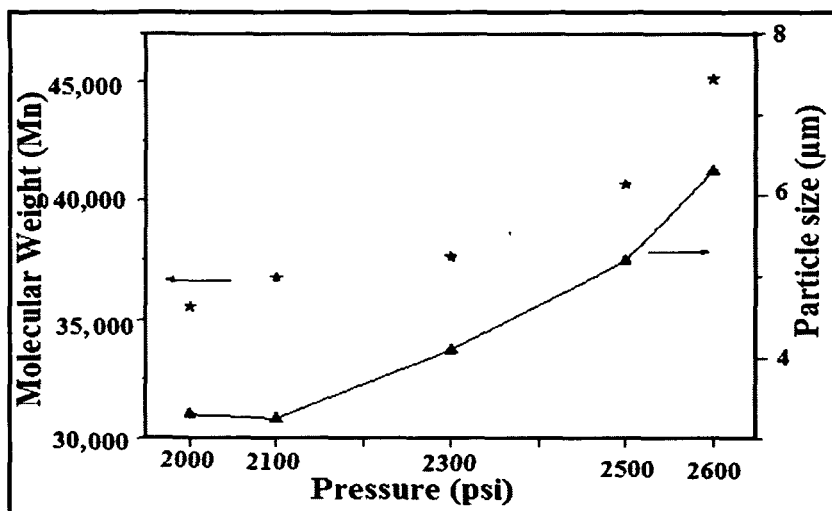
Fig.2.10: Molecular weight (M$_n$), particle size vs. pressure plot

2.5.2.3 Particle size

Fig.2.9. depicts change of particle size with the variation of pressure of polymerization. Particle size gradually increases with the pressure. At 2,000-2,300 psi, the particle sizes are in the range of 3.3-4.1 μm and particles are spherical and uniform sizes (Fig.10). At 2500 and 2600 psi, particles are in the range of 5.2-6.3 μm and a bimodal particle size distribution is observed. The high pressure facilitates the nucleation of growing particles and hence results in formation of larger particles. The higher solvency of CO$_2$ at higher pressure leads to the formation bimodal particle sizes. The operating pressure has significant effect on particle size as well as on reaction rate but not observed any particular trend on the yield of the products. The stirring speed has also significant effect on the sizes of polymer particle but this is not discussed in this thesis.

2.5.2.4 Thermal behavior

The thermal behavior of the polymer samples were studied by the Thermogravimetric analysis. TGA curves of all the polymer samples are shown in Fig. 2.11. From the TGA analysis, it can be conferred that the polymer samples show a single step degradation pattern and show a thermal stability up to 320°C.
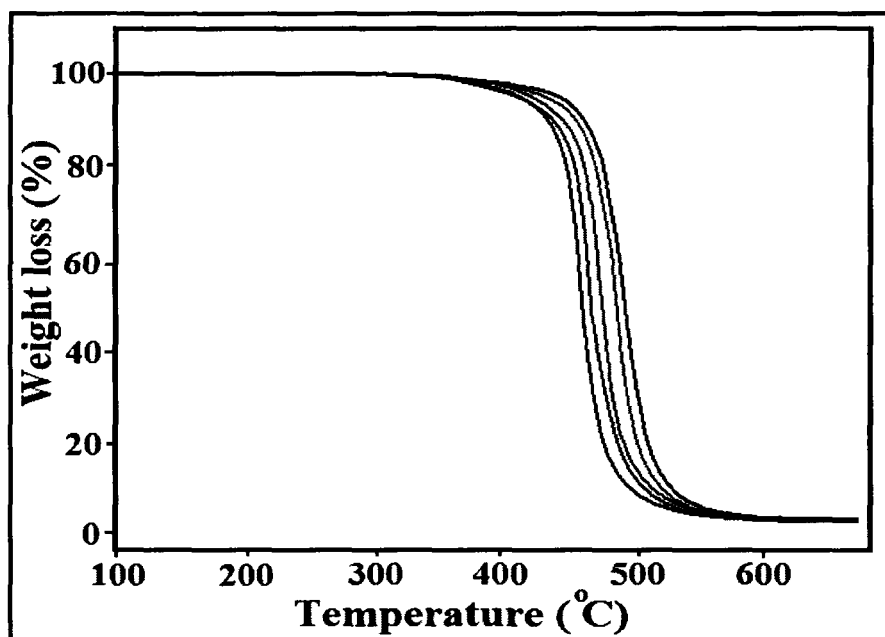
Fig. 2.11: TGA thermogram of the polymer samples

2.6 Comparison of the physical properties of the polymers synthesized by the two stabilizers (C₇F₁₄ and PDMS)

Both the stabilizers viz. (trifluoromethyl)undecafluorocyclohexane (C_7F_{14}) and polydimethylsiloxane (PDMS) are found to be good stabilizers for emulsion polymerization in sc-CO_2 medium. The yield of the product was found to be independent of the stabilizer concentration in both the cases (PDMS and C_7F_{14}). Similarly, molecular weight and polydispersity indices did not follow any particular trend with change in stabilizer concentrations (PDMS and C_7F_{14}). But, the stabilizer concentration has significant effect on the size of the polymer particles. In both the

cases, the particle size of the polymer decreases with increase in stabilizer concentrations. The morphology of the polymer products is found to be spherical in both the stabilizer systems.

2.7 CONCLUSIONS

Supercritical carbon dioxide is a versatile alternative solvent for the emulsion polymerization technique. Polystyrene microparticles in sc-CO$_2$ can be synthesized using different concentrations of initiator (AIBN) and stabilizer (trifluoromethyl)-undecafluorocyclohexane (C$_7$F$_{14}$), under different pressure at temperature 75 °C. With the increase in the stabilizer concentration from 0.2% to 10.0%, the particle size of the polymer decreases from 1.80μm to 0.25μm. As the number of surfactant/stabilizer molecule increases, the number of surfactant stabilized micelles also increases which results in the formation of smaller particle size. The increase in initiator concentration from 0.10% to 0.50%, the molecular weight of the polymer decreases from 55,000 g/mol to 45,000 g/mol and the particle size of the polymer also decreases from 4μm 1.8μm, which are in accordance with the nucleation mechanism of an emulsion polymerization. The increase in pressure of CO$_2$ (2,100-2,500 psi) did not have so much effect on the yield of polymerization. It influences the particle size, with the increasing pressure, particle size increases (2.2μm-1.0μm) and also the reaction rate during polymerization. At higher pressure, monomer droplets coalescing each other results in the larger particle size.

The powdered polystyrene micro particles of has been successfully synthesized by emulsion polymerization in supercritical carbon dioxide (sc-CO$_2$) using (polydimethylsiloxane) (PDMS) as a surfactant/stabilizer and azobisisobutyronitrile (AIBN) as initiator. It is observed that the pressure during polymerization has significant effect on the size and molecular weight and yield of the polymer particles. This technique can be easily applied for the synthesis of powdered polymeric particles to a large number of polymers. Molecular weight (M$_n$) of the polymer is in the range of

35,542 to 45,078 g/mol, polydispersity is 1.45-1.86 and particle size in the range of 3.25μm-6.3μm. The polymeric particles synthesized at higher pressure are free flowing, fine powdered in nature. These powdered particles may be used in powder coating, pigments in paint industry, packing in column for chromatography, redispersible emulsions etc. The product can be redispersed in aqueous to form stable, uniform white latex.
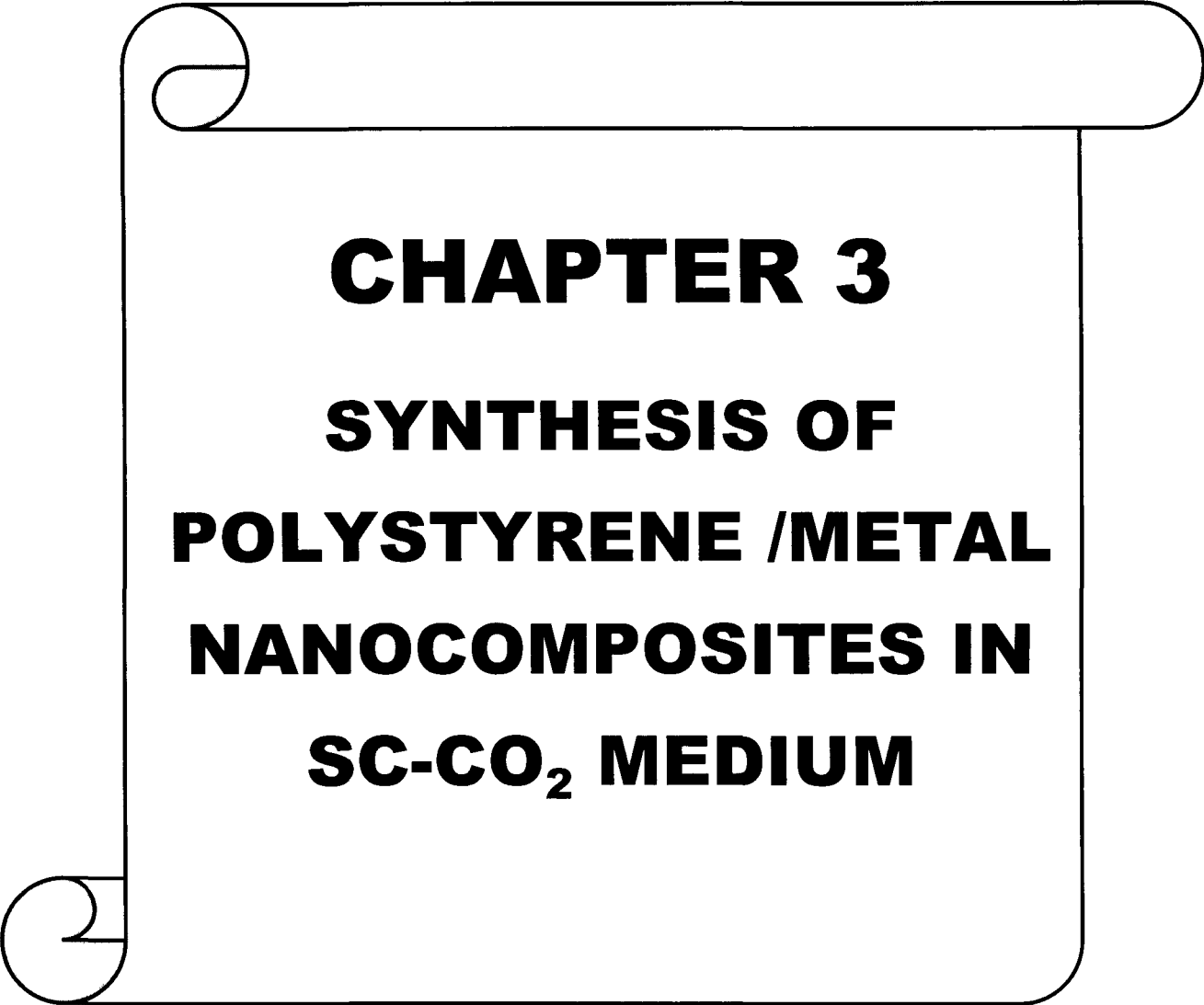
REFERENCES

1. Anikeev, V.I. Transformations of organic compounds in supercritical fluid solvents: From experiments to kinetics, thermodynamics, simulation, and practical applications, *Kinetic. and Cat.* **50**, 284-296 (2009).

2. Keskin, S; Talay, D.K.; Akman, U.; Hortacsu, O. A review of ionic liquids towards supercritical fluids, *J. Supercrit. Fluids.* **43**, 150-180 (2007)

3. Jaramillo-Soto, G. *et al.* Effect of stabilizer concentration and controller structure and composition on polymerization rate and molecular weight development in RAFT polymerization of styrene in supercritical carbon dioxide, *Polymer* **50**, 5024–5030 (2009)

4. Zhao, X. *et al.* Preparation and characterization of camptothecin powder micronized by a supercritical antisolvent (SAS) process, *J. Supercrit. Fluid.* **51**, (2010) 412–419

5. James, P. D.; Timothy, J.R.; DeSimone, J.M. *Fluoropolymers1: synthesis* 205 (2006).

6. Yue, B.; Yang, J. Particle encapsulation with polymers via in situ polymerization in supercritical CO_2, *Powder Technol.* **146**, 32–45 (2004).

7. Sze Tu, L.; Dehghani, F.; Foster, N.R. Micronisation and microencapsulation of pharmaceuticals using a carbon dioxide antisolvent, *Powder Technol.* **126**, 134-149 (2002).

8. Breitenbach, A.; Mohr, D.; Kissel, T. Biodegradable semi-crystalline comb polyesters influence the microsphere production by means of a supercritical fluid extraction technique (ASES), *J. Control. Release* **63**, 53–68 (2000).

9. Garay, I.; Pocheville, A.; Madariag, L. Polymeric microparticles prepared by supercritical antisolvent precipitation. Powder Technol. **197**, 211–217 (2010).

10. Dixon, D.J.; Johnston, K.P.; Bodmeier, R.A. Polymeric materials formed by precipitation with a compressed fluid antisolvent. *AIChE J.* **39** (1), 127–139 (1993).

11. Roderic , P.Q.; Taejun, Y.; Youngjoon, L.; Jungahn, K.; Bumjae, L. Applications of 1,1-Diphenylethylene chemistry in anionic synthesis of polymers with controlled structures, *Adv. Polym. Sci.* **153**, 70-100 (2000).

12. Reverchon, E. Supercritical antisolvent precipitation of micro- and nano-particles, *J. Supercrit. Fluid.* **15**, 1-21(1999).

13. Zhao, Y. *et al.* CO$_2$-controlled reactors: epoxidation in emulsions with droplet size from micron to nanometre scale, *Green Chem.* **12**, 452-457, (2010).

14. Urbanczyk, L. *et al.*, Batch foaming of SAN/clay nanocomposites with sc-CO$_2$: A very tunable way of controlling the cellular morphology, *Polymer* **51**, 3520-3531 (2010).

15. Kim, J.B.; Cho, K.S.; Park, S.J., Copper oxide-decorated porous carbons for carbon dioxide adsorption behaviors, *J. Colloid Interf. Sci.* **342**, 575-578 (2010).

16. Davies, O.R. *et al.* Applications of supercritical CO2 in the fabrication of polymer systems for drug delivery and tissue engineering, *Adv. Drug Delivery Rev.* **60**, 373-387 (2008).

17. Rindfleisch, F.; Dinoia, T.P.; McHugh, M.A. Solubility of polymers in supercritical CO$_2$, *J. Phys. Chem.* **100**, 15581-15587 (1996).

18. Wang, W.V.; Kramer, E.J.; Sachse, W.H. Effects of high-pressure CO$_2$ on the glass transition temperature and mechanical properties of polystyrene, *J. Polym. Sci. Polym. Phys. Ed.* **20**, 1371-1384 (1982).

19. Collins, N.J.; Bridson, R.H.; Leeke, G.A.; Grover, L.M. Particle seeding enhances interconnectivity in polymeric scaffolds foamed using supercritical CO$_2$, *Acta Biomaterialia* **6**, 1055-1060 (2010).

20. Pollak, S.; Petermann, M.; Kareth, S.; Kilzer, A. Manufacturing of pulverised nanocomposites- dosing and dispersion of additives by the use of supercritical carbon dioxide, *J. Supercrit. Fluid.* **53**, 137-141 (2010).

21. Galia, A.; Pierro, P.; Filardo, G. Dispersion polymerization of methyl methacrylate in supercritical carbon dioxide stabilized with poly(ethylene glycol)-b-perfluoroalkyl compounds, *J. Supercrit. Fluid.* **32**, 255-263 (2004).

22. Charpentier, P.A.; DeSimone, J.M.; Roberts, G.W. Continuous Precipitation Polymerization of Vinylidene Fluoride in Supercritical Carbon Dioxide: Modeling the Rate of Polymerization, *Ind. Eng. Chem. Res.* **39**, 4588-4596 (2000).

23. Tang, M.; Wen, T.Y.; Du, T.B.; Chen, Y.P. Synthesis of electrically conductive polypyrrole–polystyrene composites using supercritical carbon dioxide II. Effects of the doping conditions, *Eur. Polym. J.* **39**, 151–156 (2003).

24. Li, X.; Vogt, B.D. Impact of thickness on CO$_2$ concentration profiles within polymer films swollen near the critical pressure, *Polymer* **50**, 4182–4188 (2009).

25. Wissinger, R.G.; Paulaitis, Swelling and sorption in polymer-CO$_2$ mixtures at elevated pressures, *J. Polym. Sci. Part B: Polym. Phys.* **25**, 2497-2510 (1987).

26. Wissinger, R.G.; Paulaitis, M.E. Glass transitions in polymer/CO$_2$ mixtures at elevated pressures, *J. Polym. Sci. Part B: Polym. Phys.* **29**, 631-633 (1991).

27. Condo, P.D.; Paul, D.R.; Johnston K.P. Glass transitions of polymers with compressed fluid diluents: type II and III behavior, *Macromolecules* **27**, 365-371 (1994).

28. Shine, A.D. Phys. *Properties of Polymer Handbook*: (J. E. Mark Ed. AIP: Woodbury NY, 1996).

29. Desimone, J.M.; Guan, Z.; Elsbernd, C.S. Synthesis of fluoropolymers in supercritical carbon dioxide, *Science* **257**, 945-947 (1992).

30. Arshady, R. Suspension, emulsion and dispersion polymerization: A methodological survey, *Coll. Polym. Sci.* **270**, 717-732 (1992)

31. DeSimone, J.M. *et al.* Dispersion polymerizations in supercritical carbon dioxide, *Science* **265**, 356-359 (1994).

32. Carson, T.; Lizotte, J.; Desimone, J.M. Dispersion polymerization of 1-vinyl-2-pyrrolidone in supercritical carbon dioxide, *Macromolecules* **33**, 1917-1920 (2000).

33. Wang, W.; Naylor, A.; Howdle, S.M. Dispersion polymerizations of methyl methacrylate in supercritical carbon dioxide with a novel ester end-capped perfluoropolyether stabilizer, *Macromolecules* **36**, 5424-5427 (2003).

34. Canelas, D.A.; DeSimone, J.M. Dispersion Polymerizations of Styrene in Carbon Dioxide Stabilized with Poly(styrene-*b*-dimethylsiloxane), *Macromolecules* **30**, 5673-5682 (1997).

35. Ye, W.; DeSimone, J.M. Emulsion polymerization of N-ethylacrylamide in supercritical carbon dioxide, *Macromolecules* **38**, 2180-2190 (2005).

36. Rahul, P.B.; Kartic, C.K. Effects of intermicellar exchange rate on the formation of silver nanoparticles in reverse microemulsions of AOT, *Langmuir* **16**, 905-910 (2000).

37. Gardon, J.L. Emulsion polymerisation ii: Review of experimental data in the context of the revised Smith-Ewart theory. J. Polym. Sci. A **6**, 643-664 (1968).

38. Smith, W.V.; Ewart, R.W. Kinetics of emulsion polymerization, *J. Chem. Phys.* **16**, 592-601 (1948).

39. Hansen, F.K.; Ugelstad, J. Particle nucleation in emulsion polymerization. I. A theory for homogenous nucleation, *J. Polym. Sci. Part A: Polym. Chem.* **16**, 1979 (1978).

40. Shiho, H.; DeSimone, J.M. Dispersion polymerization of acrylonitrile in supercritical carbon dioxide, *Macromolecules* **33** (**5**), 1565-1569 (2000).

CHAPTER 3

SYNTHESIS OF POLYSTYRENE /METAL NANOCOMPOSITES IN SC-CO$_2$ MEDIUM

Synthesis of metal (Ag, Cu) nanoparticles and their nanocomposites with polystyrene using water in (sc-CO$_2$) medium

3.1 Introduction

Polymer/metal nanocomposites have been receiving great scientific interest because of their effectiveness in catalysis and antibacterial activity.[1-6] The antibacterial potential of metal nanoparticles (Ag, Cu etc.) allures the global scientific community to use this property for the welfare of mankind. There are numerous methods available in literature for the preparation of metallic nanoparticles. The synthesized nanoparticles cannot be directly used for the antimicrobial purpose without any support. Polymer molecules are found to be very effective support for the stabilization of nanoparticles. The application of nanoparticles varies widely on the basis of its physical properties like apparent density, surface area and morphology and these are strongly related to the method of preparation.[7]

Supercritical carbon dioxide (sc-CO$_2$) has been attracting interest as a polymerization and processing medium, primarily driven by the need to replace conventional solvents with more environmentally benign and economically viable systems.[8] It is an attractive substitute for the organic non-polar solvents for a variety of reactions.[9-17] It possesses many advantages like non-flammability, high diffusivity, low cost, low viscosity, compressibility nature etc..[18-34]

Moreover, the product can easily be separated by depressurizing CO$_2$. Many reagents/chemicals are insoluble in CO$_2$, but they can easily be emulsified in sc-CO$_2$ by selecting proper fluorinated or siloxane-based surfactants/stabilizers.[35,36]

Johnston et al.[37] pioneered the preparation of stable microemulsion of water in sc-CO$_2$ (w/c) by incorporation of fluorinated perfluoropolyether (PFPE) stabilizers. Fluorinated stabilizers cover the water droplet which prevents Van-der-Waals force of attraction for coalesce of droplets. Many stabilizers/surfactants like polydimethyl siloxane (PDMS), Perfluoropolyether (PFPE), Sodium bis(3,5,5-trimethyl-1-hexyl)sulfosuccinate (AOT-TMH), (trifluoromethyl)undecafluorocyclo-hexane (C$_7$F$_{14}$) etc. are found to be suitable for the formation of stable micro emulsion of water in CO$_2$ (w/c).[38,39] Micellar droplets possess a dynamic exchange of their contents that facilitates the reaction between reactants dissolved in different droplets. The micellar exchanges have been used to synthesize size controlled crystallites by carrying out a wide variety of reactions in nanodroplets. Water in sc-CO$_2$ is utilized for the synthesis of nanoparticles (like Ag, Cu, Pd, Cd etc.).[40] The antibacterial potential of nano sized particles (Ag, Cu etc.) is a subject of great interest to chemists in the recent years. The synthesis and dispersion of Cu nanoparticles in water-in supercritical carbon dioxide (sc-CO$_2$) microemulsion using a surfactant system consists of a mixture of sodium bis (2-ethylhexyl)sulfosuccinate with a fluorinated cosurfactant, a perfluoropolyether surfactant phosphate ether was reported by Min Je et al..[41] The synthesis of copper nanoparticles in water in sc-CO$_2$ medium was studied by Hiroyuki Ohde et al..[42]

DeSimone et al.[43] pioneered the dispersion polymerization of methyl methacrylate in sc-CO$_2$. The CO$_2$-soluble fluorinated homo-polymer [poly (dihydroperfluorooctyl acrylate) PFOA] was used as a stabilizer for the polymerization reaction. Dry, free flowing and powdered polystyrene microparticles can be synthesized by emulsion polymerization using polydimethylsiloxane (PDMS) stabilizer in supercritical carbon dioxide medium.[39] The operating pressure has sound effect on monomer conversion, molecular weight, particle size and on polydispersity index of the

polymer microparticles. Similarly, the same reactions by emulsion polymerization of styrene in supercritical carbon dioxide medium can be carried out using fluorinated stabilizer.[44] Zhang et al.[45] reported the synthesis of polystyrene nanospheres immobilized with silver nanoparticles by using compressed CO$_2$ as the medium and AOT as the stabilizer. Yang et al.[46] used an organometallic precursor complex to synthesize hybrid metal–polymer nanocomposites based on in situ free radical suspension and bulk polymerization.

Horsch et al.[47] studied the synthesis of clay/polymer nanocomposites in sc-CO$_2$ by dispersing nanoclays within the polymer matrix. It was observed that the extent of clay dispersion in sc-CO$_2$ medium was dependent on the CO$_2$-philicity of the nanoclay layers. Wong et al.[48] prepared gold/silica nanocomposites in sc-CO$_2$ medium. They observed that the average size of gold particles was in the range of 3.7-6.6 nm. Following the similar procedure, gold nanoparticles was dispersed within a wide number of polymers like polyamide, polypropylene and poly (tetrafluoroethylene) (PTFE) in sc-CO$_2$. Wallace et al.[49] reported the synthesis of Ag colloid from AgNO$_3$ under microwave irradiation. They showed that the Ag nanoparticles could direct the self assembly of different protein superstructures. Thirumurgan et al.[50] studied the antibacterial activity of silver nanoparticles against several pathogenic bacteria at a concentration of 5μg/ml. Silver nanoparticles showed very good antibacterial activity against a number of pathogenic bacteria. Though the use of supercritical carbon dioxide (sc-CO$_2$) for the synthesis of nanoparticles/nanocomposites is a common green practice, but limited literatures are available on the antibacterial activity of nanocomposites particles synthesized in water-in-sc-CO$_2$ medium.

This chapter describes the synthesis and characterization of metal nanoparticles like Ag and Cu using water in supercritical carbon dioxide (sc-CO$_2$) medium, nanoparticles encapsulated polystyrene particles and its antibacterial activity etc. Polydimethylsiloxane (PDMS) was used as stabilizer and sodium borohydrate (NaBH$_4$) was used as the reducing agent in the synthesis of metal nanoparticles. The synthesized

metal nanoparticles (Ag, Cu) were encapsulated into polystyrene particles in supercritical carbon dioxide (sc-CO_2) medium. The antibacterial activity of these nanocomposites particles are also described elaborately in this chapter.

3.2 Experimental

3.3 Materials

Silver nitrate ($AgNO_3$) (Aldrich), Copper chloride ($CuCl_2$) (Aldrich), sodiumborohydrate ($NaBH_4$) (Merck), Sodium bis (2-ethylhexyl)sulfosuccinate (Aldrich), Sodium (bis-2ethylhexyl) sulfosuccinate (AOT), Sodium dodecyl sulfate (SDS) (Aldrich) and polydimethylsiloxane (PDMS) (Fluka) were used as received. Styrene (Merk) was washed with 10% NaOH solution and then double distilled water to make inhibitor free. Azobisisobutyronitrile (AIBN) (Allied Industries, Bombay) was recrystallized twice from methanol. Carbon dioxide (SCF/SFE Grade) (99.99 %pure) (Rass Chryogenics) was used as received.

3.4 Apparatus

All experiments were carried out in a 60 ml, high-pressure stainless steel reactor (SCF-System, Reaction Eng. Inc. Korea). The schematic diagram of the apparatus is shown in Fig.3.1.
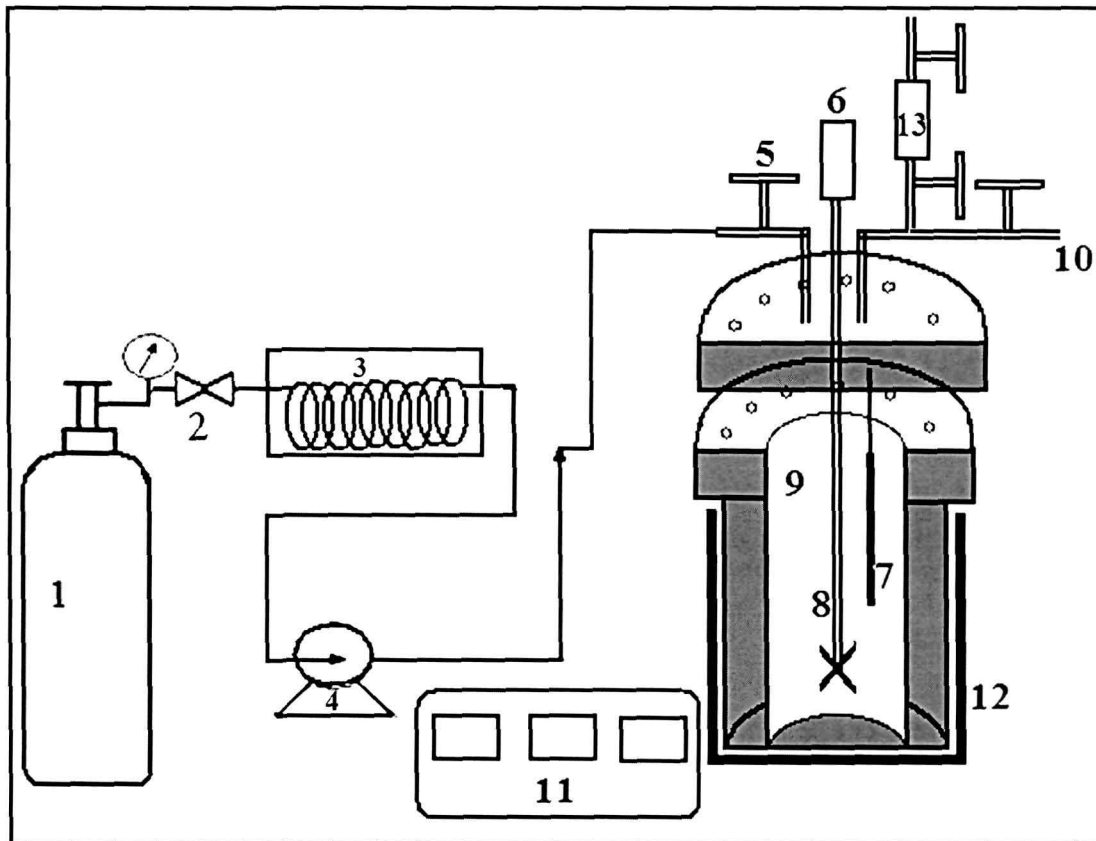
Fig.3.1: Schematic diagram of the reactor

1. Carbon dioxide cylinder 2. Back pressure valve 3. Refrigeration Unit 4. High pressure liquid Pump 5. Pressure valve 6. Motor for mechanical stirrer 7. Heating probe 8. Mechanical stirrer 9. SFE Vessel 10. Vent 11. Digital display unit. 12. Heating jacket 13. Specially designed dropper

The SCF equipment was connected with the high pressure CO_2 cylinder, a high pressure metering pump and an efficient cooler. There is a provision for continuously addition of reactants to the reactor during the reaction at high pressure (13 in Fig. 1). The pressure inside the reactor can be raised upto 6,000psi. The pressure inside the reactor was measured with a pressure transducer.

3.5 Procedure

3.5.1 Synthesis of Ag nanoparticles using water in supercritical Carbon dioxide (sc-CO$_2$) medium

Silver nitrate (AgNO$_3$) with a concentration of 0.03 mol/L and sodium borohydrate (NaBH$_4$) with a concentration of 0.02-0.05 mol/L in water was prepared. 10 ml of silver nitrate solution, 0.2 ml of polydimethylsiloxane (PDMS) and 0.25 g SDS were taken in a round bottom flask and it was mixed thoroughly by stirring. The solution was then purged into the stainless steel sc-CO$_2$ reactor. The pressure inside the reactor was raised up to 2,000 psi and the temperature was raised to 45 °C. The sodium borohydrate solution was then added slowly dropwise into the AgNO$_3$ solution. The solution was stirred with a rotation speed of 900 rpm and the process was conducted for 4 h. After depressurizing the CO$_2$, the brown colloid containing silver nanoparticles was collected.

3.5.2 Synthesis of Cu nanoparticles in supercritical Carbon dioxide (sc-CO$_2$)

Copper (II) Chloride (CuCl$_2$) with a concentration of 0.03 mol/L and sodium borohydrate (NaBH$_4$) with a concentration of 0.02-0.05 mol/L in water was prepared. To the 10ml of copper chloride solution, 0.2 ml of polydimethylsiloxane (PDMS) and 0.20 g sodium-bis-(2-ethylhexyl) sulfosuccinate (AOT) were added and it was mixed thoroughly by stirring. The solution was then purged into the stainless steel reactor of the SCF reactor. The pressure inside the reactor was raised upto 2,000 Psi and the temperature was raised to 40°C. The sodium borohydrate (NaBH$_4$) solution was then added slowly dropwise into the CuCl$_2$ solution. The solution was agitated vigorously with the help of a magnetically coupled mechanical stirrer at a rotation speed of 700 rpm and the reaction was allowed for 4 h. When the reaction got completed, colloid containing Cu nanoparticles was collected by slowly depressurizing the reactor CO$_2$. All the reactions were repeated twice to get the reproducibility of the experiments.

3.5.3 Synthesis of Ag/PS nanocomposite particles

Polydimethylsiloxane (PDMS) and AIBN were mixed thoroughly in double distilled water in a round bottom flask. Styrene monomer was added slowly to the mixture and stirred vigorously to make a pre-emulsion. The pre-emulsion was purged into the SCF reactor. The reactor was filled with CO_2 and the pressure inside the reactor was raised to 20.68 MPa. The temperature inside the reactor was set at 75°C and stirred at a rotation speed of 900 rpm. After half an hour, the dispersed Ag nanoparticles were added slowly to the reaction mixture and the reaction was allowed to continue for 8 h. The reactor was depressurized and the milky white emulsion was separated from the reactor as soon as the polymerization reaction was over. The emulsion was precipitated in methanol and washed thoroughly with water and ethanol for several times. The whole reaction was repeated at various pressures upto 3,500 psi and with different amounts of Ag nanoparticle dispersions. Each experiment was repeated to ensure reproducibility of the results.

3.5.4 Synthesis of Cu/polystyrene nanocomposite particles

In a typical reaction, polydimethylsiloxane (PDMS) and AIBN were mixed thoroughly in double distilled water in a round bottom flask. To this mixture, styrene monomer was added with vigorous stirring for the preparation of pre emulsion. The pre emulsion was then purged into 60 ml stainless steel reactor. The reactor was filled with CO_2 and the pressure inside the reactor was raised upto 20.68 MPa. The temperature inside the reactor was set at 75°C and the stirred at a rotation speed of 900 rpm. After half an hour, the stable dispersion of Cu nanoparticles (0.5% V/V of dispersed Cu nanoparticles solution with respect to monomer) was added dropwise to the reaction mixture. The concentration of Cu nanoparticles in the nanocomposite was varied from 0.5% -1.5% (V/V of the stable dispersion with respect to monomer). The reaction was continued for 8 h. After polymerization, the reactor was depressurized and the milky white emulsion was separated from the reactor. The emulsion was precipitated out in

94

methanol and washed thoroughly with water and ethanol for several times. The whole reaction was performed at various pressures upto 3,400 psi. Each reaction was repeated twice to obtain the reproducible data.

3.6 Characterization

3.6.1 UV-Visible spectrophotometer

The UV-Visible (UV-Vis) spectrophotometer provides information about structure and stability of the materials in solution. Various kinds of electronic excitation may occur in organic molecules by absorbing the energies available in UV-Vis region. The spectrophotometer records the wavelengths at which absorption occurs, together with the degree of absorption at each wavelength. The resulting spectrum is presented as a graph of absorbance versus wavelength. UV-Visible spectra were recorded on a HitachiU-2001 UV-visible spectrophotometer.

3.6.2 X-ray diffraction

X-ray diffraction (XRD) technique gives the information about the crystallographic structure, chemical composition and physical properties of the materials. X-ray diffraction technique is based on the elastic scattering of X-rays from structures that have long range order. XRD data were collected on a Rigaku Miniflex X-ray diffractometer Cu Kα radiation (λ=0.15418nm) at 30 kV and 15mAmp, with a scanning rate of 0.05 degree/sec in 2θ ranges from 10° to 90°.

3.6.3 SEM analysis

SEM analysis of the polymer particles were obtained from Jeol-Jsm-6390LV scanning electron microscope (SEM). For SEM analysis, samples were mounted on an aluminum stub using an adhesive carbon tab and were coated with platinum to a

95

thickness of 200 A$^\circ$ in high vacuum. SEM analysis gives the morphology of the polymer particles.

3.6.4 TEM analysis

TEM analysis of the nanoparticles and the nanocomposites was studied using JEOL, JEMC XII transmission electron microscopy (TEM) at an operating voltage of 80 kV. For TEM analysis, 2-3 drops of the emulsion were transferred on to a 3 mm diameter carbon coated copper grid. The solvent was allowed to evaporate at room temperature before loading the sample in the microscope. Conventional bright field imaging was used to observe the particle morphology with diffraction patterns.

3.6.5 Thermogravimetric analysis (TGA)

Thermogravimetric analysis (TGA) reveals the thermal characteristics of polymers including degradation temperature, absorbed moisture content, the level of oligomer in polymer etc. It determines the weight loss with respect to temperature. Thermogravimetric analysis (TGA) was conducted on a Shimadzu TGA-50 thermo gravimetric analyzer with a heating rate of 5° C/min under nitrogen atmosphere. Analysis was performed at 0-500 °C temperature range.

3.6.6 Antibacterial activity test

Four bacterial strains Pseudomonas fluorescens *BS3*, Bacillus circulens *BP2*, Eschericia coli and Staphylococcus aureus strains were selected for the experiment. The test organisms were grown on nutrient agar plates by evenly spreading over the entire surface of the agar plates. After the agar surface was dried, 50 µl of the test nanocomposite samples i.e., 0% Ag/Cu (a), 0.5% Ag/Cu (b), 1.0% Ag/Cu (c) and 1.5% Ag/Cu (d) were placed on each bacterial colony and each experiment was repeated thrice. The antibacterial activity was determined by measuring the diameter of the zone

of inhibition to the nearest mm of the well on the plate. Wider the zone surrounding the well more is the susceptibility of the test organism to the nanocomposite. The antibacterial activity test was performed only for qualitative and comparative purposes.

3.7 Result and discussion

It is well known that weak intermolecular forces, such as van der Waals attraction, H-bonding, π-π interaction etc. are responsible for the aggregation of nanoparticles.[51] The synthesis of metal nanoparticles is very sensitive to many experimental conditions like temperature, concentration of the reactants, and the rate of addition of the reactants.[52] The formation of nanoparticles can be tracked by UV-visible spectra of the solutions. Water-in-sc-CO_2 offers an excellent medium to synthesize metal nanoparticles and their nanocomposites. Our experiment involved preparation of Ag-nanoparticles by the reduction of $AgNO_3$ with $NaBH_4$ and preparation of Cu nanoparticles by reduction of $CuCl_2$ with $NaBH_4$ in the water-in-sc-CO_2 medium. After completion of the reaction, CO_2 is depressurized and finally a stable colloidal dispersion of Ag and Cu nanoparticles in water is obtained. The dispersion is kept at room temperature for observing stability of the dispersion and it is found to be stable up to 60 days. UV-visible spectra, WAXD diffractogram and the TEM micrograph confirm the formation and dispersion of Ag nanoparticles.

3.7.1 Synthesis of Ag nanoparticles using water in supercritical carbon dioxide (sc-CO₂) medium

The synthesized silver nanoparticles using water in sc-CO_2 medium are characterized by different techniques like UV-visible spectroscopy, XRD, TEM and STM analysis. The UV-visible spectroscopic analysis shows absorption peak at 400-430 nm due to surface Plasmon of the silver nanoparticles. The synthesis of Ag nanoparticles was carried out by varying the amount of stabilizer from 0.1 ml to 0.25 ml and pressure from 2,000 psi to 2,500 psi. This dispersion was kept at room temperature

for observing stability of the dispersion. It was observed that the dispersion was stable up to 90 days with 0.2 ml stabilizer and 0.25 g SDS. The stability of the dispersion of Ag nanoparticles synthesized at different stabilizer concentration and different pressures are summarized in Table.3.1.

Table.3.1: Experimental conditions for the synthesis of Ag nanoparticles

Sample no.	PDMS(ml)	Pressure(Psi)	Temp.(^{o}C)	Stability of Dispersion
1	0.2	2000	45	Stable for 90 Days
2	0.2	2300	45	Stable for 90 Days
3	0.2	2400	45	Stable for 90 Days
4	0.2	2500	45	Stable for 90 Days
5	0.25	2400	45	Stable for 90 Days
6	0.1	2300	45	Stable for 30 Days
7	0.13	2300	45	Stable for 45 Days
8	0.15	2300	45	Stable for 60 Days

(In all the reactions, water to surfactant (SDS) ratio was constant, Rotation per minute = 700 rpm)

At lower stabilizer concentration (0.1ml), the dispersion was stable upto 30 days (Table.1). However the pressure has no significant effect on the stability of dispersion at room temperature. It was observed that if the reaction was performed using SDS surfactant (without adding the PDMS stabilizer) in the sc-CO$_2$, the particle size was larger and irregular in size and shape and the dispersion was not stable for a long time.

3.7.1.1 UV Visible Spectroscopic Analysis

The UV-Visible spectroscopic analyses were carried out in the wavelength range of 250-800 nm and are shown in Fig.3.2. The analysis of the various samples showed the absorption peak in a region of 400-430 nm, which confirms the formation of silver nanoparticles. In all the above experiments (Table.3.1) the absorption peak was found to be in the range of 400-430 nm.
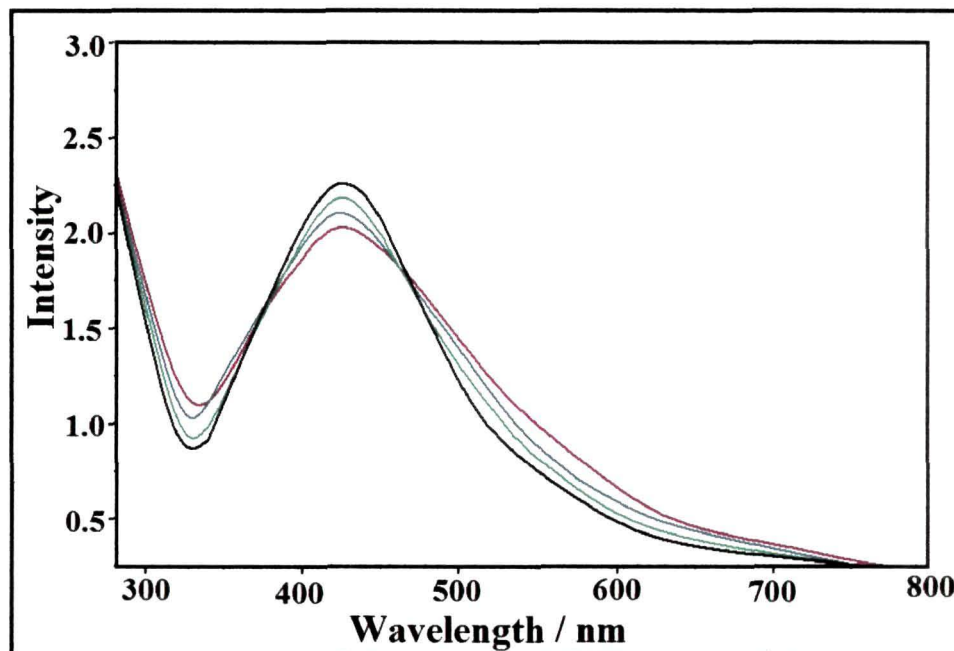
Fig.3.2: UV-Visible spectra of the Ag nanoparticles

3.7.1.2 XRD Analysis

The WAXD pattern of the synthesized Ag nanoparticles shows a cubic crystal structure. The major strong characteristic peaks of Ag nanoparticles are at $2\theta=38.16°$, $44.28°$, $64.38°$and $77.74°$, which are in consistent with crystal faces of (111), (200), (220) and (311) of Ag (Fig.3.3). All these reflection peaks could be indexed to face-centered cubic (FCC) silver and the results indicate that Ag nanoparticles prepared in water-in-sc-CO$_2$ did not change the crystalline structure of neat Ag nanoparticles. According to the full width at half-maximum of the diffraction peaks, the average size of the particles could be estimated from the Scherrer equation (equation no. 1) to be about 5.3 nm[reaction conditions: t=45 °C, c(AgNO$_3$)= 0.033 mol/L]. These results are in consistent with the TEM images.

99
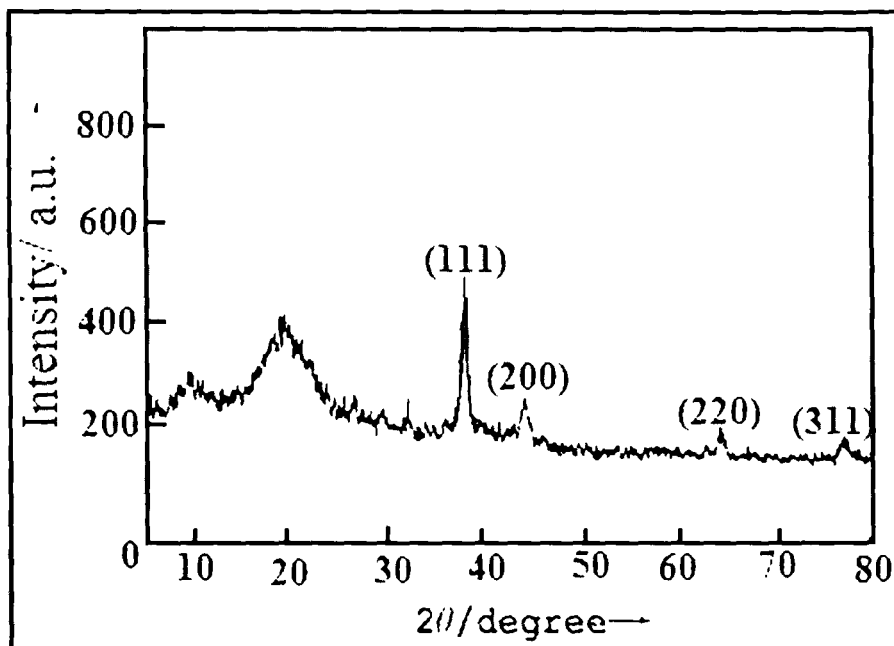
Fig.3.3: WAXD pattern of the Ag nanoparticles

The particle size calculation was performed by using the Scherrer's formula.

$$t = K\lambda / B\cos\theta \qquad \text{----------------} (1)$$

Where t is the mean dimension of the Ag nanoparticles, B is the corrected X-ray diffraction broadening, K is a constant dependent on crystalline shape, and θ is Bragg angle.

3.7.1.3 TEM Analysis

TEM image of the prepared silver nano particles is shown in the Fig.4. The Ag nano particles are spherical in shape with a smooth surface morphology. The diameter of the nano particles is found to be approximately 5-15 nm. The nano particles are more or less uniform in size and shape.
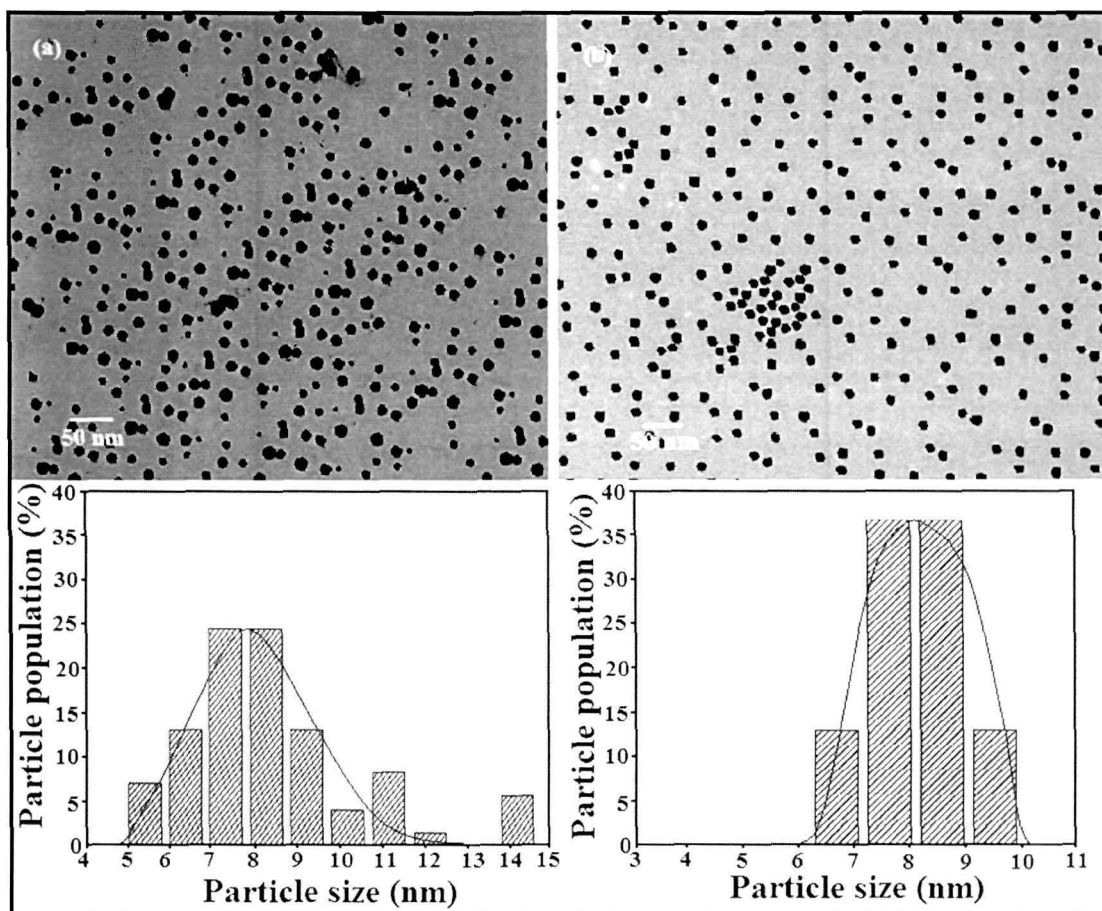
Fig.3.4: TEM image of the Ag nanoparticles

(a) at 2,500 psi and (b) at 2,000 psi

The TEM micrograph shows that the nanoparticles are smaller, discrete and uniform at lower pressure (2,000 psi) (Fig.3.4.b). At higher pressure (2,500 psi), (Fig.3.4.a) nanoparticles are agglomerated. At higher pressure the concentration of the solution increases, so the size of the nanoparticles formed is larger in size and also irregular in shape. The bar diagrams shows the particle size distributions at pressure 2,000 psi and 2,500 psi. The nanoparticles at lower pressure (b) are of more uniform in size (6-10 nm) than at higher pressure (a) (5-15 nm).

3.7.1.4 STM Analysis

The surface morphology of the synthesized nanoparticles was analyzed by tapping mode – Scanning Tunneling Microscopy (STM) analysis (Fig.3.5). The surface of the film shows randomly distributed tunneling current in regions of 20 nm in dimension.
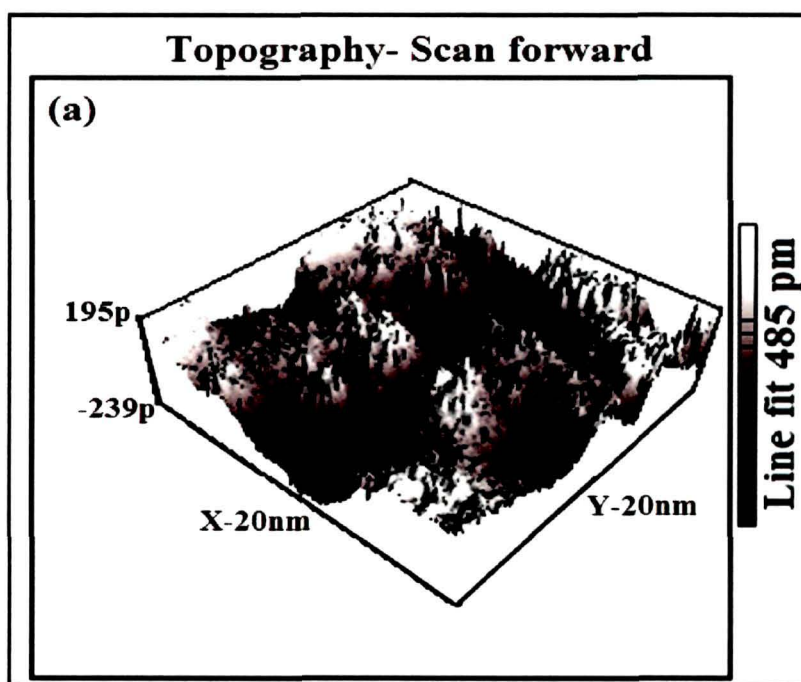
Fig.3.5: STM image of the Ag nanoparticles

3.7.2 Synthesis of Cu nanoparticles in supercritical Carbon dioxide (sc-CO₂)

In this experiment, we have used PDMS as stabilizer along with AOT surfactant for stabilizing the dispersion of the Cu-nanoparticles and observed that these nanoparticles dispersion are stable up to 60 days. Cu nanoparticles are formed by the chemical reduction of $CuCl_2$ with $NaBH_4$ in water in sc-CO₂ medium. The surfactant AOT covers the nanoparticles by forming micro emulsions and thereby controls the size of the size of the particles. The agglomeration of these nanoparticles is restricted by an

102

extra cover formed by the stabilizer PDMS which is compatible with CO$_2$. After formation of nanoparticles the CO$_2$ is depressurized, although some amount of CO$_2$ still dissolved in the colloid that are directly linked with the stabilizer PDMS. AOT molecules dissolved in water medium interact with the nanoparticles by van der Waals interaction to form stable micro emulsion in water. Simultaneously, PDMS also covers the microemulsions to aid extra stability to the nanoparticles in water medium.

PDMS is a non-polar, hydrophobic polymer and found to be one of the best stabilizers for stabilizing the microemulsions in the sc-CO$_2$ medium.[39] The stability of these colloidal dispersions containing Cu nanoparticles is found to be up to 60 days (Table 2). But simply taking AOT as a surfactant/stabilizer, it is observed that the dispersion can be stabilized only for a short period of time. It is the PDMS (along with AOT) stabilizer system which is responsible for stabilizing the nanoparticles in water in sc-CO$_2$ medium.

Table.3.2: Experimental conditions for the synthesis of Cu nanoparticles

Sample	PDMS (mL)	Pressure(psi)	Temp(^{o}C)	Stability of Dispersion
1	0.2	2,000	40	Stable for 60 Days
2	0.2	2,300	40	Stable for 60 Days
3	0.2	2,400	40	Stable for 60 Days
4	0.2	2,500	40	Stable for 60 Days
5	0.25	2,400	40	Stable for 90 Days
6	0.1	2,300	40	Stable for 30 Days
7	0.13	2,300	40	Stable for 40 Days
8	0.15	2,300	40	Stable for 50 Days

(In all the reactions, the water to surfactant (AOT) ratio was constant, Time 4 h and RPM=700)

UV-visible spectra show absorption at 560-590 nm due to surface plasmon transition of the Cu nanoparticles. The synthesis of Cu nanoparticles was carried out using different amount of stabilizer 0.1ml to 0.25 ml and pressure was varied in the range 2,000 psi to 2,400 psi. This dispersion is kept at room temperature for observing stability of the

dispersion. It was observed that the dispersion is stable for 60 days with 0.2 ml stabilizer. At lower stabilizer concentration (0.1ml), the dispersion is stable up to 30 days (Table 2). However the pressure has no significant effect on the stability of the dispersion at room temperature. If the reaction is performed using AOT surfactant (without adding the PDMS stabilizer) in the sc-CO₂, the particle size is larger in size and irregular in shape and the dispersion is not stable for long period. PDMS is a non-polar, hydrophobic polymeric stabilizer which is used in the dispersion polymerization for synthesizing polymer microparticles in sc-CO₂ in earlier all works. Here, we have used PDMS stabilizer for stabilizing metal nanoparticles synthesized in water in sc-CO₂ in presence of AOT surfactant and observed that it acts as a very good stabilizer in stabilizing metal nanoparticles.

3.7.2.1 UV-visible spectroscopic analysis

The UV-visible spectroscopic analyses of the stable dispersion of Cu nanoparticles were carried out in the 400-800 nm range and the curves are shown in Fig. 3.6. The analyses of the various samples show the absorption peak in a region of 560-590 nm, which confirms the formation of Cu nanoparticles. In all the above experiments (Table. 1) the absorption peak was found to be in the range of 560-590 nm.
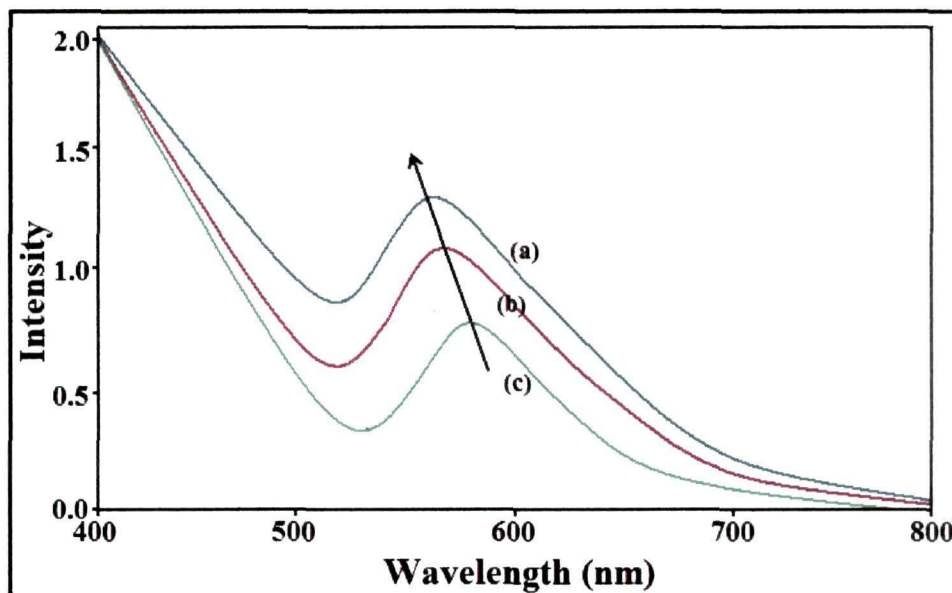
Fig.3.6: UV-visible spectra of the Cu nanoparticles

From the UV-visible spectroscopic analysis we have observed a characteristic blue-shift with the decrease in pressures, 2,500 psi - 2,000 psi. This may be due to the formation of smaller and uniform particles formed with the decrease in pressure, which is in consistent with the TEM images. At lower pressures, the size of the nanoparticles is smaller than at higher pressures.

3.7.2.2 XRD Analysis

The XRD analysis of the synthesized Cu nanoparticles shows a cubic crystal structure and is shown in Fig.3.7. The major strong characteristic peaks of Cu nanoparticles are at $2\theta=43.16°$, $50.28°$ and $74.74°$, which were in consistent with crystal faces of (111), (200) and (220) of Cu. All these reflection peaks could be indexed to face-centered cubic (FCC) copper and the results indicate that Cu nanoparticles prepared in water-in-scCO$_2$ did not change the crystalline structure of neat Cu nanoparticles.

105
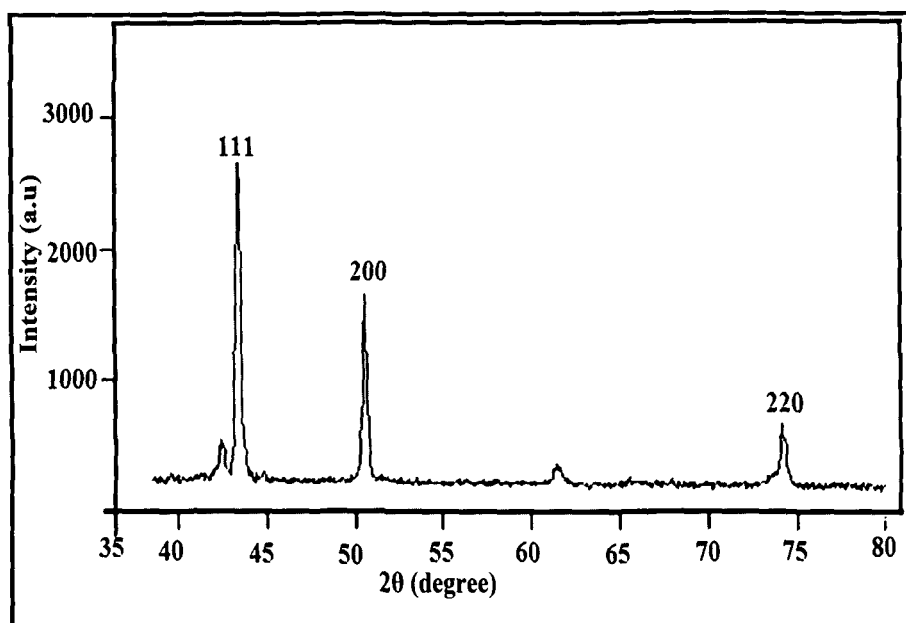
Fig.3.7: XRD pattern of the Cu nanoparticles

The lattice constant is calculated to be 3.614 A° which is in good agreement of pure copper crystals.[53] The crystalline size distribution is determined from the analysis of line broadening method using Schrrer equation.[54] According to the full width at half-maximum of the diffraction peaks, the average size of the particles could be estimated from the Scherrer equation (equation no. 1) to be about 4.8 nm for nanoparticles synthesized at lower pressure, 2,000 psi [reaction conditions: t=40 °C, c(CuCl$_2$)= 0.033 mol/L]. These results are in consistent with the TEM images.

The particle size calculation was performed by using the Scherrer's formula.

$$t = K\lambda/(B\cos\theta) \quad \text{-----------------(1)}$$

Where t is the mean dimension of the Cu nanoparticles, B is the corrected X-ray diffraction broadening, K is a constant dependent on crystalline shape, and θ is Bragg angle. The calculation yields an average particle dimension of 8 nm in diameter at higher pressure (2,400 psi). These values are also in good agreement with the TEM results.

106

3.7.2.3 TEM Analysis

A TEM image of the prepared Cu nanoparticles is shown in the Fig.3.8. The Cu nano particles are spherical in shape with a smooth surface morphology. The diameter of the nano particles (Fig.3.8.a) synthesized at higher pressure (2,400 psi) is found to be approximately 6-8nm and the nanoparticles (Fig.3.8.b) synthesized at lower pressure (2,000 psi) is found to be 4-5 nm. TEM image also shows that the produced nano particles are uniform in size and shape.
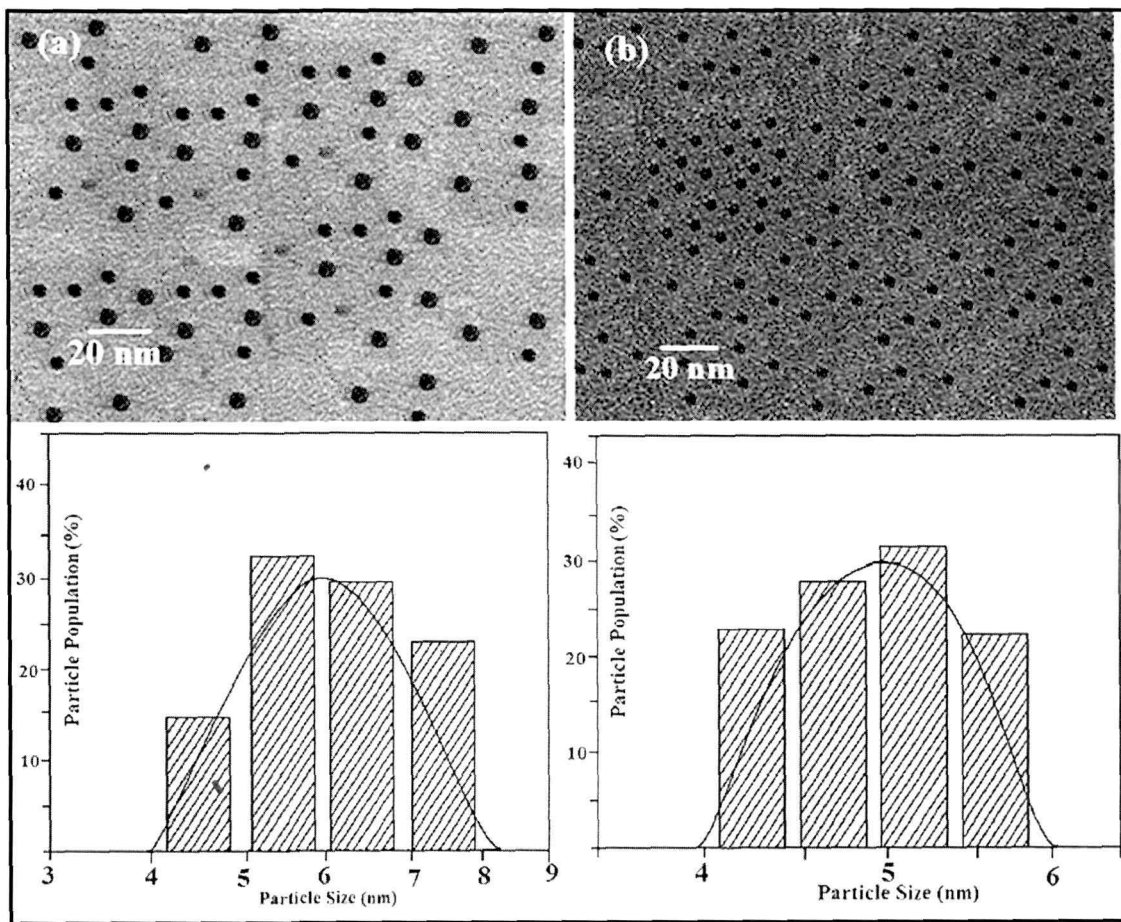
Fig.3.8: TEM image of the Cu nanoparticles (a) at 2,400 psi and (b) at 2,000 psi

The TEM micrograph shows that the particle size of the nanoparticles is smaller, uniform and discrete at lower pressure (2,000psi) than at higher pressures (2,400psi). At

higher pressure the concentration of the solution increases, so the size of the nanoparticles formed is larger and also irregular in shape. The bar diagrams show the particle size distributions at pressure 2,000 psi and 2,400 psi. The nanoparticles that were formed at lower pressure (b) are of more uniform in size (4-5nm) than at higher pressure (a) (6-8nm).

Cu nanoparticles without stabilizers represent typical lyophobic colloids with very low steadiness. That is why high molecular compounds and various substances are used to stabilize nanoparticles. For the nanoparticles synthesized in water in sc-CO_2 medium, PDMS is found to be the best stabilizer. As a result of such steric stabilization, nanoparticles turn out to be enveloped by a preserving barrier consisting of a continuous layer of long solvate polymer chains. The colloidal system becomes absolutely stable unless the protecting layers get damaged. The stabilizer PDMS along with the surfactant AOT makes aids the colloidal dispersion an extra stability for which it is stable upto two months.

3.7.2.4 STM Analysis

The surface morphology of the synthesized nanoparticles was analyzed by tapping mode-Scanning Tunneling Microscopy (STM) analysis and is shown in Fig.3.9. The surface of the film shows randomly distributed tunneling current in regions of 20 nm in dimension. A three dimensional STM image of the colloid containing Cu nanoparticles is shown in Fig.3.9.

108
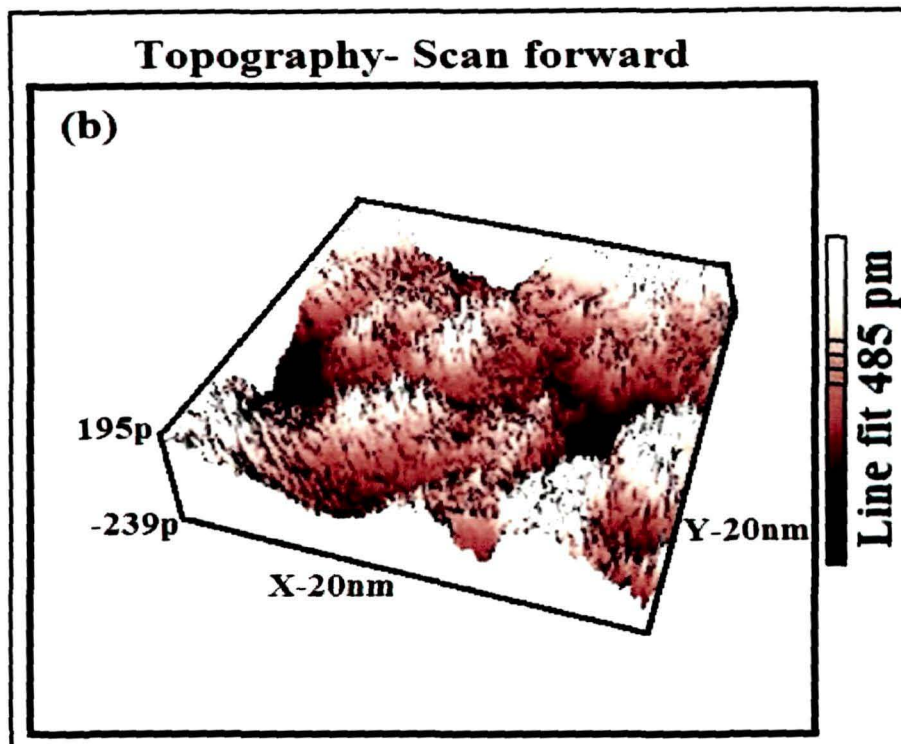
Fig.3.9: STM image of the Cu nanoparticles

3.7.3   Synthesis of Ag/PS nanocomposite particles

Ag nanoparticles are dispersed into the micro emulsion of the monomers to prepare Ag/polystyrene nanocomposite in the water-in-sc-CO$_2$ medium in the presence of PDMS stabilizer. The monomers interact with Ag nanoparticles forming some active monomer droplets. The delocalized π-electrons in the aromatic ring of styrene monomer interact with the d-electrons of Ag nanoparticles. The initiator added to the mixture undergoes decomposition at 75°C and generate the free radical in the active monomer droplets. These active monomer droplets contain the Ag nanoparticles at the center and undergo free radical polymerization on the surface of the nanoparticles. The TEM images (Fig.3.13) of the Ag-polystyrene nanocomposite particles reveal that the nanoparticles are encapsulated within the polymer particles. Nanoparticles possess very

109

high chemical activity due to its high active surface area. Polymer molecules itself act as good stabilizers for the metal nanoparticles.[49,52]

The amount of Ag nanoparticles loaded per polystyrene particles can be controlled mainly by maintaining the ratio of the stable dispersion of the nanoparticles to the amount of monomers in the reaction. The amount of nanoparticles encapsulated within the particle is directly proportional to the amount of stable dispersion of nanoparticles taken. Moreover, some reaction parameters like agitation speed, rate of addition of dispersed nanoparticles have also significant effect on the amount of encapsulated metal nanoparticles within the nanocomposites. From the TEM image (Fig.3.13), it is clear that majority of the composite particles contain 2-3 agglomerated Ag nanoparticles. Stabilization of metal nanoparticles in the polymer matrix is affected by the polymer nature and its functional groups. More the electron donor properties of the polymer functional groups, the stronger is their adhesion to dispersed phase particles.[51] In case of polystyrene, the aromatic π-electrons interact with the atoms of the metal surface layer which increase the stability of the nanoparticles in the Ag/polystyrene nanocomposites. By incorporating nanoparticles into polymer matrix, it is possible to create reliable protection against corrosion and other undesirable factors.[55]

3.7.3.1 UV-visible spectroscopic analysis

The UV-Visible spectra are shown in Fig.3.10. The analysis of the various samples showed the absorption peak at the range of 400-430 nm, which confirmed the formation of silver nanoparticles. The size and shape of the nanoparticles have the pronounced influence on the nature of the UV-visible absorption peak. The position of the plasmon band is also strongly dependent on the average size of the nanoparticles.
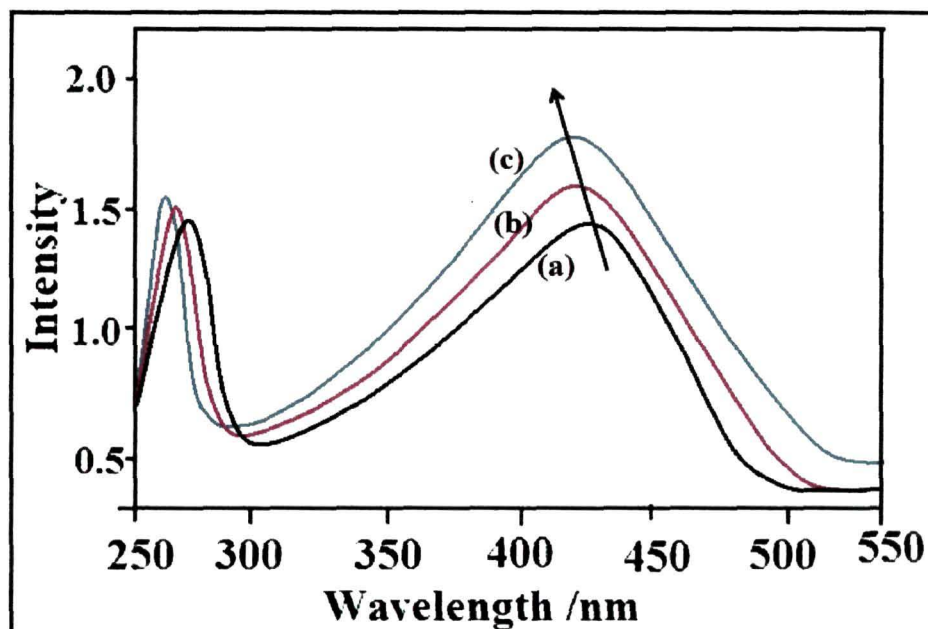
Fig.3.10: UV-Visible spectra of Ag nanoparticles

With the decrease in reaction pressure from 3,400 psi to 3,000 psi, the Ag-nanoparticles show a characteristic blue-shift in the UV-visible spectra (Fig.3.10). This shift may be attributed to the decrease in particle size with decrease in pressure.

3.7.3.2 XRD analysis

The WAXD patterns of (a) Ag nanoparticles, (b) pure polystyrene and (c) Ag/polystyrene nanocomposite particles are shown in Fig.3.11. The XRD diffractogram of the synthesized pure (a) Ag-nanoparticles showed cubic crystal structure. The major characteristic diffraction peaks of Ag particles are found at $2\theta=38.16°$, $44.28°$, $64.38°$ and $77.74°$, which are in conformity with the crystal faces of (111), (200), (220) and (311) of Ag. All these difraction peaks could be indexed to face-centered cubic (FCC) silver.

111
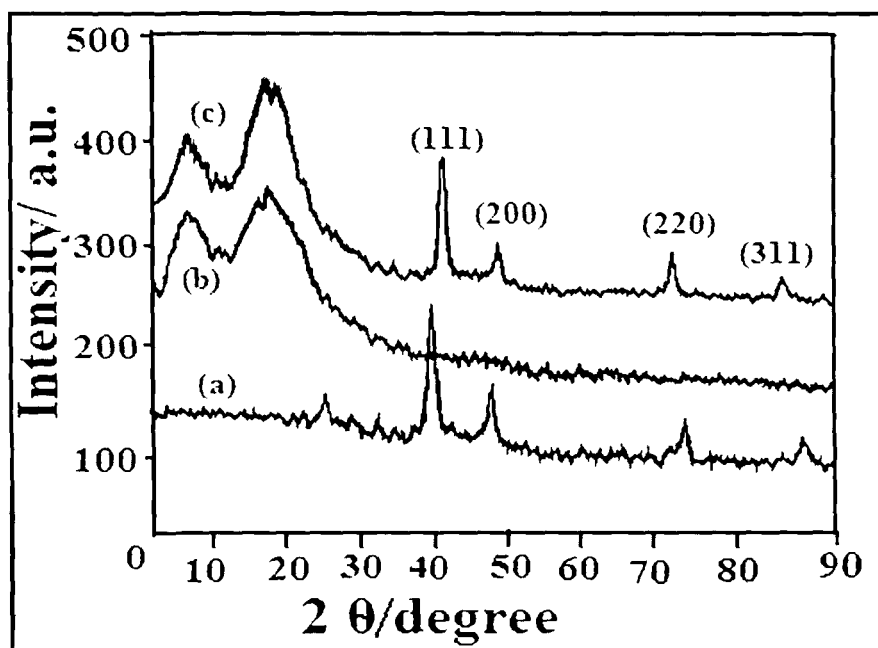
Fig.3.11: WAXD pattern of Ag/polystyrene nanocomposites

(a) Ag nanoparticles (b) pristine polymer and (c) Ag-polymer nanocomposite

According to the full width at half-maximum of the diffraction peaks, the average size of the particles is estimated from the Scherrer equation[54] and is found to be about 8 nm [reaction conditions: t=45°C, c(AgNO$_3$)= 0.033 mol/L, P= 20.68 MPa] and is found to be in consistent with the TEM results. The WAXD diffractogram of the pristine polystyrene (b) particles showed a broad peak at $2\theta=10°-21°$ indicating the amorphous nature of the polymer. However, with the incorporation of Ag into the polymer matrix, the same peak is observed with higher intensity and narrower width. The diffraction pattern of the Ag/polystyrene nanocomposite manifested the broad peak of polystyrene and the peaks responsible for Ag nanoparticles. This indicates the presence of Ag nanoparticles in the polymer matrix.

112

3.7.3.3 SEM analysis

The SEM micrographs of the pristine polymer and the silver-polystyrene nanocomposites are shown in Fig.3.12. The morphology of the pristine polymer particles and Ag/polymer nanocomposites is found to be slightly different.
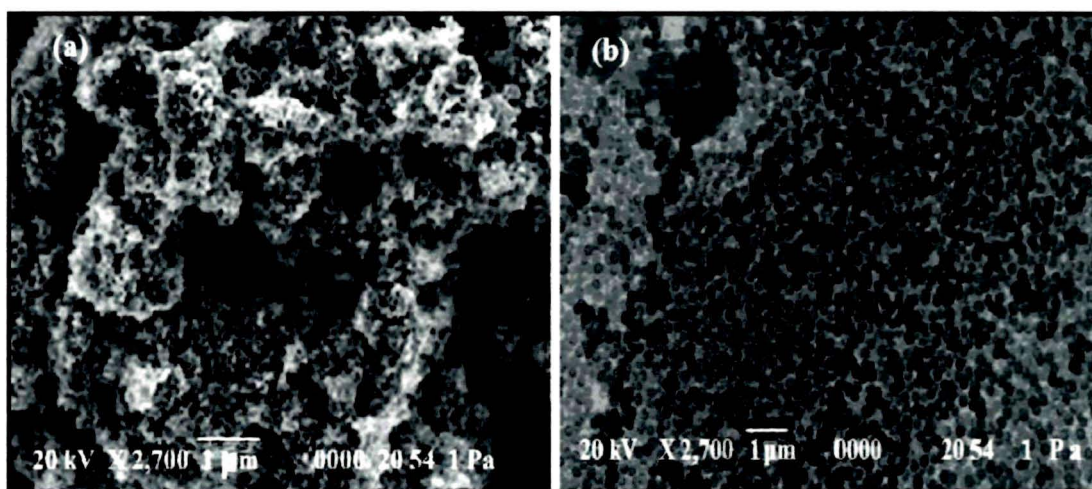
Fig.3.12: SEM image of (a) pristine polymer, (b) Ag-polystyrene nanocomposites

In SEM micrographs for Ag/polymer nanocomposite samples, discrete particles are observed. However in case of pristine polymer, the polymer particles are found to be interlinked like the foam structures. This may be due to the interaction of the aromatic π-electrons of the polystyrene and the free electrons of the metal nanoparticles.

3.7.3.4 TEM analysis

TEM images of the prepared silver nanoparticles and Ag/polystyrene nanocomposite particles are shown in Fig.3.13. The representative TEM images demonstrated the homogeneous dispersion of silver nanoparticles in the medium. The Ag nanoparticles are spherical in shape with a smooth surface morphology. The average size of silver nanoparticles is 8 nm, which is in good agreement with the XRD analysis. TEM image also showed that the silver nanoparticles are nearly uniform in size and

113

shape. The TEM image of the Ag/polystyrene nanocomposites clearly demonstrated that the silver nanoparticles are encapsulated into the polymer particles (Fig.3.13.b) without leaving any bare Ag nanoparticles.
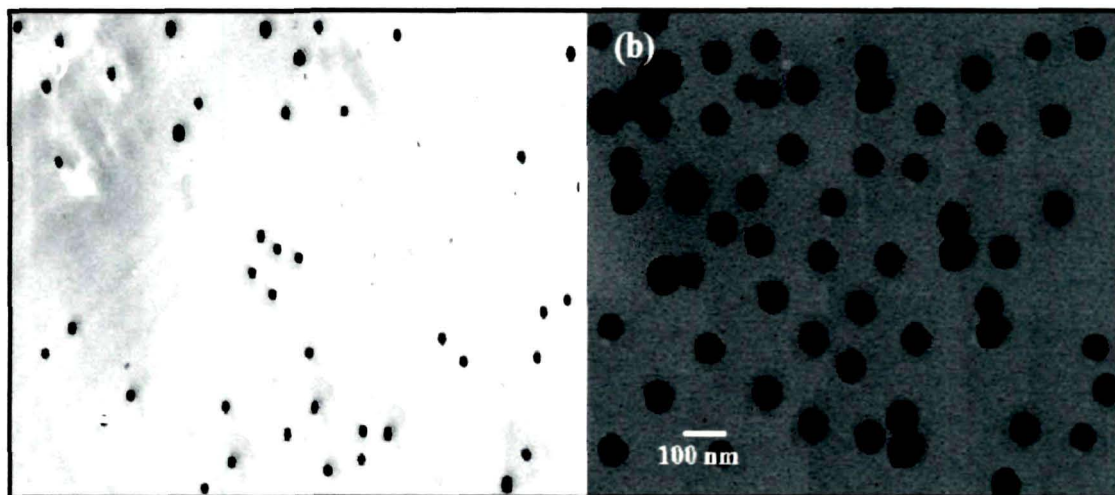
Fig.3.13: TEM micrographs of (a) Ag nanoparticles and (b) Ag-polystyrene nanocomposites

The average size of the Ag/polymer nanocomposite particle is determined to be 70 nm. An interesting observation from the TEM image (Fig.3.13) revealed that in each of the nanocomposite particles, more than two agglomerated nanoparticles are encapsulated. This may due to the agglomeration of Ag nanoparticles during polymerization. Once the metal nanoparticles are encapsulated within the polymer particles, there is no further chance of getting agglomeration of metal nanoparticles. Thus the stability of the nanoparticles within the polymer particle is enhanced after polymerization. On the other hand, the nanoparticles are compatible with the monomer and the resulting polymer phase due to the interaction of the free electrons of the metal with the delocalized π-electrons of the benzene ring in the monomer for which more than two agglomerated nanoparticles are encapsulated within the polymer particles.

3.7.3.5 Thermo gravimetric analysis (TGA)

The TGA curves for the pristine polymer (a) and for the metal polymer nanocomposite (b) are shown in the (Fig.3.14). The onset of degradation for pristine polymer is 300°C and for nanocomposite is 315°C. The degradation temperature of the pristine polystyrene is 320°C and that of Ag/polystyrene nanocomposite is 350°C. Evidently, the decomposition onset for Ag/polystyrene nanocomposite is shifted to the higher temperature compared to the pristine polystyrene. Here the Ag nanoparticles act as the nucleating agent for enhancing the crystallization which restricts the movement of the polymer chains.
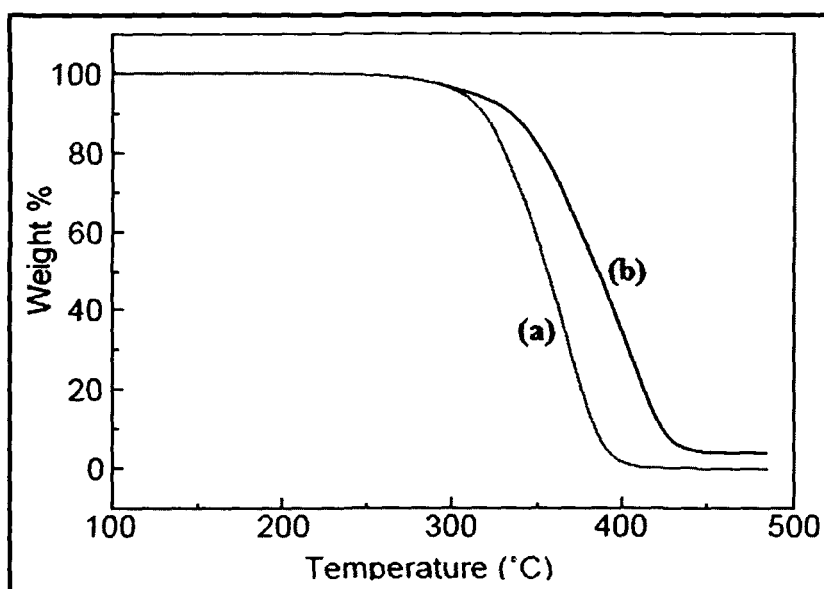
Fig.3.14: TGA of the (a) pristine polymer and (b) Ag-polystyrene nanocomposites

Significant improvement in the thermal stability of nanocomposite compared to pristine polymer is observed from TGA curves. With the increase in amount of nanoparticles, the polymer chain restriction increases considerably due to the interaction of nanoparticles. The Ag nanoparticles in the polymer matrix act as the hardening (virtual cross linking) point in the polystyrene particles and thereby helping the soft segments to arrange in a regular pattern and thus improve the crystalline behavior.[56]

Therefore, by incorporating the silver nanoparticles within polymer, the thermal stability of the Ag/polymer nanocomposites can be enhanced.

3.7.3.6 Antibacterial activities

The bacteriostatic effect of Ag/polymer nanocomposite particles was studied against four bacterial species, Pseudomonas fluorescens *BS3*, Bacillus circulens *BP2*, Eschericia coli and staphylococcus aureus as given in Table.3.3.

Table.3.3: The antibacterial activity of the Ag-polystyrene nanocomposite against different bacterial strains

Sl. No	Micro organisms	Average diameter zone of inhibition (mm)			
		0% Ag-(pure polystyrene)	0.5% Ag-polystyrene	1% Ag-polystyrene	1.5% Ag-polystyrene
1	Pseudomonas fluorescens	$0^b (0)^a$	$12^b (1)^a$	$17^b (2)^a$	$21^b (2)^a$
2	Bacillus circulens	0 (0)	14 (2)	19 (2)	27 (2)
3	Eschericia coli	0 (0)	8 (1)	9 (1)	12 (1)
4	staphylococcus aureus	0 (0)	5 (2)	10 (2)	15 (1)

a Standard deviation, b Average diameter

The figure depicting the antibacterial activity of the nanocomposites is shown in Fig.3.15. It clearly indicates that the test sample with Ag nanoparticles concentration 1% Ag (c) and 1.5% Ag (d) show inhibitory effect against all four bacterial species. Sample (d) i.e, with concentration of 1.5% Ag nanoparticles show the highest inhibition of all four bacterial species, in which the zone of inhibition (diameter) is the largest. The sample without Ag nanoparticles, i.e. pristine polymer (a) does not show any antibacterial activity. The sample with 0.5% Ag nanoparticles (b) shows a very little

effect against the test organisms. The antibacterial activity test carried out against these different kinds of bacterial strains has been performed qualitatively for a comparative study. However, plate counting are necessary for detailed evaluation of the antibacterial activity.
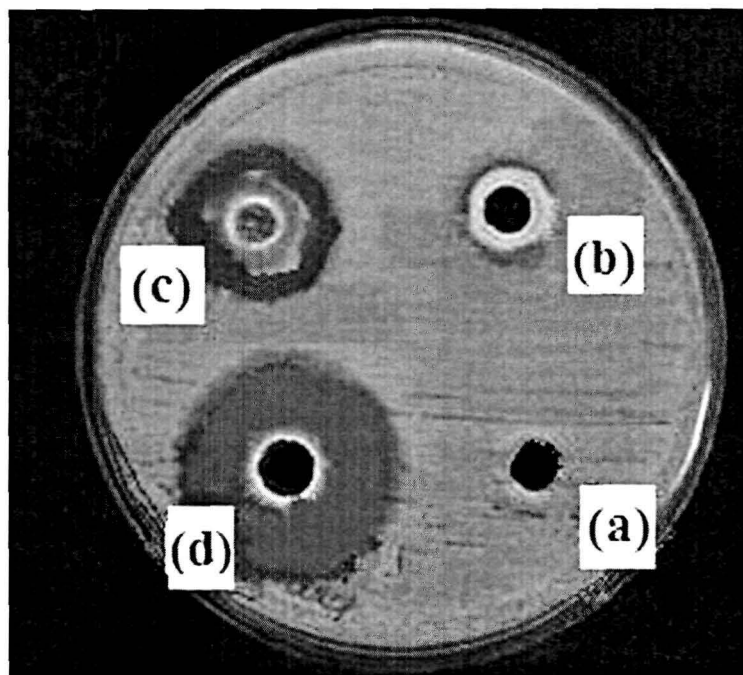
Fig.3.15: Antibacterial activity of the nanocomposites

The test samples (a) did not show antibacterial activity against the test organism Bacillus circulens *BP2*, but both (c) and (d) were found to be positive with high antibacterial activity.
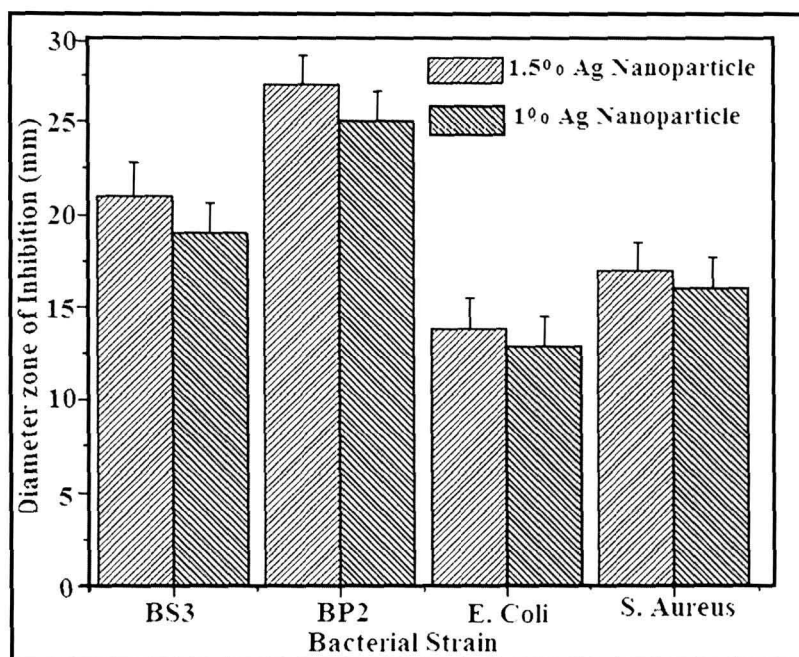
Fig.3.16: Bar diagram showing the antibacterial activity

The bar diagram (Fig.3.16) depicts the antibacterial activity of the nanoparticles encapsulated polystyrene particles towards the four different kinds of bacterial strains. The inhibitory effect of the samples with 1% Ag nanoparticles (c) and 1.5% Ag nanoparticles (d) are shown in the figure. The results indicated that Bacillus circulens *BP2* bacteria is very sensitive towards Ag-encapsulated polystyrene nanocomposite particles. Eschericia coli are the least sensitive to Ag/polymer nanocomposite. The neat silver nanoparticles showed very good antibacterial activity against a number of pathogenic bacteria.[49] But the current study reflects that the Ag-nanoparticles encapsulated polystyrene particles synthesized in sc-CO$_2$ also bear promising potential to be used as antibacterial agent.

3.7.4 Synthesis of Cu/polystyrene nanocomposite particles

Nanoparticles have very high chemical activity due to its high active surface area. Polymer molecules are very good stabilizer for the stabilization of the metal

118

nanoparticles.[57] By incorporating nanoparticles into polymer matrix, it is possible to create reliable protection against corrosion and other undesirable factors.[55]

The Cu-nanoparticles are well dispersed into the micro emulsion of the monomers in the water-in-sc-CO$_2$ medium in presence of PDMS stabilizer. The monomers interact with the Cu nanoparticles forming some active monomer droplets. The initiator added to the mixture undergoes decomposition at 75°C and generate the free radical on the active monomer droplets. These active monomer droplets contain the Cu-nanoparticles at the center and undergo free radical polymerization on the surface of the nanoparticles. Thus the nanoparticles are encapsulated into the polymer particles (Fig.3.13. b). Stabilization of nanoparticles in the polymer matrix is affected by the polymer nature and its functional groups. The excess fragments of polystyrene molecules aggregate the nanoparticles to enhance the stability of the nanoparticles. More is the electron donor properties of the polymer functional groups, the stronger is their adhesion to dispersed phase particles.[57] In case of polystyrene, the aromatic π-electrons interact with the atoms of the metal surface layer which increase the stability of the nanoparticles in the Cu/polystyrene nanocomposite.

3.7.4.1 UV-visible spectroscopic analysis

The analysis of the various samples show the absorption peak in a range of 580-600 nm, which confirms the formation of Copper nanoparticles.[54] A characteristic blue-shift is observed from the analysis with the decrease in the pressure of CO$_2$ (3,400-3,000 psi) in the reaction (Fig.3.17).
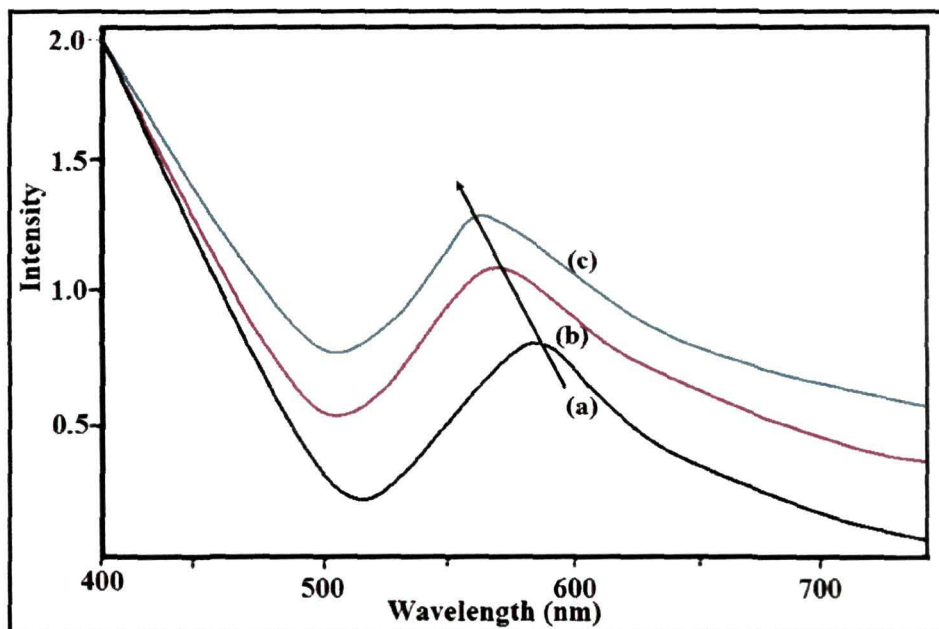
Fig.3.17: UV-Visible spectra of the Cu nanoparticles

This particular blue-shift implies that with the decrease in pressure, the particle size of Cu nanoparticle decreases. At higher pressure the concentration of the fluid (sc-CO$_2$) increases which leads to formation of larger particle size.

3.7.4.2 XRD Analysis

The XRD analysis of the synthesized Cu nanoparticles shows a cubic crystal structure. The major strong characteristic peaks of Cu nanoparticles are at $2\theta=46.16°$, 57.28°and 73.74°, which are in consistent with crystal faces of (111), (200) and (220) of Cu. All these reflection peaks can be indexed to face-centered cubic (FCC) copper. Cu nanoparticles prepared using water-in-scCO$_2$ do not change the crystalline structure of neat Cu nanoparticles. The lattice constant is calculated to be 3.614 A° which is in good agreement of pure copper crystals. The WAXD patterns of pure Cu nanoparticle (a), pristine polymer (b) and polymer/Cu nanocomposite (c) are shown in Fig.3.18. The XRD pattern confirms the proper incorporation of Cu nanoparticles into the polymer microparticles which can be further confirmed from TEM images.

120
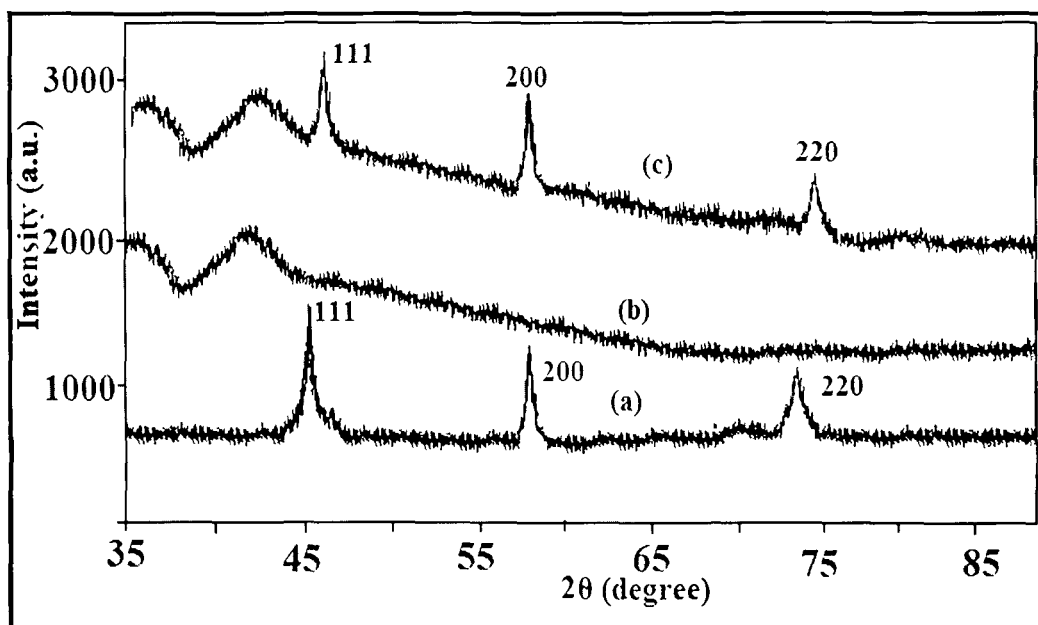
Fig.3.18: WAXD pattern of the Cu nanoparticles and Cu-polystyrene nanocomposites

The crystallite size distribution is determined from the analysis of line broadening method using Schrrer equation.[45] According to the full width at half-maximum of the diffraction peaks, the average size of the particles could be estimated from the Scherrer equation to be about 6.3 nm [reaction conditions: t=40°C, $c(CuCl_2)$= 0.033 mol/L]. These results are in consistent with the TEM images.

3.7.4.3 SEM analysis

The SEM images of the pristine polymer (a) and the Copper-polystyrene nanocomposite particles (b) are as shown in the Fig.3.19. The morphology of the pristine polymer particle and Cu/polymer nanocomposite particles are different. In the pristine polymer, the polymer particles are interlinked like foam structures. It is observed that the particle formation in the nanoparticles encapsulated polymer particle is clearer than the pristine polymer.
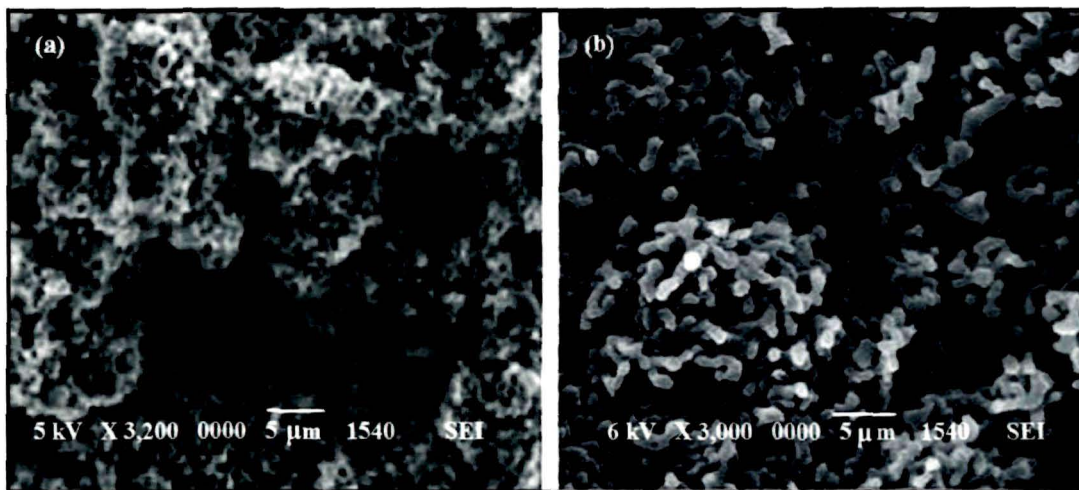
Fig.3.19: SEM micrographs of (a) pristine polymer and (b) Cu-polystyrene nanocomposites

Cu nanoparticles inside the monomer droplets enhance the particle formation for which discrete particle formation are observed in the Cu/polystyrene nanocomposite particles. This is possibly due to the electronic interaction between Cu and unsaturated styrene monomers.

3.7.4.4 TEM analysis

TEM image of the prepared Copper nanoparticles are shown in the Fig.3.20. The representative TEM images demonstrate the homogeneous dispersion of Copper nanoparticles in the medium. Cu nano particles are spherical in shape with a smooth surface morphology. The TEM image of the Copper nanoparticle yielded an average size of 7 nm. This value is in good agreement with that from the XRD analysis.
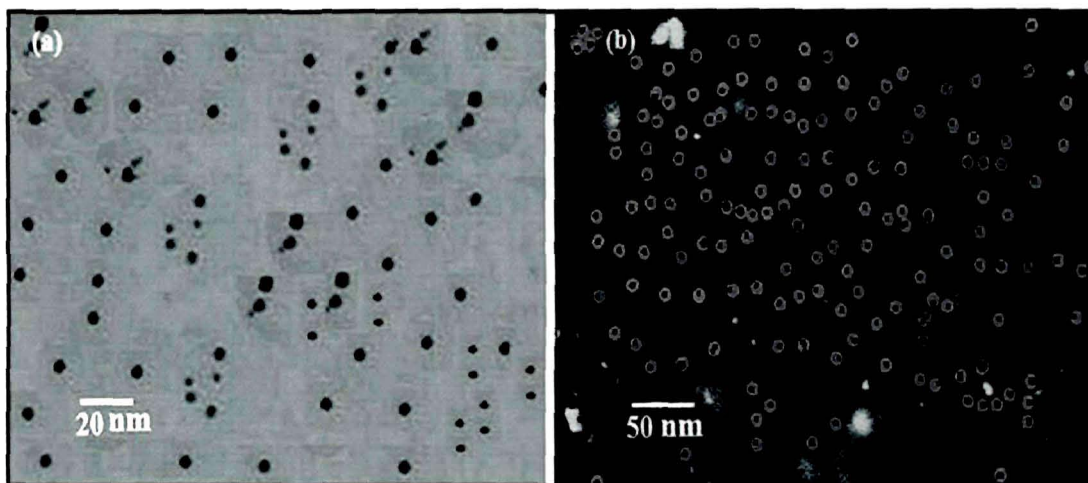
Fig.3.20: TEM image of (a) Cu nanoparticles and (b) Cu-polystyrene nanocomposites

TEM image also shows that the produced nano particles are more or less uniform in size and shape. The Copper nanoparticles are encapsulated into the polymer particles which can be clearly observed in the Fig. 20. (b). No bare Cu nanoparticles left out within the polymer matrix. The average size of the Cu/polymer nanocomposite particle is 20 nm.

3.7.4.5 GPC analysis

The molecular weight distribution and polydispersity indices of the polymer samples were obtained from gel permeation chromatographic (GPC) data. All the data are summarized in Table.3.4. The copper nanoparticles present in the composites were separated by making a solution in THF and centrifuging at 5,000 rpm for 1 h.

Table.3.4: Molecular weight of the Cu/polymer nanocomposites

Sl no	Polymer	Mol. Weight (g/mol) (M_n)	Polydispersity Index	Yield (%)
1	Pure Polystyrene	44,000	1.31	80
2	0.5% Cu/Polystyrene	43,000	1.26	81
3	1% Cu/Polystyrene	44,000	1.34	85
4	1.5% Cu/Polystyrene	45,000	1.30	82

The nanoparticles settled down and the clear solution was collected for polymer molecular weight determination. Number average molecular weight (M_n) of the polymer was found to be in the range of 43,000-45,000 g/mol. The polydispersity indices of the polymers are observed in the range of 1.26-1.34. From these GPC data, it can be confirmed that the molecular weight and the polydispersity indices of the polymer nanocomposite is independent of the percentage of nanoparticles present in the composite. In all the cases, the yields of the polymer were found to be above 80%.

3.7.4.6 TGA analysis

The thermal stability of the polymer was studied by thermo gravimetric analysis (TGA). TGA curves (residual weight percentage versus temperature) for pristine polymer (a) and for the metal polymer nanocomposite (b) are shown in the Fig.3.21. The onset of degradation is defined as 5% of degradation and degradation temperature is defined as 20% degradation. The onset of degradation for pristine polymer is 300°C and for Cu/polystyrene nanocomposite is 317°C respectively.
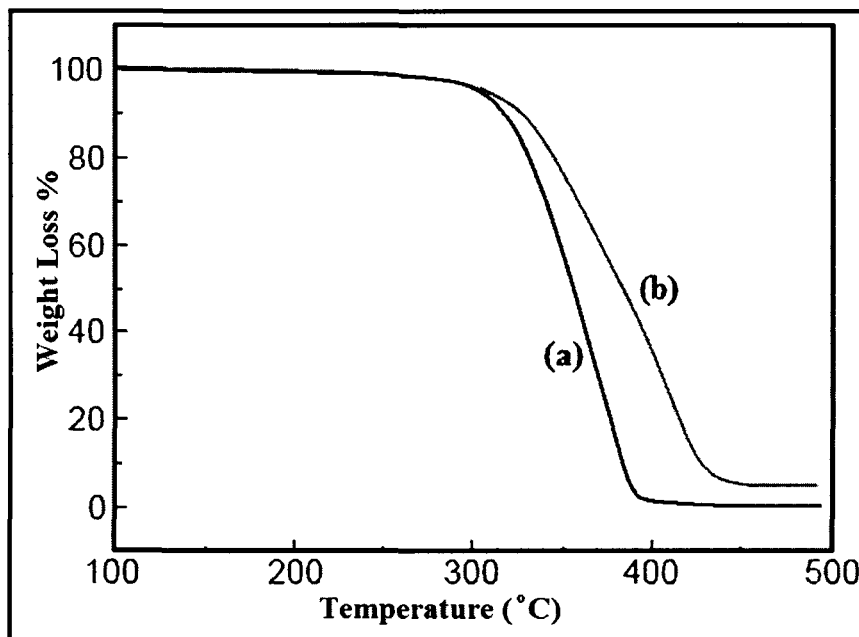
Fig.3.21: TGA of (a) pristine polymer and (b) Cu-polystyrene nanocomposites

The degradation temperature of the pristine polystyrene is 320°C and the Cu/polystyrene nanocomposite is 350°C. Evidently, the decomposition onset for Cu/Polystyrene nanocomposite shifts to higher temperature compared to pristine polystyrene polymer. This shows that the thermal stability of the polymer/metal nanocomposite is higher than the pristine polymer. The Cu-nanoparticles in the polymer matrix act as the hardening (virtual cross linking) point in the polystyrene particles and thereby helping the soft segments to arrange in a regular pattern and thus improve the crystalline behavior.[56] Therefore, by incorporating the copper nanoparticles within polymer, the thermal stability of the Cu/polymer nanocomposites can be enhanced.

3.7.4.7 Antibacterial activities

The bacteriostatic effects of the Cu/polymer nanocomposite particles were studied against four kinds of bacterial strains i.e, Pseudomonas fluorescens BS3, Bacillus circulens BP2, Eschericia coli DHSa and staphylococcus aureus strain. It is clear from the Fig.3.22. and Table. 3.5. that the test samples with a Cu nanoparticles

125

concentration 1% Cu nanoparticles (c) and 1.5% Cu nanoparticles (d) show inhibitory effect against all the four bacterial strains. The sample with 1.5% Cu nanoparticles concentration show the highest degree of inhibition against all the four kinds of bacterial strains for which the diameter of zone of inhibition is more. The sample with no Cu nanoparticles (a) did not show any antibacterial activity towards the bacterial strains, sample with 0.5% Cu nanoparticles show a very little affect against the test organism and therefore the inhibitory zone of this sample is very narrow. The test samples (a) and (b) shows no antibacterial activity against the test organism. Thus the test samples (c) and (d) exhibit good bacteriostatic effect on the tested bacteria.
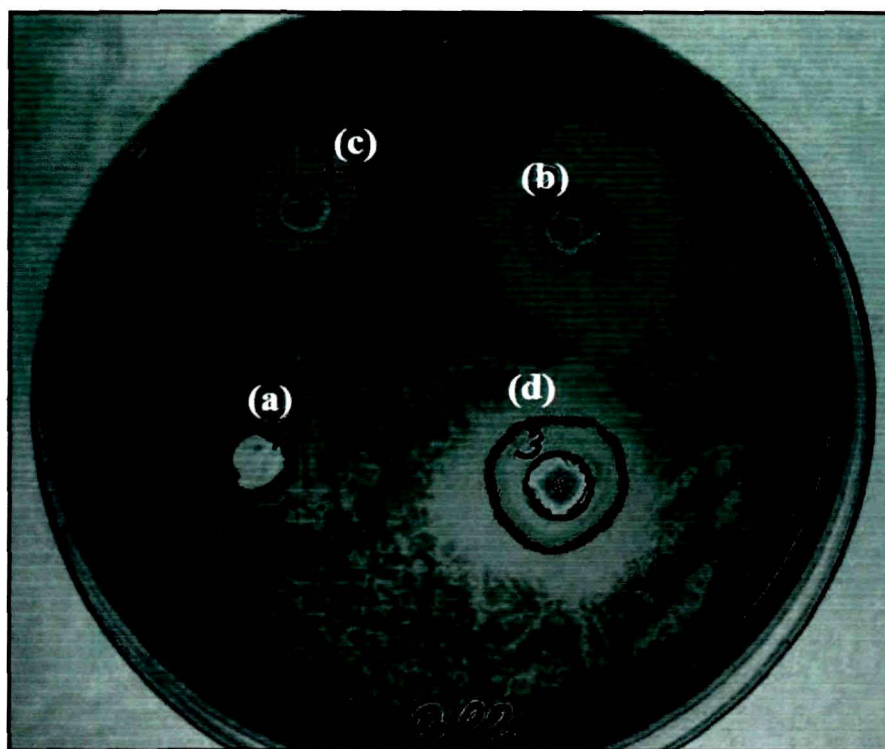
Fig.3.22: Antibacterial activity of the Cu-polystyrene nanocomposites

It has been proposed that the bacterial DNA loses its replication ability once the bacteria have been treated with copper nanoparticles.[58] Other studies have shown evidence of structural changes in the cell membrane as well as the formation of small electron-dense granules formed by silver.

126

Table.3.5: The antibacterial activity of the Cu-polystyrene nanocomposite against different bacterial strains

Sl. No	Micro organisms	Average diameter zone of inhibition (mm)			
		0% Cu-(pure polystyrene)	0.5% Cu-polystyrene	1% Cu-polystyrene	1.5% Cu-polystyrene
1	Pseudomonas fluorescens	$0^b (0)^a$	$9^b (0.1)^a$	$13^b (0.2)^a$	$19^b (0.2)^a$
2	Bacillus circulens	0 (0)	11 (0.2)	16 (0.2)	24 (0.2)
3	Eschericia coli	0 (0)	7 (0.1)	8 (0.1)	10 (0.1)
4	Staphylococcus aureus	0 (0)	4 (0.2)	10 (0.2)	13 0.1)

*Average diameter zone is reported from the average of three experiments and the value in the bracket shows standard deviation.

Copper nanoparticles when come in contact with the bacteria, it destroys the cell walls of the bacteria showing its antibacterial activity.[59]
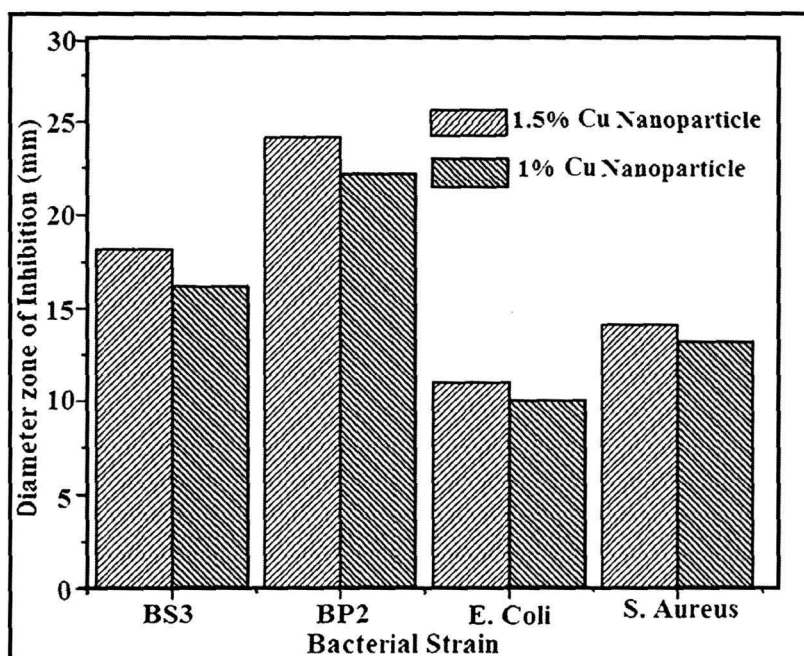
Fig.3.23: Bar diagram of the antibacterial activity of the nanocomposites

The bar diagram (Fig.3.23) shows the antibacterial activity towards the four different kinds of bacterial strains. The inhibitory effect of the samples with 1% Cu nanoparticles (c) and 1.5% Cu nanoparticles (d) are shown in the diagram. It is clear from the above set of tests that Bacillus circulens *BP2* bacteria is very sensitive towards the Cu encapsulated polystyrene nanocomposite particles and Eschericia coli DHSα shows the lowest degree of inhibition.

3.8 Conclusions

In summary, this chapter describes a route to synthesize the silver nanoparticles by the chemical reduction technique in a water-in-sc-CO_2 medium using polydimethylsiloxane (PDMS) as a stabilizer. The dispersion of silver nanoparticles remains stable up to three months with the polydimethylsiloxane (PDMS) stabilizer and SDS surfactant. At high concentration of PDMS, the stability is more. The size of the Ag nanoparticles is found to be in the range of 5 nm-17 nm. At lower pressure (2,000 psi) the particles are smaller and uniform in size. On the other hand, at higher pressure the particles are larger and irregular in size. This process may easily be applied to a range of inorganic/polymer composite nanoparticles with different size and compositions.

Again, a route to synthesize the Cu nanoparticles by the chemical reduction technique in a water-in-sc-CO_2 medium using polydimethylsiloxane (PDMS) as a stabilizer is described in this chapter. The dispersion of Cu nanoparticles remains stable upto two months with the polydimethylsiloxane (PDMS) stabilizer and AOT surfactant. At high concentration of PDMS, the stability is more. The size of the Cu nanoparticles is in the range of 4-8 nm. At lower pressure (2,000 psi) the particles are smaller and uniform in size. On the other hand at higher pressure the particles are larger and irregular in size. This process may easily be applied to a range of inorganic/polymer composite nanoparticles with different size and compositions.

The work describes an easy method to synthesize the silver/polystyrene nanocomposite particles by *ex-situ* addition of Ag nanoparticles during the polymerization. The average size of Ag nanoparticles is found to be 8 nm and of nanocomposite particles to be 70 nm. The metal nanoparticles are uniformly distributed inside the polymer particles without leaving any bare Ag nanoparticles within the polymer matrix. The inclusion of the metal precursor had no influence on the polymerization process. Moreover, the method possessed potential advantages for applications as it is simple, time saving, environmentally benign and the solvent (sc-CO$_2$) could be recycled. The Ag-polystyrene nanocomposite shows enhanced thermal stability than the pristine polymers. The antibacterial activity of silver/polystyrene nanoparticles was tested against four species of bacteria, Pseudomonas fluorescens *BS3*, Bacillus circulens *BP2*, Eschericia coli and Staphylococcus aureus. Amongst all the bacterial species, Bacillus circulens *BP2* is found to be highly sensitive towards the Ag encapsulated polystyrene nanocomposite particles.

Similarly, an easy method to synthesize the Copper/polystyrene nanocomposites by ex-situ addition of Cu nanoparticles during the polymerization is also summarized in this chapter. The size of the nanoparticles can be easily controlled by adjusting the pressure inside the reactor. The average size of the Cu nanoparticles was found to be 7 nm. The metal nanoparticles were uniformly distributed inside the polymer particles and the inclusions of the metal precursor have no significant influence on the polymerization process. Moreover, this method has some potential advantages for applications as it is simple, timesaving, and the solutions can be recycled. The polymer nanocomposite particles show thermal stability upto 350°C, whereas the pristine polymer shows stability up to 320°C. Molecular weight of the polymer particles are found to be in the range of (43,000-45,000g/mol). The antibacterial activity of the of the Copper/polystyrene nanoparticles were tested against four different bacterial strains, Pseudomonas Fluorescens BS3, Bacillus Circulens BP2, Eschericia Coli DHSα and Staphylococcus Aureus. Amongst all the bacterial strains, Bacillus Circulens BP2 is very sensitive towards the Cu encapsulated polystyrene nanocomposite particles.

129

References

1. Kopeikin, V.V.; Panarin, E.F. Water-soluble nanocomposites of zerovalent metallic silver with enhanced antimicrobial activity, *Dokl. Chem.* **380**, 277–279 (2001).

2. Zezin, A.B.; Rogacheva, V.B.; Feldman, V.I.; Afanasiev, P.; Zezin, A.A. From triple interpolyelectrolyte-metal complexes to polymer-metal nanocomposites, *Adv. Colloid Interf. Sci.* Article in Press. doi:10.1016/j.cis.2009.09.002.

3. Hasell, T. *et al.* A facile synthetic route to aqueous dispersions of silver nanoparticles, *Mater. Lett.* **61**, 4906–4910 (2007).

4. Yang, J.; Hasell, T.; Wang, W.; Howdle, S.M. A novel synthetic route to metal–polymer nanocomposites by in situ suspension and bulk polymerizations, *Eur. Polym. J.* **44**, 1331–1336 (2008).

5. Sterk, L.; Gorka, J.; Jaroniec, M. Polymer-templated mesoporous carbons with nickel nanoparticles, *Colloid. Surf. A: Physicochem. Eng. Aspects* **362**, (2010) 20–27.

6. Van NGO, T.T.; Rumeau, J.D.; Whittaker, A.K.; Gerard, J.F. Processing of nanocomposite foams in supercritical carbon dioxide. Part I: Effect of surfactant, *Polymer* **51**, 3436-3444 (2010).

7. Zahir, M.H.; Suzuki, T.; Fujishiro, Y.; Awano, M. Perovskites with cotton-like morphology consisting of nanoparticles and nanorods: Their synthesis by the combustion method and their NO$_x$ adsorption, *Appl. Catal. A* **361**, 86-92 (2009).

8. Johnston, K.P.; Rocha, S.R.P. Colloids in supercritical fluids over the last 20 years and future dire, *J. Supercrit. Fluid* **47**, 523–530 (2009).

9. Romang, A.H.; Watkins, J.J. Supercritical Fluids for the Fabrication of Semiconductor Devices: Emerging or Missed Opportunities, *Chem. Rev.* **110**, 459–478 (2010).

10. Zhang, H.; Cooper, A.I. Synthesis and applications of emulsion-templated porous materials, *Soft. Matter.* 107–113 (2005).
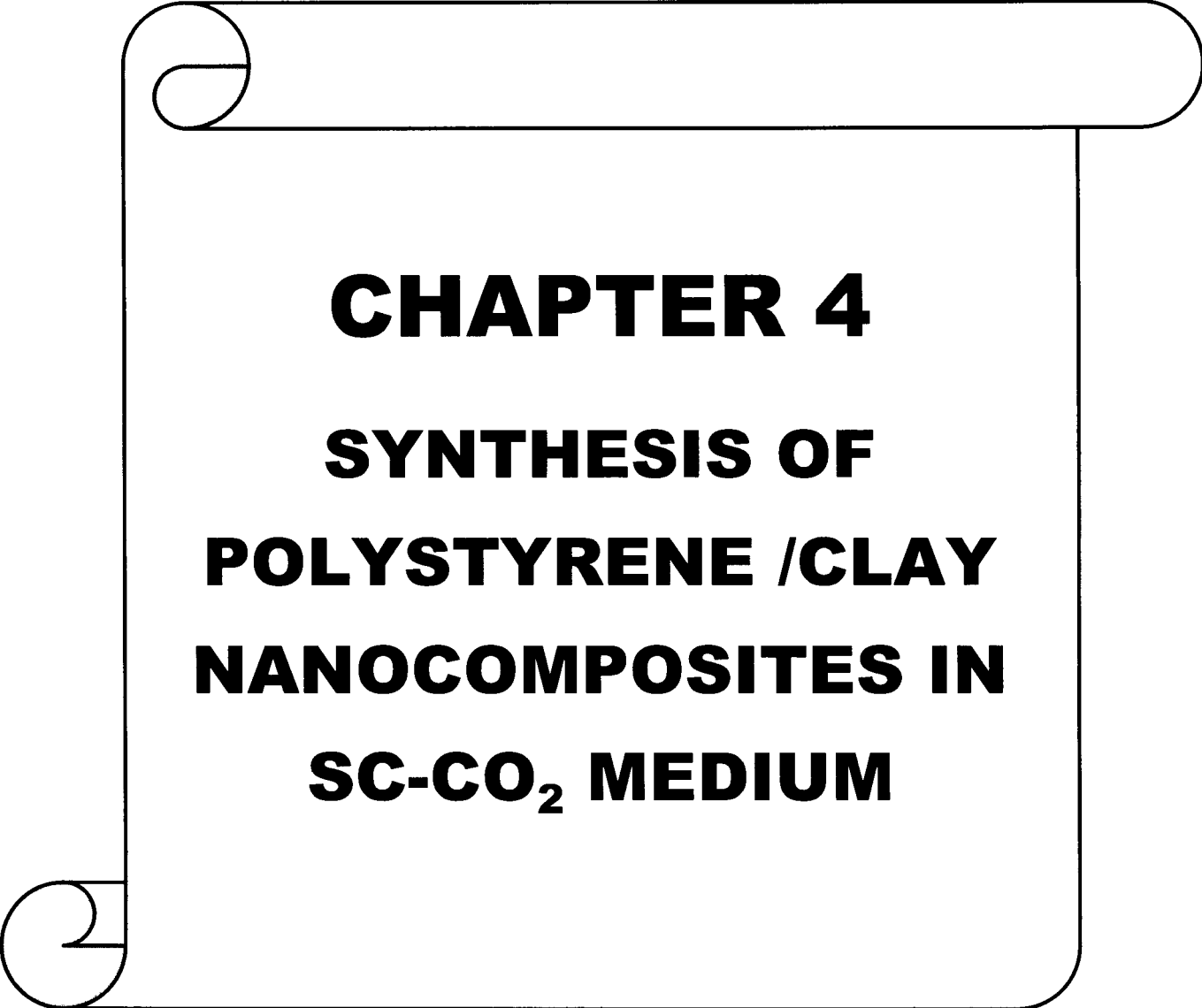
11. Chattopadhyay, P.; Gupta, R.B. Supercritical CO_2 based production of magnetically responsive micro- and nanoparticles for drug targeting, *Ind. Eng. Chem. Res.* **41,** 6049-6058 (2002).

12. Zhang, J.; Han, B. Supercritical CO_2-continuous microemulsions and compressed CO_2-expanded reverse microemulsions, *J. Supercrit. Fluid.* **47,** 531-536 (2009).

13. Shimizu, R.; Nibe, A.; Sawada, K.; Enokida, Y.; Yamamoto, I. Preparation of hydrophobic platinum catalysts using a water-in-CO_2 microemulsion, *J. Supercrit. Fluid.* **44,** 109-114 (2008).

14. Liua, J.; Shervania, Z.; Raveendrana, P.; Ikushima, Y. Micellization of sodium bis(2-ethylhexyl)sulfosuccinate in supercritical CO_2 with fluorinated co-surfactant and its solubilization of hydrophilic species, *J. Supercrit. Fluid.* **33,** 121-130 (2005).

15. Hojjati, B.; Charpentier, P.A. Synthesis of TiO_2-polymer nanocomposite in supercritical CO_2 via RAFT Polymerization. Polymer **51,** 5345-5351 (2010).

16. Zhong, X.; Dehghani, F. Solvent free synthesis of organometallic catalysts for the copolymerisation of carbon dioxide and propylene oxide, *Appl. Catalysis B: Env.* **98,** 101-111 (2010).

17. Ellis, J.L. *et al.* Supercritical CO_2 sterilization of ultra-high molecular weight polyethylene, *J. Supercrit. Fluid.* **52,** 235-240 (2010).

18. Jacobs, L.J.M.; Danen, K.C.H.; Kemmere, M.F.; Keurentjes, J.T.F. Quantitative morphology analysis of polymers foamed with supercritical carbon dioxide using Voronoi diagrams, *Comput. Mater. Sci.* **38,** 751-758 (2007).

19. Su, L.; Li, L.; Li, H.; Tang, J.; Zhang, Y.; Yu, W.; Zhou C. Preparation of polysiloxane modified perfluorosulfonic acid composite membranes assisted by supercritical carbon dioxide for direct methanol fuel cell, *J. Power Sources* **194,** 220-225 (2009).

20. Keskin, S.; Talay, D.K.; Akman, U.; Hortacsu, O. A review of ionic liquids towards supercritical fluid applications, *J. Supercrit. Fluid.* **43,** 150-180 (2007).

21. Yuvaraj, H. Dispersion polymerization of styrene in supercritical CO$_2$ in the presence of non-fluorous random copolymeric stabilizers, *J. Supercrit. Fluid.* **42**, 351–358 (2007).

22. Meziani, M.J.; Pathak, P.; Beacham, F.; Allard, L.F.; Sun Y.P. Nanoparticle formation in rapid expansion of water-in-supercritical carbon dioxide microemulsion into liquid solution, *J. Supercrit. Fluid.* **34**, 91–97 (2005).

23. Yue, B.; Yang, J. Particle encapsulationwith polymers via in situ polymerization in supercritical CO$_2$,*Powder Techno.* **146**, 32–45 (2004).

24. Sze Tu, L.; Dehghani, F.; Foster, N.R. Micronisation and microencapsulation of pharmaceuticals using a carbon dioxide antisolvent, *Powder Technol.* **126**, 134–149 (2002).

25. Breitenbach, A.; Mohr, D.; Kissel, T. Biodegradable semi-crystalline comb polyesters influence the microsphere production by means of a supercritical fluid extraction technique (ASES), *J. Control. Release.* **63**, 53–68 (2000).

26. Garay, I.; Pocheville, A.; Madariag, L. Polymeric microparticles prepared by supercritical antisolvent precipitation, *Powder Technol.* **197**, 211–217 (2010).

27. Dixon, D.J.; Johnston, K.P.; Bodmeier, R.A. Polymeric materials formed by precipitation with a compressed fluid antisolvent, *AIChE J.* **39** **(1)**, 127–139 (1993).

28. Roderic, P.Q.; Taejun, Y.; Youngjoon, L.; Jungahn, K.; Bumjae, L. Applications of 1,1-Diphenylethylene chemistry in anionic synthesis of polymers with controlled structures, *Adv. Polym. Sci.* **153**, 70-100 (2000).

29. Reverchon, E. Supercritical antisolvent precipitation of micro- and nano-particles, *J. Supercrit. Fluid.* **15**, 1–21 (1999).

30. Zhao, Y. *et al.* CO$_2$-controlled reactors: epoxidation in emulsions with droplet size from micron to nanometre scale, *Green Chem.* **12**, 452-457, (2010).

31. Urbanczyk, L. *et al.*, Batch foaming of SAN/clay nanocomposites with sc-CO$_2$: A very tunable way of controlling the cellular morphology, *Polymer* **51**, 3520-3531, (2010).

32. Kim, J.B.; Cho, K.S.; Park, S.J., Copper oxide-decorated porous carbons for carbon dioxide adsorption behaviors, *J. Colloid. Interf. Sci.* **342**, 575–578, (2010).

33. Zielinski, R.G.; Kline, S.R.; Kaler, E.W.; Rosov, N. A small-angle neutron scattering study of water in carbon dioxide microemulsions, *Langmuir* **13**, 3934-3937 (1997).

34. Lee, H.; Terry, E.; Zong, M.; Arrowsmith, N.; Perrier, S.; Thurecht, K.J.; Howdle, S.M. Successful dispersion polymerization in supercritical CO₂ using polyvinylalkylate hydrocarbon surfactants synthesized and anchored via RAFT, *J. Am. Chem. Soc.* **130**, 12242–12243 (2008).

35. Butler, R.; Davies, C.M.; Cooper, A.I. Emulsion templating using high internal phase supercritical fluid emulsions, Advanced Materials **13**, 1459–1463 (2001).

36. Kemmere, M.; Cleven, M.; Schilt, M. Keurentjes, J. Process design for the removal of residual monomer from latex products using supercritical carbon dioxide, *Chem. Eng. Sci.* **57**, 3929-3937 (2002).

37. Johnston, K.P.; Rocha, S.R.P. Colloids in supercritical fluids over the last 20 years and future directions, *J. Supercrit. Fluid.* **47**, 523-530 (2009).

38. Kwon, S.; Lee, K.; Bae, W.; Kim, H. Synthesis of biocompatible polymer using siloxane-based surfactants in supercritical carbon dioxide, *J. Supercrit. Fluid.* **45**, 391-399 (2008).

39. Canelas, D.A.; DeSimone, J.M. Dispersion polymerizations of styrene in carbon dioxide stabilized with poly(styrene-b-dimethylsiloxane), *Macromolecules* **30**, 5673-5682 (1997).

40. Debenedetti, P.G. *Supercritical fluids as particle formation media, in: Fundamentals for application*, (Kluwer Academic publishers. Boston, 700-719 1994).

41. Ji, M.; Chen, X.; Wai, C.M.; Fulton, J.L. Synthesizing and dispersing silver nanoparticles in water-in- sc-CO₂ microemulsions, *J. Am. Chem. Soc.* **121**, 2631-2639 (1999).

42. Ohde, H.; Hunt, F.; Wai, C.M. Synthesis of silver and copper nanoparticles in a water-in-supercritical-carbon dioxide microemulsion, *Chem. Mater.* **13**, 4130-4135 (2001).

43. Shiho, H.; DeSimone, J.M. Dispersion polymerization of glycidyl methacrylate in supercritical carbon dioxide, *Macromolecules* **34 (5)**, 1198-1203 (2001).

44. Rosell, A.; Storti, G.; Morbidelli, M. Dispersion polymerization of methyl methacrylate in supercritical carbon dioxide using a pseudo-graft stabilizer: role of reactor mixing, *Macromolecules* **37**, 2996-3004 (2004).

45. Zhang, J. *et al.* A novel method to synthesize polystyrene nanospheres immobilized with silver nanoparticles by using compressed CO₂, *Chem.-A Eur. J.* **10**, 3531-3536 (2004).

46. Yang, J.; Hasell, T.; Wang, W.; Howdle, S.M. A novel synthetic route to metal–polymer nanocomposites by in situ suspension and bulk polymerizations, *Eur. Polym. J.* **44**, 1331-1336 (2008).

47. Horsch, S.; Serhatkulu, G.; Gulari, E.; Kannan, R.M. Supercritical CO₂ dispersion of nano-clays and clay/polymer nanocomposites, *Polymer* **47**, 7485-7496 (2006).

48. Wong, B.; Yoda, S.; Howdle, S.M. The preparation of gold nanoparticle composites using supercritical carbon dioxide, *J. Supercrit. Fluid.* **42**, 282-287 (2007).

49. Wallace, J.M. *et al.* Silver-colloid-nucleated cytochrome c superstructures encapsulated in silica nanoarchitectures, *Langmuir* **20**, 9276-9281 (2004).

50. Thirumurugan, G.; Shaheedha, S.M.; Dhanaraju, M.D. In-vitro evaluation of antibacterial activity of silver nanoparticles synthesized by using phytophthora infestans, *Int. J. Chem. Tech. Res.* **3**, 714-716 (2009).

51. Dutta, A.; Dolui, S.K. Preparation of colloidal dispersion of CuS nanoparticles stabilized by SDS, *Mater. Chem. Phys.* **112**, 448–452 (2008).

52. Bernade, A.G.; Kramer, M.; Olah, B.; Haag, R. Syntheses and phase-transfer properties of dendritic nanocarriers that contain perfluorinated shell structures *Chem. A Eur. J.* **10**, 2822-2830 (2004).

53. Feng, J.; Zhang, C.P. Preparation of Cu-Ni nanocrystallites in water in oil microemulsions, *J. Colloid. Interf. Sci.* **293**, 414-419 (2006).

54. Raja, M.; Shanmugaraj, A.M.; Ryu, S.H. Preparation of template free zinc oxide nanoparticles using sol-gel chemistry, *J. Nanosci. Nanotech.* **8**, 4224-4426 (2008).

55. Ershov, B.G.; Gordeev, A.V. Silver nanoparticles stabilised with heteropolyanions in an aqueous solution: optical properties and electronic polarization, *Mendeleev Commun.* **11**, 147-148 (2001).

56. Deka, H.; Karak, N.; Kalita, R.D.; Buragohain, A.K. Bio-based thermostable, biodegradable and biocompatible hyperbranched polyurethane/Ag nanocomposites with antimicrobial activity, *Polym. Degrad. Stabil.* **95**, 1509-1517 (2010).

57. Pomogailo, A.D.; Kestelman,V.N. Metallopolymer Nanocomposites 375, 65 (2005).

58. Feng,Q.L.; Wu, J.; Chen,G.Q.; Cui, F.Z.; Kim, T.N.; Kim, J.O. A mechanistic study of the antibacterial effect of silver ions on escherichia coli and staphylococcus aureus, *J. Biomed. Mater. Res.* **52**, 662-665 (2000).

59. Singh, M.; Singh, S.; Prasad, S.; Gambhir, I.S. Digest J Nanoparticles Bioclusters 3, 115 (2008).

CHAPTER 4

SYNTHESIS OF POLYSTYRENE /CLAY NANOCOMPOSITES IN SC-CO$_2$ MEDIUM

Synthesis of polystyrene/bentonite clay nanocomposites by emulsion polymerization in aqueous and in supercritical carbon dioxide (sc-CO$_2$) medium

4.1 Introduction

Improvement of pristine polymer properties through the formation of nanocomposites is found to be one of the best ways in the current scenario.[1-9] Polymer nanocomposites in which even a small percentage (<5wt%) of nanoparticles embedded in a polymer matrix exhibit significant improvement in material properties like dimensional stability, mechanical properties, thermal stability, flame retardancy, gas barrier properties etc. compared to the neat polymer.[10,11] The high surface to volume ratio and easy intercalation ability of the nanoclay account for such enhancements of the properties compared to the conventional composites. The polymer chain dynamics are highly altered due to the restricted conformational degree of freedom of the polymer chains as imposed by the clay layers.[12,13] There are several approaches to synthesize polymer/clay nanocomposites, among which *in-situ* polymerization has proved to be the most successful one. A few researchers from Toyota Motor Company first synthesized the exfoliated nylon-6/clay hybrid for automotive applications.[14] Since then several useful vinyl polymer/clay nanocomposites have been prepared by *in-situ* polymerization. Among the vinyl monomers the most commonly used are styrene and methyl methacrylate.

The modification of the clay is an important factor to make it compatible with the polymer chain. For this purpose, the sodium ions of the pristine clay are usually replaced with an alkyl ammonium or phosphonium cations containing surfactant via an ion exchange reaction.[15]

This renders increase in inter-gallery spacing and making the clay organophilic. The well dispersion of the organophilic or modified clay can be done in a variety of methods. A wide range of nanocomposites have been modified by melt mixing, solution casting and *in-situ* polymerization. However a drawback of *in-situ* polymerization is that it typically involves large amount of solvents which are not environmentally friendly and costly for an industrial scale applications.

Volatile organic solvents and water are basically used all over the world in the industrial applications for the synthesis and processing of polymers. Water is used as a polymerizing medium due to its easy availability and low cost. But there are some serious problems associated with organic solvents as they cause environmental pollution. Moreover, complete purification of the product (removal of solvent from the product) is also a tedious job in this procedure.

To overcome these problems, one new green synthesis medium, supercritical carbon dioxide (sc-CO$_2$) is used recently by the researchers.[16-22] It has attracted extensive interest as polymerization and polymer processing medium. The key factor for using supercritical carbon dioxide as polymerizing medium is that it is environmentally benign and economically viable.[23] It has a lot of advantages over conventional organic as well as aqueous solvents because of their "gas-like" diffusivity, liquid like density, low viscosity and low surface tension.[24] In short supercritical carbon dioxide has emerged as an important supercritical fluid, (SCF) because of many desirable attributes such as low cost, abundance, low toxicity, and readily accessible supercritical conditions (T$_c$=31.1°C, P$_c$=7.38MPa).[22] Above the critical condition, the physicochemical properties of CO$_2$ can be tuned between gas like and liquid like limits by maintaining the pressure and temperature. Horsh *et al.* has successfully dispersed nanoclays in supercritical carbon dioxide and synthesized polymer clay nanocomposites in the same medium. They observed significant dispersion of dry Cloisite 93A nanoclays in the medium. They have used PDMS as the stabilizer for synthesizing the polymer clay nanocomposite.[25] Zhao *et al.* has made a comparative study on the synthesis of poly(methyl methacrylate) and

polystyrene/clay nanocomposites in supercritical carbon dioxide (sc-CO$_2$) medium. They have synthesized both the nanocomposites via pseudo dispersion polymerization in the presence of surfactant modified clay (PDMS-clay) in (sc-CO$_2$) medium.[26] L. Urbanczyk *et al.* have studied the synthesis of polylactide/clay nanocomposites by *in-situ* interactive polymerization in (sc-CO$_2$) medium. They prepared the polylactide/clay nanocomposite by *in-situ* ring opening polymerization in (sc-CO$_2$).[27] The clay polymer/clay nanocomposites exhibits enhanced mechanical properties, thermal properties, reduced gas permeability and improved chemical stability.[31] These types of polystyrene/clay nanocomposites are widely used in biomedical applications as they are inert, in packaging industries, in manufacturing CD cases, disposable razor, low cost containers, bottles etc. the polymer clay nanocomposites due to its light weight and high mechanical strength properties are used in replacing wood and metal furnishers used in the household purposes.[33]

This chapter describes the synthesis of Polystyrene/bentonite clay nanocomposites by emulsion polymerization in aqueous and in supercritical carbon dioxide (sc-CO$_2$) medium using organically modified bentonite clay. The modified clay is dispersed within the monomer via ultrasonication and the mixture is allowed to undergo *in-situ* emulsion polymerization resulting in the formation of polymer/clay nanocomposites. A comparative study of the properties of the nanocomposites synthesized in the two media is carried out. The effects of clay concentration on polymer conversion, molecular weight, morphology and mechanical properties have been investigated. Sodium dodecylbenzene sulfonate (SDBS) is used as a stabilizer in aqueous medium and Polydimethylsiloxane (PDMS) as stabilizer in sc-CO$_2$ medium. The nanocomposites were characterized by XRD, SEM, TEM, GPC and TGA.

4.2 Experimental

4.3 Materials

Styrene (Merk) was deinhibited with 10% NaOH solution and washed with distilled water, azobisisobutyronitrile (AIBN) (Allied Industries, Bombay) was recrystallized twice in methanol. Sodiumdodecyl benzene sulfonate (Aldrich), organically modified bentonite clay (Sigma Aldrich), and polydimethylsiloxane (PDMS) (Fluka) was used as received. Carbon dioxide (Rass Cryogenics) (99.99 % pure) was used as received.

4.4 Supercritical fluid (SCF) Reactor

The reactions in water medium were performed in a three necked round bottom flask. All reactions in supercritical carbon dioxide medium was performed in a 60 ml, high-pressure stainless steel reactor (SCF-System, Reaction Eng. Inc. Korea). The schematic diagram of the apparatus is shown in earlier chapters. The SCF equipment is connected with the high pressure CO$_2$ cylinder, high pressure metering pump and an efficient cooler. The pressure inside the reactor can be raised up to 6,000 psi. The pressure inside the reactor is measured with a pressure transducer.

4.5 PROCEDURE

4.5.1 Synthesis of polystyrene/clay nanocomposites in aqueous medium

All reactions in aqueous medium were performed in a three necked round bottom flask fitted with a mechanical stirrer, a condenser and a thermometer. 50 ml of distilled water was taken in the three necked round bottom flask and 0.02 g SDS was added to it. 0.3 g of bentonite clay (6.0 wt % with respect to monomer) was mixed with 5 ml of distilled water and sonicated for 30 min, and then added to the reaction mixture. Then

styrene monomer (5 ml) and 0.2g initiator AIBN (0.5 wt % with respect to monomer) was added to the reaction mixture and stirred vigorously and 0.06wt% of PVA solution was added as a stabilizer. The temperature was raised upto 80 °C and allowed the reaction for 6 h at nitrogen atmosphere. The dirty white emulsion of the nanocomposite is separated out from the round bottom flask. The emulsion was centrifuged at 5,000 rpm for 2 h. The nanocomposite was washed for several times with distilled water and methanol.

4.5.2 Synthesis of polystyrene/clay nanocomposite in supercritical carbon dioxide (sc-CO_2) medium

0.5 ml PDMS, 0.02 g AIBN, 5 ml of styrene monomer and 0.3 g organically modified bentonite clay were mixed thoroughly in a beaker and then the mixture was sonicated for 30 min. The whole reaction mixture was then purged into the stainless steel SCF reactor. The reactor was charged with CO_2 for few seconds and vented the gas to make the reactor free from air. Then the reactor was filled with CO_2 gas and the pressure was raised to 3,000 psi at 80 °C. The reaction was continued for 8 h. After completing the reaction, the pressure inside the reactor was released and the dirty white dry nanocomposite particles were collected from the reactor and washed several times with methanol.

4.6 Sample preparation for mechanical test

Polystyrene/bentonite clay nanocomposite particles were dissolved in THF and ultrasoniated for few minutes to make a well dispersed solution. The solutions were casted on glass plates (75x25x1.39 mm^3) and dried in oven. These films were peeled out and cut by manual sample cutter as per ASTM D 412-51T for mechanical test. All the films were of 60-70 μm thickness.

4.7 CHARACTERIZATION

4.7.1 SEM analysis

SEM analysis of the polymer particles were obtained from Jeol-Jsm-6390LV scanning electron microscope (SEM). For SEM analysis, samples were mounted on an aluminum stub using an adhesive carbon tab and were coated with platinum to a thickness of 200 A° in high vacuum. SEM analysis gives the morphology of the polymer particles.

4.7.2 TEM analysis

TEM analysis of the nanoparticles and the nanocomposites was studied using (TEM) of model JEM 2100, JEOL, Japan at operating voltage of 200 kV. For TEM analysis, 2-3 drops of the emulsion were transferred on to a 3 mm diameter carbon coated copper grid. The solvent was allowed to evaporate at room temperature before loading the sample in the microscope. Conventional bright field imaging was used to observe the particle morphology with diffraction patterns. The size distribution of the clay layers were studied using transmission electron microscope (TEM).

4.7.3 Thermogravimetric analysis (TGA)

Thermogravimetric analysis (TGA) reveals the thermal characteristics of polymers including degradation temperature, absorbed moisture content, the level of oligomer in polymer etc. It determines the weight loss with respect to temperature. Thermogravimetric analysis (TGA) was conducted on a Shimadzu TGA-50 thermo gravimetric analyzer with a heating rate of 5 °C per min under nitrogen atmosphere. Analysis was performed at 30-500 °C temperature ranges.

4.7.4 Differential scanning calorimetry (DSC)

Differential scanning calorimetry (DSC) is used widely for polymers. It evaluate glass transition temperature (T$_g$), melting temperature (T$_m$), purity of the polymers. The result of a DSC experiment is a curve of heat flux versus temperature or versus time. Differential scanning calorimetry (DSC) of the polymers was accomplished on DSC-60 (Shimadzu) with a heating rate of 10 °C per minute under nitrogen atmosphere. Analysis was performed at 30-300 °C temperature ranges.

4.7.5 X-ray diffraction

X-ray diffraction (XRD) technique gives the information about the crystallographic structure, chemical composition and physical properties of the materials. X-ray diffraction technique is based on the elastic scattering of X-rays from structures that have long range order. XRD data were collected on a Rigaku Miniflex X-ray diffractometer Cu Kα radiation (λ=0.15418 nm) at 30 kV and 15 mA, with a scanning rate of 0.05 degree/sec in 2θ ranges from 2° to 15°.

4.7.6 GPC analysis

Molecular weight of the polymers was determined by gel permeation chromatography (GPC, Waters, USA, Model 515) solvent delivery system at a flow rate of 1.0 ml/min through a set of three ultrastyregel columns. Analysis was done at controlled temperature at 45 °C using HPLC grade tetrahydrofuran (THF) as eluent, and the instrument was standardized with polystyrene standards.

4.7.7 Mechanical property study

The mechanical properties such as tensile strength and elongation at break were measured by universal testing machine (UTM) of model Zwick Z010, Germany with a

10-kN load cell and crosshead speed of 50 mm/min. The casted nanocomposites sheets ($\approx$1 mm thickness) were cut by the manual sample cutter with dimension as per ASTM D 412-51T for mechanical testing.

4.8 RESULT AND DISCUSSION

4.8.1 Effect of concentration of nano clay on polymerization of styrene

The polystyrene/bentonite clay nanocomposites have been prepared in both aqueous medium and supercritical carbon dioxide medium using same concentration of clay. SEM micrographs (Fig.4.3, Fig.4.4) show that the polymer/clay nanocomposites in both the cases primarily consist of spherical particles. Some particles are free and some particles are in the agglomerated form. These particles show a relatively broad size distribution, presumably due to the ill-defined interaction between monomers and insoluble clay platelets as compared to monomers and soluble polymeric surfactants.[32] As the concentration of clay increases from 4-15%, the particle size of the nanocomposite. This is due to the formation of large number of nano clay centered monomer droplets, which undergo in-situ polymerization to form the nanocomposite particles. With the increase in clay percentage, the number of nano clay centered monomer droplets will be more. That is why, the number of nanocomposite particles increase with the increase in clay loading. In addition, the molecular weights of polystyrene increases with the increase in clay concentration as shown in the Table.1.

Table.4.1: Physical properties of the nanocomposites synthesized in the two media

Medium	Entry	Clay %	Yield %	M$_n$ (g/mol)	Sample description	Particle size (μm)
In Water	1	4	67	55,000	Dirty white emulsion	4 Agglomerated
	2	7	70	57,000	Dirty white emulsion	1-2 Agglomerated
	3	10	82	60,000	Dirty white emulsion	1.7 Agglomerated
	4	15	83	62,000	Dirty white emulsion	1.5 Agglomerated
In sc-CO$_2$	5	4	71	43,000	Aggregated powder	2.2 discrete
	6	7	76	45,000	Fine powder	2 discrete
	7	10	80	47,000	Fine powder	1- 1.9 discrete
	8	15	88	48,000	Fine powder	1.8 discrete

[*] Particle size is calculated from SEM, Molecular weight from GPC analysis

This is due to the nano clay layers present in the nanocomposite particles which restricts the chain termination rate during the polymerization process. Though the molecular weight is increasing in both the media, the molecular weight of the polystyrene in case of supercritical carbon dioxide is lower than in aqueous medium. In our earlier observations also it was noticed that the molecular weight of the polymers synthesized in sc-CO$_2$ medium was quite low than in organic and aqueous medium.[29] This is possibly due to the presence of CO$_2$, which restricts the growth of the polymer chains in sc-CO$_2$ medium.

4.8.2   XRD analysis of PS/clay nanocomposites synthesized in the two media

XRD is a powerful tool to investigate the degree of dispersion and delamination of clay layers into polymer matrix. In general intercalated layers show intense peak in the range of $1.5°-10°$ (2θ value). Fig.4.1 shows the XRD patterns of the bentonite clay and polymer clay nanocomposites. The pristine bentonite clay showed a characteristic diffraction peak at $2\theta \approx 4.2°$ which corresponds to an intergallery distance 2.36 nm. The d-spacing of the organically modified clay was calculated on the basis of Bragg's equation.[28] The XRD of the pristine polymer did not show any peak. The peak of the clay was shifted to $2\theta \approx 2.4°$ which corresponds to an intergallery distance 3.67 nm in the nanocomposites synthesized in aqueous medium (10% and 15% clay loading), which is due to the delamination of the layers in the polymer matrix by the polymer chains. The peak of the clay was shifted to $2\theta \approx 2.1°$ (corresponding to inter layer distance 4.2nm) in the nanocomposites synthesized in sc-CO$_2$ medium (10% and 15% clay loading). In sc-CO$_2$, the inter layer distance of the clay layers shifted up to 4.9 nm for 7% clay loading (corresponding peak at $1.8°$), which implies that the clay layers are more exfoliated in sc-CO$_2$ medium.
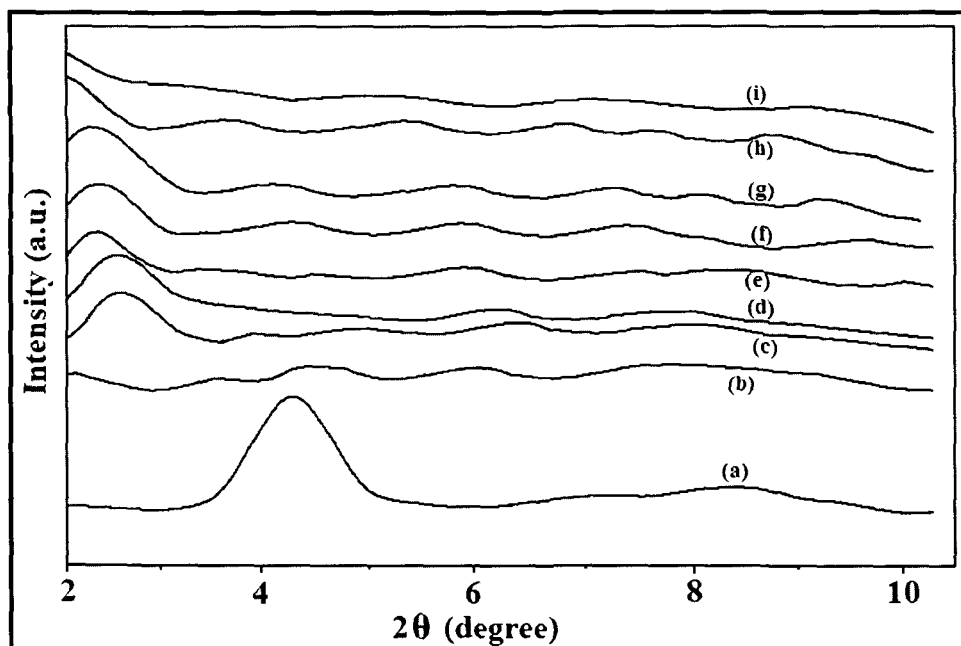
Fig.4.1: XRD of the nanocomposites and the pristine polymer

(a) Modified bentonite clay, (b) Pristine polymer, (c) Nanocomposite with 15% Clay in water medium, (d) Nanocomposite with 10% Clay in water medium, (e) Nanocomposite with 7% Clay in water medium, (f) Nanocomposite with 15% Clay in sc-CO$_2$ medium, (g) Nanocomposites with 10% Clay in sc-CO$_2$ medium, (h) Nanocomposites with 7% clay in sc-CO$_2$ medium, (i) Nanocomposite with 4% Clay in sc-CO$_2$ medium.

In supercritical carbon dioxide, the delamination efficiency of the clay is more due to very high pressure. CO$_2$ gas helps in delamination of the clay layers under vigorous stirring inside the reactor and the monomer penetrate the layers of the nanoclay. The *in-situ* processing of the clay in sc-CO$_2$ medium is shown in the Fig.4.2. But in aqueous medium, the increase in interlayer distance of the nanoclay is lower compared to CO$_2$ medium.

146
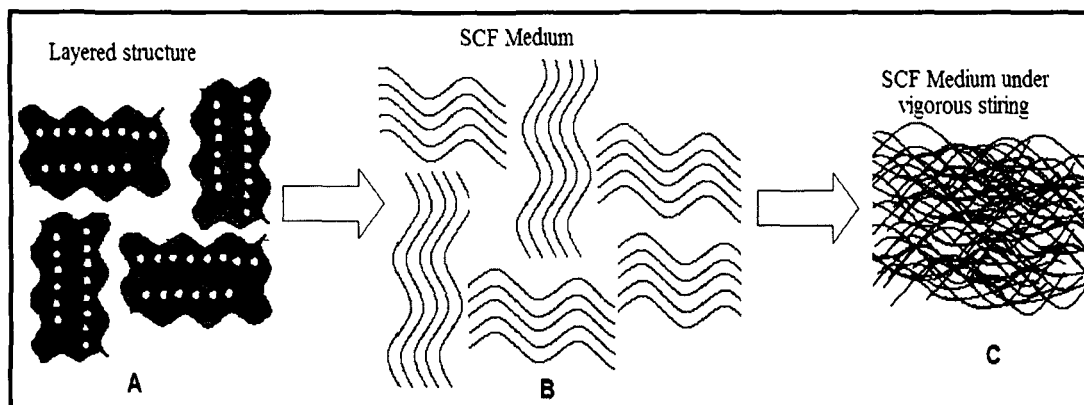
Fig. 4.2: Scheme for processing of nanoclay in sc-CO₂ medium

A. Layered clay structure, B. Clay layers in sc-CO₂ medium, C. Clay layers in sc-CO₂ under vigorous stirring

4.8.3 SEM analysis of PS/clay nanocomposites synthesized in the two media

SEM micrographs of the polymer clay nanocomposite particles synthesized in aqueous medium and in supercritical carbon dioxide (sc-CO₂) medium are as shown in Fig.4.3 and Fig.4.4. The SEM micrographs imply that the nanocomposite particles synthesized in aqueous medium in the agglomerated form. But the polystyrene/clay nanocomposite particles synthesized in sc-CO₂ medium are in the form of discrete particles.

Fig.4.3: SEM images of the nanocomposites synthesized in water medium

(a) 4% Clay loading, (b) 7% Clay loading, (c) 10% Clay loading, (d) 15% clay loading

It is also observed that with the increase in concentration of clay dosing from 4 to 15%, the average diameter of the nanocomposite particles decreases. In addition, the molecular weight of the polymers also decreases with the increase in concentration of the nanoclays. In both the media, the nanocomposite particles were in the form of some spherical particles (as evident from the SEM images). However, there was an interesting observation from the SEM images that the microparticles of the polystyrene/clay nanocomposite synthesized in sc-CO_2 medium are more discrete and uniform in nature than the nanocomposite particles synthesized in aqueous medium. At high pressures, very good processing of the nanoclay and the nanocomposites take place resulting in the

148

formation of uniform and discrete nanocomposite particles. This is because, at high pressure, CO_2 penetrates into the layered structures of the nanoclay for which the monomers can undergo penetrating in between the layers of the nanoclay and undergo polymerization to form the nanocomposite particles.
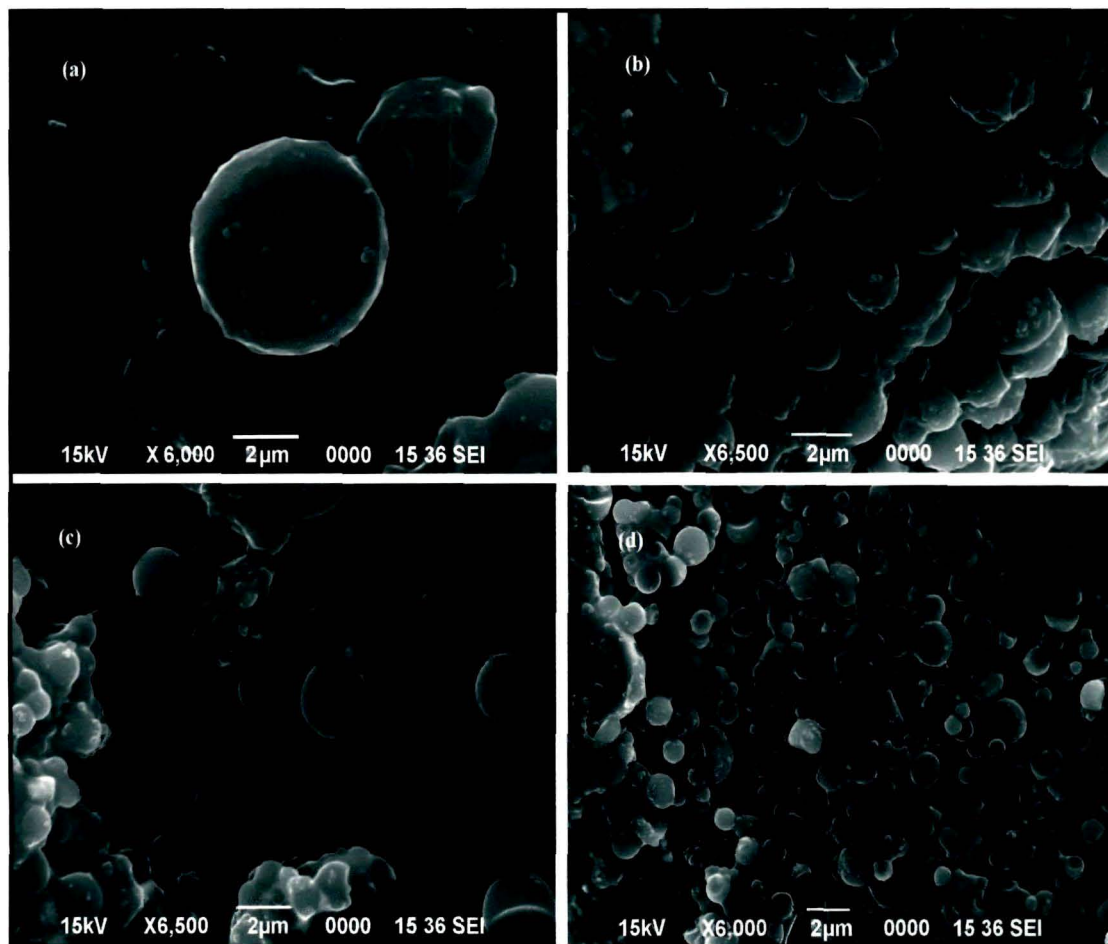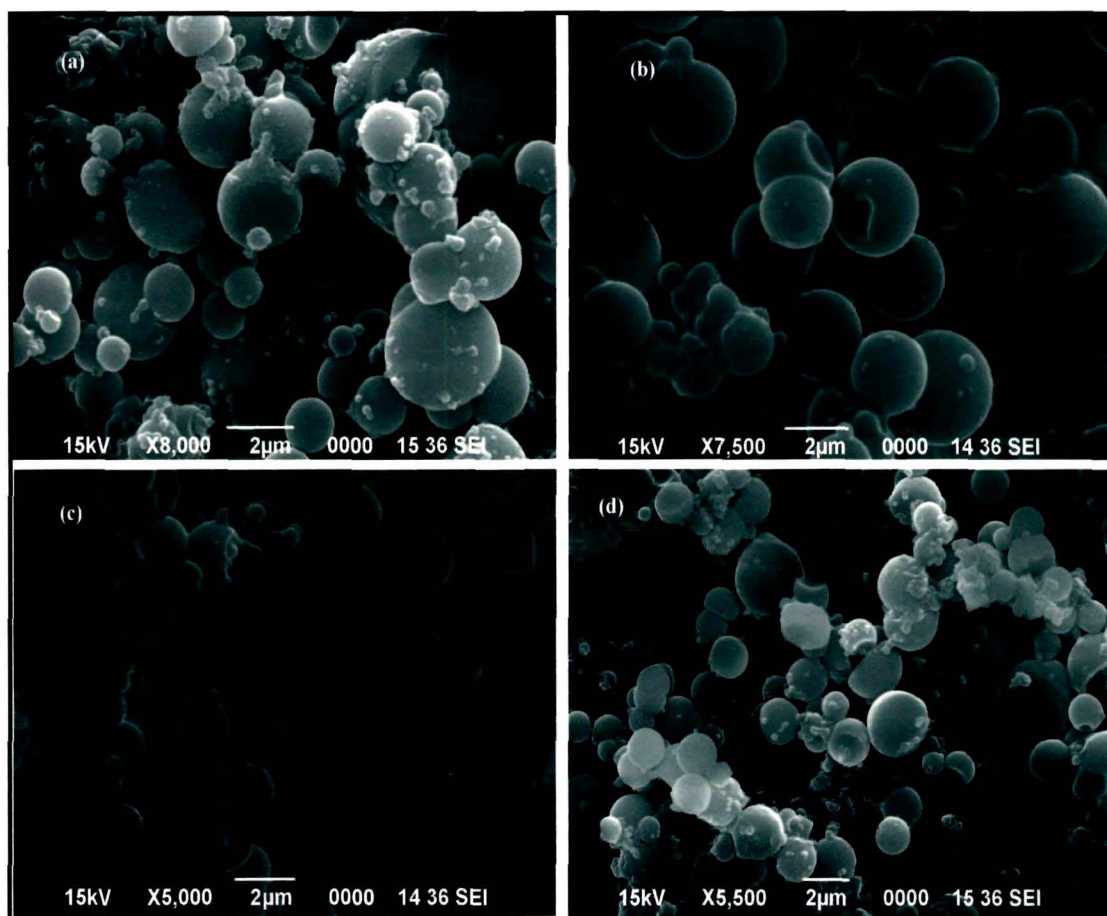

Fig.4.4: SEM images of the nanocomposites synthesized in sc-CO_2 medium

(a) 4% clay loading, (b) 7% Clay loading, (c) 10% Clay Loading, (d) 15% Clay loading

That is why uniformly distributed nanocomposite particles are obtained without any agglomeration in supercritical carbon dioxide medium than in aqueous medium. This is in good agreement with the TEM results. Relatively low molecular weight of the

polymers is formed in supercritical carbon dioxide than in aqueous medium. Powdered nanocomposite particles are directly obtained in supercritical carbon dioxide medium.

4.8.4 TEM images of PS/clay nanocomposites synthesized in the two media

The TEM micrographs of single particle of the polymer clay nanocomposite particles are shown in Fig.4.5 which clearly indicates the exfoliated and intercalated nature of the nanoclay. In the supercritical carbon dioxide medium totally exfoliated clay layers are observed. But in the nanocomposites synthesized in aqueous medium, the degree of exfoliation nature is less as compared to the sc-CO_2 medium.

Fig.4.5: TEM images of the nanocomposites

(a) in water medium, (b) in sc-CO_2 medium, (c) in water medium, (d) in sc-CO_2 medium

150

This is due to the high degree of penetration of the CO_2 gas in between the layers of the nanoclay at very high pressure and temperature (Fig.4.2). The monomers can easily penetrate through the layers of the exfoliated clay layers and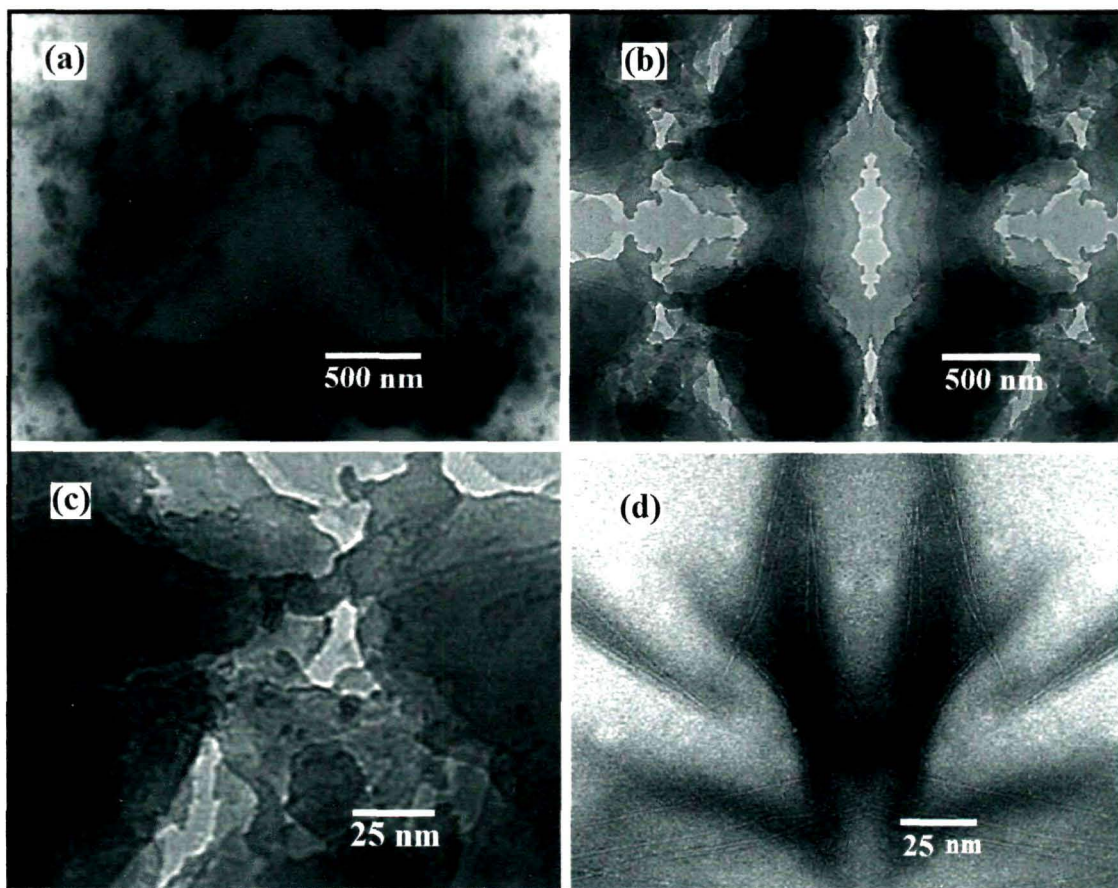 undergo polymerization to form the nanocomposite particles. From the TEM image, it is also clear that the clay layers are dispersed and disordered randomly inside the polymer particles. The disorderness and the randomness of the clay layers are more in the case of polymer nanocomposites synthesized in supercritical carbon dioxide medium than the aqueous medium.

The TEM images of the nanocomposite (Fig.4.5.b) synthesized in sc-CO_2 medium clearly points out the exfoliated nature of the nanocomposite whereas the nanocomposite particles synthesized in aqueous medium showed the intercalated nature (Fig.4.5.a).

4.8.5 Thermal properties of PS/clay nanocomposites synthesized in the two media

The thermal properties of the nanocomposite were studied by (TGA) and (DSC) analysis. The TGA curves are shown in Fig.4.6 and Fig.4.7. Single step degradation pattern with enhanced thermal stability of the polymer/clay nanocomposite is observed in both the media. The thermal properties of the polymer-clay nanocomposites are significantly improved may be due to the fact that the nanoclays act as a heat barrier, which enhances the overall thermal stability of the system. It also assists in the formation of char after thermal decomposition. The incorporation of the clay layers restricts the thermal motion of the polymer in the confined space and prevents chain scission or delays the emission of volatile decomposed products as a result of reduced permeability.[30]
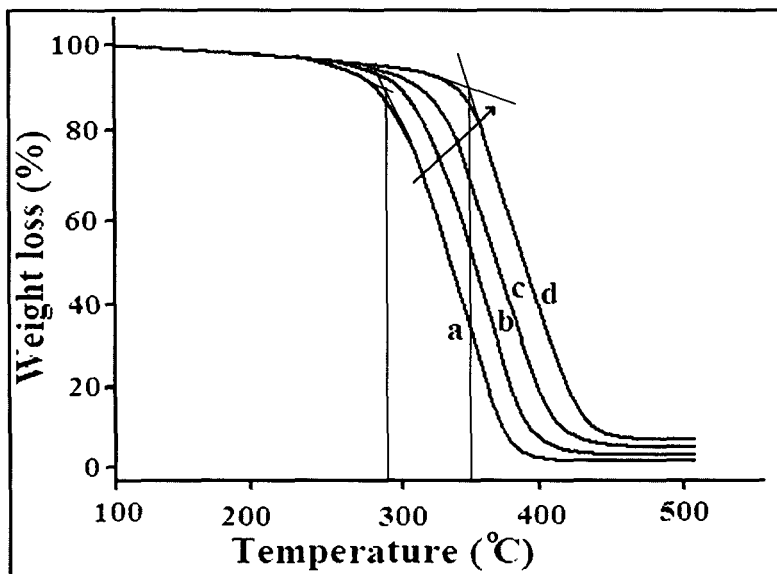
Fig.4.6: TGA of the nanocomposites synthesized in water medium
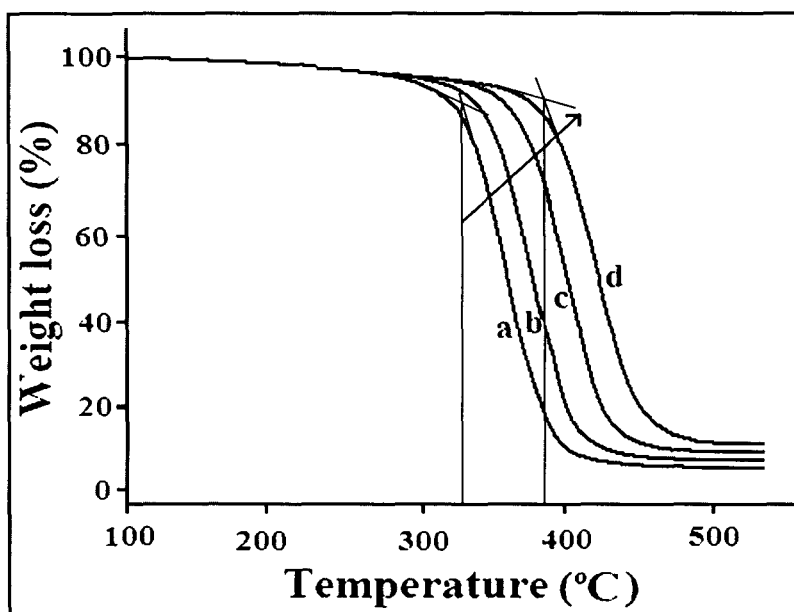
Fig.4.7: TGA of the nanocomposites synthesized in sc-CO$_2$ medium

The polymer nanocomposites showed thermal stability up to 390°C. The thermal properties of the polystyrene-clay nanocomposites are summarized in Table 4.2.

Table 4.2: Thermal properties of the clay/polystyrene nanocomposites

Medium	Entry	Clay (%)	Glass Transition temperature (T$_g$ °C)	Decomposition Temperature (°C)
In water medium	1	4	75	290
	2	10	78	317
	3	15	81	350
In sc-CO$_2$ medium	4	4	75	320
	5	10	81	375
	6	15	87	390

With the increase in the clay percentage in the nanocomposite, the thermal stability of the nanocomposite increases. This is because, the well dispersed nanoclay layers are acting as the physical barrier to the decomposed products for escaping from the matrix.[29,30]
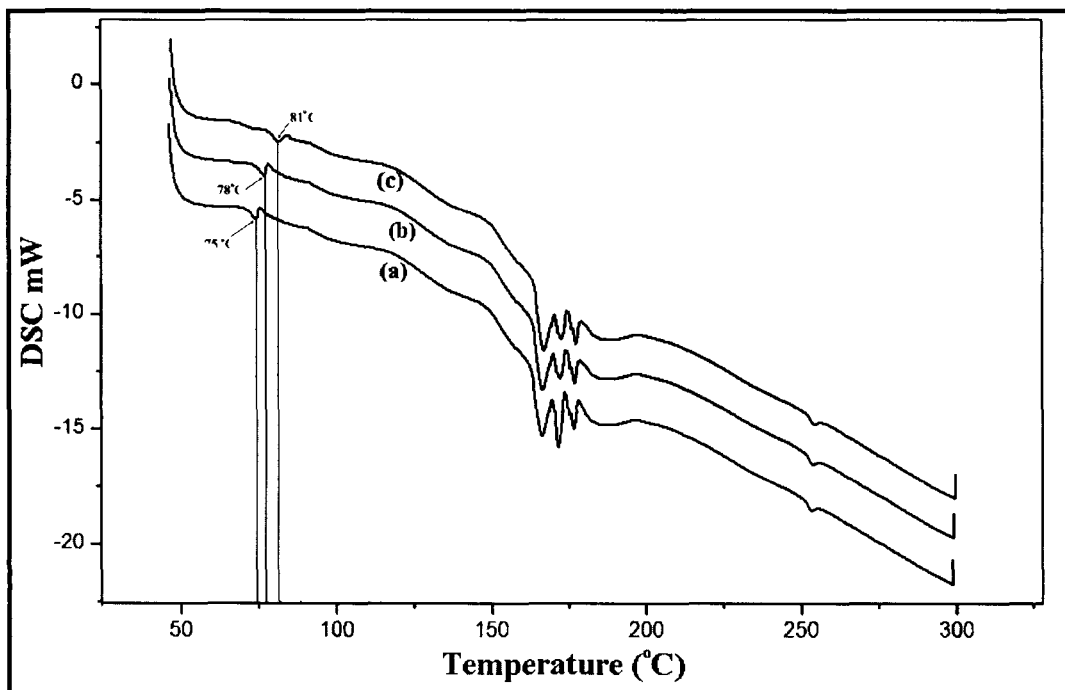
Fig.4.8: DSC of the nanocomposites synthesized in water medium

(a) 4% clay-polystyrene nanocomposites, (b) 10% clay-polystyrene nanocomposites and

(c) 15% clay-polystyrene nanocomposites.

153

In the DSC curves (Fig.4.8 and Fig.4.9), distinct hump formation was observed indicating the glass transition temperature (T$_g$) of the polystyrene clay nanocomposites. With the increase in clay percentage in the nanocomposites, the T$_g$ value also increases. The restriction on the segmental chain movement imposed by the clay particles is the cause of this behavior.[15] However, the increase in glass transition temperature of the nanocomposites synthesized in supercritical carbon dioxide is more than in aqueous medium.
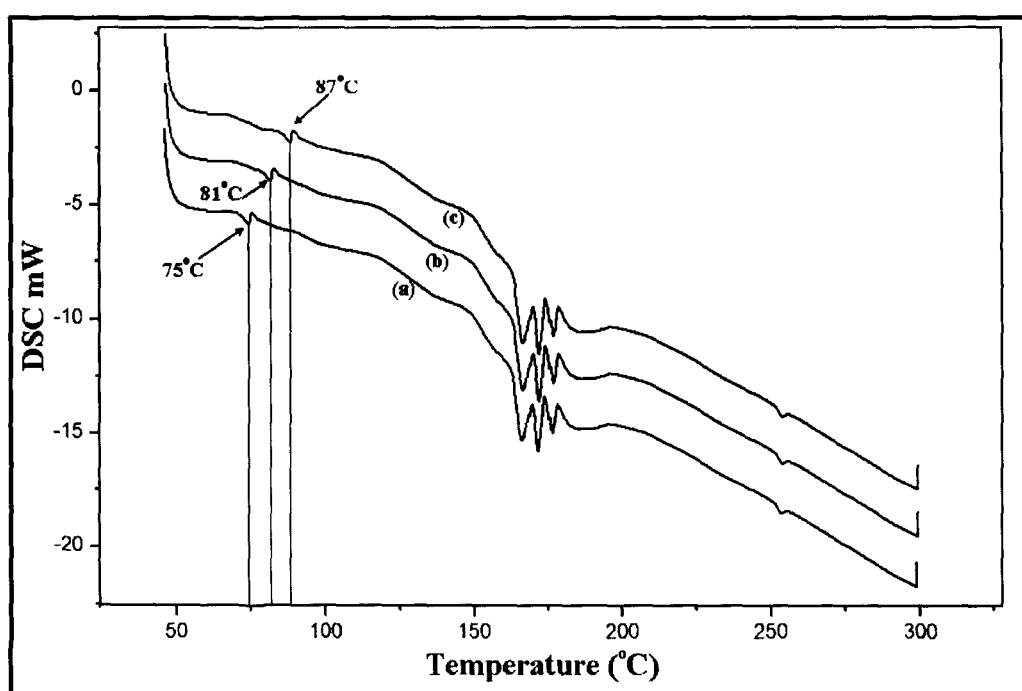
Fig.4.9: DSC of the nanocomposites synthesized in CO$_2$ medium

(a) 4% clay-polystyrene nanocomposites, (b) 10% clay-polystyrene nanocomposites and

(c) 15% clay-polystyrene nanocomposites

Thus the volatile polymer products have to come across a torturous path way during thermal degradation. Again the thermal motion of the polymer was quite reduced by the increased interfacial interaction between the clay and the matrix. This also helped in improvement of thermal stability. The thermal stability as well as residual weight of the nanocomposites increases with increase in clay content. The polystyrene/clay

154

nanocomposites synthesized in the supercritical carbon dioxide medium showed a better thermal stability than the in the aqueous medium. The thermal decomposition temperature of the nanocomposite with 4% clay synthesized in aqueous medium is 290°C, while the decomposition temperature of the nanocomposite with 4% clay synthesized in sc-CO₂ medium is 320°C. Similarly in other clay percentages also the degradation temperatures of the nanocomposites synthesized in sc-CO₂ medium show improved in the thermal stability.

4.8.6 Mechanical properties of PS/clay nanocomposites synthesized in the two media

The mechanical properties of the polystyrene/bentonite clay nanocomposites synthesized in aqueous and sc-CO₂ medium are summarized in Table 3. All these experiments were conducted in triplicate and the values in bracket represents the standard deviations.

Table 4.3: Mechanical properties of nanocomposites and the pristine polymer

Medium	Entry	Clay %	Tensile Strength (MPa)	Elongation at break (%)
	1	0	18 (±1)	470 (±3)
In	2	4	25 (±2)	450 (±1)
Water	3	7	32 (±1)	443 (±3)
	4	10	36 (±2)	436 (±4)
Medium	5	15	43 (±1)	429 (±1)
In	6	4	28 (±3)	463 (±3)
Sc-CO₂	7	7	36 (±2)	452 (±2)
	8	10	39 (±1)	445 (±3)
medium	9	15	48 (±2)	438 (±2)

The tensile strength of the nanocomposite increases with increase of nanoclay content, while the value of elongation at break decreases. This is because of the reinforcement of the matrix by organically modified bentonite clay layers. Generally, with the increase in the degree of exfoliation, the effective aspect ratio and surface area of

the nanofiller increase and hence better reinforcement of the mechanical properties observed.[30] The secondary chemical forces like van der Waals interaction, H-bonding, dipolar interaction etc. between the clay layers and the matrix at the interface are responsible for the improvement of the mechanical properties.[28] The tensile strength of the nanocomposites is far better in case of supercritical carbon dioxide than in aqueous medium.

This may be due to better exfoliated structure formation in supercritical carbon dioxide than in aqueous medium. The tensile strength (MPa) versus clay loading (%) curve for the polystyrene/clay nanocomposites are shown in Fig.4.10.
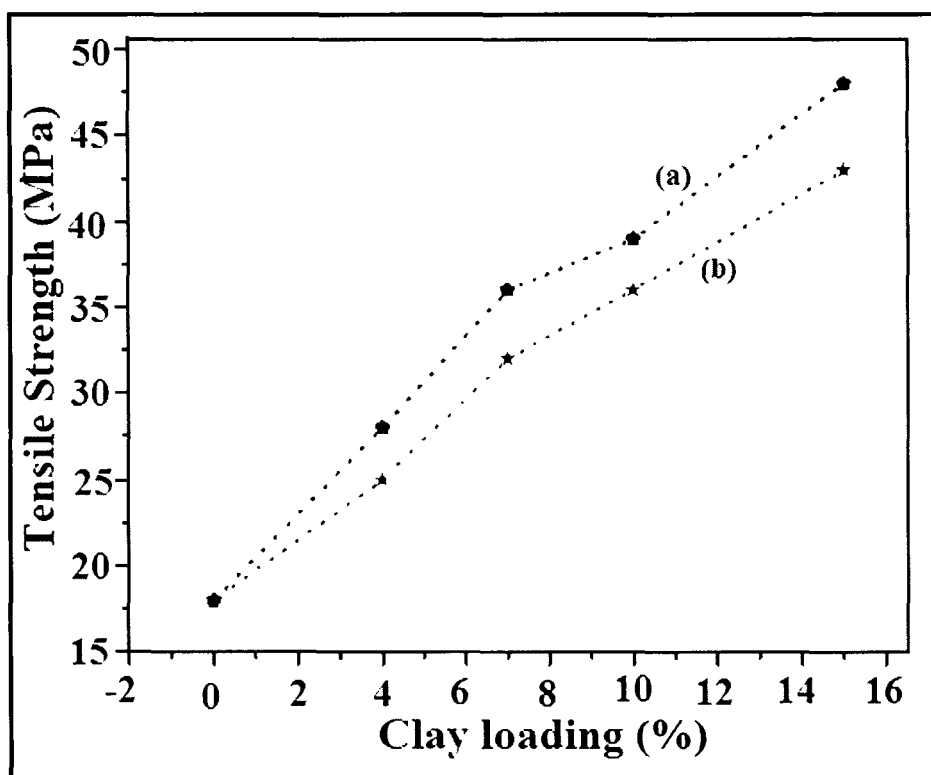
Fig.4.10: Tensile strength of nanocomposites

(a) in sc-CO₂ and (b) in water medium

In sc-CO₂, the processing of the modified nanoclay layers is far satisfactory than in aqueous medium. The formation of exfoliated structures of the nanoclay enhances the

interface interactions through bridge, loop and tail linkages of the polymer chains with the nanoclay layers. The organically modified bentonite nanoclay layers reinforce the polystyrene matrix causes the increase in tensile strength of the nanocomposite. The hydrogen bonding and some chemical linkages between the clay layers and the polystyrene matrix at the interface is responsible for the reinforcement of the mechanical strength.

4.9 Conclusion

Polystyrene/bentonite clay nanocomposites have been prepared by emulsion polymerization in both aqueous and supercritical carbon dioxide (sc-CO$_2$) medium. The particle size of the nanocomposites decreases with the increase in clay loading in both the media. But discrete and uniform sized particles are observed in sc-CO$_2$ medium, while agglomerated particles are obtained in aqueous medium. TEM and XRD results indicated that exfoliated nature of clay layers in the nanocomposites synthesized in sc-CO$_2$ medium, while intercalated and low exfoliation observed in nanocomposites synthesized in aqueous medium. The inter layer distance of the clay increases from 2.36 nm to 4.9 nm in sc-CO$_2$ medium, while in aqueous medium, it increases from 2.36 nm to 3.67 nm. The mechanical properties of the nanocomposite synthesized in sc-CO$_2$ medium are higher than in aqueous medium. Similarly, thermal properties and the particle forming efficiency of the nanocomposite are far better in supercritical carbon dioxide medium than in aqueous medium.
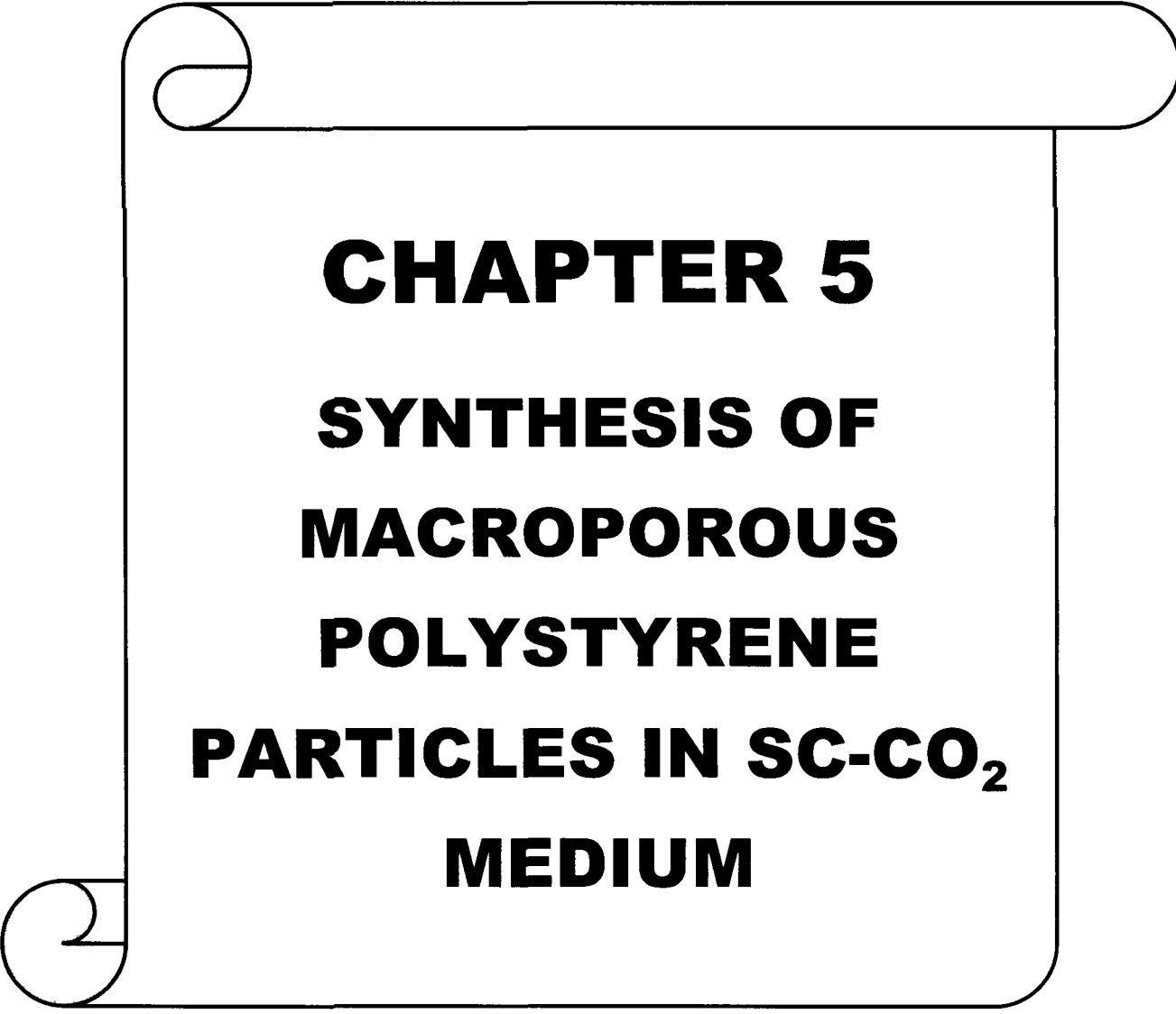
REFERENCES

1. Cho, J.; Joshi, M.S.; Sun, C.T.; Effect of inclusion size on mechanical properties of polymeric composites with micro and nano particles, *Compos. Sci. Technol.* **66**, 1941–1952 (2006).

2. Reynaud, E.; Jouen, T.; Gautheir, C.; Vigier, G.; Varlet, J.; Nanofillers in polymeric matrix: a study on silica reinforced PA6, *Polymer* **42**, 8759–8768 (2001).

3. Luo, J.J.; Daniel, I.M.; Characterization and modelling of the mechanical behaviour of polymer/clay nanocomposites, *Compos. Sci. Technol.* **63**, 1607–1616 (2003).

4. Hasell, T. *et al.* A facile synthetic route to aqueous dispersions of silver nanoparticles, *Mater. Lett.* **61**, 4906–4910 (2007).

5. Yang, J.; Hasell, T.; Wang, W.; Howdle, S.M. A novel synthetic route to metal–polymer nanocomposites by in situ suspension and bulk polymerizations, *Eur. Polym. J.* **44**, 1331–1336 (2008).

6. Yoksan, R.; Chirachanchai, S. Silver nanoparticle-loaded chitosan–starch based films: Fabrication and evaluation of tensile, barrier and antimicrobial properties, *Mater. Sci. Eng. C* **30**, 891–897 (2010).

7. Jhang, J. *et al.* A Novel Method to Synthesize Polystyrene Nanospheres Immobilized with Silver Nanoparticles by Using Compressed CO₂, *Chem. Eur. J.* **10**, 3531-3536 (2004).

8. Tai, H.; Wang, W.; Howdle, S.M. High molecular weight graft stabilisers for dispersion polymerization of vinylidene fluoride in supercritical carbon dioxide: the effect of architecture, *Polymer* **46**, 10626–10636 (2005).

9. Bell, P.W. *et al.* Stable Dispersions of silver nanoparticles in carbon dioxide with fluorine-free ligands, *Langmuir* **21**, 11608-11613 (2005).

10. Anand, M. *et al.* Synthesis and steric stabilization of silver nanoparticles in neat carbon dioxide solvent using fluorine-free compounds, *J. Phys. Chem. B* **110**, 14693-14701 (2006).

11. Chang, J.H.; An, Y.U.; Nanocomposites of polyurethane with various organoclays: thermomechanical properties, morphology and gas permeability, *J. Polym. Sci. B Polym. Phys.* **40**, 670-678 (2002).

12. Tseng, C.R.; Wu, J.Y.; Lee, H.Y.; Chang, F.C.; Preparation and characterization of polystyrene–clay nanocomposites by free radical polymerization, *J. Appl. Polym. Sci.* **85**, 1370-1377 (2002).

13. Alexandre, M.; Dubois, P. Polymer-layered silicate nanocomposites: preparation, properties and uses of a new class of materials, *Mater. Sci. Eng. Report.* **28**, 1-63 (2000).

14. Bhiwankar, N.N.; Weiss, R.A. Melt intercalation/exfoliation of polystyrene–sodium montmorillonite nanocomposites using sulfonated polystyrene ionomer compatibilizers, *Polymer* **47**, 6684-6691 (2006).

15. Kojima, Y.; Matsuoka, T.; Takahashi, H.; Kurauchi, T.; Crystallization of Nylon-6/ Clay hybrid by annealing under elevated pressure, *J. Appl. Polym. Sci.* **51**, 683-687 (2003).

16. Deka, H.; Karak, N.; Vegetable oil-based Bio-based hyperbranched thermosetting polyurethane/clay nanocomposites, *Nanoscale Res. Let.* **4**, 758-765 (2009).

17. Zhao, X. *et al.* Preparation and characterization of camptothecin powder micronized by a supercritical antisolvent (SAS) process, *J. Supercrit. Fluid.* **51**, 412-419 (2010).

18. Hossain, M.D.; Kim, W.S.; Hwang, H.S.; Lim, K.T. Role of water on PMMA/clay nanocomposites synthesized by in situ polymerization in ethanol and supercritical carbon dioxide, *J. Colloid. Interf. Sci.* **336**, 443-448 (2009).

19. Jhang, J.; Han, B. Supercritical CO$_2$-continuous microemulsions and compressed CO$_2$-expanded reverse microemulsions, *J. Supercrit. Fluid.* **47**, 531-536 (2009).

20. Su, L. *et al.* Preparation of polysiloxane/perfluorosulfonic acid nanocomposite membranes in supercritical carbon dioxide system for direct methanol fuel cell, *Int. J. Hydrogen Energ.* **34**, 6892-6901 (2009).

21. Garay, I.; Pocheville, A.; Madariaga, L. Polymeric microparticles prepared by supercritical antisolvent precipitation. *Powder Technol.* **197**, 211-217 (2010).

22. Lee, H. *et al.* Successful Dispersion Polymerization in Supercritical CO₂ Using Polyvinylalkylate Hydrocarbon surfactants Synthesized and Anchored via RAFT, *J. Am. Chem. Soc.* **130**, 12242-12243 (2008).

23. Leitner, W. Supercritical Carbon Dioxide as a Green Reaction Medium for Catalysis, *Account. Chem. Res.* **35**, 746-756 (2002).

24. Anderson, P.E.; Badlani, R.N.; Mayer, J.; Mabrouk, P.A. Electrochemical synthesis and characterization of conducting polymers in supercritical carbon dioxide, *J. Chem. Res.* **124**, 10284-10285 (2002).

25. Horsch, S.; Serhatkulu, G.; Gulari, E.; Kannan, R.M. Supercritical CO₂ dispersion of nano-clays and clay/polymer nanocomposites. Polymer **47**, 7485-7496 (2006).

26. Zhao, Q.; Samulski, E.T. A comparative study of poly(methyl methacrylate) and polystyrene/clay nanocomposites prepared in supercritical carbon dioxide, *Polymer* **47**, 663-671 (2006).

27. Urbanczyk, L.; Ngoundjo, F.; Alexandre, M. Jerome, C. Detrembleur, C. Calberg, C. Synthesis of polylactide/clay nanocomposites by in situ intercalative polymerization in supercritical carbon dioxide, *Eur. Polym. J.* **45**, 643-648 (2009).

28. Dutta, A.; Dolui, S.K. Preparation of colloidal dispersion of CuS nanoparticles stabilized by SDS, *Mater. Chem. Phys.* **112**, 448–452 (2008).

29. Kim, Y.K.; Choi, Y.C.; Wang, K.H.; Chung, I.J. Synthesis of polystyrene–Na MMT nanocomposites via emulsion polymerization, *Chem. Mater.* **14**, 4990–4995 (2002).

30. Karak, N. *Fundamentals of polymers raw materials to finish products,* (PHI Learning Pvt. Ltd., New Delhi, 2009).

31. Meneghetti, P.; Qutubuddin, S. Synthesis, thermal properties and applications of polymer-clay nanocomposites, *Thermochim. Acta.* **442**, 74-77 (2006).

32. Yalcinkaya, S.E.; Yaldiz, N.; Sacak, M.; Calimli, A. Preparation of polystyrene/ montmorillonite nanocomposites: optimization by response surface methodology(RSM), *Turk. J. Chem.* **34**, 581-592 (2010).

33. Carastan, D.J.; Demerquette, N.R. Polystyrene/clay nanocomposites, *Int. Mater. Rev.* **52**, 345-380 (2007).

CHAPTER 5

SYNTHESIS OF MACROPOROUS POLYSTYRENE PARTICLES IN SC-CO$_2$ MEDIUM

Synthesis of macroporous polymer particles by suspension polymerization using supercritical carbon dioxide as a pressure-adjustable porogen

5.1 Introduction

Supercritical carbon dioxide (sc-CO_2) is a nontoxic, inexpensive, recyclable, nonflammable and green solvent for polymer synthesis and processing.[1-17] It is a highly compressible solvent and the solvent properties can be varied over a wide range by changing the pressure and hence the density.[18-23] In principle, it allows control over variables such as phase behavior, and should permit "tuning" of solvent properties in certain chemical reactions and polymerizations. It has been widely used as a polymerization medium for the synthesis of a variety of polymers. De Simone and his co-workers have shown that sc-CO_2 is a versatile medium for both homogeneous and heterogeneous polymerization.[24] Cooper et al.[25,26] synthesized cross-linked divinylbenzene-based polymers in sc-CO_2 by free-radical precipitation polymerization and dispersion polymerization. Microparticulate powders (0.4-10 μm) were formed, but in all the cases, the polymers were found to be completely nonporous. Canelas et al. have synthesized microparticles of polystyrene by dispersion polymerization using sc-CO_2 as polymerization medium and poly(styrene-b-dimethylsiloxane) as stabilizer.[27] The particle size was (0.5-1.0 μm) and all these particles are all nonporous in nature. Again in another study, Hsiao et al. synthesized free flowing, fine powdered polymethyl methacrylate microparticles using supercritical carbon dioxide as the polymerizing solvent.[28] The SEM images of these microparticles depicted that these particles were all nonporous in nature.

Microporous particles are of particular interest because they possess characteristics such as high surface-to-volume ratio, low density, and low coefficients of thermal expansion. These characteristics facilitate the manipulation of the surface properties of the interior or the exterior of the microspheres. Macroporous polymeric particles with high and uniform pore interiors and high surface area play an important role in microencapsulation and have been used in both drug delivery and biomedical imaging.[29,30] Macroporous polymers are important in a wide range of applications such as ion-exchange resins, chromatographic separation media, solid-supported reagents, and supports for combinatorial synthesis. They are commonly prepared by dispersion polymerization, emulsion polymerization, phase separation, suspension polymerization etc. by adding some suitable porogen. These porogens are mainly some organic solvents which are completely miscible with the monomers and are "good" solvent for the growing polymer networks. But the complete removal of the solvent and porogenic material from the polymer particles is not possible. That is why these macroporous polymer particles are not advisable for particular applications like drug delivery, temporary artificial matrix for cell seeding, chromatographic separation media, ion exchange resin etc., which demand high purity of the product.[31] But, by using sc-CO_2 as pressure adjustable porogen, we can overcome these problems and can obtain highly pure porous polymeric particles. Again in this case, one can have very fine control over the pore size and the diameter of the microparticles which was not possible in conventional porogenic solvents.

Cooper *et al.* in 2001 first reported the synthesis of macroporous polymeric beads by using sc-CO_2 as the porogens.[32] They have showed that these reaction conditions can be modified to generate well-defined macroporous polymer monoliths, thereby using sc-CO_2 as a porogenic solvent. They have used [trimethylolpropane trimethacrylate (TRIM)] monomer for synthesizing the macroporous polymer beads. In earlier all works sc-CO_2 was used as the polymerizing medium and the resulting polymer particles are all nonporous in nature. The solvent properties of supercritical carbon dioxide can be tuned in such a way that it can be used for the synthesis of macroporous polymer beads and the porosity in the beads can be controlled by varying

the CO_2 pressure.[33] A number of well established works are available in literatures regarding the synthesis of porous polymer blocks or porous polymers scaffolds in supercritical carbon dioxide. But very few works are available regarding the synthesis of macroporous polymer beads using supercritical carbon dioxide as pressure adjustable porogen.

In this chapter, one green route for synthesizing macroporous polystyrene particles by using sc-CO_2 as the porogens is reported. The solvent strength of sc-CO_2 was tuned continuously over a significant range by varying the pressure.[32] As such, sc-CO_2 can be thought of as a "pressure-adjustable porogen" for synthesis of macroporous polymer beads.

5.2 Materials

Styrene (Merck) was deinhibited by washing with 10% NaOH solution followed by washing with double distilled water. Polyvinyl alcohol (MERCK) and Tetrahydrofuran (THF, Ranbaxy), Divinylbenzene (DVB) (Aldrich) were used as received. Azobisisobutyronitrile (AIBN) (G.S. Chemical Testing Lab. & Allied Industries, Bombay) was recrystallized twice from methanol. Carbon dioxide (SCF/SFE Grade) (99.99% pure) (Rass Cryogenics) was used as received.

5.3 Supercritical fluid (SCF) reactor

All experiments were conducted in a 60 ml, high-pressure reactor (SCF-System, Korea). The stainless steel reactor can withstand a pressure up to 6,000 psi. The schematic diagram of the apparatus is already shown in chapter 1 and chapter 2. The supercritical fluid (SCF) equipment is attached with the high pressure CO_2 cylinder, high pressure metering pump and an efficient cooler. The pressure inside the reactor was measured with a pressure transducer and a digital display. The internal temperature of the reactor was measured with thermocouple. The temperature controlling is done via

some internal water circulating coil inside the reactor, heating with the help of highly efficient jacket thermocouple.

5.4 Procedure

5.4.1 Synthesis of macroporous polymer particles

In a typical polymerization reaction, monomer (5 ml of styrene), 0.1 g initiator (AIBN), 6ml stabilizer (PVA 5% w/v), 0.5 ml cross-linker (DVB) and double distilled water (35 ml) were mixed thoroughly in a three necked round bottom flask in nitrogen atmosphere to make a pre emulsion. On vigorous stirring, micro droplets of monomer were formed and suspended in water medium. The stabilizer polyvinyl alcohol (PVA) inhibits the coalescence of the monomer droplets. The pre emulsion was transferred into the high pressure SCF reactor. The reactor was then pressurized to the desired pressure (1,015-4,640 psi) with the help of high pressure pump. Then the mixture was agitated with a magnetically coupled mechanical stirrer at rotation speed of 700 rpm. The temperature of the reactor was allowed to reach desired reaction temperature (75 °C) and the desired pressure (1,015-4,640 psi) was attained with the addition of CO_2. The reaction was allowed to run for 8 hours and at the end, the reaction system was allowed to cool down to room temperature. The pressure was then slowly released and at atmospheric pressure and the polymeric product was recovered from the autoclave as white latex. All these reactions were repeated twice for reproducibility of the result. The polymer particles were separated by centrifuging at 5,000 rpm for one hour. The polymer was collected by decanting clear aqueous layer, and the polymer particles were dried under vacuum at 50 °C overnight. The control reactions in absence of CO_2 were carried out under identical conditions. In absence of CO_2, white latex was again observed but this was also accompanied by large quantities of coagulum.

5.5 Characterization

The yield of polymerization reaction was measured gravimetrically.

5.5.1 GPC Analysis

Molecular weight of the polymer particles was determined by gel permeation chromatography, a modular Waters 600 gel permeation chromatograph (GPC) with ultra styragel columns of 10^3 and 10^4 $^\circ$A porosities and a 410 differential refractometer was used for determination of molecular weight distributions. Tetrahydrofuran (THF) was used as a mobile phase with a flow rate of 1.0 ml/min, and the instrument was standardized with PS standards.

5.5.2 SEM analysis

Morphology of the polymer particles were obtained from JEOL-JSM-6390LV scanning electron microscope (SEM) and using JEOL, JEMCXII transmission electron microscopy (TEM). TEM was performed at an operating voltage of 80 kV. For SEM analysis, samples were mounted on an aluminum stub using an adhesive carbon tab and were coated with platinum to a thickness of 200 $^\circ$A.

5.5.3 BET analysis

Polymer particle surface area and porosity were measured using the BET method with a Micromeritics ASAP 2010 nitrogen adsorption analyzer. Samples were out-gassed for 3 h at 160°C under a N_2 flow before analysis.

5.6 Result and discussion

5.6.1 Preparation of macroporous polymer particles

Polymer particles are formed in water in supercritical carbon dioxide medium. The solvent property of supercritical carbon dioxide can be tuned by changing the pressure inside the reactor. At high pressure, CO_2 is partially soluble in monomer droplets thereby trapped inside the droplets. These monomer droplets undergo polymerization at high pressure resulting polymer particles into which the CO_2 gas is entrapped.
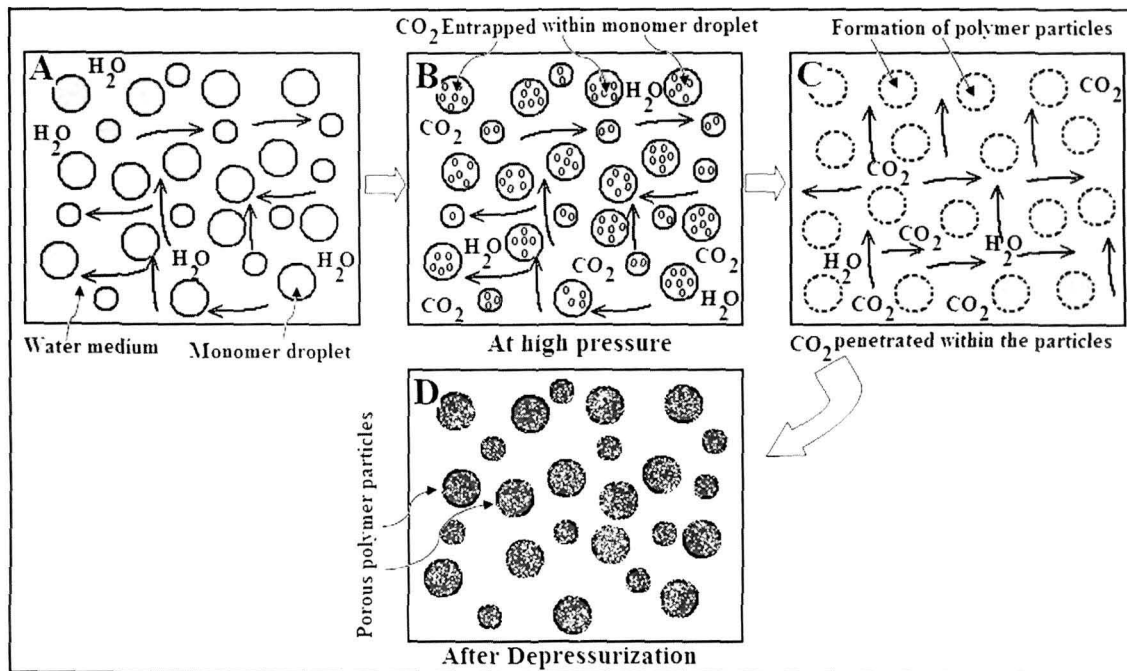
Fig.5.1: Mechanism for synthesis of porous polymer particles

While releasing the pressure, gaseous CO_2 comes out from the polymer particles which results a porous surface. Here sc-CO_2 acts as a reaction medium as well as a porogen. The particle size, pore diameter and surface area of the particles are dependent on the pressure. The formation of porous polymer beads in the SCF reactor is shown schematically in Fig. 5.1. At first, the monomer droplets are stabilized in the water

167

medium by the PVA stabilizer (A in Fig. 5.1). When CO_2 is introduced into the reactor, a large amount of CO_2 get dissolve in the water medium and a few amount of it dissolve in the monomer droplets and entrapped within the droplets (B). As soon as the temperature is raised to 75 $^{\circ}$C, polymerization starts and the dissolved CO_2 gas in the monomer droplets get entrapped within the polymer particles. Once the reactor is depressurized, the CO_2 gas comes out from the polymer particles and form some pores in the polymer particles.

Table.5.1: Physical property of the particles synthesized at different pressures

Sl no	Pressure (psi)	Stirring (rpm)	Mean diameter (µm)	Pore size (nm)	Surface area (m^2/g)	Yield (%)
1	14	700	8	0	< 4	70
2	1,015	700	10	20	<6	60
3	1,450	700	13	36	< 8	55
4	2,175	700	15	80	150	68
5	2,900	700	16	209	170	76
6	3,625	700	17	106	230	84
7	4,350	700	20	70	250	91
8	4,640	700	22	40	280	90

Table 5.1 summarizes the physical properties of the macroporous polymer particles. The experiments were carried out at various pressures (1,015-4,640 psi) keeping temperature and agitation speed constant. The monomer droplets and their corresponding particles during polymerization in water in sc-CO_2 medium are stabilized by the PVA molecules. Below 1,015 psi, particles are nonporous in nature. Here, solvency of CO_2 is very poor and is incapable to penetrate the monomer droplets. As the pressure of CO_2 is increased, the solvency of the gas increases for which large amount of CO_2 got dissolved into the monomer droplets. These monomer droplets undergo polymerization to form particles with high pore diameter and high surface area.

Each polymerization reactions were repeated twice over a range of pressures (1,015-4,640 psi) and keeping other parameters constant for reproducibility of the results. The size of the polymer particles increases (8-22 µm) with the increase in pressure (1,015-4,640 psi). The surface area of the polystyrene particles was also found to increase (8-280 m^2/g) with the increase in pressure. This is because, with the increase in pressure, the amount of CO_2 dissolved within the monomer droplets increases. The solvent property of CO_2 can be tuned to over a wide range by changing the pressure (i.e. density) inside the reactor. The pore diameter of the particles increases with the increase in pressure and reaches a maximum value 209 nm at pressure 2,900 psi (Table 5.1), and then it gradually decreases at higher pressures >2,900 psi. This is because at elevated pressures (>2,900 psi), the solvency of CO_2 increases which affects the phase separation process during the polymerization process. So the pore diameter starts decreasing above 2,900 psi but surface are increases. The degree of solvation imparted by the porogen is an important factor for determining the physical structure of the porous channels in the polymer particles. By tuning the pressure (density), we can have a control over different physical properties such as average pore diameter, pore size distribution and surface area. In normal organic porogenic solvents, the above mentioned properties can be achieved by optimizing reaction variables such as nature and proportion of porogen, proportion of cross-linker etc. However fine controlling over the pore size is always a challenging factor. But by using supercritical carbon dioxide, we can have a fine control over the pore size and the surface area of the polymer particles. Our results showed that the average particle size, average pore diameter and the surface area can be controlled by controlling the reaction pressure. Again the yield of the reaction is also increasing with increase in pressure (70 % - 91 %). When polymerization was carried out at 1,015 psi, porous polymer beads were obtained, but the pore size was relatively low (20 nm) and the surface area of the particles were also low (<6 m^2/g). This is because of the phase separation at lower pressures; at lower pressures CO_2 is not completely miscible with the reaction mixture. A pressure (psi) vs pore diameter (nm) and surface area (m^2/g) plot is given in Fig. 5.2, which shows that with the increase in pressure, the pore diameter of the particles increased and hence the surface area (upto 2,900 psi) (Fig. 5.3).

At pressure >2,900 psi, the pore diameter gradually decreases but the surface area gradually increases upto 280 m^2/g at 4,640 psi (Table 5.1).
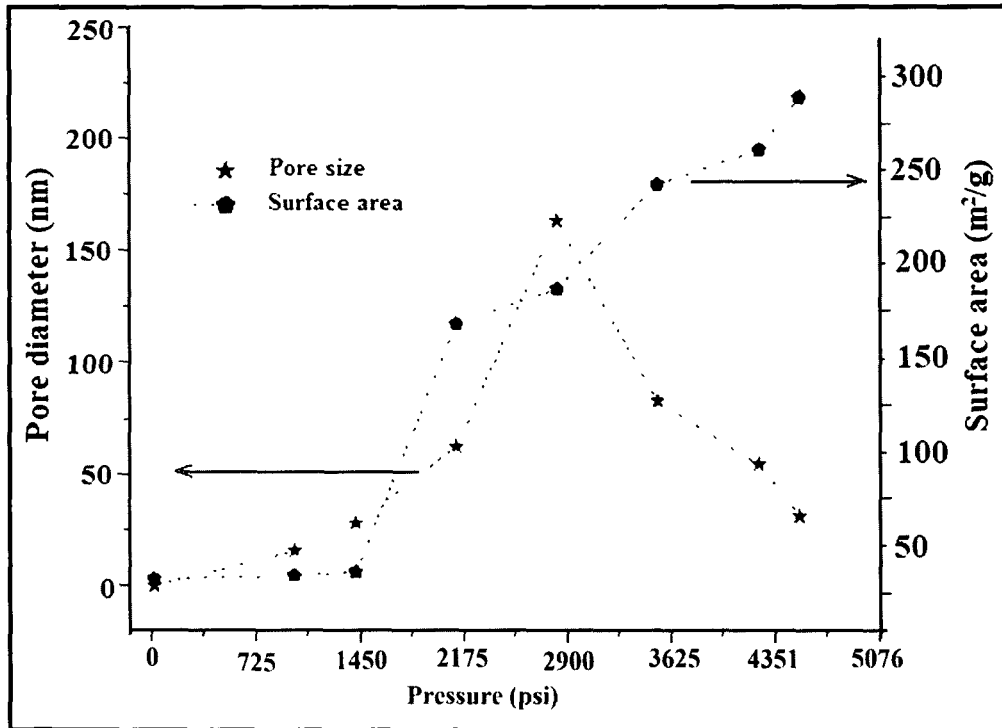

Fig.5.2: Variation of pore size and surface area with pressure

5.6.2 SEM Analysis

The scanning electron microscopic (SEM) images of the porous polystyrene particles are shown in Fig. 5.3.
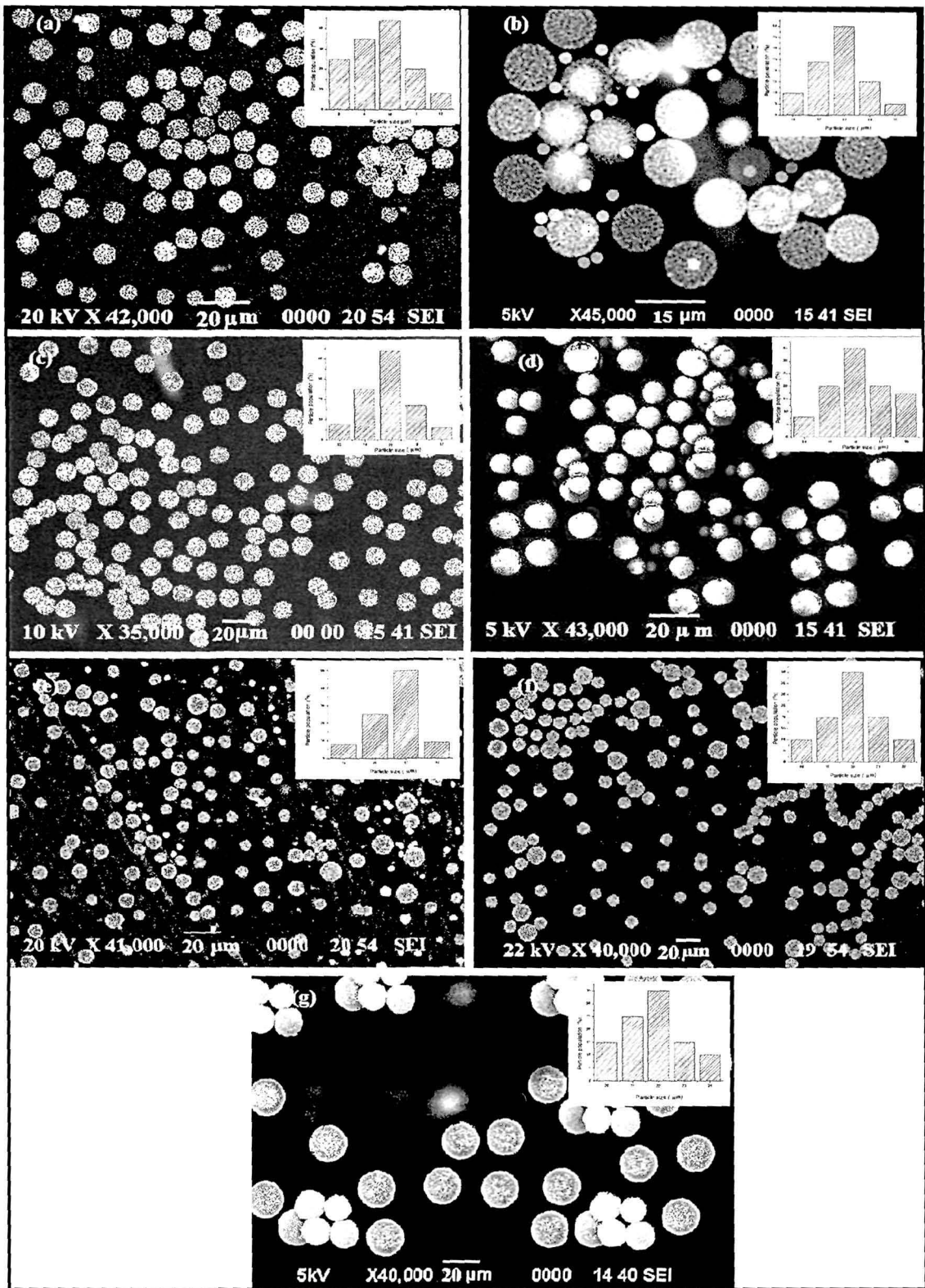
Fig.5.3: SEM micrographs of porous polymer particles

The SEM micrographs show the formation of spherical and uniform sized polymer particles. Some dark spots are observed in the polymer particles which are due to the porosity of the particles. It is observed from the SEM image that the particle diameter increase with the increase in pressure. The surface area of the particles also gradually increases with the increase in pressure. The solvency power of carbon dioxide increases with the increase in the pressure. This higher solvency power is responsible for the high density of CO_2 at higher pressures. This higher solvency affects the phase separation that occurs during the polymerization and is responsible for the increase in surface area, pore size and also the yield.

5.6.3 TEM Analysis

The Transmission electron micrograph (TEM) of the polymer particles is shown in Fig. 5.4. TEM micrograph of the polymer particles clearly indicates the formation of porous polymer particles. Highly porous polymer particles with various pore sizes are observed in the TEM micrograph.
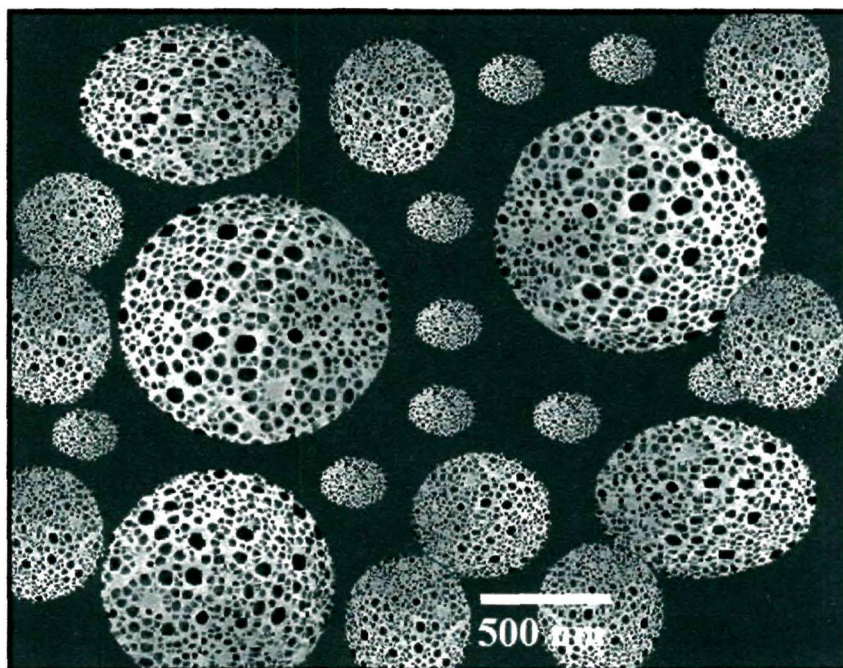
Fig. 5.4: TEM micrograph of porous polymer particles

5.6.4 Nitrogen adsorption/desorption characterization of porous polymer particles

The nitrogen adsorption/desorption isotherms and pore size distribution curves of one representative porous polystyrene particles synthesized in sc-CO_2 sample is shown in Fig.5.5. The BET plot of the porous polystyrene particles gives the pore size distribution, surface area and the average size of the pores. The BET surface area is calculated to be 170m^2/g and pore diameter 209 nm for particles synthesized at 2,900 psi and 700 rpm Fig.5.5. Relative pressure versus volume of N_2 adsorbed/desorbed plot gives curves of similar nature showing the porous behavior.

The BET surface area of the porous particles increase with the increase in pressure, but the pore size of the particles increase up to 2,900 psi and then it decreases.

Fig.5.5: BET analysis of the porous polymer particles

5.6.5 Gel permeation chromatographic (GPC) analysis

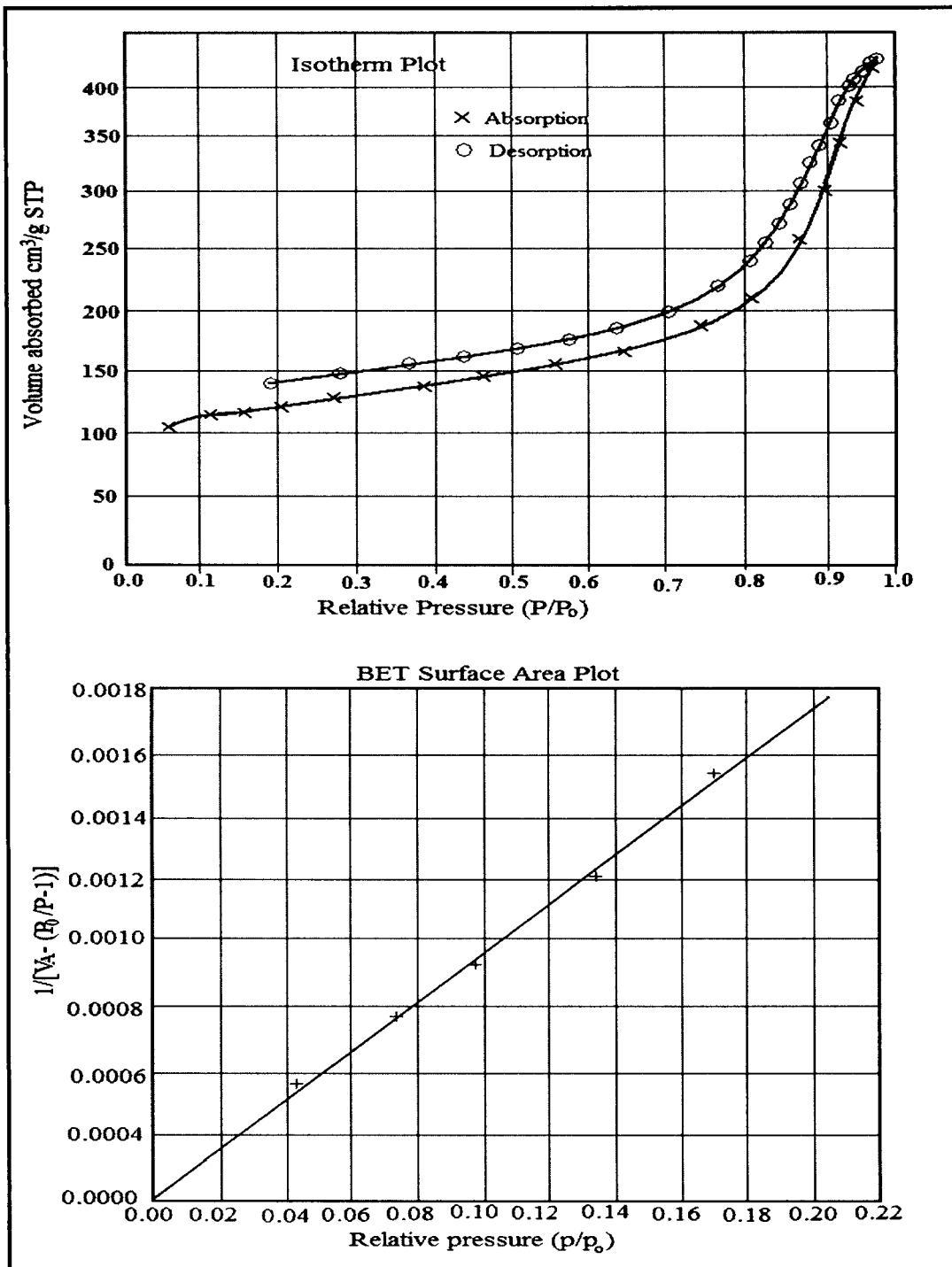The molecular weight distribution and polydispersity indices of the polymer samples were obtained from gel permeation chromatographic (GPC) data. All the data are summarized in Table. 5.2. Number average molecular weight (Mn) of the polymer was found to be in the range of (43,050-50,070 g/mol) and follows no fixed trend with the change in pressure.

Table 5.2: Molecular weights of the porous polymer particles

Sl no	Polymer synthesized at pressures (psi)	Mol. Wt. (g/mol) (Mn)	Polydispersity Index
1	14	48,450	1.31
2	1,015	44,300	1.26
3	1,450	43,050	1.43
4	2,175	44,070	1.34
5	2,900	45,660	1.64
6	3,625	47,000	1.30
7	4,350	47,550	1.53
8	4,640	50,070	1.67

The polydispersity indices (PDI) of the polymers are observed in the range of (1.26-1.67). From these GPC data it can be confirmed that the polydispersity indices and molecular weight of the polymer particles is independent of the pressure at which the polymer was synthesized.

Conclusion

Here, in this chapter, it is shown that sc-CO_2 can also be used as a porogenic solvent for the synthesis of porous polymer particles. The solvent property of sc-CO_2 can be tuned over a wide range for the synthesis of macroporous polymer particles by changing the pressure inside the reactor. The pore size, pore size distribution, surface

area and the average diameter of the particles can be fine controlled by controlling the pressure. The diameter of the particles increases (8-20 μm) with the increase in pressure (1,015-4,640 psi). Similarly the surface area of the particles also increase (4-280 m^2/g) with the increase in pressure. The pore size of the particles increases with increase in pressure and reaches a maximum 209 nm at 2,900 psi and then it gradually decreases with increase in pressure. The use of sc-CO$_2$ for synthesizing porous polymer particles is superior to the other conventional systems that are used for synthesizing porous particles regarding the purification of the products and environmental pollution. By simply depressurizing the gas, the porogen from the porous particles can be removed completely; no extra washing or drying steps are required.
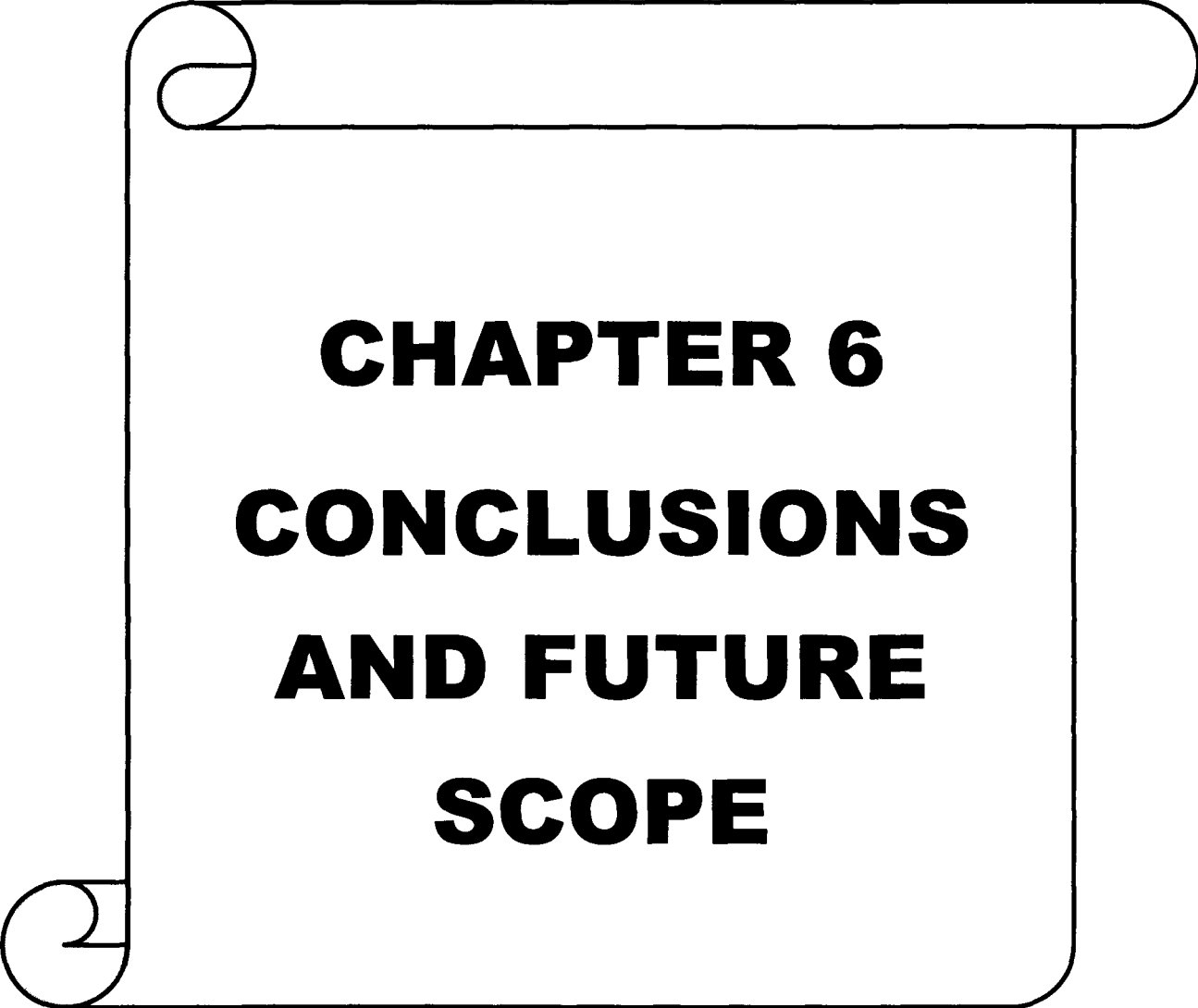
REFERENCES

1. Canelas, D.A.; DeSimone, J.M. Polymerizations in liquid and supercritical carbon dioxide, *Adv. Polym. Sci.* **133**, 103-144 (1997)

2. Kendall, J.L.; Canelas, D.A.; Young, J.L.; DeSimone, J.M. Polymerizations in supercritical carbon dioxide, *Chem. Rev.* **99**, 543-563 (1999).

3. Consani, K.A.; Smith, R.D. Observations on the solubility of surfactants and related molecules in carbon dioxide at 50°C, *J. Supercrit. Fluid.* **3**, 51-65 (1990).

4. Rosell, A.; Storti, G.; Morbidelli, M. Dispersion polymerization of methyl methacrylate in supercritical carbon dioxide using a pseudo-graft stabilizer: Role of reactor mixing, *Macromolecules* **37**, 2996-3004 (2004).

5. Wang, W.; Howdle, S.M.; Yan, D. One-step seed dispersion polymerisation in supercritical carbon dioxide, *Chem. Commun.* 3939–3941 (2005).

6. Hebb, A.K.; Senoo, K.; Cooper, A.I. Synthesis of porous cross-linked polymer monoliths using 1,1,1,2-tetrafluoroethane (R134a) as the porogens, *Compos. Sci. Technol.* **63**, 2379–2387 (2003)

7. Wang, X.; Sanchez, I.C. Anomalous sorption of supercritical fluids on polymer thin films, *Langmuir* **22**, 9251-9253 (2006).

8. Lee, H. *et al.* Successful dispersion polymerization in supercritical CO_2 using polyvinylalkylate hydrocarbon surfactants synthesized and anchored via RAFT, *J. Am. Chem. Soc.* **130**, 12242–12243 (2008).

9. Paul, E.; Anderson, Rachna, N.B.; Jamie, M.; Patricia, A.M. Electrochemical synthesis and characterization of conducting polymers in supercritical carbon dioxide, *J. Am. Chem. Soc.* **124**, 10284-10285 (2002).

10. Tan, B.; Lee, J.Y.; Cooper, A.I. Synthesis of emulsion-templated poly(acrylamide) using CO_2-in-water emulsions and poly(vinyl acetate)-based block copolymer surfactants, *Macromolecules* **40**, 1945-1954 (2007).

11. Thurecht, K.J.; Gregory, A.M.; Wang, W.; Howdle, S.M. "Living" Polymer Beads in Supercritical CO_2, *Macromolecules* **40 (9)**, 2965-2967 (2007)

12. Young, J.L.; DeSimone, J.M. Advantages of supercritical carbon dioxide for composite particle synthesis using water-soluble or water-reactive monomers, *Macromolecules* **38**, 4542-4544 (2005).

13. Clark, M.R.; Kendall, J.L.; DeSimone, J.M. Cationic dispersion polymerizations in liquid carbon dioxide, *Macromolecules* **30**, 6011-6014 (1997).

14. Lee, J.Y.; Tan, B.; Cooper, A.I. CO_2-in-water emulsion-templated poly(vinyl alcohol) hydrogels using poly(vinyl acetate)-based surfactants, *Macromolecules* **40**, 1955-1961 (2007).

15. Ji, M.; Chen, X.; Wai, C.M.; Fulton, J.L. Synthesizing and dispersing silver nanoparticles in a water-in-supercritical carbon dioxide microemulsion, *J. Am. Chem. Soc.* **121**, 2631-2632 (1999).

16. Hoefling, T.A.; Enick, R.M.; Beckman, E.J. Microemuisions in near-critical and supercritical CO_2, *J. Phys. Chem.* **95**, 7127-7129 (1991).

17. Galia, A.; Pierro, P.; Filardo, G. Dispersion polymerization of methyl methacrylate in supercritical carbon dioxide stabilized with poly(ethylene glycol)-b-perfluoroalkyl compounds, *J. Supercrit. Fluid.* **32**, 255-263 (2004).

18. Talay, D.K.; Akman, U.; Hortacsu, O. Supercritical carbon dioxide immobilization of glucose oxidase on polyurethane/polypyrrole composite *J. Supercrit. Fluid.* **44**, 457-465 (2008).

19. Heitz, M.P. *et al.* Water core within perfluoropolyether-based microemulsions formed in supercritical carbon dioxide, *J. Phys. Chem. B* **101**, 6707-6714 (1997).

20. Ohde, H.; Wai, C.M.; Rodriguez, J.M. The synthesis of polyacrylamide nanoparticles in supercritical carbon dioxide, *Colloid. Polym. Sci.* **285**, 475–478 (2007)

21. Ohde, H.; Hunt, F.; Wai, C.M. Synthesis of silver and copper nanoparticles in a water-in-supercritical-carbon dioxide microemulsion, *Chem. Mater.* **13**, 4130-4135 (2001).

22. Liu, Z.T.; Erkey, C. Water in carbon dioxide microemulsions with fluorinated analogues of AOT, *Langmuir* **17**, 274-277 (2001).

23. Yuvaraj, H. *et al.* Dispersion polymerization of styrene in supercritical CO_2 in the presence of non-fluorous random copolymeric stabilizers, *J. Supercrit. Fluid.* **42**, 351-358 (2007).

24. Young, J.L.; DeSimone, J.M. Advantages of supercritical carbon dioxide for composite particle synthesis using water-soluble or water-reactive monomers, *Macromolecules* **38**, 4542-4544 (2005).

25. Cooper, A.I.; Hems, W.P.; Holmes, A.B. Synthesis of cross-linked polymer microspheres in supercritical carbon dioxide, *Macromol. Rapid. Commun.* **19**, 353-357 (1998).

26. Cooper, A.I.; Hems, W.P.; Holmes, A.B. Synthesis of highly cross-linked polymers in supercritical CO_2 by heterogeneous polymerization, *Macromolecules* **32**, 2156-2166 (1999).

27. Canelas, D.A.; DeSimone, J.M. Dispersion polymerizations of styrene in carbon dioxide stabilized with poly(styrene-b-dimethylsiloxane), *Macromolecules* **30**, 5673-5682 (1997).

28. Hsiao, Y.L.; Maury, E.E.; DeSimone, J.M. Dispersion polymerization of methyl methacrylate stabilized with poly(1,1-dihydroperfluorooctyl acrylate) in supercritical carbon dioxide, *Macromolecules* **28**, 8159-8166 (1995).

29. Hodge, P.; Sherrington, D.C. *Syntheses and Separations using Functional Polymers*, (Wiley, New York 1989).

30. Sherrington, D.C. Preparation, structure and morphology of polymer supports, *Chem. Commun.* 2275-2286 (1998).

31. Park, Y.J. *et al.* Porous poly(lactide) membranes for guided tissue regeneration and controlled drug delivery: membrane fabrication and characterization, *J. Control. Release.* **43**, 151-160 (1997).

32. Wood, C.D.; Cooper, A.I. Synthesis of macroporous polymer beads by suspension polymerization using supercritical carbon dioxide as a pressure-adjustable porogens, *Macromolecules* **34**, 5-8 (2001).

33. Cooper, A.I.; Wood, C.D.; Holmes, A.B. Synthesis of well-defined macroporous polymer monoliths by sol-gel polymerization in supercritical CO_2, *Ind. Eng. Chem. Res.* **39**, 4741-4744 (2000).

CHAPTER 6

CONCLUSIONS AND FUTURE SCOPE

6.1 Conclusions:

Supercritical carbon dioxide exhibits large number of advantages over conventional polar and non-polar solvents. Besides its applications in extraction of natural products, synthesis of different organic compounds and inorganic complexes, it can also be used as a green medium for the synthesis of polymers, metal nanoparticles and different nanocomposites.

In this thesis, I provide insights into the synthesis, characterization and concomitant thermal, physical, mechanical properties of the synthesized polymer particles, nanoparticles and nanocomposites. A considerable effort has been devoted to the synthesis of polymer/metal nanocomposites with special emphasis on their antibacterial activities against a number of bacterial strains. The thesis also provides an account of the synthesis of macroporous polymer particles by using supercritical carbon dioxide as a pressure adjustable porogens.

The major findings of the thesis are described below

(I) Polymerization of styrene using siloxane and fluorine based stabilizers in supercritical carbon dioxide (sc-CO$_2$) medium.

➤ Supercritical carbon dioxide is a versatile alternative solvent for the emulsion polymerization technique. Dry, free flowing polystyrene microparticles in sc-CO$_2$ were successfully synthesized using initiator (AIBN) and stabilizer using siloxane based polydimethylsiloxane (PDMS) and fluorine based (trifluoromethyl)-undecafluorocyclohexane (C$_7$F$_{14}$) stabilizers at temperature 75 °C.

➤ The stabilizer concentration has sound effect on the polystyrene particle size. With the increase in stabilizer concentration, there is a subsequent decrease in the size of the polymer microparticles.

181

➤ With the increase in initiator concentration from 0.10% to 0.50%, the molecular weight of the polymer decreases from 55,000 g/mol to 45,000 g/mol and the particle size of the polymer also decreases from 4 μm 1.8 μm, which are in accordance with the nucleation mechanism of an emulsion polymerization.

➤ The increase in pressure of CO_2 (2,100-2,500 psi) influences the particle size. With the increasing pressure, particle size increases (2.2-1.0 μm) as well as the reaction rate get increased during polymerization.

➤ The powdered polystyrene microparticles of has been successfully synthesized by emulsion polymerization in supercritical carbon dioxide (sc-CO_2) using polydimethylsiloxane (PDMS) as a stabilizer and AIBN as initiator.

(II)Synthesis of metal (Ag, Cu) nanoparticles and their nanocomposites with polystyrene using water in (sc-CO₂) medium

➤ A green route has been developed for the synthesis of silver (Ag) and copper (Cu) nanoparticles by the chemical reduction technique in a water-in-sc-CO_2 medium using polydimethylsiloxane (PDMS) as a stabilizer.

➤ The dispersion of silver nanoparticles remains stable up to three months with the polydimethylsiloxane (PDMS) stabilizer and SDS surfactant. At high concentration of PDMS, the stability is more. The size of the Ag nanoparticles is found to be in the range of 5-17 nm. At lower pressure (2000psi) the particles are smaller and uniform in size.

➤ The dispersion of Cu nanoparticles remains stable up to two months with the polydimethylsiloxane (PDMS) stabilizer and AOT surfactant. At high concentration of PDMS, the stability is more. The size of the Cu

nanoparticles is in the range of 4 nm-8 nm. At lower pressure (2,000 psi) the particles are smaller and uniform in size.

➤ An easy, green method is developed to synthesize the silver/polystyrene and copper/polystyrene nanocomposite particles by ex-situ addition of Ag/Cu nanoparticles during the polymerization.

➤ The average size of Ag nanoparticles is found to be 8 nm and of nanocomposite particles to be 70 nm. The average size of the Cu nanoparticles is found to be 7 nm.

➤ The metal nanoparticles are uniformly distributed inside the polymer particles without leaving any bare Ag nanoparticles within the polymer matrix. The inclusion of the metal precursor had no influence on the polymerization process. Moreover, the method possess potential advantages for applications as it is simple, time saving, environmentally benign and the solvent (sc-CO_2) can be recycled.

➤ The antibacterial activity of silver/polystyrene and copper/polystyrene nanocomposite particles were tested against different bacterial strains like Pseudomonas fluorescens *BS3*, Bacillus circulens *BP2*, Eschericia coli and Staphylococcus aureus. Amongst all the bacterial species, Bacillus circulens *BP2* is found to be highly sensitive towards the Ag/Cu encapsulated polystyrene nanocomposite particles.

(III) *Synthesis of polystyrene/bentonite clay nanocomposites by emulsion polymerization in aqueous and in supercritical carbon dioxide (sc-CO_2) medium*

➤ Polystyrene/bentonite clay nanocomposites have been successfully synthesized by emulsion polymerization in both aqueous and sc-CO_2 medium.

➤ The particle size of the nanocomposites decreases with the increase in clay loading in both the media. But discrete and uniform sized particles are observed in sc-CO_2 medium, while agglomerated particles are obtained in aqueous medium.

➤ TEM and XRD results indicated that exfoliated nature of clay layers in the nanocomposites synthesized in sc-CO_2 medium, while intercalated and low exfoliation observed in nanocomposites synthesized in aqueous medium. The inter layer distance of the clay increases from 2.36-4.9 nm in sc-CO_2 medium, while in aqueous medium; it increases from 2.36-3.67 nm.

➤ The mechanical properties of the nanocomposites synthesized in sc-CO_2 medium are far enhanced than in aqueous medium. Similarly, thermal properties and the particle forming efficiency of the nanocomposite are better in supercritical carbon dioxide medium than in aqueous medium.

(IV) *Synthesis of Macroporous Polymer particles by Suspension Polymerization Using Supercritical Carbon Dioxide as a Pressure-Adjustable Porogen*

➤ The solvent property of sc-CO_2 can be tuned over a wide range for the synthesis of macroporous polymer particles. Supercritical carbon dioxide (sc-CO_2) can be used as a porogenic solvent for the synthesis of porous polymer particles.

➤ The pore size, pore size distribution, surface area and the average diameter of the polymer particles can be controlled by tuning the operating pressure. The diameter of the particles get increases (8-20 μm) with the increase in pressure (1,015-4,640 psi).

➤ The surface area of the polymer particles increases (4-280 m^2/g) with the increase in pressure. The pore size of the particles also increases with

184

increase in pressure and reaches a maximum 209 nm at 2,900 psi and then it gradually decreases with increase in pressure.

➢ By simply depressurizing the gas, the porogen from the porous particles can be removed completely; no extra washing or drying steps are required.

6.2 Future Scope

Supercritical carbon dioxide (sc-CO_2) is an attractive substitute for organic non polar solvents for a variety of chemical reactions. It has been attracting extensive interest as a polymerization and processing medium, primarily driven by the need to replace conventional organic solvents with more environmentally benign and economically viable systems. It has many advantages over conventional organic solvents. Moreover, the product can easily be separated out from solvent gas by depressurizing the gases. It is widely used for synthesis of organic compounds, inorganic complexes and in extraction of natural products in a greener way. In the contrary, it has been getting special interest as a reaction medium for synthesizing polymers, nanoparticles, and nanocomposites for its different environmental as well as product benefits. Although we have done a little works in the field of synthesis polymers, metal nanoparticles and nanocomposites, there are a lot of future directions to proceed in this field.

Some of the future directions of study of this present investigation.

✦ Synthesis of conducting polymers and its nanocomposites with metal nanoparticles using sc-CO_2 medium with special reference to its electrical conductivity.

✦ Encapsulation of some drug molecules in to the porous polymer particles and study their control release profile.

✦ Synthesis of some porous membranes using sc-CO_2 medium.

185

- Synthesis of fluoropolymers using sc-CO_2 medium.

- Polymerization of different monomers inside the microreactors in sc-CO_2 medium.

- Synthesis of conjugated polymers in supercritical carbon dioxide (sc-CO_2) medium for electronic applications.

LIST OF PUBLICATIONS

PAPERS IN INTERNATIONAL JOURNALS

1. **Kamrupi, I.R.**; Borthakur, L.J.; Dolui, S.K. Emulsion polymerization of styrene in supercritical carbon dioxide (sc-CO_2) stabilized with (Trifluoromethyl)-undecafluorocyclohexane (C_7F_{14}), *J. Polym. Mater.* **27**, 113-123 (2010).

2. **Kamrupi, I.R.**; Dolui, S.K. Synthesis of powdered polymeric microparticles by using supercritical carbon dioxide (sc-CO_2) as polymerizing medium, *Mater. Manuf. Process* **25**, 700-704 (2010).

3. **Kamrupi, I.R.**; Phukon, P.; Konwer, B.K.; Dolui, S.K. Synthesis of silver-polystyrene nanocomposite particles in water in supercritical carbon dioxide (sc-CO_2) medium and its antimicrobial activities, *J. Supercrit. Fluid.* **55**, 1089-1094 (2011).

4. **Kamrupi, I.R.**; Dolui, S.K. Synthesis of Copper-polystyrene nanocomposite particles in water in supercritical carbon dioxide (sc-CO_2) medium and its antimicrobial activities, *J. Appl. Polym. Sci.* **120**, 1027-1033 (2011).

5. Pokhrel, B.; **Kamrupi, I.R.**; Maiti, J.; Adhikari, B.; Dolui, S.K. Synthesis, Characterization, and Photovoltaic Properties of Poly(3-Phenyl Azomethine Alkylthiophene) Polymers, *J. Electron. Mater.* **40**, 149-156 (2011).

6. **Kamrupi, I.R.**; Dolui, S.K. Synthesis of polystyrene/bentonite clay nanocomposites by emulsion polymerization in water and in supercritical carbon dioxide (sc-CO_2) medium, *J. Compos. Mater.* (Article in Press) (Online DOI: 10.1177/0021998311401094).

7. **Kamrupi, I.R.**; Dolui, S.K. Synthesis of stable dispersion of Copper nanoparticles in a water-in-supercritical carbon dioxide (sc-CO_2) using polydimethyl siloxane (PDMS) as the stabilizer, *J. Exp. Nanosci.* (Article in Press).

8. Pokhrel, B.; **Kamrupi, I.R.**; Adhikary, B.; R.; Baruah, M.; Dolui, S.K. Study of optical and photovoltaic properties of n-alkyl substituted polycarbazole

derivative and its copolymer with thiophene, *Mater. Manuf. Process.* (Article in Press).

9. **Kamrupi, I.R.**; Pokhrel, B.; Kalita, A.; Baruah, M.; Baruah, R.; Dolui, S.K. Synthesis of macroporous polymer particles by emulsion polymerization using supercritical carbon dioxide as polymerizing medium, *Adv. Polym. Tech.* (Article Accepted)

10. **Kamrupi, I.R.**; Dolui, S.K. Synthesis of Colloidal dispersion of Silver nanoparticles in a water-in-supercritical carbon dioxide (sc-CO_2) medium using polydimethylsiloxane (PDMS) as stabilizer, *Mater. Manuf. Process.* (Revision submitted).

11. Kalita, A.; **Kamrupi, I.R.**; Dolui, S.K. Polymer supported heterogeneous titanium based Ziegler-Natta catalyst for ethylene polymerization, *J. Appl. Polym. Sci.* (Revision submitted).

12. **Kamrupi, I.R.**; Dolui, S.K. Dispersion polymerization of styrene in supercritical carbon dioxide (sc-CO_2) using polydimethylsiloxane (PDMS) as the stabilizer, *Int. J. Chem. React. Eng.* (Communicated).

13. **Kamrupi, I.R.**; Dolui, S.K. A new synthetic method for polymerization inside the micro reactors in supercritical carbon dioxide (sc-CO_2)", (Under Communication).

14. **Kamrupi, I.R.**; Dolui, S.K. Synthesis of core-shell polymer particles by using single monomer system using sc-CO_2 as polymerizing medium, (Under Communication).

15. **Kamrupi, I.R.**; Dolui, S.K. Dispersion polymerization of methylmethacrylate (MMA) in supercritical carbon dioxide (sc-CO_2) medium using PDMS as stabilizer", (Under Communication).

16. **Kamrupi, I.R.**; Dolui, S.K. Synthesis of styrene-butyl acrylate copolymers by emulsion polymerization in water and in supercritical carbon dioxide (sc-CO_2) medium (Under Communication).

17. **Kamrupi, I.R.**; Dolui, S.K. A review on synthesis of polymer microparticles by using supercritical carbon dioxide (sc-CO_2) as polymerizing medium (Under Communication).

PATENT FIELD

1. **Kamrupi, I.R.**; Dolui, S.K. *Efficient method for emulsion polymerization of styrene in supercritical carbon dioxide (sc-CO_2)*, Patent, (Application no. 1147/KOL/2009 dated 14.9.2009).

2. **Kamrupi, I.R.**; Dolui, S.K. *Synthesis of porous polymer beads by using sc-CO_2 as pressure adjustable porogen*, (Under preparation).

PRESENTATION IN CONFERENCES

1. **Kamrupi, I.R.**; Dolui, S.K. Synthesis of porous polymeric particles by emulsion polymerization using sc-CO_2 as polymerizing medium", 45th Annual Convention of Chemists 2008 and International Conference on Recent Advances in Chemistry, Dharwad University, Karnataka, (2008)

2. **Kamrupi, I.R.**; Dolui, S.K. Successful emulsion polymerization of styrene in sc-CO_2 using (trifluoromethyl)undecafluorocyclohexane stabilizer, National Conference on Frontiers in Polymer Science and Technology (POLY-2009), Saurastra University, Rajkot, (2009).

3. Dolui, S.K.; **Kamrupi, I.R.**, A novel method for the synthesis of silver-polystyrene nanocomposite particles using water in sc-CO_2 medium, National Conference on Smart Nanocluster (NCSN-2011), Tezpur University, Assam, (2011).

4. **Kamrupi, I.R.**; Dolui, S.K., Synthesis of Cu-polystyrene nanocomposites using water in sc-CO_2 medium and its antibacterial activity, National conference on Frontiers in Polymer Science and Technology (POLY-2011), Jadavpur University, Kolkata, (2011).